

TELEVISION RECEIVER
DESIGN
I.F. STAGES

The Series of books on Electronic Valves includes:

- Book I Fundamentals of Radio Valve Technique
 547 pages, 6" × 9", 384 illustrations.
- Book II Data and Circuits of Radio Receiver and Amplifier Valves
 424 pages, 6" × 9", 531 illustrations (1933/39).
- Book III Idem, 220 pages, 6" × 9", 267 illustrations (1940/41).
- Book IIIA Idem, 487 pages, 505 illustrations (1945/50).
- Book IIIB Idem, 1951/52, in preparation.
- Book IIIC Idem, on Television Valves, in preparation.
- Book IV Application of the Electronic Valve in Radio Receivers and Amplifiers (Part 1)
(1) R.F. and I.F. amplification. (2) Frequency changing. (3) Determination of the tracking curve. (4) Interference and distortion due to curvature in characteristics of the receiving valves. (5) Detection.
 440 pages, 6" × 9", 256 illustrations.
- Book V Application of the Electronic Valve in Radio Receivers and Amplifiers (Part 2)
(6) A.F. amplification. (7) Output stage. (8) Power supply.
 434 pages, 6" × 9", 343 illustrations.
- Book VI Application of the Electronic Valve in Radio Receivers and Amplifiers (Part 3) (in preparation).
(9) Inverse feedback. (10) Control devices. (11) Stability and instability of circuits. (12) Parasitic feedback. (13) Interference phenomena (hum, noise and microphony). (14) Calculation of receivers and amplifiers.
- Book VII Transmitting Valves, 284 pages, 6" × 9", 256 illustrations.
- Book VIIIA Television Receiver Design, Monograph 1.
 I.F. Stages. 188 pages, 150 illustrations.
- Book VIIIB Television Receiver Design, Monograph 2.
 Flywheel Synchronization of Saw Tooth Generators.

BOOK VIII A
TELEVISION RECEIVER DESIGN
I. F. STAGES

TELEVISION RECEIVER DESIGN

Monograph 1

I. F. STAGES

U.D.C. 621.397.62

by

A. G. W. UITJENS

Bibliotheek
Centraal Laboratorium PTT
St. Paulusstraat 4
Leidschendam

1953

PHILIPS' TECHNICAL LIBRARY

All rights reserved by N.V. Philips' Gloeilampenfabrieken
Eindhoven (Holland)

All data in this book are given without prejudice
to patent rights of the above company

AFGEVOERD

C.L.



P440, 8a

First published 1953
Printed in the Netherlands

FOREWORD

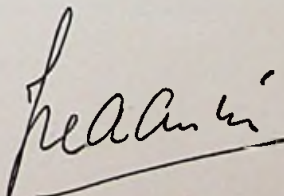
Parts IV, V and VI *) of this series of books deal with all those problems which relate to the application of the electronic valve in radio receivers and amplifiers. As explained in their prefaces, the material has been based mainly on Philips' publications, but the articles have been arranged in a logical sequence and, where necessary, revised and supplemented so as to bring the subject matter up to date.

In this manner a work has been compiled which, as a guide and source of information, is indispensable to set-makers and at the same time is greatly valued as material for practical study in secondary and higher technical training institutions.

It was, therefore, not surprising that suggestions have been received from various quarters that a similar work on the problems encountered in the design and construction of television receivers should be published. Although the technique of television reception is still in its infancy and has by no means reached a stabilized state, it has been decided to publish such a work under the title of *Television Receiver Design*, but in a slightly different format. In the work on radio receivers, chapters dealing with the many different aspects of the subject are printed in three bound volumes, but *Television Receiver Design* will comprise a series of 6 to 8 parts, each dealing with a specific aspect of television receiver design, and the whole forming a complete and comprehensive treatise.

The first part, entitled "I. F. Stages", deals with the application of the pentode in the intermediate frequency section of a superheterodyne receiver and the high frequency stages of a T.R.F. receiver. The second part, now at press, treats of flywheel circuits and synchronization. Other parts will cover such subjects as deflection circuits, problems related to the high-frequency stages, etc.

It is hoped that this work will prove to be just as valuable in its particular sphere as are the series of books on the construction of radio receivers.



J. HAANTJES

PHILIPS ELECTRONIC TUBE DIVISION

* Part VI is now in course of preparation.

PREFACE

This monograph deals particularly with pentode amplifiers operating in a frequency range lying roughly between 10 Mc/s and over 100 Mc/s. The high-frequency amplifiers of T.R.F. receivers (40 Mc/s to 70 Mc/s) also come under this definition, and thus, while not strictly coming within the scope of this book, have had to be included for the sake of completeness. On the other hand, the choice of the intermediate frequency has not been touched upon because this is so closely related to the problem of high-frequency amplification and frequency changing that it is considered better to deal with this subject in a separate book.

In order that the exposition may be quite clear to the reader, it has been necessary to use in some parts of the text formulae which do not directly follow from the preceding comments. The derivations of these formulae are to be found in the appendices at the end of the book.

Finally, a word of recognition is to be added, not only for the use that has been made of the literature quoted, but also for the support given by many colleagues, among whom I am particularly indebted to Jhr. Ir. H. van Suchtelen for many discussions and valuable advice, to Mr. H. Kater for editing the manuscript and to Mr. Harley Carter A.M.I.E.E. of Mullard Ltd., London, who scrutinized the manuscript.

The Author

Eindhoven, October 1952.

CONTENTS

1 GAIN AND BANDWIDTH WITH TWO-TERMINAL COUPLING NETWORKS	
1.1 The (GB) product	1
1.2 The gain reference frequency	3
1.3 Corrected equations	7
1.3.1 Consequences of stray capacitances, etc.	7
1.3.2 Input stage of the amplifier	8
1.3.3 Output stage of the amplifier	12
2 RESPONSE CURVE OF THE COMPLETE AMPLIFIER	
2.1 Total gain and total bandwidth with synchronous circuits	15
2.2 Staggered tuning	16
3 DISTORTION	
3.1 Distortion in double sideband systems	23
3.2 Distortion in vestigial sideband systems	25
3.3 Distortion in practical amplifiers	28
3.4 Graphical determination of the step function	30
4 GAIN, BANDWIDTH AND DISTORTION WITH FOUR-TERMINAL COUPLING NETWORKS	
4.1 " π " Network	50
4.2 Double-tuned band-pass filters	53
5 NOISE	
5.1 Definitions	59
5.2 Calculation of the noise factor	63
5.2.1 Noise factor of an amplifier without input damping	63
5.2.2 Noise factor of an amplifier with input damping	64
5.2.3 Noise factor of an amplifier with matching transformer	65
5.3 Causes of noise in a valve	67
5.3.1 Emission and partition noise	67
5.3.2 Induced grid noise	69
5.4 Calculation of the noise factor at metric waves	70
5.4.1 General equations	70
5.4.2 Range above f_0'	74
5.4.3 Range below f_0'	76
5.5 Effect of reducing the cathode lead conductance	78
5.6 Calculation of the signal-to-noise ratio from the noise factor	80

6 FEEDBACK

6.1 General	83
6.2 Basic formulae	84
6.3 Feedback from anode to grid	86
6.3.1 Negative feedback by a resistance	86
6.3.2 Feedback by the anode-to-grid capacitance	88
6.3.3 Maximum permissible values of p^2	92
6.3.4 Staggered tuning	95
6.3.5 Maximum permissible gain	97
6.3.6 Coupling by means of band-pass filters (I.F. transformers)	98
6.3.7 Deviations at higher frequencies	102
6.4 Feedback by the cathode-to-grid admittance	103
6.4.1 Self-inductance in the cathode lead	104
6.4.2 Reducing the conductance by means of a cathode capacitor	106
6.4.3 Small resistor in the cathode lead	108
6.4.4 Stabilization of the input admittance	110
6.4.5 Valves with double cathode connection	112
6.5 Feedback by the anode-to-cathode capacitance	113
6.6 Other forms of feedback	114

7 PRACTICAL CONSIDERATIONS FOLLOWING ON THE THEORY

7.1 Sensitivity	116
7.2 Gain	116
7.2.1 Gain of the input circuit	117
7.2.2 Gain of the I.F. amplifier	117
7.3 Selection of the valves	119
7.4 Staggered tuning system	122
APPENDIX I	134
APPENDIX II	152
APPENDIX III	154
APPENDIX IV	163
APPENDIX V	166
TABLE 1	168
TABLE 2	170
TABLES 3 and 4	172
LIST OF SYMBOLS	173

1 GAIN AND BANDWIDTH WITH TWO-TERMINAL COUPLING NETWORKS

1.1 THE (GB) PRODUCT

An essential difference between H.F. or I.F. amplifiers in sound receivers, whether for F.M. or A.M. signals, and the corresponding amplifiers in the video section of television receivers is that the latter have to pass a much wider frequency band. This means that amplifiers for the video section must include circuits in which the ratio of bandwidth to resonant frequency is comparatively high. Such circuits are said to have a low quality factor Q and, as is well known, they have a lower impedance than circuits with a high Q value.

Now the gain obtainable with a pentode is proportional to the anode impedance, so that the gain of an H.F. or I.F. stage in the video section may be expected to be lower than that of the corresponding stage in a sound receiver. It is therefore of prime importance so to design the circuits that the maximum gain is obtained for a given Q , and to ensure this the circuit capacitances must be reduced to the lowest practicable values.

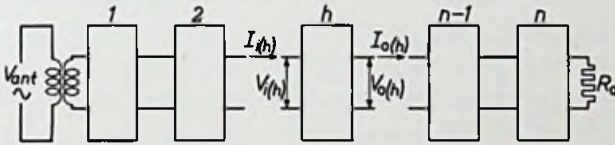


Fig. 1. Block diagram of an amplifier each stage of which comprises a valve with a mutual conductance S and an anode load Z .

This becomes clear when the gain and bandwidth of an amplifying stage forming part of the amplifier depicted in fig. 1 are calculated. The valve of this stage may be regarded as a current source $V_i \cdot S_{eff}$ shunted by an impedance Z , i.e. the internal resistance of the valve and the anode load connected in parallel. Hence:

$$V_o = V_i S_{eff} Z,$$

or, expressing Z in terms of admittance:

$$V_o = \frac{V_i S_{eff}}{Y},$$

giving for the gain of stage h :

$$G_h = \left(\frac{V_o}{V_i} \right)_h = \left(\frac{S_{eff}}{Y} \right)_h, \quad (1)$$

where S_{eff} is the dynamic mutual conductance of the valve, which may be taken to be equal to the static mutual conductance provided the cathode impedance is zero. At the frequencies considered, transit time effects do not influence the mutual conductance to any appreciable extent.

In investigating stage h more closely, the circuit of fig. 2, consisting of two amplifying valves and an interstage coupling formed by a parallel tuned circuit, will be considered. Here:

- g_a = anode conductance of valve h ,
- r_a = internal resistance of valve h ,
- C_o = output capacitance of valve h ,
- R_a = anode load of valve h ,
- L_c = self-inductance of the interstage circuit,
- R_c = shunt resistance of the interstage circuit,
- C_c = capacitance of the interstage circuit,
- R_g = grid leak of valve $h + 1$,
- g_i = input conductance of valve $h + 1$,
- C_i = input capacitance of valve $h + 1$,

The anode-to-grid capacitances C_{ag} will be disregarded.

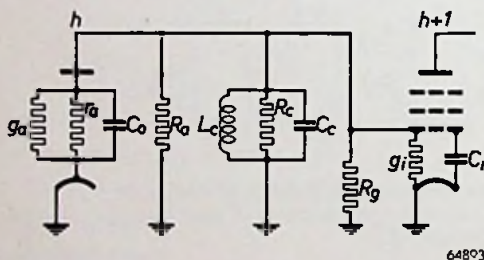


Fig. 2. Interstage coupling in which the various symbols are indicated.

If the two valves are coupled via an anode resistor and a tuned grid circuit, $1/R_g = 0$; if, on the other hand, the anode circuit is tuned and the following valve is coupled via a grid capacitor and a grid leak, $1/R_a$ may be set equal to zero (see fig. 2).

In what follows $g_a + 1/r_a$ will be termed the output conductance g_o , while $1/R_a + 1/R_c + 1/R_g$ will be called the circuit conductance g_c ¹). The admittance Y of eq. (1) can now be expressed by:

$$Y_h = g_i + g_o + g_c + j\omega C_c + j\omega C_o + j\omega C_i + \frac{1}{j\omega L_c}. \quad (2)$$

At correct tuning eq. (2) becomes:

$$Y_h = g_i + g_o + g_c. \quad (3)$$

¹) The symbol g_c has been introduced here as a logical corollary to the use of L_c, C_c , etc. in fig. 2, although it is recognized that this symbol is also used occasionally for the conversion conductance of frequency changers.

1.2 The gain reference frequency

while the gain G per stage is:

$$G = \frac{S_{\text{eff}}}{g_i + g_o + g_c} \quad (4)$$

Considering an amplifier with n identical stages and disregarding differences caused by different input and output circuits of the amplifier, the total gain G_{tot} is:

$$G_{\text{tot}} = \left(\frac{S_{\text{eff}}}{g_i + g_o + g_c} \right)^n \quad (5)$$

Denoting by B the bandwidth within which the circuit impedance varies 3 db, the conductance of the intervalve circuit of valves h and $h + 1$ may be expressed by:

$$g = g_i + g_o + g_c = 2\pi BC = 2\pi B (C_i + C_o + C_c) \quad (6)$$

(see Appendix Ia)

Substitution of this expression in eq. (4) gives:

$$G \cdot B = \frac{S_{\text{eff}}}{2\pi (C_i + C_o + C_c)} \quad (7)$$

This equation shows that **the quantities which determine the gain and bandwidth are so related that a high gain can be obtained only at the cost of the bandwidth.** The product $G \cdot B$ reaches the maximum when the circuit capacitance C_c (including the stray capacitances) is zero and when the dynamic mutual conductance S_{eff} is equal to the static mutual conductance S . In that case this product is entirely determined by the valve characteristics and will be denoted as:

$$(GB) = \frac{S}{2\pi (C_i + C_o)} \quad (8)$$

Eq. (8) shows that this (GB) product merely depends on the ratio of valve characteristics. If, for a given (GB) product, one of the quantities G or B is given, the maximum value of the other is fixed. It is, however, impossible to increase the gain G beyond a certain value by decreasing the bandwidth B . This is explained by eq. (3) in which the value of $g_i + g_o + g_c$ cannot be decreased indefinitely.

So long as $g_i + g_o$ is smaller than $2\pi B(C_i + C_o + C_c)$ (cf. eq. (6)) the bandwidth can be adjusted to the desired value by suitable choice of g_c until g_c has reached the minimum value obtainable. Beyond this limit it is impossible to decrease B by decreasing g_c . (For the present it will be assumed that it is possible to reduce g_c to zero.)

1.2 THE GAIN REFERENCE FREQUENCY

Another important difference between amplifiers for television and for broadcast receivers is that the television signal frequencies (for both

picture and sound) are very much higher than for normal broadcasting, being about 40 Mc/s to 200 Mc/s, and that intermediate frequencies in the order of 20 Mc/s to 50 Mc/s are employed.

At these high frequencies damping due to the valve conductances contributes largely to the total circuit damping. Now the input and output conductances of a valve, g_i and g_o , depend on the frequency which is to be amplified. The higher the frequency, the greater will be the damping, and the lower will be the maximum gain, until, at a certain frequency, the gain becomes unity, in other words the valve no longer amplifies. At still higher frequencies, the signal is even attenuated¹). The frequency at which the maximum gain is unity is called the **gain reference frequency** (symbol f_1).

It will be shown in Section 6 that the relationship between the conductances and frequency in the very-high frequency range (metric waves) is practically the same for all valves, and follows a square law, viz.:

$$g_i + g_o = \text{const.} \times f^2. \quad (9)$$

The magnitude of the constant in this expression depends on the valve characteristics and differs for each type of valve.

This implies that **the maximum gain which can be obtained with a given valve is determined by the frequency and by a valve constant**, for if g_c is put equal to zero to obtain the maximum gain, then, according to eqs (1) and (3), the gain is determined by the dynamic mutual conductance S_{eff} and $g_i + g_o$. The maximum value of S_{eff} is equal to the static mutual conductance S . Since at the frequencies under consideration there is little difference between the dynamic and static mutual conductances provided no additional impedances are included in the cathode lead, the maximum gain may be expressed by:

$$G_{\text{max}} = \text{const.} \times f^{-2}.$$

At the gain reference frequency f_1 the maximum gain $G_{\text{max}} = 1$, so that this expression may also be written as:

$$G_{\text{max}} = \left(\frac{f_1}{f}\right)^2. \quad (10)$$

The possibilities of an amplifier can now be investigated more closely. In practice the design of the amplifier is always based on the required bandwidth B_0 . It is obvious that this governs the gain obtainable, G_0 , and the required value of $g_i + g_o + g_c$. Considering the possibilities at in-

¹) M. J. O. Strutt, Gain and Noise Figures at V.H.F. and U.H.F., *Wireless Eng.* XXV, p. 21, 1948 (No. 292).

1.2 The gain reference frequency

creasing frequency, $g_i + g_o$ will obviously increase, and this could be compensated up to a certain limit by decreasing g_c . At a particular frequency the circuit conductance g_c would have to be reduced to zero, and this frequency is denoted by f_0 . Beyond f_0 the gain must necessarily

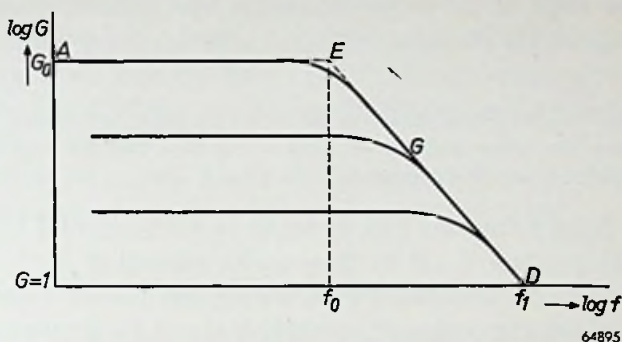


Fig. 3. Diagram representing $\log G$ as a function of $\log f$ in the case of R_c being so adjusted that the minimum bandwidth is B_0 . Three different values B_0 are shown.

decrease and the bandwidth will then increase, provided the circuit capacitance remains unchanged. The conductance of the circuit will be equal to $g_i + g_o$, both of which vary according to eq. (9).

The variation of B and G has been plotted in figs 3 and 4, in which

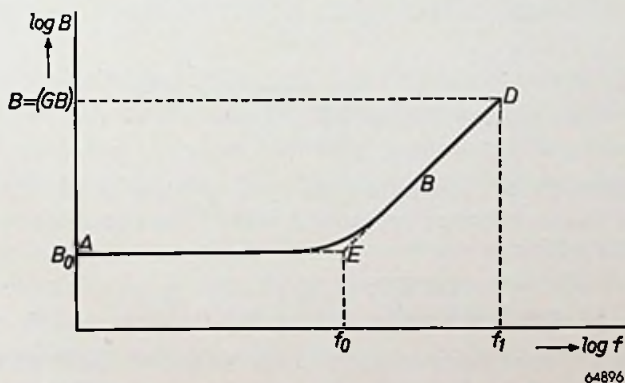


Fig. 4. Diagram representing $\log B$ as a function of $\log f$.

S_{eff} is considered constant and equal to S over the frequency range considered.

The graph in fig. 3 shows $\log G$ as a function of $\log f$ and consists of two linear parts—the horizontal part AE , the position of which depends on the chosen value of B , and the descending part ED , the position of

which is determined by the characteristic quantity f_1 . The slope of the latter part is determined by the square-law relation (9) existing between f and G .

A similar graph showing $\log B$ as a function of $\log f$ has been plotted in fig. 4. The slope of the ascending part is also determined by a square-law relation and the characteristic goes through the point $f = f_1$, $B = (GB)$.

It is obvious that the graph shown in fig. 4 can be made to coincide with that in fig. 3 by using the same unit for plotting — $\log B$ as that for plotting $\log G$ and making the point $B = (GB)$ coincide with $G = 1$.

The $\log B/\log f$ diagram can be made to be horizontal beyond f_0 by reducing the product $G \cdot B$ at frequencies exceeding f_0 . As shown by eq. (7), this may be achieved by increasing the circuit capacitance C_c .

For this reason the design of amplifying stages for frequencies exceeding f_0 must be based upon considerations differing from those governing the design of amplifying stages for lower frequencies. It is, therefore, of interest to know the position of point E in figs 3 and 4.

The position of point E depends on the choice of B_0 (and therefore of G_0) and on the value of f_1 . Since the point E must be situated both on the line AE and on the line ED , it is possible to calculate f_0 from eq. (10) by setting $f = f_0$ and $G_{\max} = G_0$. This gives:

$$f_0 = \frac{f_1}{\sqrt{G_0}} \quad (11)$$

or

$$f_0 = f_1 \sqrt{\frac{B_0}{(GB)}} \quad (12)$$

Example

As indicated in Table I (see p. 168) the (GB) product of the EF 42 valve is 100 Mc/s and its gain reference frequency f_1 is 325 Mc/s. According to eq. (12), for a bandwidth of 5 Mc/s:

$$f_0 = f_1 \sqrt{\frac{B_0}{(GB)}} = 325 \sqrt{\frac{5}{100}} = 73 \text{ Mc/s.}$$

At 50 Mc/s, i.e. at a frequency below f_0 , eqs (7) and (8) apply, giving:

$$G = G_0 = \frac{(GB)}{B_0} = \frac{100}{5} = 20.$$

At 100 Mc/s, i.e. at a frequency above f_0 , eq. (10) applies, giving:

$$G = \left(\frac{f_1}{f}\right)^2 = \left(\frac{320}{100}\right)^2 = 10;$$

hence

$$B = \frac{(GB)}{G} = \frac{100}{10} = 10 \text{ Mc/s.}$$

1.3 CORRECTED EQUATIONS

This simple method of calculation has been made possible only by a very idealized representation of the amplifier and it is now necessary to investigate what corrections are required to render the results more accurate and to extend their validity.

The two simplifications made in the preceding calculations were:

- (1) It was assumed that the total circuit capacitance is equal to $C_i + C_o$ and that the dynamic mutual conductance S_{eff} is equal to the static mutual conductance S .
- (2) The calculations were based on the assumption that the amplifying stage is preceded and followed by an identical stage.

1.3.1 Consequences of stray capacitances, etc.

The extent to which it is permissible to ignore the circuit capacitances C_c will first be investigated.

In broadcast receivers the choice of the circuit capacitance C_c is often determined by the desire to obtain a high value of Q ; but, as explained above, a high Q is not possible in T.V. receivers. In a receiver containing circuits with a high Q value tuning must be very accurate because a small relative detuning corresponds to a large proportion of the bandwidth. A small fractional shift of the resonant frequency of one of the circuits therefore results in quite a considerable modification of the response curve.

Now the valve capacitances are not entirely constant (for example the variation ΔC_i in the case of gain control being applied, see also Section 6), and it is therefore desirable to minimize the effect of these variations by ensuring that the valve capacitances are small compared with the total circuit capacitance.

This argument does not apply in T.V. receivers in view of the very low quality factors of the circuits. It is nevertheless desirable to keep these variations within reasonable limits; the circuit capacitance can then be reduced to the minimum. This is advantageous because the gain at a given bandwidth can then be increased to its maximum value.

It is of course not practicable to reduce the total circuit capacitance to $C_i + C_o$, owing to the existence of unavoidable stray capacitances of the wiring, the coils, etc. and "electronic" capacitance of the valve. These stray capacitances are represented by an additional term C_s , which is added to the circuit capacitance.

It is, therefore, no longer permissible to replace $G \cdot B$ simply by the

(GB) product, but it should be written:

$$G \cdot B = F_x (GB), \quad (13)$$

in which

$$F_x = \frac{C_i + C_o}{C_i + C_o + C_x}. \quad (14)$$

This becomes obvious when eq. (7), in which C_c is put equal to C_x , is compared with eq. (8). It is moreover seen that in eq. (8) the term S occurs instead of the term S_{eff} in eq. (7). To remove this discrepancy, eq. (13) will be rewritten as:

$$G \cdot B = F_s F_x (GB), \quad (13a)$$

in which

$$F_s = \frac{S_{\text{eff}}}{S}. \quad (15)$$

If, for example, a non-bypassed cathode resistor R_k is used, then:

$$F_s = \frac{1}{1 + S_k R_k},$$

where S_k denotes the cathode transconductance $\partial I_k / \partial V_g$.

Not only is it necessary to revise the calculation of $G \cdot B$ as shown above, but that of G_{max} must also be corrected. Eq. (10) for this quantity includes only terms depending on the mutual conductance and no term related to the circuit capacitances. The corrected equation, therefore, contains no term F_x and becomes:

$$G_{\text{max}} = F_s \left(\frac{f_1}{f} \right)^2. \quad (10a)$$

The calculation of f_0 can now easily be corrected, eqs (11) and (12) becoming:

$$f_0 = f_1 \sqrt{\frac{F_s}{G_0}}, \quad (11a)$$

and

$$f_0 = f_1 \sqrt{\frac{B_0}{F_x \cdot (GB)}}. \quad (12a)$$

1.3.2 Input stage of the amplifier

The assumption that an identical stage precedes the stage of which the gain is to be calculated does not hold for the first stage of the amplifier, and the necessary correction for this stage will now be investigated for the case of a "straight" (T.R.F.) receiver.

The gain of the first valve, between control grid and anode, can be calculated as before. The valve is, however, preceded by a transformer for matching the input impedance of the amplifier to the aerial. Correct matching is particularly important in T.V. receivers in order to avoid

reflections in the aerial cable, the effects of which are commonly termed "ghosts".

The matching transformer contributes to the voltage gain of the receiver. This additional gain is partly determined by the characteristics of the first valve in very much the same way as are the stage gain and bandwidth. In this case, too, there is a frequency range over which the gain is determined only by the bandwidth and a range over which the bandwidth and gain are determined by the frequency (see fig. 5).

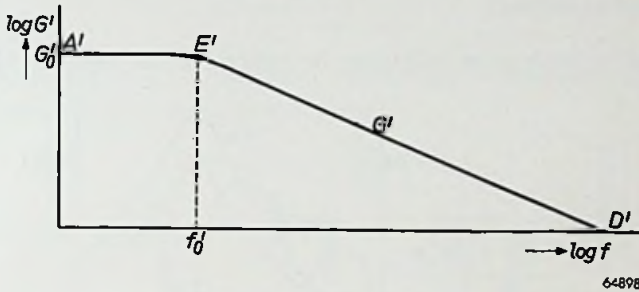


Fig. 5. The logarithm of the aerial gain G' as a function of $\log f$, R_c being so adjusted that the minimum bandwidth is B_0 and the value of w being such as to give correct matching.

This will now be investigated quantitatively. It is obvious that the largest possible proportion of the available power in the aerial will be transferred to the grid circuit if the load resistance is equal to the internal resistance of the source, i.e. when:

$$w^2 R_{\text{ant}} = \frac{1}{g_i + g_c'} \quad (16)$$

in which w is the transformer ratio and R_{ant} is the aerial resistance.

Under these conditions the output voltage V_{ant} of the source is equal to half the no-load voltage V_{rad} . For a normal dipole aerial and a given peak value of the field strength H :

$$V_{\text{rad}} = \frac{H\lambda}{\pi},$$

from which it can easily be calculated that:

$$V_i = \frac{V_{\text{rad}}}{2} w = \frac{H\lambda}{2\pi} w. \quad (17)$$

For a normal dipole aerial the value of R_{ant} depends not only on the characteristic aerial impedance

$$Z_{\text{ant}} = K' \log_e l/d - K'',$$

but also on the ratio l/λ (see fig. 6).

Since the reactive component X_{ant} of the aerial impedance also depends on l/λ , in practice this ratio must necessarily be made 0.5 or 1.0. The disadvantage of choosing $l/\lambda = 1.0$ is that R_{ant} then largely depends on Z_{ant} . It is true that the dependence of R_{ant} on l/λ is somewhat greater when the ratio l/λ is made 0.5 instead of 1.0, but the dependence on l/d is greatly diminished.

The aerial resistance R_{ant} is about 75Ω for a normal dipole aerial and about 300Ω for a folded dipole aerial. For correct matching of a normal dipole to an amplifier the condition:

$$w = \frac{1}{\sqrt{75(g_i + g_c)}}$$

must therefore be satisfied.

The total voltage gain will now be taken as the ratio of the output

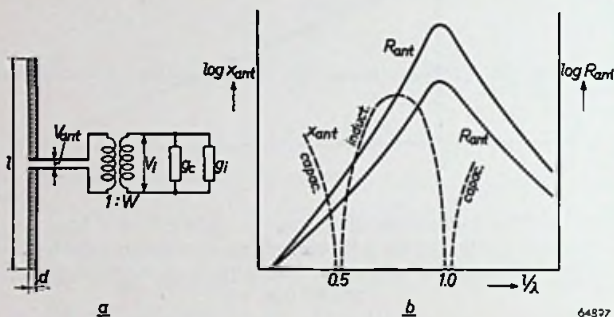


Fig. 6. *a* Dipole aerial having a length l and a diameter d . *b* The aerial reactance X_{ant} (broken line), which may be either capacitive or inductive, and the aerial resistance R_{ant} (full lines) as functions of the ratio l/λ for two different values of Z_{ant} .

voltage V_o to the no-load voltage V_{rad} of the aerial. This gain is equal to the product of the gain of all stages multiplied by the gain of the aerial circuit. At correct matching the gain G' of the aerial circuit is:

$$G' = \frac{V_i}{V_{rad}} = \frac{w}{2}.$$

It should be realized that in this equation w must not be considered as a constant quantity. If g_i is changed for choice of the bandwidth or frequency dependence, it is also necessary to change w to satisfy the condition given by eq. (13). Hence:

$$G' = \frac{w}{2} = \frac{1}{\sqrt{4R_{ant}(g_i + g_c)}} \quad (18)$$

At correct matching the transformed aerial resistance R_{ant} is just equal to $1/(g_i + g_c)$, so that the bandwidth of the aerial circuit is doubled when the aerial is connected. The bandwidth is therefore given by:

$$2(g_i + g_c) = 2\pi B' (C_i + C_x). \quad (19)$$

It is now clear, for the input stage, that it is not the product $G' \cdot B$ but the product $G' \cdot \sqrt{B'}$ which is constant. Eq. (13) of Section 1.3.1 now becomes:

$$G' \sqrt{B'} = F_x' (GB)' \quad (13b)$$

in which

$$(GB)' = \frac{1}{\sqrt{4\pi R_{ant} C_i}} = \frac{32.5}{\sqrt{C_i}} \quad (7a)$$

and

$$F_x' = \sqrt{\frac{C_i}{C_i + C_x'}} \quad (14a)$$

The maximum gain of the aerial circuit can be calculated by putting g_c in eq. (18) equal to zero, which gives:

$$G_0' = \frac{1}{\sqrt{4 R_{ant} g_i}}$$

where g_i is again $\text{const.} \times f^2$, so that:

$$G_0' = \frac{f_1'}{f} \quad (10b)$$

The position of the transitional point at f_0' is now given by:

$$f_0' = \frac{f_1'}{G_0'} \quad (11b)$$

or

$$f_0' = f_1' \frac{\sqrt{B_0'}}{F_x' (GB)'} \quad (12b)$$

Example

A normal dipole aerial is tuned to exactly 60 Mc/s and correctly matched to the input circuit preceding an EF 42 valve. The wiring capacitances are 3 pF. What is G' if $B_0' = 5$ Mc/s?

According to Table 1 (p. 168), the gain reference frequency $f_1' = 190$ Mc/s and the figure of merit $(GB)' = 10$ (B in Mc/s).

Since $C_i = 9.5$ pF:

$$F_x' = \sqrt{\frac{C_i}{C_i + C_x}} = \sqrt{\frac{9.5}{9.5 + 3}} = 0.87.$$

From eq. (12b):

$$f_0' = \frac{f_1' \sqrt{B_0'}}{F_x' (GB)'} = \frac{190 \sqrt{5}}{0.87 \times 10} \approx 50 \text{ Mc/s.}$$

Since f is higher than f_0' , eq. (10b) applies:

$$G' = \frac{f_1'}{f} = \frac{190}{60} = 3.2,$$

¹) Here it would in fact be more correct to write $(G \sqrt{B})'$ instead of $(GB)'$.

giving, according to eq. (13b):

$$B' = \left\{ \frac{F_x' (GB)'}{G'} \right\}^2 = \left(\frac{0.87 \times 10.5}{3.8} \right)^2 = 5.8 \text{ Mc/s.}$$

According to whether the receiver operates at a frequency above or below f_0 and f_0' , four cases arise:

- (1) the frequency lies below both f_0 and f_0' ;
- (2) the frequency lies below f_0 but above f_0' ;
- (3) the frequency lies above both f_0 and f_0' ;
- (4) the frequency lies above f_0 but below f_0' .

It will be seen later (Section 7) that in order to decide upon the most favourable design of the amplifier and input transformer it is of interest to know which of these cases applies.

T.R.F. receivers will usually be so designed that case (1) applies, but at higher frequencies (about 70 Mc/s) case (2) may occur. In superheterodynes, at the high T.V. band (about 200 Mc/s) case (2) always applies.

In view of the low gain per stage obtainable in case (3) this case will be avoided wherever possible. Case (4) does not occur in practice, f_0 hardly ever being lower than f_0' . This becomes obvious when f_0 and f_0' are calculated at $B_0 = B_0'$. From eqs (12a) and (12b):

$$\frac{f_0'}{f_0} = \frac{f_1'}{f_1} \cdot \frac{\sqrt{F_x(GB)}}{F_x'(GB)'} = \frac{\sqrt{F_x}}{F_x' \sqrt{2}} \cdot \sqrt{\frac{g_i + g_o}{g_i}} \cdot \sqrt{\frac{C_i}{C_i + C_o}} \approx \frac{1}{\sqrt{2}}.$$

It should be understood that the above considerations are based on the assumption that g_c can always be made negligible with respect to $g_i + g_o$. In practice, however, the minimum value of g_c may be quite considerable, especially in the aerial circuit. The implications of this in the above theory are dealt with in Section 7.

1.3.3 Output stage of the amplifier

In calculating the gain of the last valve of the amplifier it should be borne in mind that this stage is not followed by an identical amplifying stage but by a detector, so that a correction must be made also for this stage.

The two principal types of detector used in T.V. receivers are the anode-bend detector (pentode) and the diode detector.

For the anode-bend detector, which is not often employed, the valve is usually of the same type as that in the preceding amplifier. In this case the last I.F. stage can be considered as being followed by an "identical

stage", at any rate from the point of view of I.F. gain, so that the gain of the last stage is then equal to that of the preceding stages.

If, however, the valve used as an anode-bend detector is of a type suitable for use also as a video output valve, its input capacitance will usually be somewhat greater than that of a normal H.F. or I.F. pentode. As a result F_x will have a slightly lower value for the last stage, viz.:

$$F_x = \frac{C_i + C_o}{C_{id} + C_o + C_x} \quad (14b)$$

in which C_{id} is the input capacitance of the detector valve.

In principle, the same argument applies to the use of a diode detector. In that case, however, it is not permissible to put C_{id} equal to the diode capacitance, since the diode forms an additional load owing to the current flowing at the peaks of the signal voltage. This is equivalent to a resistance of approximately

$$R_d = \frac{R_l}{2\eta_D}$$

in which R_l is the load resistance of the detector valve and η_D is the efficiency of the detector. Moreover, when the smoothing capacitor has a fairly low value, as is usually the case with video detectors, R_d is shunted by a capacitance C_d , which also depends on η_D .

At first sight it might be supposed that the original circuit impedance could be restored by increasing the damping resistor across the last I.F. stage. This, however, is undesirable since, in a diode detector, η_D and therefore R_d depends on the signal amplitude. With very small signals (for example 0.1 V) η_D is very low, so that R_d may be high, but with large signals (for example > 5 V) η_D approaches its maximum limit, which is determined by the magnitude of R_l , the smoothing capacitor and the internal resistance R_i . Since the value of R_d depends on the signal strength, a response curve would then be obtained which varies with the signal amplitude¹).

These effects can be minimized by ensuring that R_p represents only a small proportion of the total circuit damping. Additional damping of the circuit by means of a fixed resistor may therefore be necessary, whilst — to ensure that the band width has the required value — some extra capacitance may have to be added. This obviously results in a lower value of F_x .

With a carefully designed detector and I.F. amplifier, however, the value of F_x for the last stage need not differ appreciably from that of the other stages.

¹) See also p. 129.

Example

Assume the maximum efficiency of a crystal diode detector, of which $R_1 = 4 \text{ k}\Omega$, to be $\eta_D = 0.65$. This gives:

$$R_d = \frac{R_1}{2\eta_D} = 3 \text{ k}\Omega.$$

When the last I.F. circuit is damped by a resistance of $2 \text{ k}\Omega$ the theoretical variation of the circuit impedance with signal amplitude will be between the limits of $2 \text{ k}\Omega$ and $1.2 \text{ k}\Omega$. In practice, however, these limits will not exceed $1.5 \text{ k}\Omega$ and $1.2 \text{ k}\Omega$, which may be considered acceptable.

It will further be assumed that $C_{id} + C_o + C_x$ has a normal value of 20 pF , which gives for the bandwidth:

$$B = \frac{g}{2\pi(C_{id} + C_o + C_x)} = \frac{10^6}{6.3 \times 20 \times 1.2} \approx 6.5 \text{ Mc/s.}$$

For television receivers this is quite a reasonable value, so that it is unlikely that much additional capacitance will have to be added.

2 RESPONSE CURVE OF THE COMPLETE AMPLIFIER

For calculating the gain it was assumed in Section 1 that the circuits were identical and that their bandwidths were known. It is true that the bandwidth of an amplifier is determined by the bandwidths of the circuits of which it is composed, but it is by no means identical to the circuit bandwidth. It will therefore be necessary to investigate how the total gain G_{tot} and the total bandwidth B_{tot} of the complete amplifier can be derived from the results calculated for one stage (G and B).

The total gain is obviously equal to the product of the gain of the separate stages, and the bandwidth of the complete amplifier will correspond approximately to the bandwidth of each of the tuned circuits.

The top of the response curve of single tuned circuits is, however, by no means flat, so that the attenuation of frequencies adjacent to the resonance peak with respect to the resonant frequency increases with the number of synchronous circuits connected in cascade. In other words, the flanks of the overall response curve become steeper and steeper and the 3 db points become closer to each other as the number of circuits is increased.

When a large number of amplifying stages is used, such as is required in T.V. receivers owing to the limited gain per stage, the total bandwidth may therefore become considerably smaller than that of the individual circuits.

Means of avoiding this without decreasing the gain are now discussed.

2.1 TOTAL GAIN AND TOTAL BANDWIDTH WITH SYNCHRONOUS CIRCUITS

The total bandwidth, B_{tot} , may be expressed as:

$$B_{\text{tot}} = F_B \cdot B, \quad (20)$$

where F_B is called the **bandwidth factor**. The value of F_B for various kinds of amplifier circuits will be briefly investigated.

The additional stray capacitance C_x will again be assumed to be zero. If it is desired to take the stray capacitances, etc., into account it suffices to introduce a factor:

$$F_x = \frac{C_i + C_o}{C_i + C_o + C_x}. \quad (14c)$$

Using the following symbols:

$$\frac{2\Delta\omega}{\omega_0} = \beta,$$

$$\frac{R}{\omega_0 L} = \omega_0 CR = Q,$$

and

$$Q\beta = x \text{ (see Appendix Ia),}$$

the function:

$$\left| \frac{Z}{Z_0} \right| = \left| \frac{1}{1 + jx} \right| = \frac{1}{\sqrt{1 + x^2}} \quad (21)$$

may be considered as the response curve of one circuit.

The response curve of an amplifier with t identical stages tuned to the same frequency may then be represented by:

$$\prod_{h=1}^{h=t} \left| \frac{Z}{Z_0} \right|_h = \left(\frac{1}{\sqrt{1 + x^2}} \right)^t. \quad (22)$$

B_{tot} can now be calculated from the value of x corresponding to the 3 db points of this response curve. Denoting this value of x for an amplifier with t synchronous circuits by x_t , and taking into consideration that for $x = x_t$ the left-hand side of eq. (22) is $1/\sqrt{2}$, it follows that:

$$1 + x_t^2 = 2^{1/t}.$$

The total bandwidth is now derived from x_t on the basis that, for $x = x_t$, $2\Delta\omega = 2\pi B_{\text{tot}}$, so that:

$$2\pi B_{\text{tot}} = \beta\omega_0 = \frac{x\omega_0}{Q},$$

which gives:

$$B_{\text{tot}} = \frac{x_t \cdot f}{Q}. \quad (23)$$

When the above equations are applied to an amplifier which contains only one tuned circuit, so that $t = 1$ and $x_t = x_1$, it is obvious that $x_1 = 1$ and $B = f/Q$. The formula for the bandwidth factor F_B of a receiver with t synchronous circuits is therefore:

$$F_B = \frac{B_{\text{tot}}}{B} = x_t = \sqrt{2^{1/t} - 1}. \quad (24)$$

2.2 STAGGERED TUNING

At high values of t the bandwidth factor F_B becomes inconveniently small, but it can be increased by applying staggered tuning, i.e. by tuning the circuits to slightly different frequencies.

For this purpose certain rules must be adhered to in order to obtain a

favourable response curve and a high gain. If the circuits were arbitrarily detuned a peculiarly shaped response curve would be obtained and the gain would not be optimum.

A simple and logical method of obtaining staggered tuning consists in dividing the amplifier into identical groups, each group consisting of a number of mutually detuned circuits. A five-stage amplifier (containing 6 circuits) may, for example, be composed of three pairs (t_1, t_2, t_3 in fig. 7a), of two triplets (t_1, t_2 in fig. 7b) or of one sextuple.

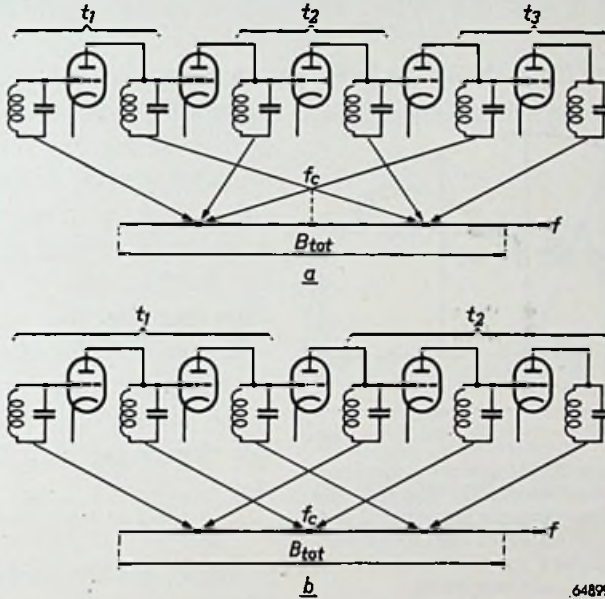


Fig. 7. Five-stage amplifier (containing 6 circuits) consisting (a) of 3 mutually detuned pairs and (b) of 2 mutually detuned triplets. f_c denotes the central frequency and B_{tot} the total bandwidth.

64899

In order to obtain for each group an optimum (GB) product and a response curve which is as flat-topped as possible, a special method of detuning and damping is applied, termed “flat staggering”. (The damping of the individual circuits also differs in this scheme.)

Assume the amplifier to be subdivided into l/s groups, each having s mutually detuned circuits. In the case of flat staggering it can be shown that the response curve of one group may be expressed by:

$$\prod_{h=1}^{h=s} \left| \frac{Z}{Z_0} \right|_h = \frac{1}{\sqrt{1+x^{2s}}} \tag{25}$$

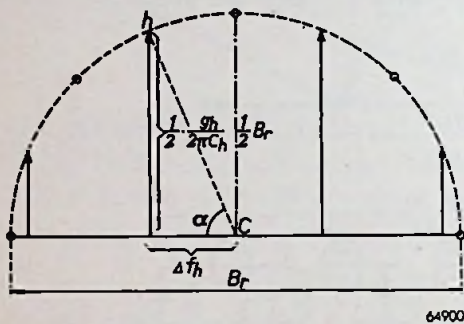
in which x is the βQ of the "reference circuit" to be defined later.

Such a "flat staggered s -tuple" can be realized as follows. From a semi-circle, subdivided into s equal parts, a perpendicular is dropped to the diameter from the centre of each part (see fig. 8). The length of the h^{th} perpendicular then represents half the required bandwidth:

$$\frac{1}{2} \cdot B_h = \frac{1}{2} \cdot \frac{g_h}{2\pi C_h}$$

of circuit number h , and the distance of its foot to the centre C represents the detuning Δf_h of this circuit with respect to the central frequency of the system ¹⁾.

The scale of fig. 8 should be so chosen that the diameter represents the required bandwidth of the group.



The dash-dot line represents the so-called central or reference circuit. Such a circuit need not actually be present in the amplifier; neither does it occur in the diagram of fig. 7a.

The gain of, for example, valve $h-1$, i.e. the valve preceding the tuned circuit h of the amplifier, can now be calculated as follows:

Fig. 8. Diagram for designing a flat staggered s -tuple, in which B_r denotes the bandwidth of the reference circuit and Δf_h represents the detuning of the circuit concerned with respect to the central frequency f_c of the system.

$$G_{h-1} = \frac{S}{g_h \sqrt{1 + x_h^2}}$$

in which for the central frequency f_c :

$$x_h = Q_h \beta_h = \frac{\omega_0 C}{g_h} \cdot \frac{2\pi \Delta f_h}{\omega_0} = \frac{2\Delta f_h}{B_h} = \frac{B_r \cos \alpha}{B_h},$$

where B_r is the bandwidth of the reference circuit and α is the angle formed by the diameter and the line interconnecting C and point h of fig. 8. According to this figure:

$$g_h = g_r \sin \alpha.$$

Since

$$g_h = 2\pi C_h B_h$$

and the damping of the reference circuit is:

$$g_r = 2\pi C_r B_r,$$

¹⁾ See i.a. George E. Valley Jr. and Henry Wallman, Vacuum Tube Amplifiers, MacGraw Hill (1948).

the value of x_h may be written:

$$x_h = \frac{g_r \cos \alpha}{g_h} = \frac{\cos \alpha}{\sin \alpha} = \cot \alpha,$$

assuming C_h to be equal to C_r . Hence

$$G_{h-1} = \frac{G_r}{\sin \alpha \sqrt{1 + \cot^2 \alpha}} = G_r. \quad (26)$$

The gain of each stage is therefore equal to that of a stage in which the reference circuit is connected to the anode of the valve (at least as far as the central frequency is concerned). The total gain can thus again be calculated from the expression:

$$G_{tot} = G_r^n.$$

At frequencies differing by $\Delta' f$ from the central frequency:

$$x_h = \frac{2(\Delta f + \Delta' f)}{B_h} = \frac{\cos \alpha + x}{\sin \alpha}, \quad (27)$$

where $x = Q\beta$ of the reference circuit. The response curve of circuit h is thus given by:

$$\left| \frac{Z}{Z_0} \right|_h = \left| \frac{\frac{1}{\sin \alpha}}{1 + j \frac{\cos \alpha + x}{\sin \alpha}} \right| = \frac{1}{\sqrt{\sin^2 \alpha + \cos^2 \alpha + x^2 + 2x \cos \alpha}} = \frac{1}{\sqrt{1 + x^2 + 2x \cos \alpha}}, \quad (28)$$

where $Z_0 = 1/g_r$ is the impedance of the reference circuit at zero detuning.

If, for each of the circuits, the values of $\cos \alpha$ are chosen according to the construction in fig. 8, then ¹⁾:

$$\prod_{h=1}^{h=s} (1 + x^2 + 2x \cos \alpha_h) = 1 + x^{2s}. \quad (29)$$

The response curve thus assumes the form given by eq. (25).

These response curves can easily be plotted on a graph the two axes of which have a logarithmic scale (see fig. 9). The curve thus obtained, which represents only (part of) one half of the response curve tends asymptotically to two straight lines, one of which runs horizontally, the other making an angle with the abscissa the tangent of which is s . The point of intersection of the two lines lies at $x = 1$, while the trend in the transitional area is determined by the gaussian logarithm of x^{2s} .

The fact that x in eq. (29) is equal to the x of the reference circuit for the frequency concerned has an important consequence: Substitution

¹⁾ The deduction of this formula is given in Appendix II, page 152.

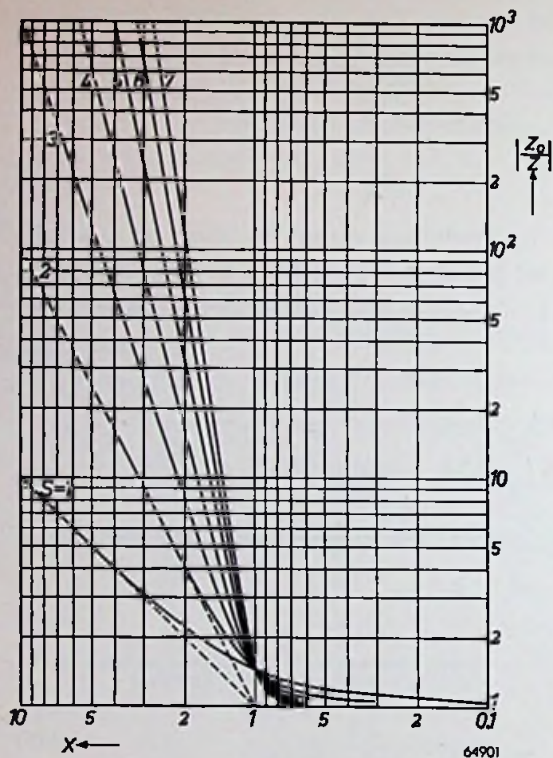


Fig. 9. Representation of the response curves according to eq. (25).

$x = 1$ in eqs (21) and (25) shows that the 3 db bandwidths (B_r of the reference circuit and the total bandwidth B_{tot} of the flat staggered s -tuple derived therefrom) are identical. For a flat staggered group the bandwidth factor F_B is therefore equal to unity.

An amplifier consisting of many stages is usually composed of several flat staggered groups, the bandwidth factor $F_{B'}$ of each of which is equal to unity; the bandwidth factor F_B of the total amplifier is then less than unity. The s -tuples are not made excessively large, because this would result in the outermost circuit requiring very little damping, which cannot very well be achieved (cf. fig. 10).

It has been shown above that all s -tuples derived from the same reference circuit have the same 3 db bandwidth, the only difference being the slope of the sides of the resonance curves (see fig. 11a).

If identical groups are connected in cascade, such as is the case in amplifiers composed exclusively either of pairs or of triplets, etc., the value of F_B can be easily calculated. If the amplifier contains for example $t/2$ pairs:

$$F_B = \sqrt[2^{t/2}]{2^{t/2} - 1} \approx \frac{1}{1.1 \sqrt[2]{t/2}} \tag{30}$$

and, if it consists of $t/3$ triplets:

$$F_B = \sqrt[2^{t/3}]{2^{t/3} - 1} \approx \frac{1}{1.06 \sqrt[3]{t/3}} \tag{30a}$$

The total bandwidth thus decreases as the

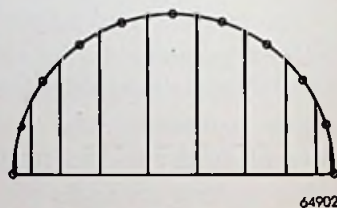


Fig. 10. Diagram showing that the outermost circuits (corresponding to the outermost perpendiculars) would have to have very little damping if the s -tuples were chosen very large.

2.2 Staggered tuning

number of groups l/s increases, see fig. 11b. In Table 2 (p. 170) the bandwidth factors F_B are given for identical groups connected in cascade.

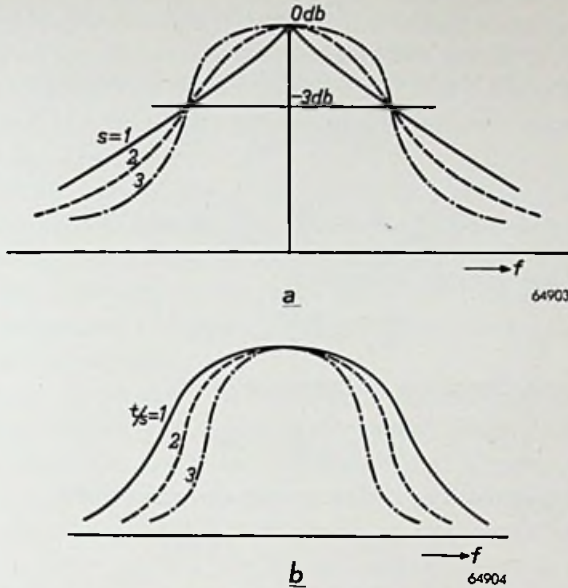


Fig. 11. (a) Response curves of three different s -tuples ($s=1$, $s=2$, $s=3$) derived from the same reference circuit. (b) Response curves showing the decrease in total bandwidth as l/s (i.e. the number of groups) increases.

With a view to avoiding undesirable low values of F_B as far as possible, the extent to which the valve characteristics restrict the possibility of obtaining flat staggered tuning will now be investigated.

The bandwidth of the most selective circuit is given by:

$$B = B_r \sin \alpha = \frac{B_{\text{tot}} \sin \alpha}{F_B}, \quad (31)$$

where α is the smallest of the angles of the semicircular staggering diagram (see fig. 8). According to eqs (10a) and (13a) the smallest bandwidth attainable at a given frequency is:

$$B_{\text{min}} = F_x (GB) \left(\frac{f}{I_1} \right)^2.$$

To enable staggering to be carried out, the following condition must therefore be satisfied:

$$B_{\text{tot}} \sin \alpha \geq F_B F_x (GB) \left(\frac{f}{I_1} \right)^2. \quad (32)$$

Example

For a five-stage amplifier with six tuned circuits $(GB) = 100$, $F_z = 0.8$, $f_1 = 300$ Mc/s and $f = 50$ Mc/s.

What is the maximum gain at $B_{tot} = 5$ Mc/s if the selectivity of the circuits may not be increased by adding extra capacitances?

According to eq. (32) the following condition must be satisfied:

$$\frac{\sin \alpha}{F_B} \geq F_z \cdot \frac{(GB)}{B_{tot}} \cdot \left(\frac{f}{f_1}\right)^2;$$

therefore:

$$\frac{\sin \alpha}{F_B} \geq 0.8 \cdot \frac{100}{5} \cdot \left(\frac{50}{300}\right)^2 \approx 0.45.$$

In the case of one sextuple (see Table 3):

$$\frac{\sin \alpha}{F_B} = \frac{0.26}{1} = 0.26,$$

which is insufficient. But in the case of two triplets:

$$\frac{\sin \alpha}{F_B} = \frac{0.5}{0.86} = 0.58,$$

which is sufficient, so that two triplets may be chosen, of which:

$$B_r = \frac{B_{tot}}{F_B} = \frac{5}{0.86} = 5.8 \text{ Mc/s},$$

while

$$G = G_0 = \frac{(GB) F_z}{B_r} = \frac{80}{5.8} = 13.8,$$

whence follows from eq. (20):

$$G_{tot} = G^5 = (13.8)^5 = 450\,000.$$

3 DISTORTION

3.1 DISTORTION IN DOUBLE SIDEBAND SYSTEMS

The method of flat staggering discussed in the previous section avoids decrease of the bandwidth as the number of circuits increases, as shown by fig. 11*b*, and the response curve assumes a more rectangular form, as depicted in fig. 11*a*.

In one important respect this is an advantage, since not only does the amplitude characteristic of the frequency range passed become flatter, but the attenuation of undesired signals also increases. For this reason networks having a rectangular response curve are usually aimed at; but it should be recognized that such networks give rise to a fairly great distortion of certain signals.

This is not due to the amplitudes being incorrectly reproduced but to the phase being shifted. The response curve and phase characteristic of the customary networks are in fact so related that a rectangular form of the amplitude characteristic always gives rise to serious non-linearity of the phase characteristic ¹⁾. If the phase characteristic of an H.F. or I.F. amplifier is linear (not necessarily constant) this merely results in the modulation being shifted over a constant time interval without the envelope of the modulated signal being distorted thereby, but if the phase characteristic is not linear the various modulation frequencies are mutually shifted in phase.

Therefore, although the distortion occurring in an amplifier is given in principle by its response curve, it is necessary in practice to know the phase characteristic in order to obtain a clear insight into the nature and seriousness of the phase distortion. The phase characteristic gives this information for sinusoidal signals of various frequencies in a form which does not show the distortion of non-harmonic waveforms and is therefore unsuitable for judging the quality of a video signal.

The common criteria for the reproduction of a video signal are adequate reproduction of the fine details present and the absence of false details. Since fine details are to be considered here as intensity variations of short duration, the reproduction of the high modulation frequencies is of particular importance.

For judging the fidelity with which high modulation frequencies are

¹⁾ Cf. Hendrik W. Bode, *Network Analysis and Feedback Amplifier Design*, Chapters XIV and XV, van Nostrand, New York.

reproduced it is necessary to understand how an impulse is reproduced; and in order to investigate the reproduction of false details, the envelope of the H.F. signal is given an easily recognizable form, which preferably contains many frequencies (i.e. the Fourier analysis of the envelope should supply an extensive spectrum). Distortion is then immediately noticed by the changed waveform of the envelope. A suitable form is the so-called unit or step function, see fig. 12, which is not only easily recognizable, but can also easily be dealt with mathematically.

A further advantage of this method is that an impulse can easily be composed of two opposed steps in rapid succession. The response to high modulation frequencies can thus easily be deduced from the envelope of the reproduced signal: the step function.

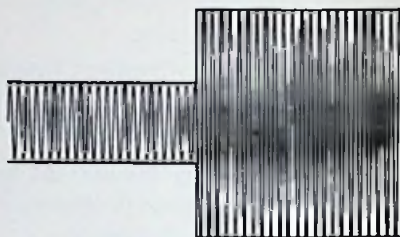
A typical form of step functions of H.F. and I.F. amplifiers is given in fig. 13.

In order to judge step function response curves quantitatively, two characteristic quantities indicated in fig. 13 must be considered: firstly the rise time τ required by the curve to increase from 1/10 to 9/10 of the ultimate value and, secondly, the overshoot δ , i.e. the amount by which the ultimate value is exceeded.

These two figures are roughly related to the form of the response curve of the amplifier. In the first place, $B_{tot} \cdot \tau = 0.7$ to 0.9; and, secondly, the overshoot is more serious

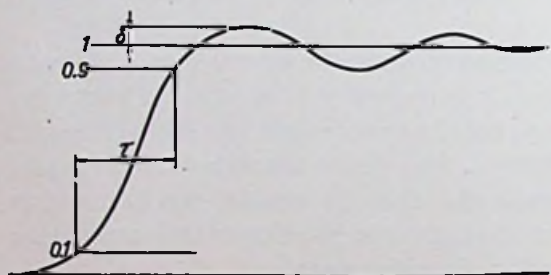
as the response curve approaches a rectangular form (see Appendix III).

By applying flat staggered tuning, several stages can thus be connected in cascade without causing the rise time τ to increase (which would be the case if the stages were synchronous), but this is at the expense of an increase of the overshoot δ . The values of δ and of the product $B_{tot} \cdot \tau$ depend on the connection of the circuits, and their tuning, etc., as indicat-



64905

Fig. 12. Example of an impulse for measuring the step function of an I.F. amplifier.



64906

Fig. 13. Example of a step function illustrating the rise time τ and the overshoot δ .

3.2 Distortion in vestigial sideband systems

ed in Table 3 (p. 172) where τ , $B_{\text{tot}} \cdot \tau$ and $B_r \cdot \tau$ are given for several identical groups of various composition connected in cascade.

It should be recognized, however, that the results quoted in this table apply only to double sideband systems; for single sideband reception the form of the step function response curve depends on other factors as well.

3.2 DISTORTION IN VESTIGIAL SIDEBAND SYSTEMS

In view of the considerable saving in bandwidth effected, the vestigial sideband system (a form of single sideband transmission) is now commonly used, and it will be useful to investigate the changes to which the step function is subject if, throughout the transmitter and receiver, one sideband is suppressed.

This may be done by considering a carrier with a sinusoidally modulated envelope corresponding to the expression

$$\sin a \sin b = \frac{1}{2} \cos (a-b) - \frac{1}{2} \cos (a + b),$$

where a represents the carrier frequency and b the modulation frequency. If throughout the whole system one sideband, e.g. the lower one, is suppressed, only the carrier plus the term $-\frac{1}{2} \cos (a + b)$ representing the upper sideband remains.

The same result would have been obtained by adding:

$$-\frac{1}{2} \left\{ \frac{1}{2} \cos (a - b) + \frac{1}{2} \cos (a + b) \right\} \quad (\text{m1})$$

to the expression:

$$\frac{1}{2} \left\{ \frac{1}{2} \cos (a - b) - \frac{1}{2} \cos (a + b) \right\}, \quad (\text{m2})$$

giving again:

$$-\frac{1}{2} \cos (a + b).$$

As follows from the well-known trigonometrical equation, the added expression (m1) is equal to:

$$\frac{1}{2} \cos a \cos b.$$

This manipulation clearly shows that **the suppression of one sideband is equivalent to the addition of a fully modulated second carrier which is in quadrature with respect to the original carrier, its modulation also being in quadrature with respect to the original modulation.** It is thus obvious that the original signal:

$$A_0 \sin 2\pi f_0 t + A_m \sin 2\pi f_m t \cdot \sin 2\pi f_0 t,$$

from which one sideband is suppressed, becomes:

$$A_0 \sin 2\pi f_0 t + \frac{1}{2} A_m \sin 2\pi f_m t \cdot \sin 2\pi f_0 t - \frac{1}{2} A_m \cos 2\pi f_m t \cdot \cos 2\pi f_0 t,$$

in which f_m and f_0 represent the frequency of the modulation and of the carrier, and A_m and A_0 represent the corresponding amplitudes.

The quadrature component (i.e. the cosine term) thus adds (in quadrature) to the original signal

a modulation component which is out of phase and gives rise to distortion. It should further be noted that the modulation depth is approximately halved.

In practice the suppression of one sideband is achieved by means of a response curve of the form shown in fig. 14a, which can be considered equivalent to the sum of the curves represented in figs 14b and c. This corresponds to the mathematical analysis given above and, moreover, takes into account the limited frequency range. It should be noted that the signal passed by the response curve of fig. 14c and that passed by the curve of fig. 14b are in quadrature.

The consequences of transmitting a modulated signal

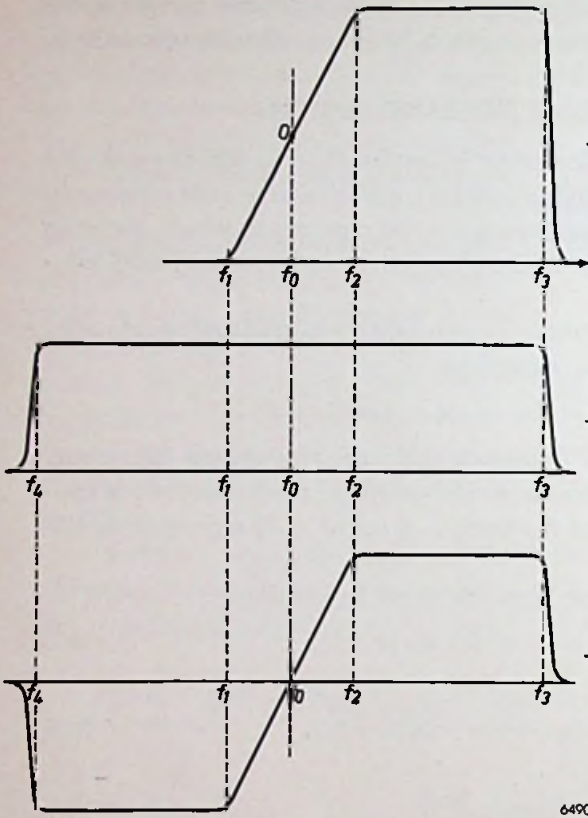


Fig. 14. *a* Asymmetrical characteristic of a vestigial sideband system which may be considered as being composed of the sum of an image-symmetrical characteristic (*b*) and a radial-symmetrical characteristic (*c*).

$$A_0 \sin 2\pi f_0 t + A_m \{ \sin 2\pi f_m t \cdot \sin 2\pi f_0 t \} = \\ = A_0 \sin 2\pi f_0 t + \frac{1}{2} A_m \{ \cos 2\pi(f_0 - f_m)t - \cos 2\pi(f_0 + f_m)t \}$$

by a system having a response curve similar to fig. 14a will now be investigated more closely.

The image-symmetrical characteristic of fig. 14b gives rise to amplitude distortion only of the sideband beyond the region from f_4 to f_3 . The frequencies within this range correspond to modulation frequencies smaller than

3.2 Distortion in vestigial sideband systems

$f_3 - f_0$ as shown by the above expression. The image-symmetrical response curve thus suppresses only modulation components with frequencies exceeding $f_3 - f_0$. This is the normal phenomenon which also occurs in double sideband systems.

For all modulation components which are passed by the image-symmetrical response curve in the manner described above, the radial-symmetrical characteristic of fig. 14c adds a modulated H.F. signal to the carrier. This H.F. signal has the same frequency as the carrier, but, since it is in quadrature, the square of this signal must be added to the square of the

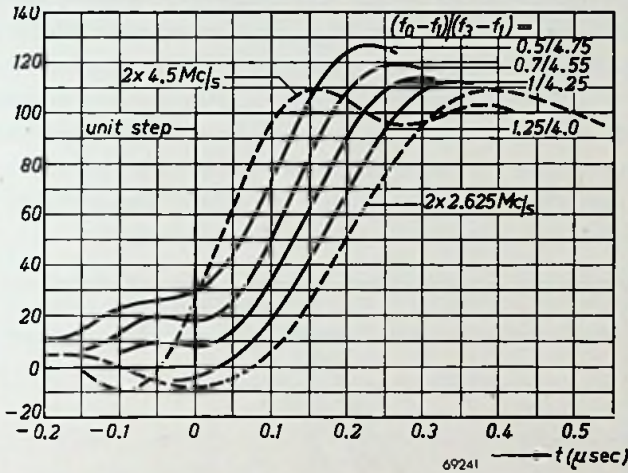


Fig. 15. Step functions of a single sideband system (full lines) with a modulation factor of 1 and an ideal filter. The total frequency band is 5.25 Mc/s. The broken lines are valid for double sideband systems.

signal originating from the image-symmetrical characteristic represented in fig. 14b.

The above considerations apply without restriction to the modulation frequencies between $f_2 - f_0$ and $f_3 - f_0$, but from fig. 14c, demonstrating the identical attenuation of the two sideband components (of the quadrature component), it is clear that the quadrature component is smaller for frequencies below $f_2 - f_0$ and tends to zero for modulation frequencies also tending to zero. This is emphasized here because the low frequencies form the most important contribution towards the video signal, and this effect renders it possible to reduce the distortion by the quadrature component for these frequencies.

It is clear that this favourable effect increases as the range from f_1 to f_2

becomes greater, because the frequency range which takes advantage of the attenuation of the quadrature component then also increases. The response curve should therefore not be made too steep in the cut-off area on both sides of the carrier frequency.

The effect of the width of the cut-off area on the total bandwidth is illustrated by fig. 15¹⁾, which shows the distortion of a voltage step (modulated on a carrier) whose components exceeding 4.25 Mc/s have been removed. The ratio $(f_0 - f_1)/(f_3 - f_1)$ has been taken as parameter. The broken lines apply to double sideband systems.

The usual characteristics of the single sideband transmission are such that the range from f_0 to f_1 can be given a maximum width of 1 Mc/s, the total bandwidth being approximately 5 Mc/s. The curve $(f_0 - f_1)/(f_3 - f_1) = 1/4.25$ may thus be considered attainable in practice.

As a result of the square of the quadrature component having to be added to the square of the carrier, the importance of the quadrature component and therefore the distortion of the step function decreases with the modulation depth.

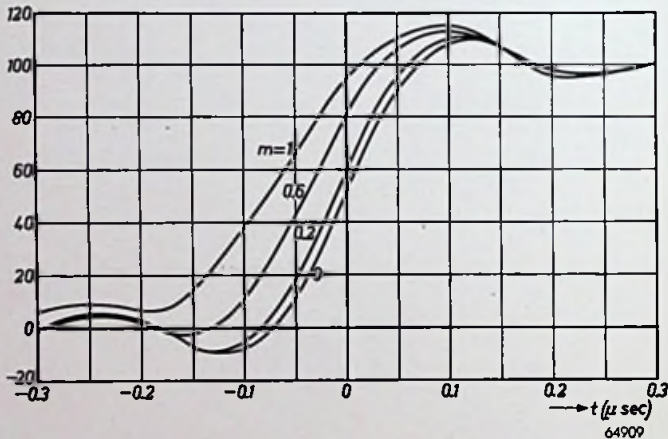


Fig. 16. Step function as shown in fig. 15 for $(f_0 - f_1)/(f_3 - f_0) = 1/4.25$, with the modulation factor m as parameter.

In fig. 16¹⁾ the variation of one envelope of fig. 15 has been plotted for four different modulation depths m .

3.3 DISTORTION IN PRACTICAL AMPLIFIERS

If the conditions imposed at the beginning of the above comments,

¹⁾ See Kell and Fredendall, Selective Side Band Transmission in Television, R.C.A. Review, April 1940.

3.3 Distortion in practical amplifiers

assuming the single sideband system to be ideal, are not satisfied, various consequences will result, as will become clear from Section 3.4.

As to the flatness of the response curve between f_2 and f_3 it can be stated that local deviations will result in incorrect reproduction of the corresponding modulation components. This will generally result in a transient with a frequency corresponding to the incorrectly reproduced modulation frequency, being added to the unit function response curve. Furthermore, the magnitude of the components in quadrature will change, so that too small a response of certain frequencies may be expected to give rise to relatively less distortion than too great a response.

The condition that the response curve of fig. 14a should be radial-symmetrical between f_1 and f_2 with respect to point O may be expressed in another way, as follows:

- (1) the amplitude response at the frequency f_0 should be half the value obtained at frequencies between f_2 and f_3 ;
- (2) the sum of the responses of two frequencies between f_1 and f_2 differing from f_0 by an equal amount should be twice the response at f_0 .

If condition (1) is not satisfied this will give rise to an incorrect D.C. component, and the lowest frequencies of the envelope will not be faithfully reproduced. This will result in "inert" distortion of the step function as shown in figs 17a and b.

Such after-effects in the television image thus point to the fact that the carrier is incorrectly situated with respect to the cut-off point of the response curve.

If condition (2) is not satisfied for a given modulation frequency the frequency concerned will not be faithfully reproduced by the image-symmetrical characteristic and neither will this be the case with the quadrature component.

This case is similar to that in which deviations occur between f_2 and f_3 , but the modulation frequencies now concerned are lower.

The condition that the phase shift should be a linear function of the

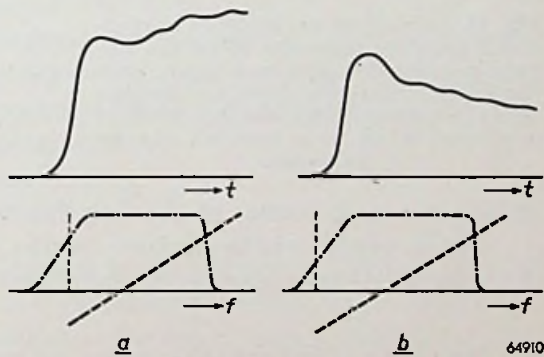


Fig. 17. Step function response curves (full lines) and corresponding amplitude and phase characteristics (dash-dot and broken lines respectively) of two detuned amplifiers. Owing to the carrier of frequency f_0 being incorrectly situated with respect to the cut-off point, a positive after-effect is experienced in (a) and a negative after-effect in (b).

frequency is difficult to fulfil in practice. The conventional coupling networks used in amplifiers have a given fixed relation between the response curve and phase characteristic, and this relation is such that no linear phase characteristic can be obtained with a response curve of the form shown in fig. 14. The deviations usually occurring in practice are sketched in figs 18*a* and *b*.

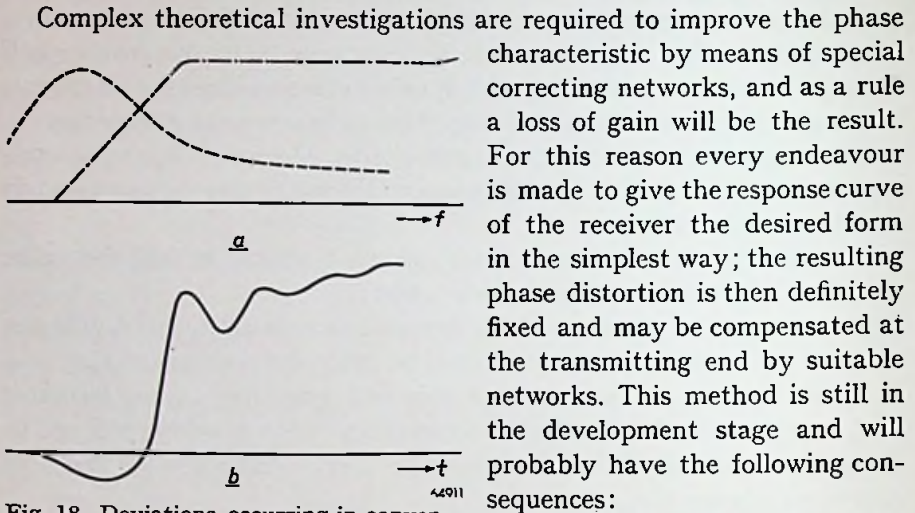


Fig. 18. Deviations occurring in conventional coupling networks. In (a) the amplitude (dash-dot line) and phase shift (broken line) are again plotted as functions of the frequency f , while the step function is plotted in (b) as a function of time (full line).

- (1) care will have to be taken that the receivers have the prescribed response curve, particularly as far as the low frequencies are concerned;
- (2) experimental testing of the unit function response curve of transmitters will have to be carried out with a receiver having an accurately prescribed response curve, instead of with a special wide-band receiver.

3.4 GRAPHICAL DETERMINATION OF THE STEP FUNCTION

For the performance of an I.F. amplifier to be judged from its step function it is useful to have available a simple and quick method for deriving this curve from the frequency response curve.

The method described below is based on the approximation of the frequency response curve by straight line segments. This method is therefore not exact, but the accuracy of the approximation may be improved *ad libitum* by increasing the number of segments.

The method offers the particular advantage of being not merely a

3.4 Graphical determination of the step function

mathematical analysis but of giving also a clear insight into the relationship between the forms of the frequency response curve and the step function. From the graphical construction of the latter it can therefore be deduced how the frequency response curve should be changed to obtain a better step function. It is, for example, possible to investigate, by means of greatly simplified frequency response curves, how their various characteristic forms influence the step function ¹⁾.

In vestigial sideband systems the contribution of the quadrature components is determined separately, so that the influence of the modulation depth on the form of the step function can easily be investigated.

The effect of phase distortion is also determined separately, this being of importance for studying for example the value of phase correction in the transmitter. It is possible, therefore, to leave the phase distortion out of consideration for the time being, thus rendering the method more easily understood.

The purpose in view is to determine the envelope E_o of the output signal when the envelope E_i of the input signal consists of a constant component (the base) E_b and a voltage step E_s at the instant $t = 0$. By means of the unit function $H(t)$ this can be expressed by:

$$E_i = E_b + E_s H(t). \quad (33)$$

To solve this problem the phase characteristic is for the time being assumed to be linear within the pass band, but with the phase angle Θ differing from zero. This means that the output signal is delayed with respect to the input signal by an amount:

$$D = \frac{-\Theta}{2\pi f}, \quad (34)$$

where Θ is the phase shift in radians at the frequency f . The delay angle $-\Theta$ thus represents the delay D expressed in radians. (The modulation frequency at which the modulation at the output lags by 360° is therefore equal to $1/D$.) Assuming that

$$t' = t - D, \quad (35)$$

the step of the output voltage is then given by:

$$E_o = G \{ E_b + E_s H_s(t') \}. \quad (36)$$

The gain G is of no consequence here and will be assumed to be equal to

¹⁾ See, for example, W. M. Lloyd, Single Sideband Receiver Design, J. Telev. Soc. 6, p. 135, Oct./Dec. (No. 4).

unity, so that it suffices to calculate the function $H_s(f')$. For this purpose the modulation response curve M is derived from the I.F. response curve A (see fig. 19).

The frequency scale of this diagram corresponds to the difference in

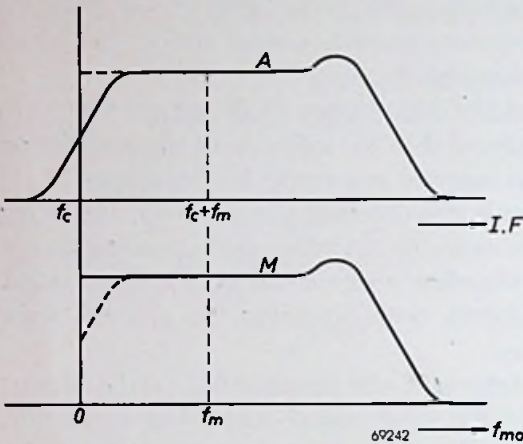


Fig. 19. I.F. response curve A from which the modulation response curve M is derived.

frequency of the carrier and the sideband component. The positive or negative sign is of no significance; the contributions of the two sidebands are simply added.

The modulation response curve is now approximated by a number of straight line segments. The extremities of each of these line segments correspond to the frequencies f' and f'' ($f'' < f'$). The difference in height between the extremities will be denoted by h , which is taken to be positive when the line segment descends towards higher frequencies, i.e. when it has a negative slope. Horizontal line segments can be disregarded in the calculation.

To determine the approximating broken line for a modulation response curve the following data are specified for each line segment:

- (1) the difference in height h ,
- (2) the highest frequency f' ,
- (3) the ratio f''/f' .

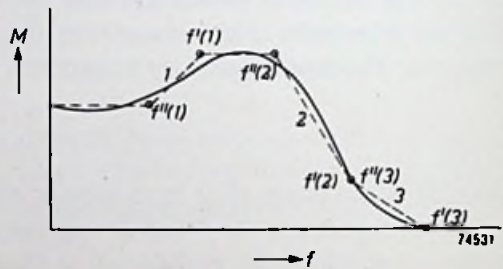


Fig. 20. Approximation of a modulation response curve by a number of straight line segments.

Example

In fig. 20 a modulation response curve is approximated by two horizontal and three inclined line segments, the latter being numbered from 1 to 3. Since the slope of segment 1 is positive, h_1 assumes a negative value.

The contribution of each of the segments towards the step function is determined by the three characteristic quantities: h , f' and f''/f' . These

3.4 Graphical determination of the step function

curves are represented by the function $S(f't')$, which has been plotted in fig. 21 with f''/f' as parameter.

The curves of fig. 21 are radial-symmetrical with respect to the point $f't' = 0$, $S(f't') = 0.5$ and are all derived from the curve for $f''/f' = 0$, which can be calculated with great accuracy by means of a series development (see Appendix III).

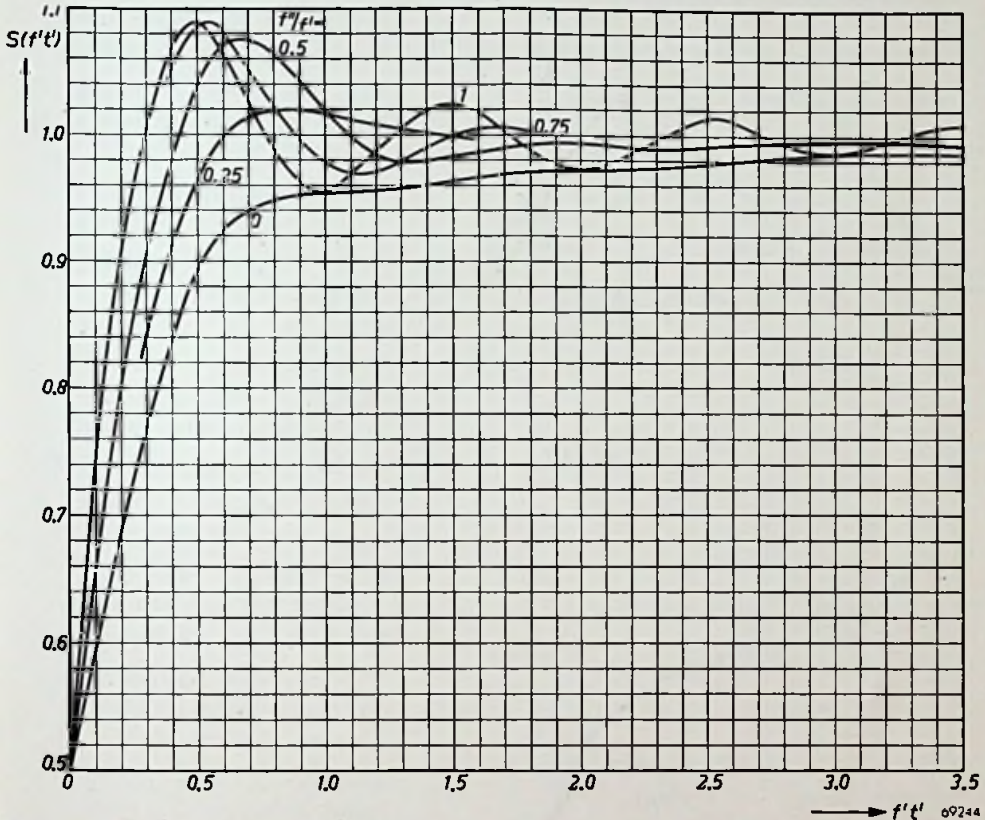


Fig. 21. Graphical representation of the function $S(f't')$ with f''/f' as parameter.

To determine the graphical representation of the step function corresponding to a given modulation response curve, it suffices to select the correct curves $S(f't')$ from the family of curves of fig. 21 (and to interpolate where necessary), after which these are redrawn on the correct scale and simply added.

This can be done, for example, by plotting for each segment a horizontal line at a distance h above the zero axis and marking the $f't'$ scale on this line. This is easily

done, since the time $t' = 1/f'$ corresponds to the point $f' t' = 1$ of fig. 21. At $t' = 0$ the curve passes through the point $0.5 h$, with respect to which it is radial-symmetrical. For negative values of t' the zero axis may therefore be imagined to correspond with the line $S(f' t') = 1$ of fig. 21, etc. The graphical construction becomes clearer when instead of the zero axis the line $S(f' t') = 0.5$ is taken as basis. See, by way of example, fig. 33.

In order to take the phase distortion into account it is necessary to

investigate the phase differences with respect to the originally assumed linear phase characteristic.

Now the modulation response can be considered as a complex quantity, the real part of which is equal to the cosine of the phase angle, and the imaginary part is equal to the sine of the phase angle. Consequently a real and an imaginary modulation response curve can be plotted (see fig. 22).

These curves are derived in the following way from the amplitude and phase characteristics. Assume that at the frequencies f_1 and f_2 , at equal distances Δf from the carrier, the amplitude and the phase angles are A_1 and A_2 and Θ_1 and Θ_2 respectively. (These are the remaining phase angles after the constant

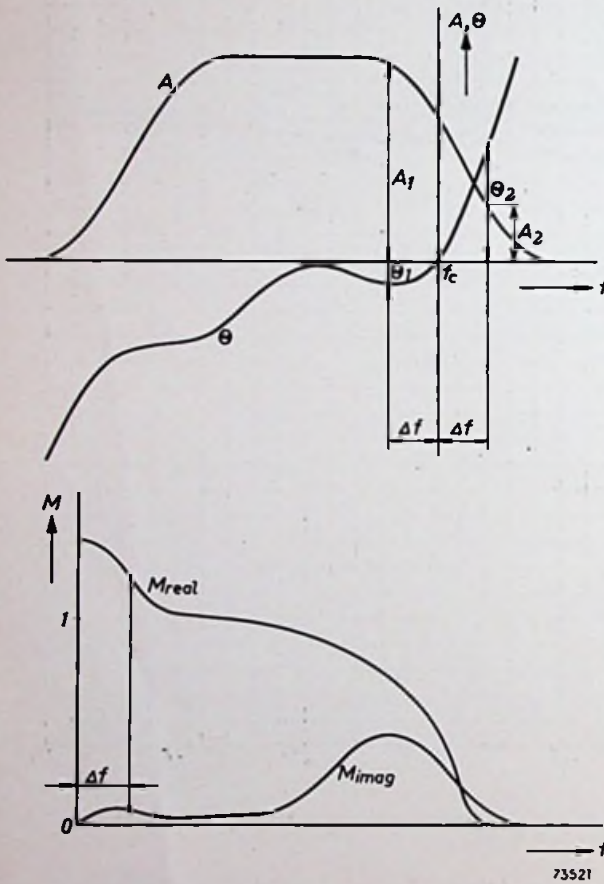


Fig. 22. Construction of the real and imaginary modulation response curves from the amplitude and phase characteristics.

delay has been subtracted.) For a modulation frequency Δf the real component of the modulation response is then:

$$M_{real} = A_1 \cos \Theta_1 + A_2 \cos \Theta_2, \tag{37}$$

3.4 Graphical determination of the step function

and the imaginary component is:

$$M_{\text{imag}} = -A_1 \sin \Theta_1 + A_2 \sin \Theta_2. \quad (38)$$

(The lower sideband should be taken for A_1 and the higher sideband for A_2 , the sign of the phase distortion being thereby given.)

Once the two modulation curves have been determined, these are again approximated by straight line segments as outlined above. Each inclined

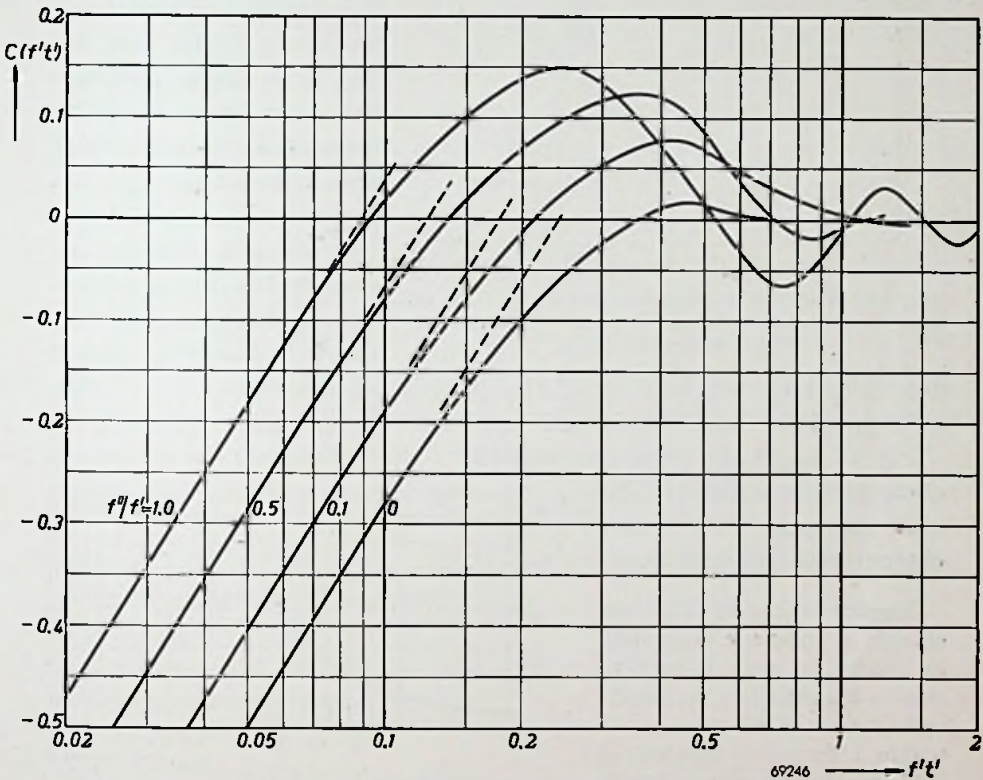


Fig. 23. Graphical representation of the function $C(f't')$ with f''/f' as parameter.

line segment of the real modulation response curve forms a contribution $S(f't')$ towards the step function, whilst each inclined segment of the imaginary modulation curve forms a contribution $C(f't')$.

The function $C(f't')$ has been plotted in fig. 23, again with f''/f' as parameter. This diagram is image-symmetrical with respect to the line $f't' = 0$. Since the curve logarithmically approaches $-\infty$ for $f't' = 0$, $f't'$ has been plotted on a logarithmic scale.

When no great accuracy is required, the $C(f''')$ diagram can be approximated by a broken line, the descending part of which has a slope of 0.72 per decade. The transitional point is situated between 0.09 and 0.25, depending on the ratio f''/f' . This procedure is followed in example 2 on p. 47.

If, in order to determine the phase distortion, the phase characteristic must be derived from the amplitude response curve (see footnote on

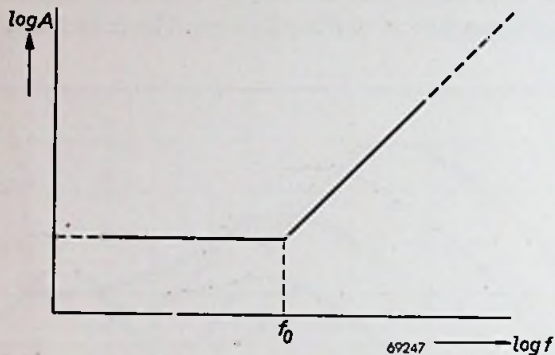


Fig. 24. Amplitude response curve plotted on logarithmic amplitude and frequency scales (semi-infinite unit slope).

page 23), the latter should preferably be plotted on logarithmic amplitude and frequency scales (see fig. 24), since the phase characteristic must be fairly accurate in the vicinity of the carrier frequency. This logarithmic amplitude characteristic can be approximated by a broken line, the shape of the phase characteristic then being

determined by the location of the transitional points and the change in slope of the line.

Fig. 25 shows the phase characteristic corresponding to the amplitude characteristic of fig. 24. The ascending part of the latter characteristic has unit slope.

Characteristics with a different change in slope are dealt with as follows. A slope is said to be of $+k$ units when the amplitude characteristic rises $2k$ db within a frequency interval of 1.25, which corresponds to $20k$ db per decade. The phase characteristic corresponding to a transitional point at which the slope changes k units is thus obtained by multiplying the vertical scale of fig. 25 by the factor k .

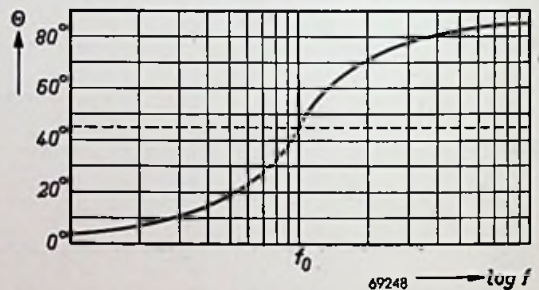


Fig. 25. Phase characteristic corresponding to the amplitude characteristic of fig. 24.

The phase characteristic of an amplitude characteristic approximated by line segments is now found by linearly adding the phase characteristics corresponding to each of the transitional points.

For accurate construction of the phase characteristic, the part of fig. 25 of greatest importance in practice has been redrawn on a linear

3.4 Graphical determination of the step function

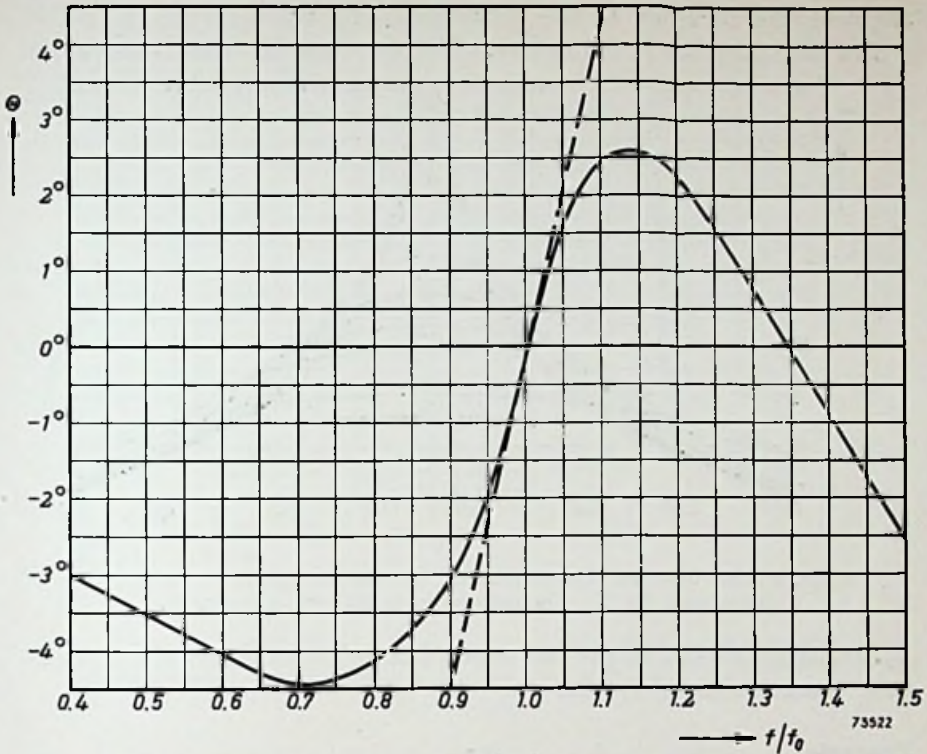


Fig. 26. Phase distortion with a semi-infinite unit slope plotted on a linear scale. The broken line shows the linear term.

scale in fig. 26. A linear term has been subtracted to give greater emphasis to the phase distortion.

A practical difficulty in determining the phase characteristic graphically lies in the fact that fairly small phase deviations sometimes correspond to the difference of two large opposed contributions originating from two adjacent opposed transitional points in the amplitude characteristic (see fig. 27).

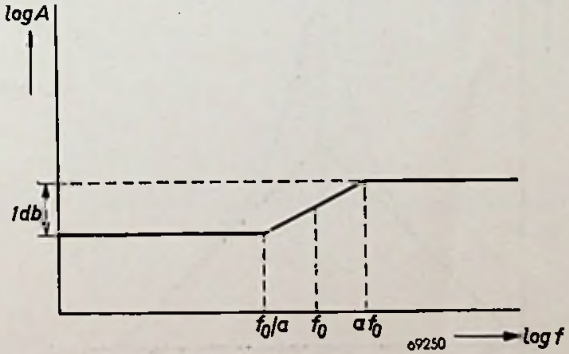


Fig. 27. Amplitude characteristic containing two adjacent opposed transitional points.

This will be the case, for example, when the amplitude characteristic has been very roughly approximated and attempts are made to

improve the accuracy of the construction by rounding off the curve. For such purposes it will be advantageous to use the phase diagram of

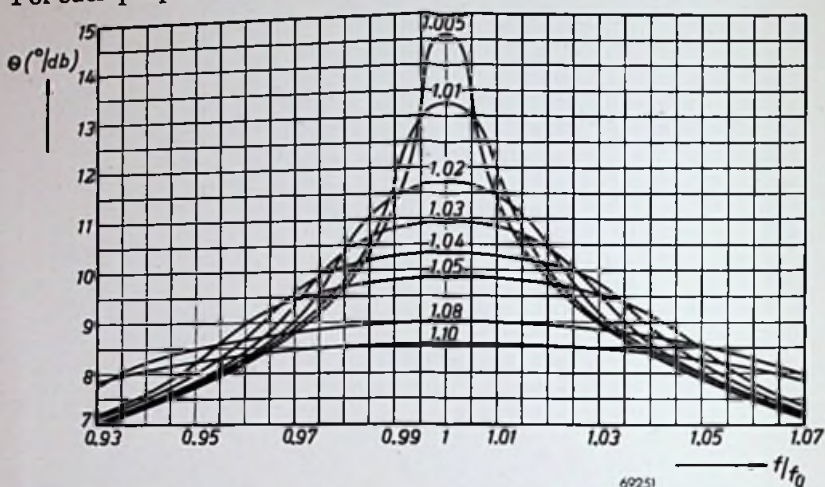


Fig. 28. Phase diagram corresponding to the amplitude characteristic depicted in fig. 27. The parameter is the term α in fig. 27.

fig. 28, corresponding to the two opposed transitional points of the amplitude characteristic of fig. 27.

Example

What will be the shape of the phase characteristic of a single resonant circuit according to the above method?

For large values of x :

$$\frac{d \log A}{d \log x} = 1,$$

in which

$$x = Q \left(\frac{\omega}{\omega_0} - \frac{\omega_0}{\omega} \right).$$

(See Appendix I)

Hence:

$$\frac{d \log A}{d \log \omega} = \frac{\omega_0}{\Delta \omega}.$$

In the case of a very large detuning:

$$\frac{\Delta \omega}{\omega_0} \rightarrow \pm 1,$$

whence

$$\frac{d \log A}{d \log \omega} \rightarrow \pm 1.$$

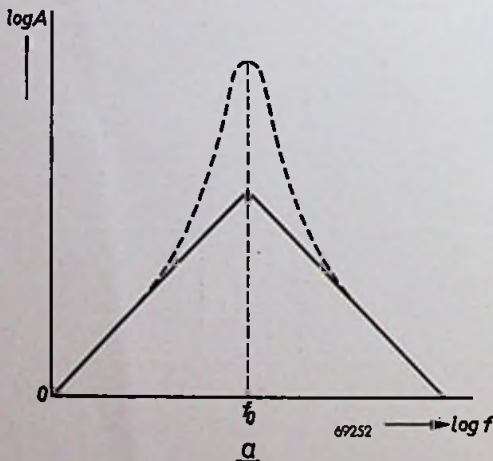


Fig. 29a. Rough approximation of the response curve of a single tuned circuit (fully drawn line). The actual response curve is indicated by the dotted line.

3.4 Graphical determination of the step function

Fig. 29b. The fully drawn line represents the phase characteristic corresponding to the approximated response curve of fig. 29a. The actual phase characteristic is indicated by the dotted line.

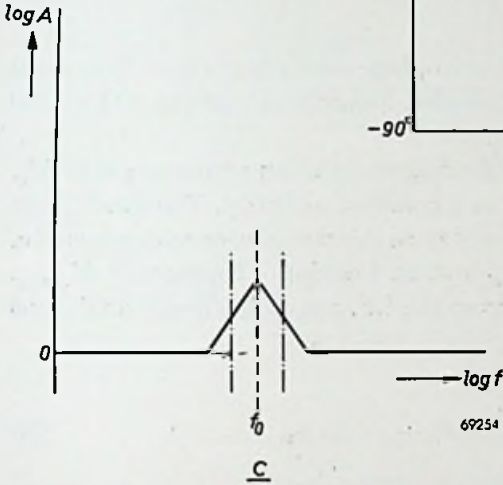
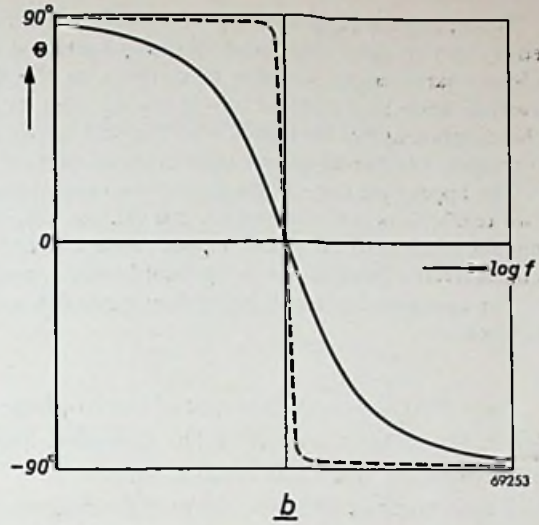


Fig. 29c. Representation of the corrections to be applied to the response curve shown in fig. 29a.

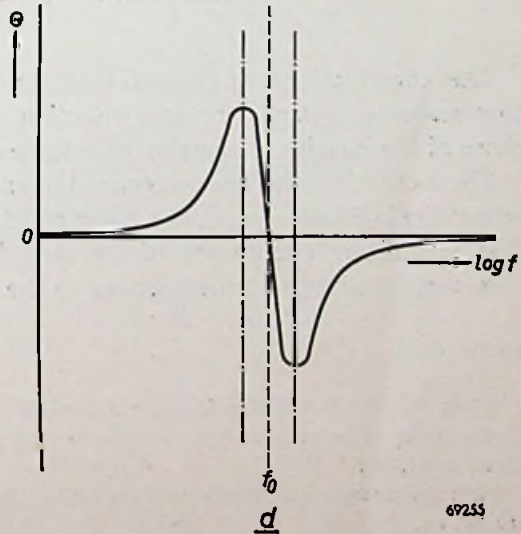


Fig. 29d. Phase characteristic corresponding to the corrections shown in fig. 29c.

When, as a first approximation, the response curve of the circuit is now represented by two straight lines, with slopes $+1$ and -1 (fully drawn lines, fig. 29a), the phase characteristic appears to conform to the diagram of fig. 25, provided its vertical scale is multiplied by -2 (see fig. 29b). In the case of very large detuning, this diagram agrees fairly well with the well-known arc tan function (see Appendix I) by which the actual phase characteristic (dotted line, fig. 29b) is given.

The approximation of the amplitude characteristic can be improved by adding two corrections indicated in fig. 29c (cf. fig. 27). A phase correction as shown in fig. 29d must then be added to the phase characteristic, so that the actual phase characteristic (broken line in fig. 29b) is very nearly approached.

The approximation can be further improved by increasing the number of these corrections.

Now that the contributions of the in-phase components have been dealt with, the determination of the so-called quadrature components of the step function will be investigated.

These components are derived from a modulation response curve M_q , which should also be considered as a complex quantity. The quadrature components can therefore be deduced from this modulation response curve, and are a real component $M_{q\text{real}}$ and an imaginary component $M_{q\text{imag}}$.

The derivation of these curves from the I.F. response curve is analogous to that of fig. 22, but now:

$$M_{q\text{real}} = A_1 \cos \Theta_1 - A_2 \cos \Theta_2, \quad (39)$$

and

$$M_{q\text{imag}} = A_1 \sin \Theta_1 + A_2 \sin \Theta_2. \quad (40)$$

The contributions of the real component of the quadrature modulation response towards the step function assume a form $jC(f't')$, whilst those of the imaginary component assume a form $jS(f't')$.

These contributions are determined in exactly the same way as described for the in-phase component, after which they are also linearly added. The quadrature component of the step function thus obtained must, however, be added in quadrature to the in-phase component.

Example 1

What shape does the step function assume at a voltage step from 1 to 2, applied to the input of an amplifier the amplitude and phase characteristics of which are given in fig. 30?

First the modulation response curves are determined for the in-phase component, see fig. 31.

3.4 Graphical determination of the step function

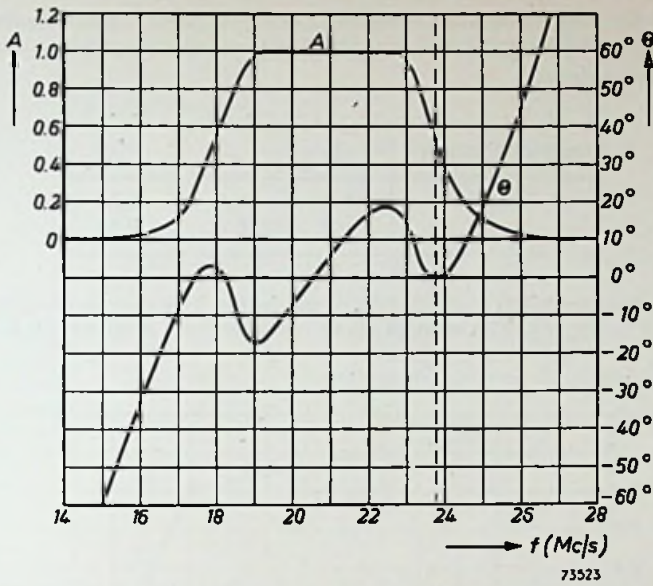


Fig. 30. Amplitude and phase characteristics of an amplifier the step function of which is to be determined. A linear term corresponding to a delay of $5 \mu\text{sec}$ has been subtracted from the phase response.

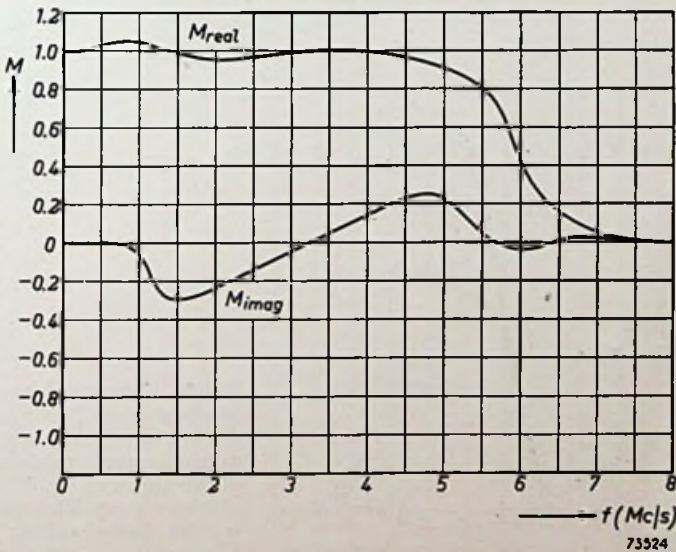


Fig. 31. Real and imaginary modulation response curves corresponding to the amplitude response curve of fig. 30.

In fig. 32 the real modulation response curve has been approximated by two inclined and two horizontal line segments. The inclined segments are characterised by the following data:

segment number	h	f'	f''/f'
1	0.2	5.5	0.55
2	0.8	6.5	0.85

The contributions $S(f't')_1$, and $S(f't')_2$ of the inclined line segments of fig. 32 have been plotted in fig. 33. The sum of these contributions is given by the dash-dot line S_{tot} .

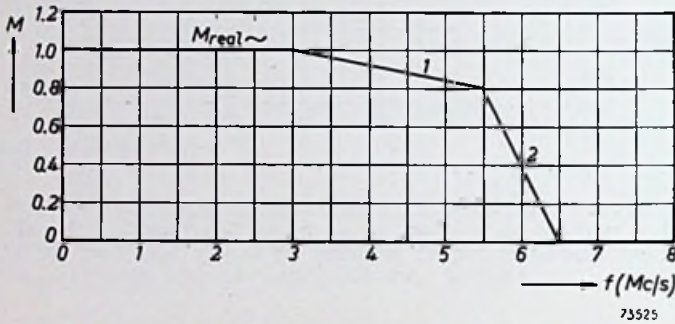


Fig. 32. Approximation of the real modulation response curve by straight line segments.

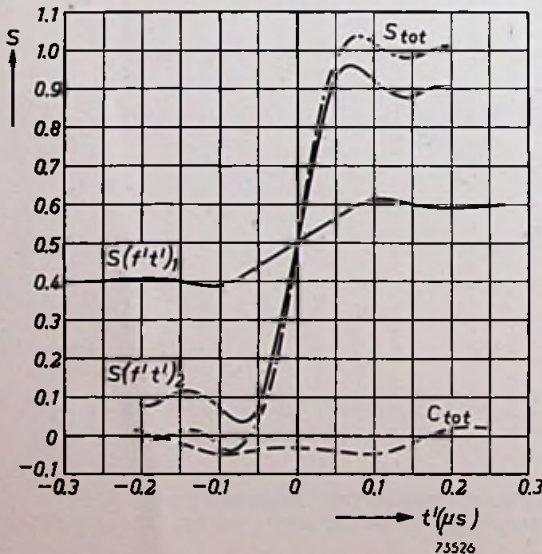


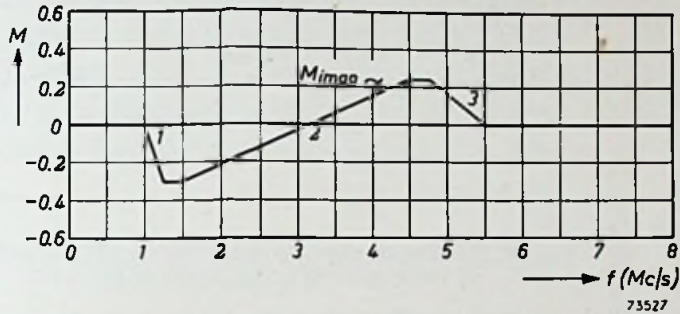
Fig. 33. Contributions of the real modulation response curve (fully drawn lines) derived from the approximated modulation response curve of fig. 32. The sum of these contributions is given by the dash-dot line S_{tot} . The broken line C_{tot} , representing the imaginary component, is derived in fig. 35.

3.4 Graphical determination of the step function

The approximated imaginary modulation response curve is given in fig. 34. This consists of three inclined line segments with the following data:

segment number	h	f'	f''/f'
1	+0.3	1.25	0.80
2	-0.55	4.5	0.33
3	+0.25	5.5	0.88

Fig. 34. Approximation of the imaginary modulation response curve by straight line segments.



The contributions to this imaginary component are plotted in fig. 35a, the sum of these contributions being given in fig. 35b.

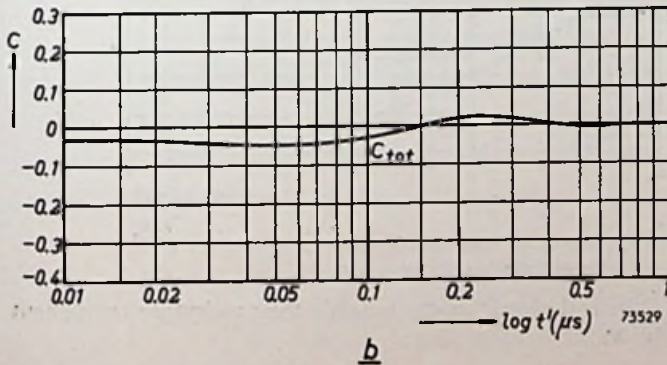
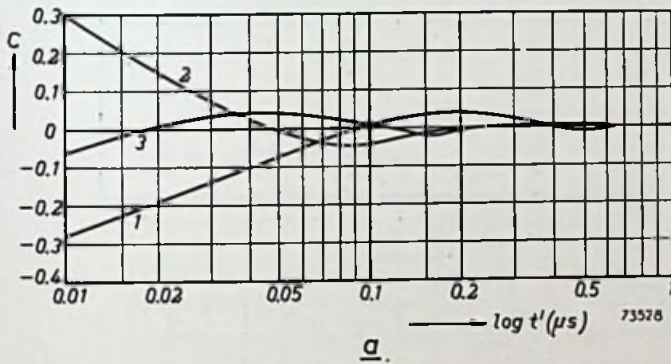


Fig. 35a. Contributions of the imaginary modulation response curve of fig. 34. The sum of the contributions $C(f't')_1$ to $C(f't')_3$ is plotted in b.

lope of the quadrature component of the signal is determined. The response characteristics serving for this purpose have been plotted

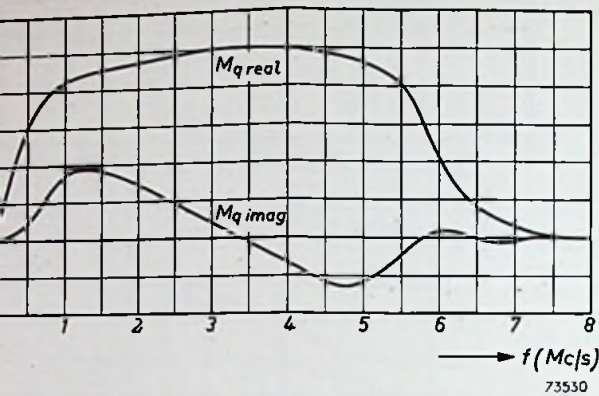


Fig. 36. Modulation response characteristics $M_{q \text{ real}}$ and $M_{q \text{ imag}}$ of the quadrature component of the signal.

These curves have been approximated in fig. 37. The inclined line segments are characterized by the following data:

Component	segment number	h	f'	f''/f'
Real	1	-0.8	0.8	0
	2	-0.2	2.5	0.32
	3	+1.0	7.0	0.85
Imaginary	1	-0.3	1.0	0
	2	+0.5	4.5	0.45
	3	-0.2	6.0	0.83

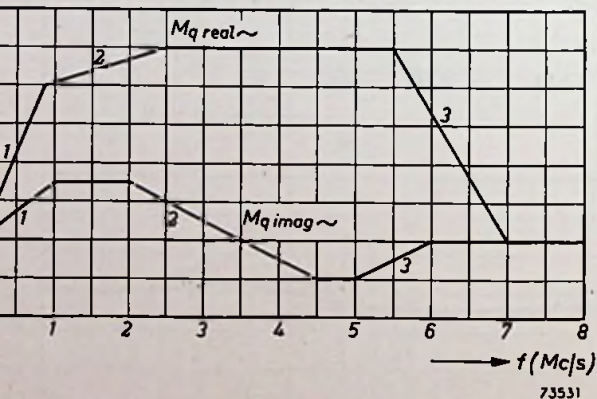


Fig. 37. Approximation of the quadrature components of the characteristics given in fig. 36.

The deviations of the real characteristic towards the quadrature component are shown in fig. 38.

3.4 Graphical determination of the step function

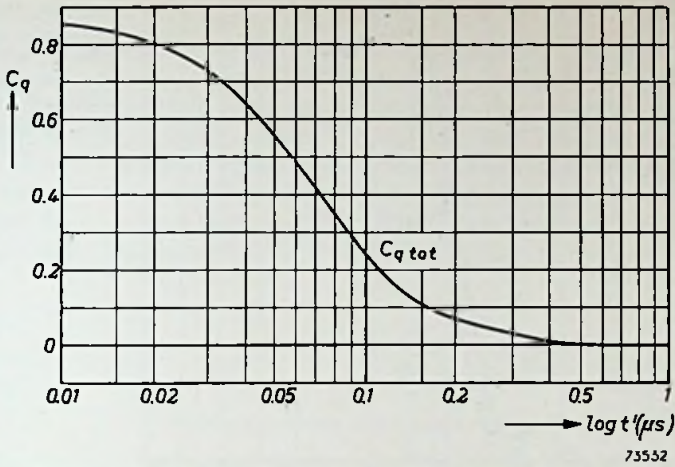


Fig. 38. Total contribution $C_{q \text{ tot}}$ of the real characteristic towards the quadrature component. The unit of the scale of the ordinate is $+j$.

In fig. 39 the contributions of the imaginary characteristic have been plotted. $S_q(f't')_1$ and $S_q(f't')_2$ are the contributions corresponding to the line sections 1 and 2 of the $M_{q \text{ imag}}$ characteristic of fig. 37. In fig. 39 the characteristic $C_{q \text{ tot}}$ of fig. 38 has been indicated by the broken line. The sum of this contribution and that of the two imaginary components is given by the dash-dot line $C_{q \text{ tot}} + S_{q \text{ tot}}$.

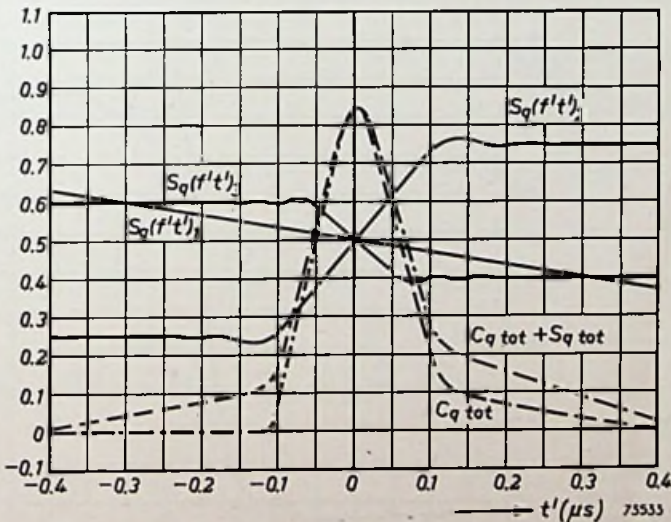


Fig. 39. $S_q(f't')_1$ and $S_q(f't')_2$ are the contributions of the imaginary characteristic, and $C_{q \text{ tot}}$ is that of the real characteristic of the quadrature component. The dash-dot line represents the sum of these contributions.

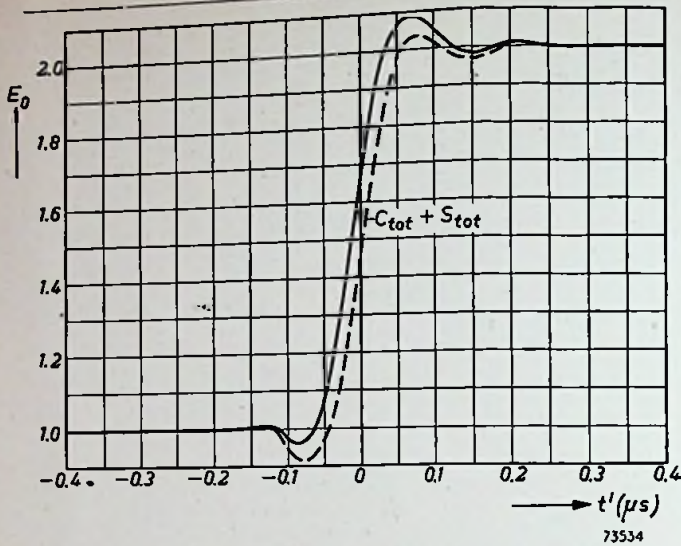


Fig. 40. Total contribution of the in-phase component (broken line) and ultimate step function (fully drawn line).

Fig. 40, finally, gives the in-phase component, i.e. the sum of the curves S_{tot} from fig. 33, C_{tot} from fig. 35 (which, for the sake of clarity, has been plotted also in fig. 33) and E_b/E_s . By adding in quadrature the contribution $C_{q\ tot} + S_{q\ tot}$ from fig. 39, the fully drawn curve representing the step function is obtained, viz.:

$$\sqrt{(C_{tot} + S_{tot})^2 + (C_{q\ tot} + S_{q\ tot})^2}.$$

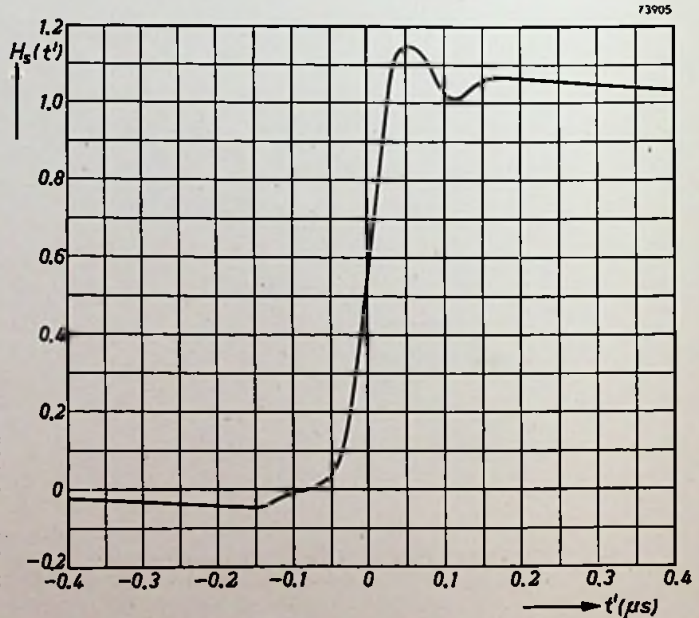


Fig. 41. In-phase component of the step function of example 1 such as would have been obtained if the irregularity at lower frequencies had not been ignored.

3.4 Graphical determination of the step function

Example 2

In example 1 the small irregularity at lower frequencies of the modulation response curve of fig. 31 was disregarded in the approximations of figs. 32 and 34. If this irregularity had been taken into account, then the in-phase component of the step function would have assumed the form depicted in fig. 41.

In this curve a variation appears to be present already at the instant $t' = -0.4 \mu\text{sec}$, i.e. before the voltage step was applied to the amplifier. This is, of course, inconsistent, since a circuit cannot possibly predict future signals. This error is due to inaccuracies of the phase characteristic in the vicinity of the carrier.

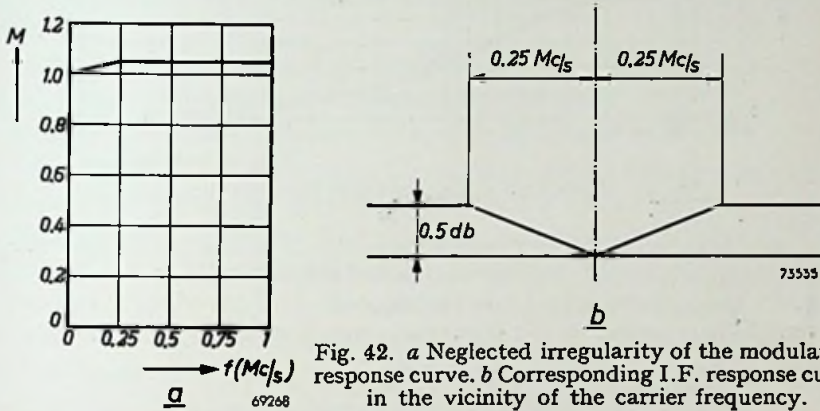


Fig. 42. *a* Neglected irregularity of the modulation response curve. *b* Corresponding I.F. response curve in the vicinity of the carrier frequency.

It will now be shown how the data required for correcting this error can be derived from the modulation response curve.

Assume for the sake of simplicity that double sideband reception takes place and that the modulation response curve has the shape as plotted in fig. 42*a*. The I.F. response curve in the vicinity of the carrier frequency will then be as depicted in fig. 42*b*.

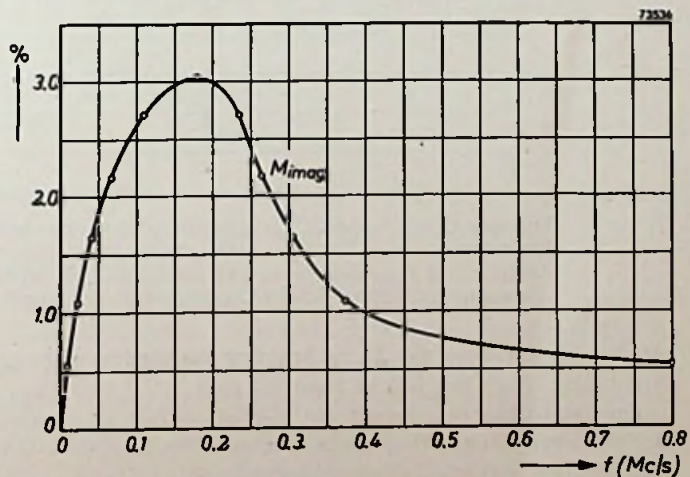


Fig. 43. Imaginary component of the correction in the modulation response.

From fig. 42 it can be derived directly that the small irregularity results in a contribution according to the fully drawn line S_{corr} in fig. 45 being added to the real component.

From fig. 42b it also follows that in the range near the carrier a phase distortion occurs as depicted in fig. 29d, but of opposed sign, so that the imaginary component of the irregularity will assume the shape as drawn in fig. 43.

The contribution C_{corr} of the in-phase component of the imaginary modulation response curve has been plotted in fig. 44 on a logarithmic scale.

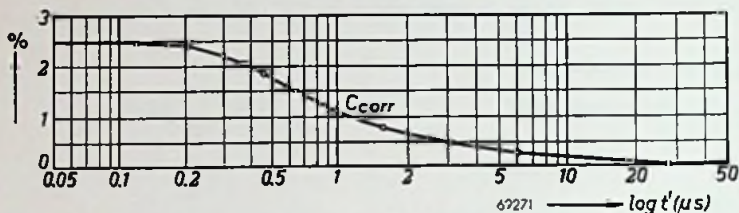


Fig. 44. Contribution C_{corr} towards the step function.

Fig. 45, finally, gives the total contribution $C_{\text{corr}} + S_{\text{corr}}$ of the in-phase component of the imaginary and the real modulation response curve towards the step function, caused by the irregularity investigated.

As was to be expected for $t' < 0$, the curve runs horizontally. The part for $t' > 0$

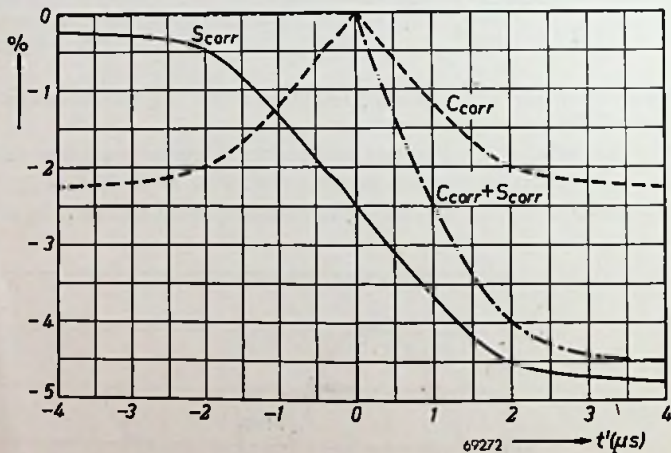


Fig. 45. Contribution C_{corr} drawn on the same scale as the contribution S_{corr} of the real modulation response curve towards the step function. The dash-dot line represents the total contribution $C_{\text{corr}} + S_{\text{corr}}$ towards the step function.

can be derived from fig. 21 by doubling the vertical scale, so that this covers the range from 0 to 1 instead of from 0.5 to 1.

The quadrature component can be dealt with in an analogous way, but in practice the corrections of this component will have less effect on the final form of the step function, so that they may be neglected.

4 GAIN, BANDWIDTH AND DISTORTION WITH FOUR-TERMINAL COUPLING NETWORKS

In the previous Sections the interstage couplings were assumed to consist of normal parallel tuned circuits, where necessary shunted by resistors, and the assumption was always made that for two successive stages the output voltage of the first stage is equal to the input voltage of the following stage. This will as a rule no longer be the case, however, if the coupling between the stages consists of more complex four-terminal networks.

The previous comments can, however, be extended to such networks by introducing the concept of **transfer admittance**. Whereas the admittance of a two-terminal network is understood to be the current divided by the voltage at the same pair of terminals, the no-load transfer admittance of a four-terminal network is here taken to be the current at the input terminals divided by the voltage at the unloaded output terminals. (The concept of **transfer impedance** can be defined in a similar way.)

Assuming again that the feedback in the valve is negligible and considering the input valve as a current source $V_i \cdot S_{\text{eff}}$, shunted by its internal resistance r_a and its anode admittance $g_o + j\omega C_o$, then it is obvious that the gain of stage h can be written as:

$$G_h = \frac{(V_i)_{h+1}}{(V_i)_h} = \frac{(I_o)_h}{Y_{h,h+1}} \cdot \frac{1}{(V_i)_h} = \frac{S_{\text{eff}}}{Y_{h,h+1}} \quad (41)$$

where $Y_{h,h+1}$ represents the transfer admittance I_i/V_o of the coupling network between the stages h and $h + 1$, including at the input side the admittance:

$$\frac{1}{r_a} + g_o + j\omega C_o,$$

and at the output side the admittance:

$$g_i + j\omega C_i.$$

For the interstage couplings now to be dealt with, it thus suffices to substitute $Y_{h,h+1}$ for Y . This having been done, the calculations can be worked out in an analogous way.

Two examples of a four-terminal coupling network, namely a so-called "π" network and a double-tuned band-pass filter, are discussed below.

The "π" network (fig. 46) is equivalent to a normal single-tuned circuit the input and output of which are "tapped", as a result of which the total circuit capacitance is reduced, since the capacitances C_o and C_i are no longer in parallel as in a single-tuned circuit. For a given frequency the

required inductance of the circuit is therefore higher. This may be an advantage at very high frequencies, since with very small values of inductance it is not easy to obtain a satisfactory quality factor.

As the voltages across C_o and C_i are in anti-phase, there will be a point in the coil L which is at zero H.F. potential. This point may be used either as the point at which the supply voltage is fed to the valves, or for interconnection by means of a screened lead with similar distant points in the receiver.

The double-tuned band-pass filter (fig. 47) differs essentially from the single-tuned circuit. It resembles a staggered pair. C_o and C_i are now parts of separate circuits, and a higher product $G \cdot B$ is obtained. The response curve has steeper flanks and is flatter, whilst the unit function response curve has a higher slope and overshoot. When more stages are connected in cascade the decrease in bandwidth is less than with single tuned circuits. This decrease can also be compensated by staggering. In this case, however, the circuits are not detuned but merely unequally damped.

4.1 "π" NETWORK

The transfer admittance of the "π" network in fig. 46, which is widely used where the layout of the amplifier makes long wiring inevitable and a small circuit capacitance is nevertheless desirable ¹⁾, may be determined as follows:

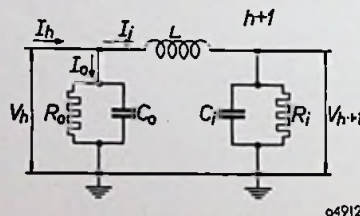


Fig. 46. Interstage coupling consisting of a "π" network.

$$Y_{h,h+1} = \frac{I_h}{V_{h+1}} \quad (42)$$

Furthermore:

$$I_i = \left(\frac{1}{R_i} + j\omega C_i \right) V_{h+1}, \quad (43)$$

and

$$I_o = \left(\frac{1}{R_o} + j\omega C_o \right) V_h. \quad (44)$$

¹⁾ Cf. A. van Weel, An Experimental Transmitter for Ultra-Short-Wave Radio-Telephony with Frequency Modulation, Philips Techn. Review 8, p. 121, 1946 (No. 4), in particular figs 4 and 5.

Moreover:

$$V_h = V_{h+1} + I_i j\omega L. \quad (45)$$

From eqs (45) and (43):

$$V_h = V_{h+1} + \left(\frac{1}{R_i} + j\omega C_i \right) V_{h+1} j\omega L, \quad (46)$$

and from eqs (46) and (44):

$$I_o = \left(\frac{1}{R_o} + j\omega C_o \right) \left\{ V_{h+1} + \left(\frac{1}{R_i} + j\omega C_i \right) V_{h+1} j\omega L \right\}. \quad (47)$$

Since $I_h = I_i + I_o$, eq. (42) finally becomes:

$$Y_{h,h+1} = \frac{1}{R_o} + \frac{1}{R_i} - \omega^2 L \left(\frac{C_o}{R_i} + \frac{C_i}{R_o} \right) + j\omega C_o + j\omega C_i + j\omega \frac{L}{R_o R_i} - j\omega^3 L C_o C_i. \quad (48)$$

At resonance the imaginary part of eq. (48) is zero, which gives:

$$C_o + C_i + \frac{L}{R_o R_i} = \omega^2 L C_o C_i,$$

whence:

$$\omega^2 = \frac{1}{L} \left(\frac{1}{C_o} + \frac{1}{C_i} \right) + \frac{1}{C_o R_o C_i R_i}. \quad (49)$$

A simplification can be introduced by making the following approximation:

$$\omega_o^2 = \frac{1}{L} \left(\frac{1}{C_o} + \frac{1}{C_i} \right). \quad (50)$$

At or near resonance the real part of $Y_{h,h+1}$ is therefore approximately:

$$\left(Y_{h,h+1} \right)_{\text{real}} = \frac{1}{R_o} + \frac{1}{R_i} - \left(\frac{1}{C_o} + \frac{1}{C_i} \right) \left(\frac{C_o}{R_i} + \frac{C_i}{R_o} \right) = - \left(\frac{C_o}{R_i C_i} + \frac{C_i}{R_o C_o} \right). \quad (51)$$

The negative sign, which is of no consequence here, will henceforth be omitted.

To determine the bandwidth the imaginary part at $\omega \neq \omega_o$ must be calculated:

$$\left(Y_{h,h+1} \right)_{\text{imaginary}} = \omega \left\{ (C_i + C_o) + \frac{L}{R_i R_o} - \frac{\omega^2}{\omega_o^2} (C_i + C_o) \right\},$$

or, if $L/R_i R_o$ is ignored and $\omega(\omega + \omega_o)/\omega_o^2$ is set equal to 2,

$$\left(Y_{h,h+1} \right)_{\text{imaginary}} = 2 \Delta\omega (C_i + C_o), \quad (52)$$

provided $\Delta\omega/\omega_o$ is small. (It should be noted that for very low frequencies the transfer admittance does not assume the very high value which might

be expected from this approximated formula.) To determine the frequency at which the attenuation is 3 db, the imaginary part must be set equal to the real part, that is to say:

$$2\Delta\omega (C_i + C_o) = \frac{C_o}{R_i C_i} + \frac{C_i}{R_o C_o} \quad (53)$$

This expression may be adapted to the previous comments by writing:

$$\frac{1}{R_i} = g_i + g_{ci} \quad (54)$$

and

$$\frac{1}{R_o} = g_o + g_{co} \quad (55)$$

where $g_o + g_{co}$ is assumed to include $1/r_a$ of the valve. Hence:

$$2\pi B(C_i + C_o) = (g_i + g_{ci}) \cdot \frac{C_o}{C_i} + (g_o + g_{co}) \cdot \frac{C_i}{C_o} \quad (56)$$

This equation thus replaces eq. (6). The gain per stage now follows from:

$$G = \frac{S}{Y_{h,h+1}} = \frac{S}{(g_i + g_{ci}) \cdot \frac{C_o}{C_i} + (g_o + g_{co}) \cdot \frac{C_i}{C_o}} \quad (57)$$

Combining eqs (57) and (56) again gives:

$$(GB) = \frac{S}{2\pi (C_i + C_o)} \quad (8)$$

The further procedure is similar to that given in Sections 1 and 2, provided $g_i + g_o$ is replaced by:

$$g_i \cdot \frac{C_o}{C_i} + g_o \cdot \frac{C_i}{C_o}$$

This means that f_1 and f_0 must be replaced by:

$$f_1'' = \gamma_2 f_1 \quad (58)$$

and

$$f_0'' = \gamma_2 f_0 \quad (59)$$

in which:

$$\gamma_2 = \sqrt{\frac{g_i}{g_i + g_o} \cdot \frac{C_o}{C_i} + \frac{g_o}{g_i + g_o} \cdot \frac{C_i}{C_o}} \approx \sqrt{\frac{C_o}{C_i}} \approx 1, \quad (60)$$

since $g_i \gg g_o$.

In practice f_1'' may be set equal to f_1 . The quantities F_s , F_B and F_x remain unchanged, so that the theory of the previous sections also applies to amplifiers where the interstage coupling is formed by the "π" network of fig. 46.

4.2 DOUBLE-TUNED BAND-PASS FILTERS

The transadmittance of double-tuned band-pass filters (fig. 47) can be determined with sufficient accuracy by means of the existing theory on band-pass filters with a high quality factor ¹⁾.

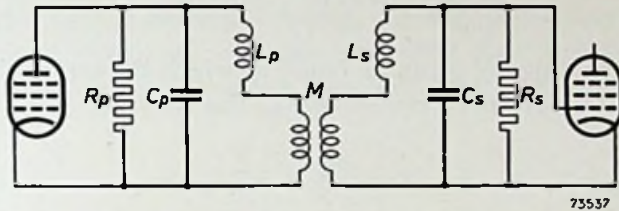


Fig. 47. Interstage coupling consisting of a double-tuned band-pass filter. In a practical circuit:

$$\begin{aligned} 1/R_p &= g_o + g_{cp} = 1/r_a + g_a + 1/R_{cp} & C_p &= C_o + C_{xp} \\ 1/R_s &= g_i + g_{cs} = g_i + 1/R_{cs} & C_s &= C_i + C_{xs} \end{aligned}$$

A more accurate theory will not be required unless the resonances of the circuit, the coupling factor, etc., are to be calculated exactly. This theory (see Appendix I) leads to the following expression:

$$Y_{h,h+1} = \frac{(1 + q^2) + jx \sqrt{2 + r + \frac{1}{r}} + (jx)^2}{jq \sqrt{R_p R_s}} \quad (61)$$

where:

$$\begin{aligned} Q_p &= \omega C_p R_p, & x &= \beta \sqrt{Q_p Q_s}, \\ Q_s &= \omega C_s R_s, & \beta &= 2 \Delta \omega / \omega_o. \end{aligned}$$

and

$$k = \frac{M}{\sqrt{L_p L_s}} \left(\text{or in the case of capacitive coupling } \frac{Ck}{\sqrt{C_p C_s}} \right),$$

while

$$r = Q_s / Q_p.$$

It can be shown that under certain conditions the frequency response given by eq. (61) corresponds to the curve $s = 2$ of fig. 9.

At resonance ($x = 0$):

$$\left(Y_{h,h+1} \right)_{\text{imaginary}} = \frac{1 + q^2}{q} \cdot \sqrt{(g_i + g_{cs})(g_o + g_{cp})} \quad (62)$$

¹⁾ See i.a. B. G. Dammers, J. Haantjes, J. Otte and H. van Suchtelen, Application of the Electronic Valve, Book IV, Philips Technical Library (1950) and C. B. Aiken, Two Mesh-Tuned Coupled Circuit Filters, Proc. I.R.E. 25, 1937 (No. 2).

from which, by means of eq. (41), the gain per stage is:

$$G = \frac{S}{\sqrt{(g_i + g_{cs})(g_o + g_{cp})}} \cdot \frac{q}{1 + q^2} \quad (63)$$

By setting:

$$\frac{dZ_{h,h+1}}{dx} = \frac{d^2Z_{h,h+1}}{dx^2} = \frac{d^3Z_{h,h+1}}{dx^3} = 0,$$

at $x = 0$, the value of q can be found at which the top of the response curve is flattest. It can be proved that at this condition (see Appendix I):

$$q = \sqrt{\frac{r + \frac{1}{r}}{2}} \quad (64)$$

If this condition is satisfied, so-called transitional coupling is obtained. In that case the frequency response corresponds to that shown in fig. 9, $s = 2$, and:

$$4\pi B\sqrt{C_o C_i} = 2\sqrt{1 + q^2}\sqrt{(g_i + g_{cs})(g_o + g_{cp})} \quad (65)$$

The maximum product of gain and bandwidth achievable by minimizing the capacitances may now be expressed by:

$$G \cdot B = \frac{S}{4\pi\sqrt{C_o C_i}} \cdot \frac{2q}{\sqrt{1 + q^2}} \quad (66)$$

This expression will be so interpreted that the first factor is considered as the (GB) product in the case where the coupling consists of a band-pass filter, and the second factor as the bandwidth factor in that case. This (GB) product is thus:

$$(GB)^n = \frac{S}{4\pi\sqrt{C_o C_i}} \quad (67)$$

This $(GB)^n$ product is identical to that given in Section 1, provided $C_i = C_o$. In practice these capacitances do not differ greatly, so that, in this case too, the theory of Section 1 remains valid to all intents and purposes. The stray capacitances can of course also be taken into account, giving:

$$Fx^n(GB)^n = \frac{S}{4\pi\sqrt{(C_i + C_{2s})(C_o + C_{xp})}}$$

where C_{ix} = the stray capacitance across the secondary and C_{ox} = the stray capacitance across the primary.

Hence:

$$Fx^n = \sqrt{\frac{C_i}{C_i + C_{2s}} \cdot \frac{C_o}{C_o + C_{xp}}} \quad (68)$$

4.2 Double-tuned band-pass filters

As indicated above, and in Section 2, the second factor of eq. (66):

$$\frac{2q}{\sqrt{1+q^2}} = \frac{2\sqrt{1+r^2}}{1+r} \quad (69)$$

represents the bandwidth factor F_B'' for one stage.

If several stages in cascade are used, the bandwidth decreases as the number of stages increases, as is the case when the coupling consists of synchronous parallel tuned circuits. This is demonstrated by the following expression:

$$F_B'' = \frac{2\sqrt{1+r^2}}{1+r} \cdot \sqrt[2^{1/i}]{1} \quad (70)$$

The second term of eq. (70) can very well be approximated by $1.1^{1/i}$; the first factor F_{B1}'' is represented by the curve of fig. 48.

There are obviously two extreme cases, viz.:

(1) $r = 1$, i.e. $Q_p = Q_s$; in that case $q = 1$, the coupling being critical. F_B is then equal to $\sqrt{2}$. With valves of which $C_i \approx C_o$ it is thus possible to improve the gain by 3 db by using a band-pass filter instead of a single tuned circuit. This obviously applies to one amplifying stage only.

(2) $r = 0$, i.e. $Q_p = \infty$. In that case the bandpass filter is damped at one side only, and the gain, compared with a single tuned circuit, may be increased by a factor as high as 2.

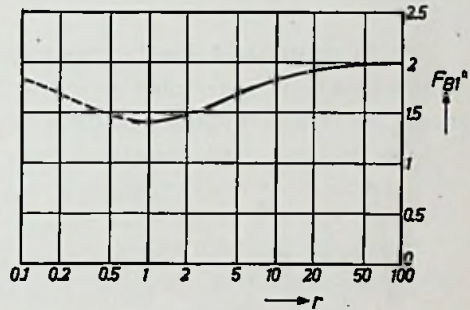


Fig. 48. Graph representing the first term of eq. (70).

The decrease of the bandwidth when synchronous band-pass filters are connected in cascade is similar to that of flat-staggered pairs connected in cascade, as is shown by a comparison of eqs (70) and (30). This decrease can be counteracted by applying so-called **staggered damping**, which has some resemblance to staggered tuning with single circuits.

This method is based on the change to which the response curve of a band-pass filter is subject when the dampings of the individual circuits are changed. Band-pass filters, one side of which is intentionally damped are used, and the well-known curves applying to symmetrical band-pass

filters no longer apply unless the values of Q are corrected¹⁾. The results are shown in figs 49 and 50, fig. 49 applying when k is varied, Q being constant, while fig. 50 shows the result when Q is varied and k is kept constant.

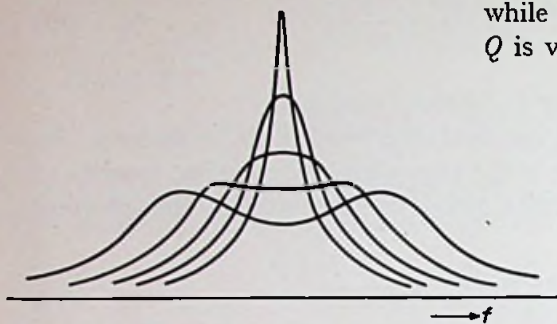


Fig. 49. Response curves of a band-pass filter one side of which is damped, with k as parameter ($Q = \text{constant}$).

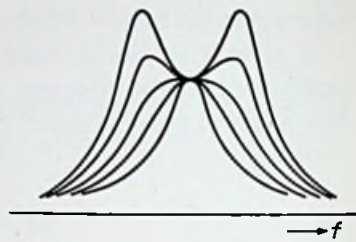


Fig. 50. Response curves of a band-pass filter one side of which is damped, with Q as parameter ($k = \text{constant}$).

Fig. 51 shows how the flat response curve is obtained from the over-coupled and under-coupled response curves. This example applies to an unequally damped band-pass filter triplet.

As in the case of the staggered tuning system, there is also a method for ensuring that staggered band-pass filters have the flattest response curve attainable. It is beyond the scope of this book to show how this method is derived, but it is applied in the following way (see fig. 52).

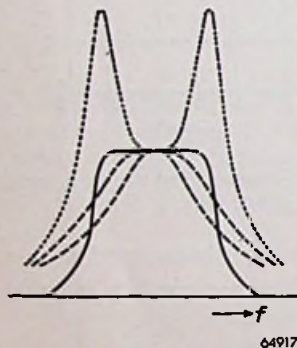


Fig. 51. Diagram showing how a flat response curve (full line) is obtained from over-coupled and under-coupled response curves (dotted and broken lines).

of the limiting radii. The lengths of these perpendiculars represent the values of g of the various circuits when the radius is equal to g_r . These values correspond to $g_i + g_{cs}$, the conductance of the band-pass filter

The values of g for the secondaries are again deduced from the value of g_r of the reference circuit, having a capacitance $C_r = 2 C_s$, in a similar way as was done for staggered tuning. A quarter arc of circle is subdivided

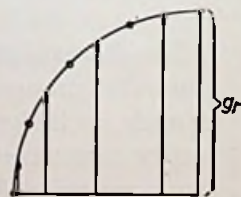


Fig. 52. Diagram for staggering band-pass filters.

¹⁾ Cf. p. 36 and p. 41 *et seq.* of the first reference quoted on p. 53.

4.2 Double tuned band-pass filters

secondary being denoted by g_{cs} (the primary conductance g_o being assumed to be zero).

The resulting bandwidth is now equal to that of the reference circuit given by:

$$2\pi B_r C_r = g_r, \quad (71)$$

provided the coupling of each of the band-pass filters is adjusted to the correct value. This will be the case when:

$$k = \frac{1}{Q_r} = \frac{g_r}{\omega_0 C_r}. \quad (72)$$

Under these conditions the gain per stage follows from the value of $|Y_{h,h-1}|$ at resonance, viz. (see Appendix Id):

$$|\hat{Y}_{h,h+1}| = 2\pi / k \sqrt{C_s C_p},$$

giving:

$$G = \frac{S}{g_r} \cdot 2 \sqrt{\frac{C_s}{C_p}} = \frac{S}{2\pi B_r \sqrt{C_s C_p}},$$

at $\Delta f = 0$, and since the bandwidth B is equal to B_r :

$$G \cdot B = F_x'' F_B'' (GB)'' = \frac{S}{2\pi \sqrt{C_s C_p}}. \quad (73)$$

Substitution of $(GB)''$ from eq. (67) now shows that for an amplifier with double tuned coupling circuits the secondaries of which are stagger-damped, F_B'' is always equal to 2.

The response curve of a set of flat staggered band-pass filters can again be derived from fig. 9, where s is the total number of tuned circuits. Since each band-pass filter comprises two tuned circuits, s is in general an even number. It is, however, possible to make a combination of stagger-damped band-pass filters with one single "fill-up" circuit, which is tuned to the central frequency. In this way overall response curves can be obtained which correspond to the odd values of s in fig. 9.

As in the case where single circuits are used, the number of elements of the staggered group should not be made too large; as a rule groups consisting of pairs or triplets are used. If such groups are connected in cascade, the total bandwidth decreases only very slightly (see Table 4, p. 172). This is due to the response curves of staggered band-pass filter groups having very sharp corners. As may be expected, the overshoot percentage is quite considerable (see Table 3, p. 172).

The possibilities of staggering are restricted also in the case of band-pass filters, owing to the limit imposed on the most selective secondary circuit

(only the secondaries of the band-pass filters are damped, R_z thus being much smaller than R_p). The following condition must be satisfied:

$$B_{\text{tot}} \sin \alpha \geq F B^n F x^n (GB)^n \left(\frac{l}{l_1}\right)^2 \sqrt{\frac{C_o + C_{oz}}{C_i + C_{iz}}} \quad (74)$$

With amplifiers having single tuned interstage circuits the quantity f_1 was determined by the sum of $g_i + g_o$. When band-pass filters are used g_i and g_o are separated by the band-pass filter, but since in practice g_i is much larger than g_o , so that $g_i + g_o$ is almost equal to g_i , there is no need to introduce here a new quantity f_1'' .

If a band-pass filter is used at the input of the amplifier the quality factors of the primary and secondary are made identical, which means that $r = 1$, so that this band-pass filter cannot very well be included in the staggering scheme. There are also other reasons for making the first band-pass filter less selective than the other circuits, especially in superheterodynes intended for reception of several channels. Moreover, by not including the input circuit in the staggering scheme, this circuit can be chosen to meet specific requirements. For example, the input circuit must also satisfy special conditions as to reflection-free termination of the aerial cable.

The selectivity of the input circuit is already reduced by the heavy damping caused by the valve and aerial. To ensure that the termination of the aerial cable is such that no reflections occur, the following condition must be satisfied:

$$R_{\text{ant}} = Z_i = 2Z_i', \quad (75)$$

where Z_i is the input impedance of the band-pass filter (at the resonant frequency) with the aerial disconnected and Z_i' is the input impedance when the aerial is connected.

Now

$$Z_i' = \frac{R_p}{1 + q'^2} + \frac{R_{\text{ant}}}{R_p + R_{\text{ant}}}$$

where $q'^2 = k^2 Q_p Q_s$ in the case of a connected aerial.

Hence, the condition to be satisfied becomes:

$$q'^2 = \frac{R_p - R_{\text{ant}}}{R_p + R_{\text{ant}}} \quad (76)$$

In the important case in which R_p is very high, q' should be made approximately equal to unity.

By means of the formulae for band-pass filters it can be calculated that (for $C_x = 0$) the product $G \cdot \sqrt{B}$ of the aerial circuit is then approximately 1.2 times that of a single-tuned aerial circuit.

A further advantage of this circuit compared to the single circuit is that less trouble is experienced from reflections at the sideband frequencies.

5 NOISE

5.1 DEFINITIONS

The signal-to-noise ratio at the output of a receiver is of considerable importance. This ratio is determined by the signal-to-noise ratio of the signal source and by the inherent noise of the amplifier. Different effects must therefore be combined for calculating the final signal-to-noise ratio. Noise voltages cannot, however, be simply added and it is the mean squares of the noise voltages or the noise powers in one and the same resistance which are additive. It is therefore useful to express signal-to-noise ratios not as ratios of signal and noise voltages but as ratios of powers, the more so as the essential problem in most amplifiers for metric waves is power gain.

Basing the considerations on these lines it is logical to introduce the concept of available power, i.e. the power obtainable from the source concerned at optimum matching. For a signal source with a no-load signal voltage E_s and an internal resistance R_s this power is:

$$P_s = \frac{E_s^2}{4R_s}$$

Similarly, the available noise power of the signal source is:

$$P_n = \frac{\overline{E_n^2}}{4R_s}$$

the noise voltage $\overline{E_n^2}$ is defined with greater accuracy later. It is obvious that no purpose is served by considering noise outside the pass-band of the amplifier.

The signal-to-noise ratio at the input of an amplifier is now taken to be P_{si}/P_{ni} , whether the amplifier is correctly matched to the signal source or not. This ratio obviously is a characteristic of the signal source.

The available powers of the signal and noise at the output of an amplifier are denoted by P_{so} and P_{no} respectively, and at a given matching between signal source and amplifier the signal-to-noise ratio is P_{so}/P_{no} . At this matching the noise factor N is by definition:

$$N = \frac{P_{si}/P_{ni}}{P_{so}/P_{no}} \quad (77)$$

The noise factor N thus indicates to what extent the signal-to-noise ratio

deteriorates when the signal passes through the amplifier ¹⁾. N is not a characteristic of the amplifier considered but of the amplifier with the signal source to which it is to be connected. Eq. (77) gives a somewhat different impression if it is written:

$$N = \frac{P_{no}}{P_{ni} \cdot \frac{P_{so}}{P_{si}}} = \frac{P_{no}}{P_{ni} \cdot (G_P)_s} \quad (77a)$$

In eq. (77a) the numerator represents the total available output noise, i.e. the sum of the noises originating from the signal source and the amplifier under the given conditions. The denominator represents the available input noise P_{ni} multiplied in the same ratio as the signal power P_{si} . In the third member of eq. (77a) this gain is denoted by $(G_P)_s$, the "available power gain". If no additional noise were introduced by the amplifier the denominator would obviously be identical to the available output noise. The noise factor N considered in this way thus represents the ratio, at the output, of the total noise from the signal source and amplifier to the noise originating from the signal source alone. This and the former definition are obviously concordant and each has its merit.

The last definition clearly shows that the signal strength has no influence on the noise factor, a fact which might not be expected so readily from eq. (77). Eq. (77a) moreover shows that the noise from the signal source on the other hand largely influences the noise factor — in other words, it again stresses the fact that the noise factor applies to the combination of amplifier, signal source and their interconnection. Therefore, when quoting a value of N *per se*, this is obviously based on the conditions of source and matching identical to those under which the amplifier will be used.

As far as the signal source is concerned, only the noise power appears to affect N , so that this source could be characterized by its internal resistance R_s . It should be recognized that the same resistance R_s has a different noise power P_{ni} at different temperatures. In quoting a value for N it is often customary to assume R_s to be at room temperature, for which the value of 288 °K is preferably employed, round figures then being obtained when a diode is used as a source of noise. Under this condition the noise factor N is considered as the **standard noise factor**.

Should the temperature of R_s differ from 288 °K or if the signal source were to contain another source of noise, owing to which the apparent

¹⁾ See, for example, H. T. Friis, Noise Figures of Radio Receivers, Proc. I.R.E. 2, p. 419, 1944.

5.1 Definitions

temperature T_s , is higher than 288 °K, this can be taken into account by introducing a so-called temperature ratio:

$$\alpha = \frac{T_s}{288}. \quad (78)$$

The **actual noise factor** N_a of an amplifier preceded by such a signal source thus differs from the standard noise factor measured with R_s at 288 °K.

It is now necessary to clarify the definition of P_{ni} . Since $\overline{dE^2} = 4kTR_sdf$, the available noise power, considered within an element df of the frequency spectrum, is:

$$dP_{ni} = d\left(\frac{\overline{E^2}}{4R_s}\right) = \frac{4kTR_sdf}{4R_s} = kTdf. \quad (79)$$

This shows, remarkably enough, that the available noise power P_{ni} is independent of the value of the internal resistance of the noise source.

As a rule only part of the entire spectrum is passed by the amplifier. If P_{ni} at the input were taken over the frequency range from zero to infinity and the integration carried out over the entire frequency spectrum, while for P_{no} at the output only the band passed by the amplifier were considered, the value of N thus obtained would obviously give an erroneous impression. Therefore, denoting the pass-band by B_n , the noise power P_{ni} at the input of the amplifier is taken to be:

$$P_{ni} = kTB_n. \quad (80)$$

The gain will usually not be uniform over B_n , and this pass-band will then have to be defined more accurately.

In deriving eq. (77a), $P_{ni} \cdot (G_P)_s$ was assumed to be the available noise output originating exclusively from the signal source. Hence:

$$P_{ni}(G_P)_s = kTB_n(G_P)_s = \int_0^{\infty} kT(G_P)_f df,$$

or

$$B_n = \frac{1}{(G_P)_s} \int_0^{\infty} (G_P)_f df, \quad (81)$$

where $(G_P)_f$ denotes the available power gain at the frequency f .

The measurement of the noise factor N of an amplifier, preceded by a standard frequency generator, is based on the third member of eq. (77a) and P_{no} is measured with a correctly matched output meter. (Correct matching at the output is, of course, not essential provided all measurements are carried out with the same matching.) $(G_P)_s$ is derived from measurements carried out with a signal which largely exceeds the noise

level P_{ni} as defined by eq. (80). B_n follows according to eq. (81) from a response curve, bearing in mind that G_P is proportional to the square of the voltage gain G . Since the noise temperature T_s of the standard signal generator usually differs from 288 °K, this measurement gives:

$$N_a = \frac{P_{no}}{k T_s B_n (G_P)_s} \quad (82)$$

k being $1.37 \cdot 10^{-23}$ joule /°K. If the noise temperature of the standard signal generator is $T_s = 288$ °K the actual noise factor N_a is equal to the standard noise factor N_{st} . As mentioned above, the noise temperature T_s of the standard signal generator usually differs from 288 °K, i.e. $T_s/288 = \alpha$, in which case N_{st} is calculated from the measured values as follows:

$$N_{st} = \frac{P_{no} - (G_P)_s k T_s B_n + (G_P)_s k 288 B_n}{(G_P)_s k 288 B_n}$$

or

$$N_{st} = \frac{P_{no}}{(G_P)_s k 288 B_n} + 1 - \alpha. \quad (83)$$

Denoting the first term in the second member of eq. (83), which strongly resembles eq. (82), by N_m , this gives:

$$N_{st} = N_m + 1 - \alpha. \quad (83a)$$

Thus N_m is a fictitious noise factor obtained when calculations are carried out according to eq. (82) and T_s is assumed to be 288 °K. To determine the actual noise factor the true value of T_s must be employed according to the definition of eq. (82), giving:

$$N_a = N_m \cdot \frac{288}{T_s} = \frac{N_m}{\alpha}. \quad (82a)$$

In the above little attention was paid to the inherent noise of the amplifier itself. This is dealt with in detail in the following section, but it will be useful to discuss a few related conceptions here.

On page 60 eq. (77a) led to a definition of N as a ratio of noise powers at the output of the amplifier, but N can also be considered as the ratio of $P_{no}/(G_P)_s$ to P_{ni} , i.e. of available powers at the signal source. $P_{no}/(G_P)_s$ then consists of a part P_{ni} originating from the signal source and a part P_{nr} which represents the equivalent amplifier noise imagined to be located in the signal source. Eq. (77a) then becomes:

$$N = \frac{P_{ni} + P_{nr}}{P_{ni}} = 1 + \frac{P_{nr}}{P_{ni}}. \quad (77b)$$

In this expression P_{nr} is the equivalent available noise power of the amplifier reflected into the signal source. This again is a figure which depends on the matching between signal source and amplifier.

A different method of expressing the inherent noise (for frequencies at which no induced grid noise occurs) has long been employed for amplifying valves, where the concept of equivalent noise resistance R_{eq} is used, i.e. a fictitious resistance at room temperature connected in series with the grid. The actual noise causes are then imagined to be absent, but R_{eq} is assumed to have a value such that the noise voltage across it gives rise to the same noise as that normally present in the anode circuit.

Similarly, it is often useful to consider the inherent noise of a complete amplifier as originating from an equivalent resistance R_n at its input, but in this case it should be recognized that the value of R_n may depend both on the signal source and on the amplifier.

5.2 CALCULATION OF THE NOISE FACTOR

It will now be shown how to calculate the noise factor N , for several cases, from the equivalent noise resistance R_n at the input grid of a given amplifier.

5.2.1. Noise factor of an amplifier without input damping

When an amplifier, the input damping g of which is assumed to be zero, is connected direct to a signal source with an internal resistance R_s (see fig. 53), the noise factor N can be calculated from the definition given by eq. (77a).

The available noise power at the output P_{no} is directly proportional to $R_s + R_n$ at the input.

If the inherent noise of the amplifier were absent ($R_n = 0$), the noise would be directly proportional to R_s . Hence:

$$N = \frac{R_s + R_n}{R_s} = 1 + \frac{R_n}{R_s}. \quad (84)$$

If the temperature ratio of the signal source is α , its noise power must be multiplied by α and the actual noise factor obviously becomes:

$$N_a = 1 + \frac{R_n}{\alpha R_s}. \quad (84a)$$

By rewriting eq. (84) as:

$$R_s + R_n = NR_s, \quad (84b)$$

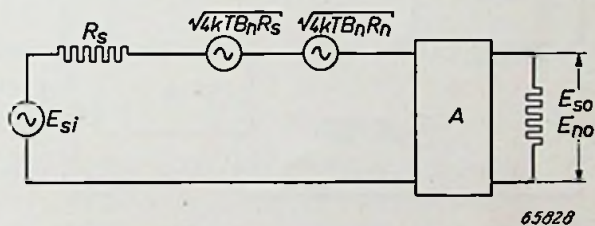


Fig. 53. Equivalent circuit of an amplifier having no input conductance and a definite, equivalent noise resistance R_n , connected to a signal generator with a noise resistance R_s and a noise temperature T .

it becomes clear that the two noise generators of fig. 53 may be replaced by one equivalent noise generator the average voltage of which is $\sqrt{4 kTNB_n R_s}$. The total noise of an amplifier preceded by a signal source may thus be imagined to be caused by R_s having a temperature NT , or it may be imagined that a noise-free signal generator is followed by an amplifier with an equivalent noise resistance NR_s having a temperature of 288 °K.

The latter representation may be useful for determining the "equivalent noise voltage" at the input of the amplifier. Advantage can then be taken of the well-known characteristic of resistances at 288 °K, i.e. that the square of the noise voltage is:

$$(4 \mu\text{V})^2 \text{ per } k\Omega \text{ and per Mc/s bandwidth.}$$

5.2.2 Noise factor of an amplifier with input damping

The calculation of the noise factor of an amplifier, which has an input conductance $g = 1/R$ and is connected direct to a signal source with a resistance R_s (see fig. 54), is based on the same lines.

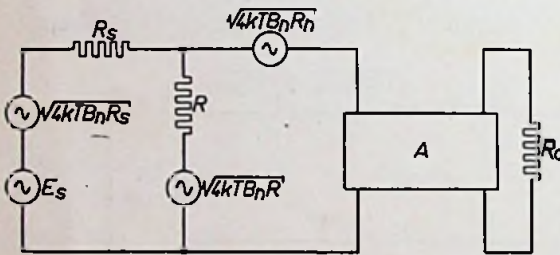


Fig. 54. Equivalent circuit similar to that of fig. 53, but with the amplifier having an input conductance $g = 1/R$.

P_{no} is determined by the combination of R_s and R connected in parallel and R_n connected in series, i.e. by

$$R_n + \frac{R R_s}{R + R_s}$$

The noise voltage of R_s is distributed over R_s and R , so that, if all inherent noise, i.e. that of R_n and R , is imagined to be zero, the available noise power at the output is determined by:

$$R_s \left(\frac{R}{R + R_s} \right)^2,$$

giving for the noise factor:

$$N = \frac{R_n + \frac{R R_s}{R + R_s}}{R_s \left(\frac{R}{R + R_s} \right)^2} = \frac{R + R_s}{R} + \frac{R_n}{R_s} \cdot \left(\frac{R + R_s}{R} \right)^2. \tag{85}$$

The limit of N for $R \rightarrow \infty$ obviously again gives eq. (84).

5.2.3 Noise factor of an amplifier with matching transformer

An amplifier connected to the signal source via a matching transformer with a ratio $1 : n$, is equivalent to an amplifier connected to a signal source having a resistance $n^2 R_s$. To calculate N it therefore suffices to replace R_s in eq. (85) by $n^2 R_s$, which gives:

$$N = 1 + \frac{n^2 R_s}{R} + \frac{R_n}{n^2 R_s} \cdot \left(1 + \frac{n^2 R_s}{R}\right)^2 \tag{86}$$

The noise factor is at a minimum when:

$$n^2 = \frac{R}{R_s \sqrt{1 + \frac{R}{R_n}}} \tag{87}$$

To avoid reflections in the aerial cable it is customary to match the H.F. amplifier of a television receiver to the aerial (having a resistance R_s) such that:

$$n^2 = \frac{R}{R_s} \tag{87a}$$

but this is not the most favourable matching with regard to the noise factor. If, however, R_n is large compared with R , eq. (87) differs but little from eq. (87a).

The practical noise factor obtained from eqs (86) and (87a) is:

$$N_{\text{pract}} = 2 + \frac{4R_n}{R} \tag{86a}$$

This expression shows that even if an amplifier with no noise ($R_n = 0$) were used, i.e. if the inherent noise were exclusively determined by the input resistance, $N_{\text{pract}} = 2$. It is seen from eq. (86) that N could be reduced by choosing n^2 smaller than R/R_s .

5.2.4 Noise factors of two amplifiers in cascade

The noise factors of two amplifiers A_1 and A_2 (of equal bandwidth B_n), to be used in cascade behind a given signal source (see fig. 55), are assumed to be N_1 and N_2 respectively. As pointed out on page 60, N_1 is valid for the combination of A_1 with the signal source S , whereas

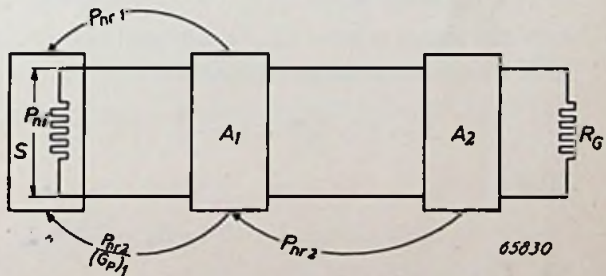


Fig. 55. Equivalent circuit of a signal source S followed by two amplifiers A_1 and A_2 in cascade.

N_2 is valid for A_2 connected to a signal source having the same impedance as the output of A_1 .

The value of the total noise factor N of two amplifiers connected in cascade, expressed in N_1 and N_2 , will now be investigated. First the inherent noise of A_2 is reflected into the input of the amplifier as an available noise power P_{nr2} originating from the output of A_1 . (This explains why N_2 has been defined as above.)

If the noise factor behind a signal source with an available noise power P_{ni} is N_2 , then, according to eq. (77b):

$$N_2 = 1 + \frac{P_{nr2}}{P_{ni}},$$

whence:

$$P_{nr2} = (N_2 - 1) P_{ni}.$$

(Since, in defining N_1 and N_2 , the noise temperature of the signal source and the bandwidth were assumed to be identical, P_{ni} at the input of A_2 and P_{ni} of the signal source are identical; see eq. (80).)

It is now possible to go a step further by imagining P_{nr2} to originate from the signal source, as an available noise power which now is $1/(Gp)_1$ times P_{nr2} . The inherent noise power of A_2 , reflected into the signal source, is therefore:

$$\frac{(N_2 - 1) P_{ni}}{(Gp)_1}. \quad (88)$$

Similarly, the inherent noise power of A_1 can also be reflected into the signal source, its value then being:

$$P_{nr1} = (N_1 - 1) P_{ni}. \quad (89)$$

The inherent noise of the total circuit connected in cascade, reflected into the signal source P_{nr} , is obviously equal to the sum of eqs (88) and (89). Calculating the total noise factor N from eq. (77b), gives:

$$N = 1 + \frac{P_{nr}}{P_{ni}} = 1 + \frac{1}{P_{ni}} \cdot \left\{ \frac{(N_2 - 1) P_{ni}}{(Gp)_1} + (N_1 - 1) P_{ni} \right\}.$$

Hence:

$$N = N_1 + \frac{N_2 - 1}{(Gp)_1}. \quad (90)$$

If the noise factor of the second stage is of the same order as that of the first stage following the signal source (the aerial), the noise contribution of the second stage is obviously negligibly small compared with the total noise, provided the power gain $(Gp)_1$ of the first stage is large.

In deducing eq. (90), the matching of A_1 to the signal source need not be

considered. It should be noted, however, that incorrect matching is necessarily accompanied by a decrease of $(G_p)_1$. In other words, incorrect matching to the aerial increases the noise contribution of A_2 .

5.3 CAUSES OF NOISE IN A VALVE

In the previous sections the inherent noise of an amplifier was represented by an equivalent noise resistance R_n or by a reflected noise power P_{nr} , without specifying the actual causes of this noise.

The amplifying valves contribute largely towards this noise and this contribution consists, in turn, of various components, each having its own origin in the valve considered.

It is very important to note that the magnitude of some of these components depends on the frequency and it is therefore obvious that these cannot be imagined to originate from an equivalent noise resistance. In fact, if the inherent noise of a valve is expressed in the customary way by the equivalent noise resistance R_{eq} (see page 63), only the components which are independent of the frequency are inferred, and at frequencies below 30 Mc/s these are indeed practically the only sources of noise.

The following are the principal causes of noise in a valve.

5.3.1 Emission and partition noise

In the simplest type of valve, i.e. the diode, the shot effect of the emission is the only source of noise. In the case of a saturated diode the mean square of the noise component in the emission current, measured within a frequency band B_n , is:

$$\overline{I_e^2} = 2 e I_k B_n \quad (91)$$

in which I_k denotes the cathode current.

When the emission current is not at saturation value the space-charge effect reduces the noise by the factor F_k , called the space-charge attenuation factor, giving:

$$\overline{I_e^2} = 2 F_k^2 e I_k B_n \quad (91a)$$

This emission noise is also present in all valves containing one or several grids and can be expressed¹⁾ in terms of the cathode temperature T_k and S' , the so-called transconductance for the effective control voltage, so that eq. (91a) becomes:

$$\overline{I_e^2} = 0.64 (4k T_k S' B_n) \quad (91b)$$

¹⁾ C. J. Bakker, The Causes of Voltage and Current Fluctuations, Philips Techn. Review 6, p. 129, 1941 (No. 5).

From eqs (91a) and (91b):

$$F_k^2 = \frac{0.64 \cdot 4 k T_k S'}{2 e I_k} \quad (92)$$

The transconductance S' is usually about 1 to 2 times the normal mutual conductance and T_k is approximately equal to 3.5 times the room temperature; hence F_k^2 lies between $0.1 S/I_k$ and $0.2 S/I_k$. For most cases a good approximation is:

$$F_k^2 \approx 0.125 \cdot \frac{S}{I_k} \quad (92a)$$

There is a striking resemblance between eq. (91b) and the expression for the Johnson noise in a resistance, viz.:

$$\overline{I^2} = \frac{\overline{E_n^2}}{R^2} = \frac{4k TR B_n}{R^2} = \frac{4k T B_n}{R} \quad (91c)$$

Clearly $1/S'$ in eq. (91b) plays the same part as R in eq. (91c).

In addition to the emission noise the irregularity of the "partition" of the current between anode and screen grid also comes into play in multigrid valves. The so-called partition noise thereby caused is given by the expression:

$$\overline{I_p^2} = 2e \cdot \frac{I_a I_{g2}}{I_k} \cdot B_n = 2F_p^2 e I_a B_n, \quad (93)$$

from which the partition noise factor is:

$$F_p^2 = \frac{I_{g2}}{I_k} \quad (93a)$$

The emission and partition noise currents are obviously manifest in the anode circuit. The emission noise has been shown to be proportional to the cathode current I_k , whereas the partition noise is proportional to the anode current I_a . If, to a first approximation, I_a is assumed to be equal to I_k in tetrodes and pentodes, and the two noise currents in the anode circuit are added, then:

$$\overline{(I_{e+p})^2} = 2F_a^2 e I_a B_n, \quad (94)$$

in which, according to eqs (91a) and (93):

$$F_a^2 \approx F_k^2 + F_p^2. \quad (95)$$

The equivalent noise resistance R_{eq} is now considered as the cause of the noise current $\overline{(I_{e+p})^2}$ according to eq. (94), and can therefore be calculated from:

$$4 k T B R_{eq} S^2 = 2 F_a^2 e I_a B,$$

which gives ¹⁾:

$$R_{\text{eq}} = \frac{e}{2kT} \cdot \frac{F_a^2 I_a}{S^2} \approx 20 \frac{F_a^2 I_a}{S^2} \text{ (k}\Omega\text{)}. \quad (96)$$

R_{eq} can further be imagined to be composed of two resistances, one of which is responsible for the emission noise, and the other responsible for the partition noise. When the latter resistance is denoted by R_p , it is obvious that:

$$\frac{R_p}{R_{\text{eq}}} = \frac{F_p^2}{F_p^2 + F_k^2} = \frac{1}{1 + \frac{F_k^2}{F_p^2}}. \quad (97)$$

This quotient will be denoted by K_3 .

A simple approximation for R_{eq} is obtained by substitution of eq. (95) in eq. (96) after eqs (92a) and (93a) have been substituted in eq. (95), viz.:

$$R_{\text{eq}} \approx \frac{I_a}{I_k} \cdot \left(\frac{2.5}{S} + 20 \cdot \frac{I_{g2}}{S^2} \right) \text{ (k}\Omega\text{)}. \quad (96a)$$

From this formula it will be clear that:

$$R_p \approx 20 \cdot \frac{I_{g2} I_a}{I_k S^2}, \quad (98)$$

and

$$K_3 \approx \frac{1}{1 + \frac{8I_{g2}}{S}}. \quad (99)$$

The following sections will show the advantage gained by splitting R_{eq} into R_p and $(R_{\text{eq}} - R_p)$. As a rule, only R_{eq} is quoted in valve data.

5.3.2 Induced grid noise

Owing to the finite transit time of the electrons the following effects occur:

(a) In a direct connection between the control grid and cathode additional fluctuations are induced, the values of which are given by:

$$\overline{I_g^2} = \text{constant} \cdot T_k S B_n \omega^2 \tau_{kg}^2, \quad (100)$$

where τ_{kg} denotes the transit time from cathode to control grid.

(b) The input circuit is subject to an additional damping g_τ , viz.:

$$g_\tau = \text{constant} \cdot S \omega^2 \tau_{kg}^2. \quad (101)$$

¹⁾ The charge of the electron $e = 1.6 \times 10^{-19}$ coulomb and $k = 1.37 \times 10^{-23}$ joule/ $^\circ\text{K}$.

As shown in the literature referred to above, the fluctuations $\overline{I_g^2}$ may be interpreted as the noise of the resistance $R_\tau = 1/g_\tau$ if the temperature is taken to be equal to about $1.43 T_k = \alpha_\tau 288$, α_τ being about 5, and assuming that there is no coherence between emission noise and induced grid noise.

This assumption is permissible here because, although there is coherence between these two kinds of noise and a possibility of noise compensation is thereby offered, such a compensation is difficult to achieve in practice. This possibility may therefore be disregarded and the more simple formulae which neglect coherence are used in this book, the slight improvement of N which might be obtained within a limited frequency range not being considered. This improvement may be expected to be less than 3 db.

5.4 CALCULATION OF THE NOISE FACTOR AT METRIC WAVES

5.4.1 General equations

The signal-to-noise ratio may undergo considerable changes due to feedback. At very high frequencies the self-inductance of the cathode lead gives rise to an additional input damping which reduces the signal strength. The noise in the input circuit (including the valve damping) is, however, also decreased by this damping and the same applies to the emission noise, which is reduced in the same proportion as the signal by the feedback in the cathode lead. The partition noise current, on the other hand, does not flow through the feedback circuit and remains unchanged.

Emission and partition noise are combined in the concept of "equivalent noise resistance", but since the feedback damping affects the emission noise and the partition noise differently, it is desirable to make a distinction between the two. For this reason, in addition to the equivalent noise resistance R_{eq} , the concept of "partition noise resistance" R_p has been introduced in Section 5.3.1, viz.:

$$R_p = \frac{F_p^2}{F_e^2} \cdot R_{eq}. \quad (102)$$

Since the fictitious resistance R_i across the input, representing the damping caused by the cathode lead inductance, can be proved to produce no additional noise ¹⁾, the equivalent is as shown in fig. 56.

¹⁾ M. J. O. Strutt and A. van der Ziel, The Noise in Receiving Sets at Very High Frequencies, Philips Techn. Review 6, p. 178, 1941 (No. 6).

The formula for expressing the noise factor of such a general circuit is very complex¹⁾ (see Appendix IV), and it is very much easier to calculate this factor for several simplified cases such as may occur or be approached in practice.

Four different cases are investigated below. These are all based on the assumption that the signal source is so matched to the amplifier that no reflections occur, i.e. that:

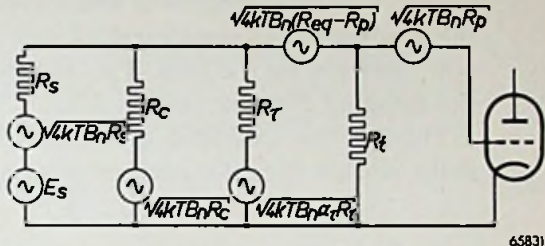


Fig. 56. Equivalent circuit demonstrating the effect of feedback (represented by the fictitious resistance R_f across the input) on the signal-to-noise ratio.

or

$$\left. \begin{aligned} \frac{1}{R_s} &= \frac{1}{R_c} + \frac{1}{R_t} + \frac{1}{R_\tau} \\ g_s &= g_c + g_t + g_\tau \end{aligned} \right\} \quad (103)$$

The input damping is not a component of g_t and g_τ and is therefore included in the circuit damping g_c .

(a) First the simplest case is considered, assuming the input damping g_i to be negligibly small with respect to the circuit damping g_c ; ($R_c \ll R_i$). This condition may occur at low frequencies and corresponds to the case dealt with in Section 5.2.3, but R_u and R should now be replaced by R_{eq} and R_c respectively. Eq. (86a) thus becomes:

$$N_{pract} = 2 + 4 \frac{R_{eq}}{R_c} \quad (104)$$

(b) In the next case to be investigated the transit time damping $g_\tau = 1/R_\tau$ of the valve is assumed to predominate, while the circuit damping $g_c = 1/R_c$ and the feedback damping $g_t = 1/R_t$ are assumed to be zero.

Following the same line as in Sections 5.2.2 and 5.2.3, the ratio of the total noise output to the noise output without inherent noise is now determined, the noise powers being assumed to be proportional to the resistances from which they originate.

At correct matching the signal source has a resistance R_τ , this being the assumed input resistance. The noise power originating from the signal source is now a constant multiplied by $\frac{1}{4} R_\tau$, the

¹⁾ L. A. Moxon, The Noise Characteristic of Radar Receivers, J.I.E.E. 93 IIIA, p. 1130, 1946 (No. 6).

factor $\frac{1}{4}$ accounting for the signal source being loaded by a resistance of the same value as the internal resistance.

The noise contribution of the transit time resistance is equal to the product of the same constant and $\frac{1}{4} \alpha_\tau R_\tau$, in which the factor $\frac{1}{4}$ now accounts for the load of R_τ by the signal source and α_τ having the meaning given in Section 5.3.2.

Finally, the unloaded resistance R_{eq} contributes towards the noise, so that the total noise originates from a resistance:

$$\frac{1}{4} R_\tau + \frac{1}{4} \alpha_\tau R_\tau + R_{eq},$$

giving for the noise factor:

$$N_{\text{pract}} = \frac{\frac{1}{4} R_\tau + \frac{1}{4} \alpha_\tau R_\tau + R_{eq}}{\frac{1}{4} R_\tau} = 1 + \alpha_\tau + 4 \frac{R_{eq}}{R_\tau}. \quad (105)$$

- (c) Whereas in the previous case only g_τ of the input conductance was taken into account, the case where only the feedback conductance g_i is present will now be investigated. The circuit conductance $g_c = 1/R_c$ is again assumed to be zero, and the resistance of the signal source is R_i .

The noise from the signal source is now directly proportional to $\frac{1}{4} R_i$. Of the total valve noise the partition noise must be taken fully into account, so that this noise contribution is proportional to R_p . The noise contribution from $(R_{eq} - R_p)$, on the other hand, is distributed over the resistance of the signal source and the resistance R_i . Since these two resistances are assumed to have the same value, only $\frac{1}{4}$ of the square of this noise voltage is operative in the amplifier.

The total noise power is therefore determined by:

$$\frac{1}{4} R_i + R_p + \frac{1}{4} (R_{eq} - R_p),$$

giving for the noise factor:

$$N_{\text{pract}} = \frac{\frac{1}{4} R_i + R_p + \frac{1}{4} (R_{eq} - R_p)}{\frac{1}{4} R_i} = 1 + 3 \frac{R_p}{R_i} + \frac{R_{eq}}{R_i}. \quad (106)$$

- (d) Finally, the two preceding cases will be combined, but for the sake of simplicity R_τ is assumed to be equal to R_i , while R_τ and R_i connected in parallel will now be denoted by R_i . The circuit conductance $g_c = 1/R_c$ is again assumed to be zero (cf. fig. 56).

The noise originating from the signal source is now determined by $\frac{1}{4} R_i$, while the partition noise is determined by R_p . The source of the transit time noise, i.e. in first instance $\alpha_\tau R_\tau$, is loaded by R_i connected in parallel with $2R_i$, that is to say by $\frac{2}{3} R_i$, and its internal

resistance is $R_\tau = 2R_i$. The transit time noise power is thus given by:

$$\alpha_\tau R_\tau \cdot \left(\frac{2}{2\frac{2}{3}}\right)^2 = \frac{1}{16} \alpha_\tau R_\tau = \frac{1}{8} \alpha_\tau R_i. \quad (107)$$

The equivalent voltage of the emission noise originating from $(R_{eq} - R_p)$ is distributed over R_i and the parallel connection of R_i and R_i , i.e. over $2 R_i$ and $\frac{2}{3} R_i$. This noise power is thus given by:

$$(R_{eq} - R_p) \left(\frac{2}{2\frac{2}{3}}\right)^2 = \frac{9}{16} (R_{eq} - R_p), \quad (108)$$

giving for the noise factor:

$$N_{\text{pract}} = \frac{\frac{1}{4} R_i + R_p + \frac{1}{8} \alpha_\tau R_i + \frac{9}{16} (R_{eq} - R_p)}{\frac{1}{4} R_i} = 1 + \frac{1}{2} \alpha_\tau + \frac{1}{4} \frac{R_p}{R_i} + \frac{3}{2} \frac{R_{eq}}{R_i}. \quad (109)$$

In the four cases investigated the matching of the signal source to the amplifier was assumed to be such that no reflection occurs. As shown in Section 5.2.3, matching may, however, be such that N is a minimum. For the calculation of this matching and of the values of N_{opt} obtained in that case, reference is made to Appendix IV.

Apart from case (a), which applies to low frequencies only, there appear to be but three quantities on which the noise factor depends, viz.:

α_τ , a constant ≈ 5 ,

R_{eq}/R_i , a quantity which depends only on the frequency and is a valve quantity¹⁾,

R_p/R_i , which can be expressed in terms of R_{eq} by means of the factor $K_3 = R_p/R_{eq}$. For triodes K_3 is obviously zero, while for pentodes $1/K_3 \approx 1 + S/8I_{g2}$, K_3 tending towards unity when the partition noise predominates, and being about $\frac{1}{2}$ in the case of high-slope pentodes.

Because of the term R_i the quantity R_{eq}/R_i is proportional to the square of the frequency, viz.:

$$\frac{R_{eq}}{R_i} = \left(\frac{f}{f_n}\right)^2, \quad (110)$$

where f_n is the **noise reference frequency** at which $R_{eq}/R_i = R_{eq} \cdot g_i$ is unity.

Taking these considerations into account, the special cases mentioned

¹⁾ It is true that R_i depends on the amount of feedback by the cathode lead, but the limit to which this effect can be reduced in practice may also be regarded as a valve characteristic.

above have been summarized in the following table in which, for the sake of simplicity, either the partition noise has been taken equal to zero ($K_3 = 0$ in the case of triodes) or the emission noise has been ignored with regard to the partition noise ($K_3 = 1$, i.e. the extreme value for pentodes). In this table the values of N_{opt} (at matching for the minimum noise factor) are also indicated.

This table permits the noise factor to be determined at various frequencies and in the various "amplification ranges" as discussed in Section 1 (cf. figs 3 and 5).

Case	N_{pract} at $K_3 = 0$ (triode circuit)	N_{pract} at $K_3 = 1$ (partition noise predominating)
<i>a</i>	$2 + 4 \frac{R_{\text{eq}}}{R_c}$	$2 + 4 \frac{R_{\text{eq}}}{R_c}$
<i>b</i>	$6 + 4 \frac{f^2}{f_n^2}$	$6 + 4 \frac{f^2}{f_n^2}$
<i>c</i>	$1 + \frac{f^2}{f_n^2}$	$1 + 4 \frac{f^2}{f_n^2}$
<i>d</i>	$\frac{1}{2} + 4 \frac{f^2}{f_n^2}$	$\frac{1}{2} + 4 \frac{f^2}{f_n^2}$
	N_{opt} at $K_3 = 0$	N_{opt} at $K_3 = 1$
<i>a'</i>	$1 + 2 \frac{R_{\text{eq}}}{R_c} \cdot \left(1 + \sqrt{1 + \frac{R_c}{R_{\text{eq}}}}\right)$	$1 + 2 \frac{R_{\text{eq}}}{R_c} \cdot \left(1 + \sqrt{1 + \frac{R_c}{R_{\text{eq}}}}\right)$
<i>b'</i>	$1 + 2 \frac{f^2}{f_n^2} \cdot \left(1 + \sqrt{1 + 5 \frac{f_n^2}{f^2}}\right)$	$1 + 2 \frac{f^2}{f_n^2} \cdot \left(1 + \sqrt{1 + 5 \frac{f_n^2}{f^2}}\right)$
<i>c'</i>	1	$1 + 4 \frac{f^2}{f_n^2}$
<i>d'</i>	$1 + \frac{f^2}{f_n^2} \cdot \left(1 + \sqrt{1 + 10 \frac{f_n^2}{f^2}}\right)$	$1 + 2 \frac{f^2}{f_n^2} \cdot \left(1 + \sqrt{1 + \frac{1}{2} \frac{f_n^2}{f^2}}\right)$

5.4.2 Range above f_0'

The conductance of the input circuit of an amplifier which is correctly matched to the aerial (assuming for the time being the noise temperature to be identical to room temperature) and which operates in the range above f_0' is due mainly to the signal source and the input conductance of the valve, and not to the circuit losses. With normal valves g_t and g_τ may

be of the same order of magnitude and for the conditions outlined here, case (d) gives a good idea of the characteristics of N .

The noise factor of a pentode with predominating partition noise is:

$$N = \frac{1}{3} + 4 \frac{f^2}{f_n^2}$$

while in the case of a triode the coefficient of f^2/f_n^2 is smaller, for in that case:

$$N = \frac{1}{4} + \frac{1}{2} \frac{f^2}{f_n^2}$$

These two expressions have been plotted in fig. 57. In comparing the triode circuit with that of the pentode, it should, however, be realized that f_n , too, has a different value in each case. (As a result of the different values of R_{eq} , the noise reference frequency f_n of a pentode usually lies between 100 and 200 Mc/s, while in the case of a triode f_n lies usually between 200 and 400 Mc/s.) The resulting difference is shown in fig. 58.

Figs 57 and 58 show that the noise factor rapidly increases above the noise reference frequency f_n . An additional factor contributing towards this increase but not yet taken into account in these two graphs is that the more f_n is increased, the nearer will the gain reference frequency f_1 be approached and the greater will be the reduction in gain. The noise of the second stage then becomes more and more important, so that the graphs must be corrected according to eq. (90). The magnitude of this correction depends on the ratio of N_1/N_2 and of f_n/f_1 of the first stage.

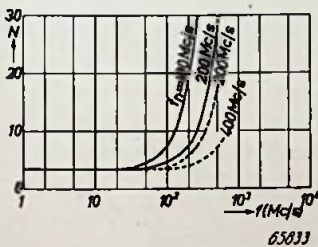


Fig. 58. Noise factor N as a function of the frequency for a valve operating above f_0 , with the noise reference frequency f_n as parameter. The full lines again apply to pentode circuits with predominating partition noise and the broken lines to triode circuits.

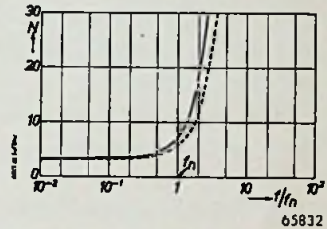


Fig. 57. Noise factor N as a function of f/f_n for a valve operating above f_0' . The full line applies to pentode circuits with predominating partition noise and the broken line to triode circuits. Matching is assumed to be correct for each frequency.

Since the 3 db bandwidth B_3 increases with the frequency when f_0' is exceeded, the noise bandwidth may also increase (provided the circuit capacitance is not increased). It is, however, by no means certain that B_n increases, because B_n depends on the response curve of the complete amplifier. B_n has no

effect on the noise factor, but it does influence the signal-to-noise ratio. It is therefore desirable that this bandwidth is not increased more than necessary for amplifying this signal.

It should finally be noted that the assumed correct matching implies that for each frequency the transformer ratio is readjusted to the optimum value.

5.4.3 Range below f_0'

If in the range below f_0' the bandwidth B is kept constant, while the circuit capacitance C is minimum, then:

$$2(g_i + g_c) = \text{constant} = 2\pi BC.$$

At the upper limit of this range, i.e. at f_0' , the circuit damping $g_c = 0$, so that $2g_i = 2\pi BC$, while at low frequencies the input damping $g_i = 0$ and $2g_c = 2\pi BC$.

Now in the extreme case of $f = f_0'$, assuming the matching to be correct, the formulae given for case (d) still apply, viz.:

$$N_{\text{pract}} = \frac{1}{3} + 4 \frac{f_0'^2}{f_n^2} = \frac{1}{3} + 4 R_{\text{eq}} \pi BC$$

if the partition noise predominates, and:

$$N_{\text{pract}} = \frac{1}{3} + \frac{2}{3} \cdot \frac{f_0'^2}{f_n^2} = \frac{1}{3} + \frac{2}{3} R_{\text{eq}} \pi BC$$

if a triode is used.

At low frequencies, however, if matching is correct, case (a) applies, giving for the above two conditions:

$$N_{\text{pract}} = 2 + 4 R_{\text{eq}} \pi BC = 2 + 4 \left(\frac{f_0'}{f_n} \right)^2$$

If a pentode is used it is seen that in the range between f_0' and, for

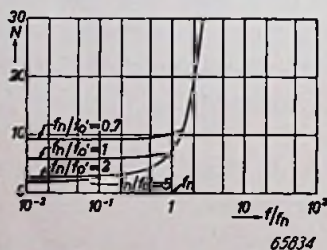


Fig. 59. Noise factor N of pentodes with predominating partition noise in the vicinity of f_n as a function of f/f_n with the ratio f_n/f_0' as parameter ($R_\tau = R_t$).

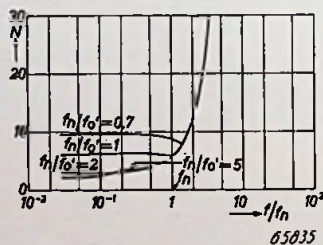


Fig. 60. Noise factor N of triodes in the vicinity of f_n as a function of f/f_n with the ratio f_n/f_0' as parameter ($R_\tau = R_t$).

example $f_0'/3$, the noise factor thus changes by about 2 units (cf. fig. 59); with triodes this improvement at decreasing frequency is less, and in some cases there may even be a deterioration (cf. fig. 60). This is because at lower frequencies the feedback conductance, which produces no noise, is replaced by a resistance at room temperature in order to obtain the required bandwidth. The advantage gained from the absence of inherent noise in the feedback damping is less in the case of a pentode than in the case of a triode.

The attenuation of the signal then exceeds the attenuation of the noise, since the cathode lead is not traversed by the partition noise.

As can be seen from figs 59 and 60, it is desirable to keep f_0' a factor of at least 2 below f_n . This means that for a satisfactory noise factor the product of B' and $C_i + C_x$ should be kept reasonably small, in other words that the gain of the aerial circuit should not be very low (cf. eq. 11b).

Eq. (111) applies when below f_0' the bandwidth is increased to the required value by shunting the input circuit by a resistance. A lower noise

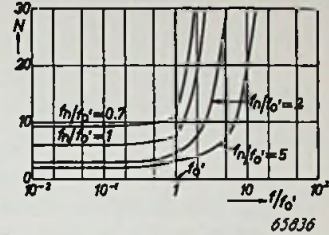


Fig. 61. Noise factor N of pentodes with predominating partition noise in the vicinity of f_0' as a function of f/f_0' with the ratio f_n/f_0' as parameter ($R_z = R_t$).

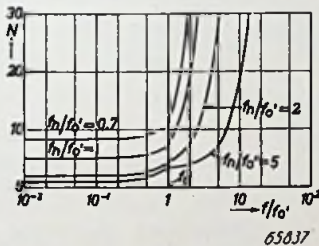


Fig. 62. Noise factor N of pentodes with predominating partition noise in the vicinity of f_0' as a function of f/f_0' with the ratio f_n/f_0' as parameter, the circuit being damped by feedback in the cathode lead only.

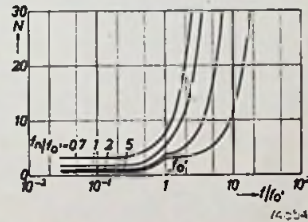


Fig. 63. Noise factor N of triodes in the vicinity of f_0' as a function of f/f_0' with the ratio f_n/f_0' as parameter, the circuit being damped by feedback in the cathode lead only.

factor may be obtained by adjusting the input damping by means of the cathode lead inductance. Here again, the results are less favourable in the case of a pentode (fig. 62) than in the case of a triode (fig. 63), as the partition noise is not fed back in the cathode lead. It is, however, difficult to apply

this method in practice, and since f_0' is usually lower than f_n , the high noise factors above f_n cannot be reduced in this way (see figs 64 and 65),

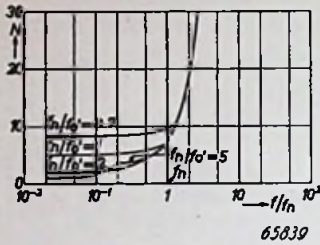


Fig. 64. Noise factor N of pentodes with predominating partition noise in the vicinity of f_n as a function of f/f_n with the ratio f_n/f_0' as parameter, the circuit being damped by feedback in the cathode lead.

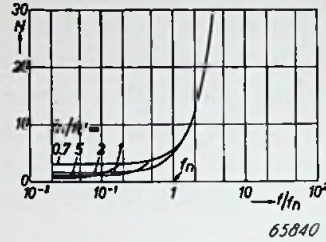


Fig. 65. Noise factor N of triodes in the vicinity of f_n as a function of f/f_n with the ratio f_n/f_0' as parameter, the circuit being damped by feedback in the cathode lead.

nor can a considerable improvement of the noise factor be obtained by changing the aerial matching at the input (see fig. 66).

5.5 EFFECT OF REDUCING THE FEEDBACK CONDUCTANCE

To investigate to what extent the noise factor of pentodes can be improved by reducing the impedance of the cathode lead, case (d), where the circuit conductance is negligible and half the input conductance is due to transit time conductance, is once again taken as a starting point. The noise factor derived for this case:

$$N_{\text{pract}} = 1 + \frac{1}{2}\alpha_{\tau} + \frac{1}{2}\frac{R_p}{R_i} + \frac{1}{2}\frac{R_{\text{eq}}}{R_i} \quad (109)$$

is now compared with the noise factor obtained when there is no feedback damping. The noise factor for the latter case is found by considering that case (b) then applies (g_c and g_t now being zero), while in this particular case the input resistance is twice the value of R_i when there is feedback, giving:

$$N_{\text{pract}} = 1 + \alpha_{\tau} + 2\frac{R_{\text{eq}}}{R_i} \quad (112)$$

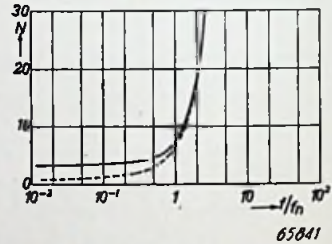


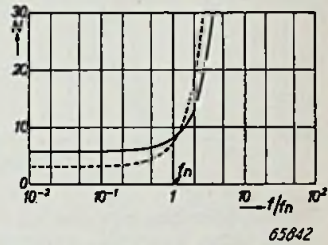
Fig. 66. Noise factor N of pentodes with predominating partition noise as a function of f/f_n for two different aerial matchings, f_n being small compared with f_0' . The full line applies when the input circuit is matched for maximum gain and the broken line when the input circuit is matched for minimum noise.

As shown by fig. 67, this amounts to an increase of N below f_n but a decrease above f_n in the case of a pentode. The deterioration below f_n is due to the ratio of the transit time noise in the input circuit to the signal energy increasing as a result of the changed matching. The improvement above f_n , on the other hand, results from the signal voltage increasing, while the equivalent noise voltage at the grid remains constant (the partition fluctuations being unaltered).

Since reduction of the cathode lead impedance, in addition to decreasing the noise factor above f_n , also increases the gain (greater aerial gain), this method is very attractive.

Apart from reducing the feedback conductance, the reduction of the cathode lead impedance leads to other improvements, limited, however, by the effects of stray capacitances, etc. and the required bandwidth. The improvement thus obtained can be determined to a first approximation by assuming that the expressions given for case (d) still apply, but that f_n is increased approximately as much as f_1 . This assumption is actually a little too optimistic, because the reduction of the feedback conductance results in an increased apparent noise temperature of the input resistance, while the emission noise increases roughly in proportion to the signal.

Owing to this latter effect the signal-to-noise ratio is independent of the feedback conductance in the case of triodes, provided the aerial transformer remains unchanged. By changing the transformer ratio in such a way that $R_s g_i$ remains equal to unity, however, the noise factor can also be improved in this case by reduction of the cathode lead conductance. The inherent deterioration of the noise temperature of g_s , however, occasionally results in the increase of the noise factor being greater than the decrease brought about by the reduction of the conductance. At very high frequencies the reduced conductance nevertheless still improves the noise factor, owing to the increased gain reducing the noise contribution of the second stage (which may then no longer be disregarded in view of the small gain). It would lead too far to investigate the difficulties arising in practice, due among other things to the grid circuit conductance being reduced simultaneously via the anode circuit.



65842
Fig. 67. Noise factor N of pentodes with predominating partition noise as a function of $1/f_n$ with the feedback conductance as parameter, the circuit conductance g_c being assumed to be zero. The full line applies when the feedback conductance is zero (case (b)) and the broken line when this conductance is equal to half the input conductance (case (d)).

Summarizing, it can be stated that the noise factor rapidly increases above f_n and, apart from improving g_i , little can be done to counteract this effect.

5.6 CALCULATION OF THE SIGNAL-TO-NOISE RATIO FROM THE NOISE FACTOR

In order to derive the signal-to-noise ratio from the noise factor it should in the first place be taken into account that so far only the standard noise factor has been considered, i.e. the noise factor of an amplifier following a signal source, the noise temperature of which is equal to room temperature.

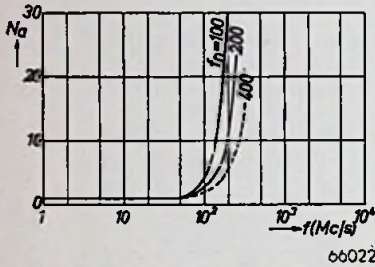


Fig. 68. Minimum value of the aerial noise factor N_a at correct matching as a function of the frequency, with f_n as parameter. The full lines apply to pentodes with predominating partition noise and the broken lines to triodes, both in case (d).

At metric waves the noise temperature T_a of an aerial largely depends on the frequency and direction, owing to the contribution of the cosmic noise¹⁾ to the noise level of the aerial. At, say, 40 Mc/s the noise temperature of the aerial may vary for example between 5000 °K and 25,000 °K.

At higher frequencies, however, the noise temperature decreases and at the highest frequencies tends towards the absolute zero point. A calculation of the effect of

the cosmic noise by means of eq. (82a) shows that, at frequencies below 100 Mc/s, N_a lies considerably below N ; see figs 58 and 68.

Owing to the influence of T_a , valve differences (differing f_n values) have a smaller effect on N_a than on N . The noise output of a receiver is now given by:

$$P_{no} = N a k T_a B_n (G_P)_s = (N - 1 + \alpha) 288 k B_n (G_P)_s,$$

while the signal output is:

$$P_{so} = \frac{H^2 \lambda^2}{4\pi^2 R_{rad}} \cdot (G_P)_s,$$

where H is the field strength in V/m and λ the wavelength in m. The signal-to-noise (power) ratio at the output is thus:

$$\frac{P_{so}}{P_{no}} = \frac{H^2 \lambda^2}{4\pi^2 (N - 1 + \alpha) (288 k B_n R_{rad})} \tag{113}$$

¹⁾ See the paper by Bakker quoted in footnote on page 67.

5.6 Calculation of the signal-to-noise ratio from the noise factor

The minimum field strength H_{\min} required for a signal-to-noise (power) ratio P_{so}/P_{no} is given by:

$$H_{\min} = \frac{\pi}{\lambda} \cdot \sqrt{\frac{P_{so}}{P_{no}}} \cdot \sqrt{N - 1 + \alpha} \cdot \sqrt{4k 288 B_n R_{\text{rad}}}$$

The last factor of this product is equal to the effective noise voltage of R_{rad} at standard room temperature over a bandwidth B_n . By putting $R_{\text{rad}} = 75 \Omega$ and $B_n = 5 \text{ Mc/s}$, this quantity becomes $2.4 \mu\text{V}$, giving:

$$H_{\min} \approx 0.05 f \sqrt{N - 1 + \alpha} \sqrt{\frac{P_{so}}{P_{no}}} \quad (\mu\text{V/m}), \quad (114)$$

f being expressed in Mc/s.

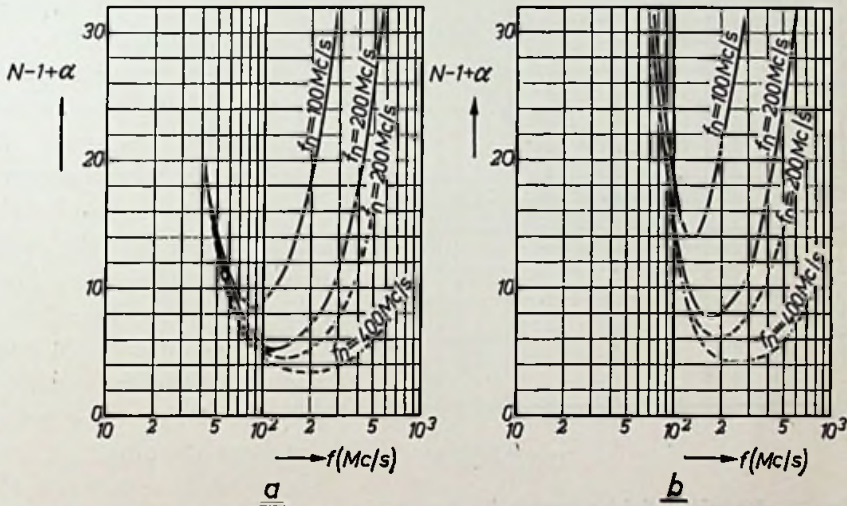


Fig. 69. The value of $(N - 1 + \alpha)$ of eq. (113) as a function of the frequency, with f_n as parameter, (a) with minimum cosmic noise and (b) with maximum cosmic noise. The full lines again apply to pentodes with predominating partition noise and the broken lines to triodes.

It should be realized that this formula gives the lowest value of H at which the desired signal-to-noise ratio could be achieved. In practice a higher value will be necessary because the aerial will not necessarily have the most suitable dimensions and direction, etc.

In fig. 69 the quantity $(N - 1 + \alpha)$ of eq. (114) has been plotted as a

function of the frequency, the cosmic noise having been assumed to be minimum in fig. 69*a* and maximum in fig. 69*b*.

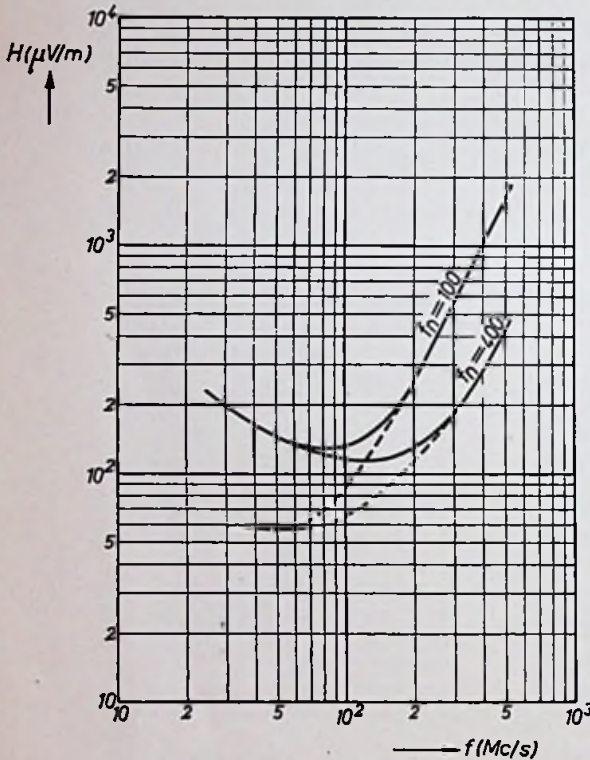
The required field strength for a signal-to-noise ratio of at least 14 db has been plotted as a function of the frequency in fig. 70.

In the foregoing the circuit impedances, the noise temperatures, the radiation resistance etc., have always been assumed to be constant over a frequency band having a width B_n , with no noise passed by the amplifier beyond this band.

In normal T.V. receivers B_n is about equal to the 3 db bandwidth of the I.F. amplifier and since this band is fairly narrow compared with the range within which the above quantities are fairly constant, this assumption is justified in practice.

It should, be recognized however, that where the receiver has undesired responses, for example for the second channel, these frequency bands also contribute towards the noise. Moreover, where the input circuit is almost as selective as the other circuits (in some straight receivers for example), B_n is no longer a constant throughout the amplifier.

The general conclusion is, therefore, that the weakest signal which can be received reasonably will depend on the frequency, on the noise condition (aerial noise) and, last but not



65845
Fig. 70. Required field strength H for obtaining a signal-to-noise ratio of 14 db, as a function of the frequency with f_n as parameter, a single dipole aerial being used. The full lines apply to maximum noise conditions and the broken lines to minimum noise conditions.

least, on the noise reference frequency f_n of the first valve. For the higher television band, conditions differ considerably from those for the lower television band, due to the frequency dependence of the cosmic noise and of the noise factor of the valves.

6. FEEDBACK

6.1 GENERAL

One of the main difficulties in constructing H.F. and I.F. amplifiers for television is how to overcome the effects of feedback. These effects are only in part due to valve characteristics. The most important causes are listed below:

- (a) Coupling between input and output leads. Provided the valve connections are so arranged that these leads can be well separated, this difficulty can always be avoided by a suitable layout.

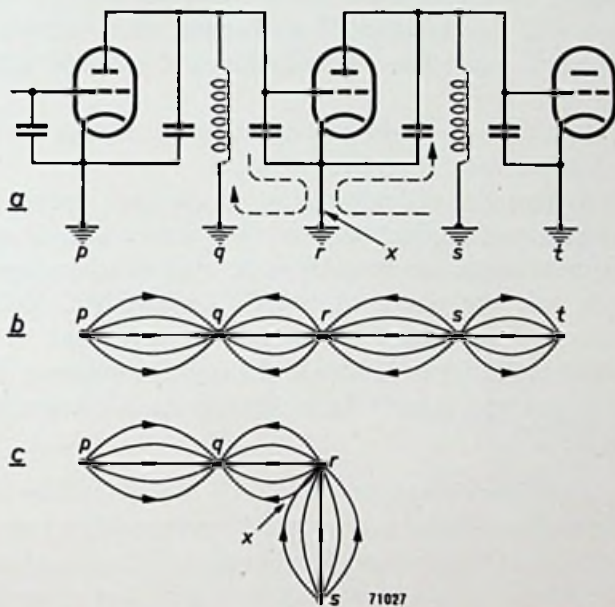


Fig. 71. Circuit diagram (a) and corresponding functional diagrams showing the currents flowing through the chassis. Diagram (b) applies to a rectilinear layout, and diagram (c) to a layout which is not rectilinear, so that undesired coupling occurs at x .

- (b) Coupling between the input and output circuits is often due also to the common earth lead. It should be recognized that the impedance of the chassis as earth lead is by no means negligible. The layout should preferably be such that the currents of the input and output circuits do not flow through the same part of the chassis (see fig. 71).

- (c) Feedback of part of the output energy due to the chassis acting as a wave guide. Many different modes are possible, each of which has a definite attenuation per unit length. Long, narrow chassis are usually advisable. A narrow chassis, permitting a high gain per unit length, can be obtained by using valves of small dimensions. The feedback can, moreover, be minimized by providing the chassis with partitions, thereby impeding the passage of guided waves.
- (d) Coupling between the stages via the filament lead. This can be avoided by by-passing these connections.
- (e) Decoupling faults. Such faults are usually due to the self-inductance of the capacitors and of their connecting leads. Good results are nevertheless obtained when these leads happen to be in series resonance with the capacitor. (For example, when working at 65 Mc/s, this will be the case when the inductance of a 200 pF capacitor and its leads is 0.03 μ H.)
- (f) Feedback via the anode-to-grid capacitance. This is the main cause of instability arising from the valves.
- (g) Feedback from the cathode circuit to the grid circuit. This effect changes the input conductance and capacitance and, though troublesome in most cases, can sometimes be used to advantage.
- (h) Feedback via the anode-to-cathode capacitance. This effect is of particular importance when taking advantage of the effect mentioned under (g) to influence the input admittance of the valve, for which purpose a fairly large impedance is incorporated in the cathode lead.

Only the effects mentioned under (f), (g) and (h) will be discussed in detail. The formulae required are derived for an amplifying stage in which all these three effects are present. The detailed discussion of each form of feedback is confined to a system in which only one of these effects is present.

6.2 BASIC FORMULAE

When considering the gain and bandwidth (see Section 1), use was made of an idealized amplifying stage in which the valve (with an input voltage V_i across the admittance Y_i) functions as a constant-current generator supplying a current $I_o = SV_i$ to the output admittance Y_o . In order to use this simplified representation when negative or positive feedback is present in the amplifying stage, it is first necessary to determine the values of the quantities S' , Y_i' and Y_o' which are substituted for S , Y_i and Y_o in

circuits where anode-to-grid, cathode-to-grid or anode-to-cathode feedback are present ¹⁾.

The investigations are based on the following notations (see fig. 72):

$$\begin{aligned}
 I_a &= S_a V_g, & I_o &= I_4 + I_5 + I_k, \\
 I_k &= S_k V_g, & I_i &= I_2 + I_4 - I_3, \\
 I_g &= 0, & V_o &= -I_i / Y_1, \\
 -I_1 &= I_a + I_3 + I_5, & V_k &= I_6 / Y_6, \\
 I_2 &= Y_2 V_i, & V_a &= V_o - V_k, \\
 I_3 &= Y_3 V_{ag}, & V_{ag} &= V_o - V_i, \\
 I_4 &= Y_4 V_g, & V_g &= V_i - V_k, \\
 I_5 &= Y_5 V_a.
 \end{aligned}$$

To simplify the formulae, the following abbreviations have been introduced:

$$\frac{Y_5}{Y_1 + Y_3 + Y_5} = \rho,$$

and

$$(1 - \rho) Y_5 = \frac{(Y_1 + Y_3) Y_5}{Y_1 + Y_3 + Y_5} = Y_7.$$

If only V_i , V_o , I_i and I_a are considered, the complicated circuit of fig. 72 can be regarded as a special case of the simpler circuit shown in

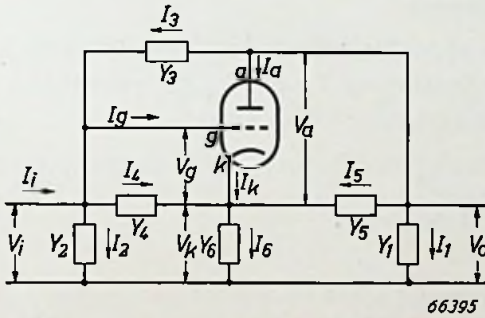


Fig. 72. Schematic representation of an amplifying stage for investigating the effect of anode-to-grid, cathode-to-grid or anode-to-cathode feedback.

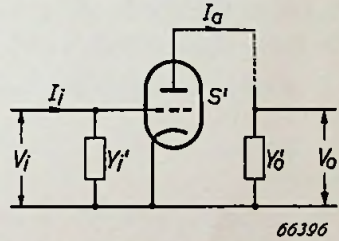


Fig. 73. Equivalent circuit of fig. 72, in which only V_i , V_o , I_i and I_a are assumed to be present.

fig. 73, in which Y_i' , S' and Y_o' have been so chosen that the relations between these four quantities remain the same. The calculations of I_i , I_a and V_o can then be based on the expressions:

$$\begin{aligned}
 I_i &= V_i Y_i', \\
 I_a &= V_i S', \\
 V_o &= I_a / Y_o'.
 \end{aligned}$$

¹⁾ Control by and feedback from the screen grid and the effect of mutual inducances in the electrode connections will be disregarded.

In order to make use of these simplified expressions, Y_i' , Y_o' and S' must be expressed in terms of Y_1, \dots, Y_7 and of the anode transconductance S_a and the cathode transconductance S_k .

As shown in Appendix V, the factor $F_s = S'/S_a$ ¹⁾ is then:

$$F_s = \frac{Y_6 + Y_7 - \rho Y_3}{Y_6 + Y_4 + Y_7 + S_k - \rho S_a}, \quad (115)$$

while

$$Y_i' = Y_2 + Y_4 F_s + Y_3 \cdot \frac{S' + Y_1 + F_s Y_5}{Y_1 + Y_3 + Y_5}, \quad (116)$$

and

$$Y_o' = \frac{Y_1 + Y_3 + Y_5}{1 - \frac{Y_3}{S'} - \frac{Y_5}{S'} \cdot (1 - F_s)} \quad (117)$$

The effect of the various types of feedback will now be investigated by means of eqs (115), (116) and (117). It is assumed that in each case only one form of feedback is present.

6.3 FEEDBACK FROM ANODE TO GRID

6.3.1 Negative feedback by a resistance

To investigate the consequences of feedback by a (high) resistance R_{ag} between the anode and grid, the admittances Y_4 and Y_5 are assumed to be zero. Hence, both ρ and Y_7 are also zero, which gives:

$$S' = \frac{S_a}{1 + \frac{S_k}{Y_6}}, \quad (118)$$

and

$$Y_o' = \frac{Y_1 + \frac{1}{R_{ag}}}{1 - \frac{1}{S' R_{ag}}}. \quad (119)$$

In practice $G \gg 1$, hence $Y_1/S' \ll 1$. Moreover, $Y_3 = 1/R_{ag}$ will usually be made smaller than Y_1 , so that also $1/S' R_{ag}$ is likely to be much smaller than unity. Hence:

$$Y_o' \approx Y_1 + \frac{1}{R_{ag}} \approx Y_o. \quad (119a)$$

It may be concluded from eqs (118) and (119a) that the gain G of the

¹⁾ In this case F_s is a complex quantity, but for the sake of simplicity this symbol was also used for the modulus in Section 1, instead of the rather unmanageable symbol $|F_s|$.

stage with negative feedback is substantially independent of the amount of feedback. This, however, is by no means the case with the gain of the preceding stage, since the input impedance of the stage in which feedback occurs is influenced by the amount of feedback. This can be shown as follows:

$$S' \gg Y_1 \text{ and } Y_1 > Y_3,$$

so that, according to eq. (116):

$$Y_i' = Y_2 + \frac{Y_3 S'}{\left(1 + \frac{Y_3}{Y_1}\right) Y_1}, \tag{120}$$

since

$$Y_1 + S' \approx S'.$$

Substituting $1 - Y_3/Y_1$ for $1/(1 + Y_3/Y_1)$ gives:

$$Y_i' \approx Y_2 + \frac{S'}{Y_1 R_{ag}} - \frac{S'}{Y_1^2 R_{ag}^2}. \tag{120a}$$

When the third term of eq. (120a) is negligible, this equation may be written:

$$Y_i' \approx Y_2 + \frac{S' Z_1}{R_{ag}}. \tag{120b}$$

Introduction of a new quantity

$$p^2 = \frac{S' \hat{Z}_1 \hat{Z}_2}{R_{ag}},$$

in which \hat{Z}_1 and \hat{Z}_2 represent Z_1 and Z_2 at the resonant frequency, gives:

$$Y_i' = Y_2 + \frac{p^2 Z_1}{\hat{Z}_2 \hat{Z}_1}. \tag{120c}$$

This expression shows that Y_i' has the form of the input admittance of a band-pass filter (see Appendix If). The response curve of the two stages is equal to that which would be obtained if they were coupled by the primary of a band-pass filter with $k^2 Q_p Q_s = p^2$ (so-called Z_i coupling, see fig. 74).

By means of this circuit the response curve can be given a flat top, as obtained by means of a band-pass filter coupling, but the sideband selectivity is inferior.

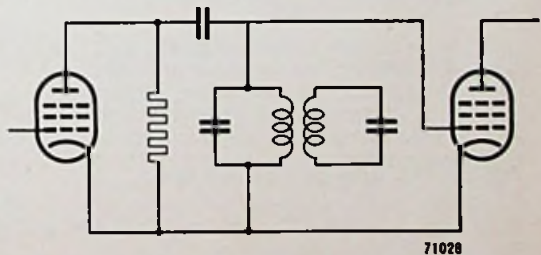


Fig. 74. Principle of the Z_i coupling.

With a feedback amplifier it is difficult to keep the response under control owing to the fact that the response of the grid circuit of a feedback stage depends both on the tuning of the anode circuit and on the gain, whilst detuning of the circuits results in an asymmetrical response curve. In I.F. amplifiers for television it is therefore not customary to apply this type of negative feedback.

6.3.2 Feedback by the anode-to-grid capacitance

In order to investigate the effect of feedback by the anode-to-grid

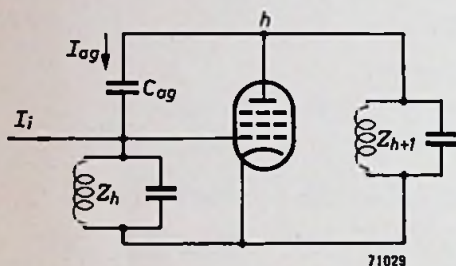


Fig. 75. Practical circuit with tuned anode and control-grid circuits. As shown by eq. (116), for calculating Y_i' the cathode impedance may be omitted, provided the correct value is substituted for S' .

capacitance C_{ag} in a multi-stage amplifier it will first be assumed that feedback occurs only in stage number h of the amplifier. The calculation is based on the circuit of fig. 75.

Z_h denotes the impedance of the input circuit of stage h , and Z_{h+1} the impedance of the output circuit, while Z_h' denotes the input impedance of stage h (including the effect of the feedback via C_{ag}), and $(Z_{h+1})'$ the output impedance of this stage.

It has already been shown that $(Z_{h+1})' = Z_{h+1}$ (cf. eq. (119a)) when there is no feedback in stage $h + 1$. Assuming that $G \gg 1$ or $|V_g| \ll |V_a|$, it can be shown that:

$$I_{ag} \approx -V_g S' Z_{h+1} j\omega C_{ag}.$$

Substitution of this expression in:

$$V_g = Z_h (I_i + I_{ag})$$

gives:

$$\frac{I_i}{V_g} = Y_h (1 + j\omega C_{ag} S' Z_h Z_{h+1}),$$

which can also be written as:

$$Y_h' = Y_h + j\omega C_{ag} S' Z_{h+1}. \quad (120d)$$

This result could of course also be derived from eq. (120) by putting:

$$Y_1 = (Z_{h+1})^{-1}, \quad Y_2 = Z_h^{-1} \quad \text{and} \quad Y_3 = j\omega C_{ag}.$$

Eq. (120d) shows that both the real and the imaginary components of

Y_h' are affected by the feedback and that this effect depends on the frequency. This is mainly due to the frequency dependence of Z_{h+1} and but little to the fact that ω occurs in this expression.

If Z_{h+1} were a pure ohmic resistance at all frequencies, this would merely be equivalent to an additional capacitance shunted across the input circuit (Miller effect), but since this is not the case, the frequency dependence of Y_h' is of a more complex nature than in the case of an ordinary parallel-tuned circuit. This is clearly demonstrated by the admittance and impedance curves (see Appendix Ia) given in figs 76 and 77, which show the polar diagrams of the input circuit, the bandwidth and tuning of the anode and grid circuits being assumed to be equal. The construction of these curves is shown later.

The admittance of the circuit, affected by the feedback, is represented by a vector with O as its origin, and with its extremity lying on the admittance curve at the point where this is intercepted by the broken line indicating the detuning $\Delta f/\frac{1}{2}B$. The horizontal projection of the vector represents the real component of the admittance, while its vertical projection represents the imaginary component. For an ordinary parallel-tuned circuit the admittance line is a vertical straight line (see Appendix I), and since in a zone near resonance the imaginary component is proportional to ω , this line can be provided with a linear frequency scale. If feedback is

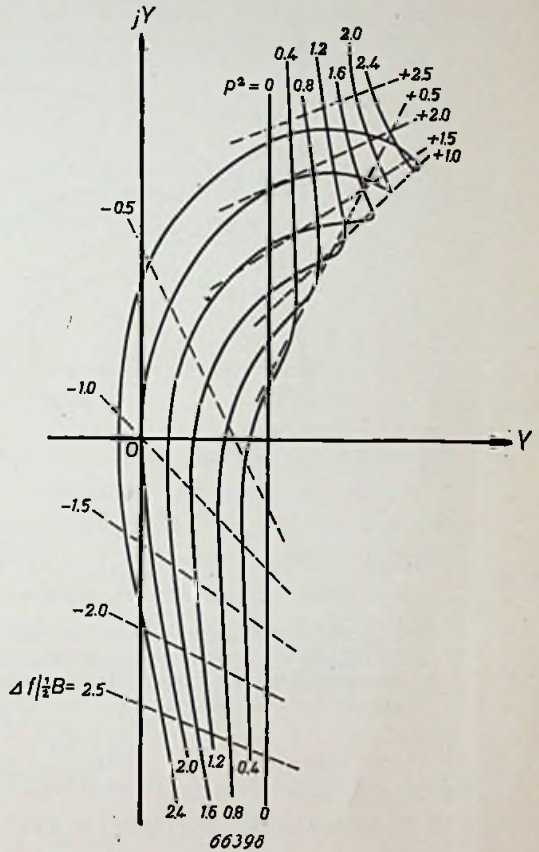


Fig. 76. Admittance curves of a grid circuit undamped by the anode-to-grid capacitance, with p^2 (a measure for the feedback) as parameter. Y at the abscissa stands for the real part of Y , and jY at the ordinate for the imaginary part of Y . The broken lines correspond to a constant detuning $\Delta f/\frac{1}{2}B$. The line for $\Delta f/\frac{1}{2}B = 0$ coincides with that for $p^2 = 0$. This diagram is derived from the construction of fig. 78.

present, the extremity of the Y_h' vector no longer lies on this straight line but on one of the curves of fig. 76.

Each of these curves shows the variation of eq. (120d) at a variable detuning, i.e. for various signal frequencies and at a fixed value of a para-

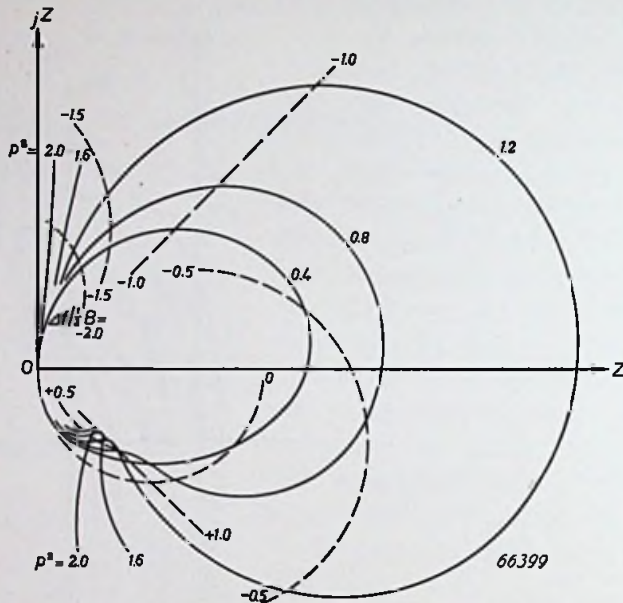


Fig. 77. Impedance curves derived from the admittance curves of fig. 76 by inversion, i.e. a simple geometric transformation by which straight lines are usually transformed into circles. Z at the abscissa stands for the real part of Z and jZ at the ordinate for the imaginary part of Z .

meter p_h^2 , which is a measure for the amount of feedback in stage h . To find this parameter, eq. (120d) is written:

$$\frac{Y_h'}{Y_h} = 1 + j\omega C_{ag} S' Z_h Z_{h+1}, \tag{120e}$$

which shows that the shape of the Y_h'/Y_h curve depends only on:

$$p_h^2 = \omega C_{ag} S' \hat{Z}_h \hat{Z}_{h+1}, \tag{121}$$

and on:

$$r_h = \frac{Q_h}{Q_{h+1}}. \tag{121a}$$

In fig. 76 the real component of Y becomes negative over a certain frequency range if $p_h^2 > 2$; this occurs first at the frequency at which the

circuits are detuned towards lower frequencies, so that an attenuation of $\sqrt{2}$ is obtained. At this frequency the circuit may become unstable if the critical value $p_h^2 = 2$ is exceeded.

The same result is obtained when the Nyquist criterion for the stability of feedback circuits is applied. According to this criterion the circuit may oscillate when in the feedback loop (grid circuit - valve - anode circuit - anode-to-grid capacitance) the gain is equal to unity at a phase shift of 0° or $n \cdot 360^\circ$, n being a whole number. This will be the case when:

$$S' Z_{h+1} \omega C_{ag} Z_h = 1$$

at a frequency such that the sum of the phase angles of the two circuit impedances is 90° , so that the phase shift due to $j\omega C_{ag}$ is compensated. When the two circuits are identical this condition is satisfied at a detuning of 45° , so that:

$$|Z| = \frac{\hat{Z}}{\sqrt{2}}.$$

The oscillatory condition is therefore:

$$\omega C_{ag} S' \hat{Z}_h \hat{Z}_{h+1} = 2.$$

The Y and Z curves of figs 76 and 77 apply to circuits which are affected by the C_{ag} of a valve loaded by a parallel-tuned circuit, the resonance frequency of which is the same as that of the grid circuit but which is not affected by feedback. In that case $(Z_{h+1})' = Z_{h+1} = Z_h$. In practice, however, several stages in cascade are used, intercoupled by circuits which are sometimes detuned and all of which are undamped by the C_{ag} of the following valve. For these conditions, eq. (120e) may be written:

$$\frac{Y_h'}{Y_h} = 1 - \frac{1}{\psi_h \cdot \frac{(Y_{h+1})'}{Y_{h+1}}}, \quad (120f)$$

in which

$$\psi_h = \frac{j \hat{Z}_r^2}{p_r^2 Z_h Z_{h+1}}, \quad (122)$$

where

$$p_r^2 = \omega C_{ag} S' \hat{Z}_r^2, \quad (123)$$

where \hat{Z}_r is the impedance of the "reference circuit" of the staggered tuning system (see Section 2.2).

By expressing $(Y_{h+1})'/Y_{h+1}$ again in terms of ψ_{h+1} and $(Y_{h+2})'/Y_{h+2}$, and so on, the expression for $(Y_{h+1})'/Y_{h+1}$ assumes the form of a continued fraction. When these continued fractions are worked out, \hat{Z}_r , the quantities p_h^2 and the circuit impedances Z_h will appear in the final result. Once the tuning frequencies, the amount of damping and the bandwidths

of all stages (without feedback) are known, the admittance curve of each of the undamped circuits is given for given values of p_n^2 . Conversely, a requirement imposed on the admittance diagram determines the maximum permissible value of p_r^2 if Z_r , S' and C_{ag} have the same values for all stages, as will often be the case.

6.3.3 Maximum permissible values of p^2

The methods for calculating maximum permissible values of p^2 will now be discussed in detail.

First, feedback will be assumed to be present only in one stage, the

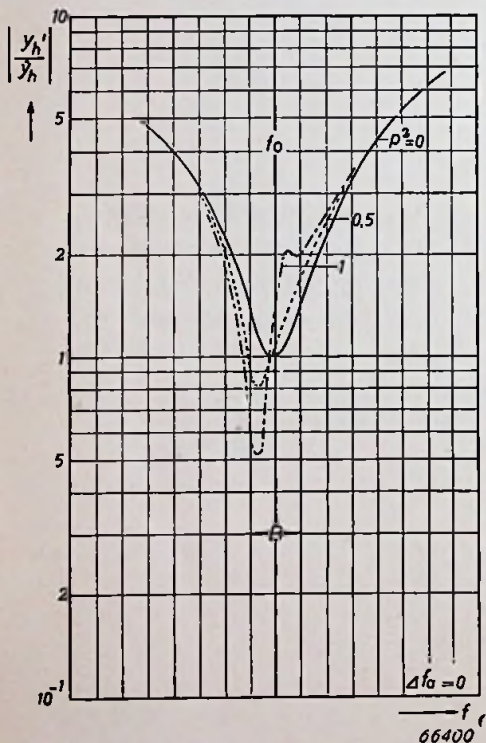


Fig. 78a. Response curves of an amplifying stage, the anode and grid circuits of which are tuned to the same frequency, for different values of p^2 .

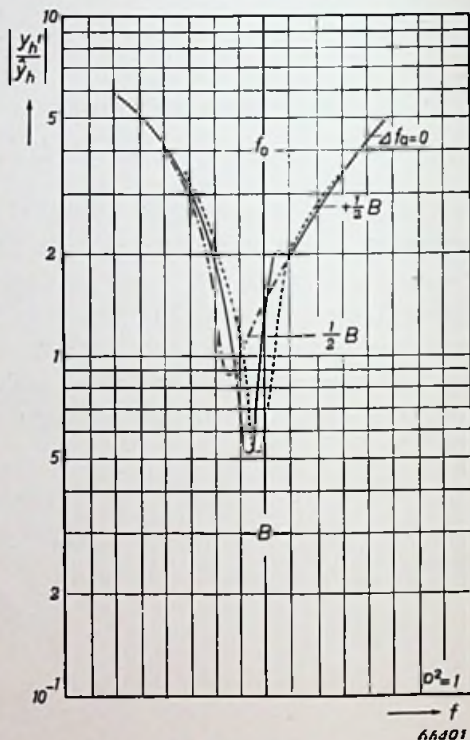


Fig. 78b. Response curves of an amplifying stage of which $p^2 = 1$, for different values of the detuning Δf_a of the anode circuit.

anode and grid circuits of which are synchronous and have the same bandwidth. The admittance curve of the grid circuit of such a stage has already been given in fig. 76. The permissible deviation of this curve from the

straight line (at $p^2 = 0$) depends on various conditions, but it is clear that p^2 must in any case remain sufficiently far below the limit value of 2.

In the case of $p^2 > 2$, the circuit will oscillate at the frequency at which the imaginary part of Y_h' is zero. This frequency is lower than the resonant frequency of the anode and grid circuits, as can be seen from fig. 76.

At $p^2 = 2$ the circuit is just bordering on instability, and it is clear that it is necessary to observe a certain margin of safety to avoid spontaneous oscillation and ensure a good response curve.

Fig. 78 shows the response curves for several values of p^2 . It appears from this figure that at $p^2 = 0.5$ the irregularities in the frequency response curve are not very pronounced and a safety factor of about 4 will therefore suffice in many cases. When, however, the gain of the stage is varied by controlling the mutual conductance of the valve, the detuning and variation of bandwidth may become excessive at $p^2 = 0.5$, so that a higher safety factor will be required. The detuning Δf_{ag} by the anode-to-grid capacitance may be roughly determined by taking the Miller capacitance as:

$$C_M = C_{ag} \cdot G = C_{ag} S \hat{Z}_{h+1},$$

hence

$$\frac{\omega C_M}{\hat{Y}_h} = p^2.$$

At a detuning of $\frac{1}{2}B$ the value of \hat{Y}_h is equal to $\omega \Delta C$ (cf. Appendix 1, fig. 107), and since

$$\frac{\Delta C_1}{\Delta C_2} = \frac{1}{2} \cdot \frac{\Delta f_1}{\Delta f_2},$$

the detuning caused by the Miller capacitance is:

$$\Delta f_{ag} = \frac{1}{4} B \cdot p^2.$$

The limit of stability can also be calculated from fig. 79a, i.e. the vector diagram from which fig. 76 was derived. The construction of fig. 79a follows from eq. (120d). A vector of length $\omega C_{ag} S' Z_{h+1}$, which is perpendicular to the Z_{h+1} vector, must be added to the Y_h vector. Now Y_{h+1} is identical to Y_h — the locus of which is a straight line — so that Z_{h+1} (derived from Y_{h+1} by inversion) is represented by a circle. The construction of Z_{h+1} is based on the fact that its phase angle is numerically equal but of opposite sign to the phase angle of Y_{h+1} . The locus of the vector $j\omega C_{ag} S' Z_{h+1}$ is also a circle, but with the point of origin shifted over 90° .

As this vector must be added to the Y_h vector, the origin of this circle (the dotted circle of fig. 79a) lies on the Y_h line. The maximum length of the vector to be added is $\omega C_{ag} S' \hat{Z}_{h+1}$, so that the diameter of the dotted circle must be:

$$\omega C_{ag} S' \hat{Z}_{h+1} = p^2 \hat{Y}_h.$$

It is obvious that the real part of Y_h' cannot become zero or negative unless $\frac{1}{2} p^2 \hat{Y}_h \geq \hat{Y}_h$, i.e. unless $p^2 \geq 2$.

The changes to which the admittance curves of the input circuit (with feedback) are subject when the anode and grid circuits are staggered, can be investigated from the construction of this diagram.

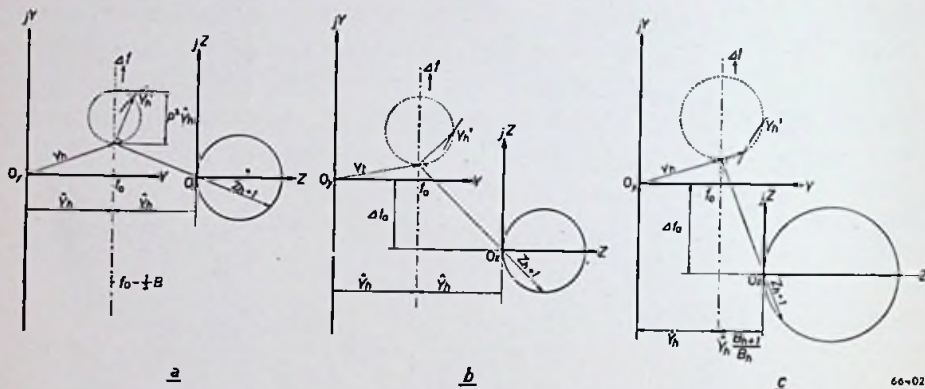


Fig. 79. Vector diagram for determining the maximum permissible value of p^2 , (a) in the case where the anode and grid circuits have the same bandwidth and are tuned to the same frequency, (b) in the case where the anode and grid circuits have the same bandwidth but are tuned to different frequencies, and (c) in the case where the anode and grid circuits have different bandwidths and are tuned to different frequencies.

If the anode circuit is detuned by an amount Δf_a with respect to the grid circuit, the origin O_z of fig. 79a is shifted vertically with respect to O_y over a distance Δf_a (see fig. 79b). The only change in fig. 76 then consists of an equally large displacement of O in the opposite direction, but the changes of fig. 78a are somewhat more complicated (see fig. 78b). In general it may be said that the detuning makes the response curve slightly more regular. The permissible value of p^2 does not, however, increase noticeably until Δf_a exceeds the value of B . When the anode circuit is tuned to a higher frequency the detuning of the grid circuit caused by the Miller capacitance decreases, whereas, when the anode circuit is tuned to a lower frequency, the damping of the grid circuit increases, and the risk of instability is reduced, though at the expense of a greater detuning.

A second change to which fig. 79a is subject in the case of staggered tuning is manifest in the change of bandwidth of the anode circuit compared with that of the grid circuit. This results in a change of the Δf_a scale of Z_{h+1} (see fig. 79c). The curves of fig. 76 are now expanded or contracted in the vertical direction, but it is clear that in this case, too, instability is likely to occur when $p_h^2 \geq 2$.

It is therefore advisable also in the case of staggered tuning to choose a value of p_h^2 which has a safety factor of, say, 4 with respect to the limit value of 2.

It is true that there are cases which are stable although $p^2 > 2$, but it is then necessary to avoid a particular value of the anode circuit detuning Δf_a . These frequencies then form the unstable region of the grid and anode circuits. This region increases with the value of p^2 and disappears at $p^2 < 2$.

If in a circuit $p^2 > 2$ it may occur that the unstable region is encountered when the set is being trimmed. During the trimming of a particular circuit the other circuits should then be damped to avoid this troublesome phenomenon.

6.3.4 Staggered tuning

In practice the staggered circuits are given different bandwidths by varying the values of \hat{Z}_h , the circuit capacitances remaining practically unchanged, i.e.:

$$\bar{Z}_h = \frac{\hat{Z}_r}{\sin \alpha_h},$$

hence:

$$p_h^2 = \frac{\omega C_{ag} S' \hat{Z}_r^2}{\sin \alpha_h \sin \alpha_{h+1}} = \frac{p_r^2}{\sin \alpha_h \sin \alpha_{h+1}},$$

in which α_h is the staggering angle of circuit h . It follows from this expression that the entire amplifier will not have the desired stability unless n conditions of the form:

$$p_r^2 \leq p_h^2 \sin \alpha_h \sin \alpha_{h+1} \quad (124)$$

are satisfied in which $p_h^2 \approx 0.5$. In these formulae the staggering angles of two successive stages will always be found, and to avoid the necessity of an extremely low value of p_r^2 , it is advisable to arrange the amplifier such that slightly and heavily detuned circuits follow each other alternately. Should this be impossible, then provision should at least be made for the successive stages to be alternately detuned, as far as possible, to either side of Z_r , the permissible value of p_h^2 being thereby slightly

increased. The fact is that if the limit of stability must necessarily be approached, more is to be feared from the reduction of damping than from the detuning caused by the feedback. In that case the grid circuit should be tuned to a higher frequency rather than the anode circuit (cf. fig. 78*b*).

It will now be investigated how the vector diagram of fig. 79 has to be constructed if the circuit $h+1$ is also the input circuit of an amplifier stage and is undamped via the anode-to-grid capacitance C_{ag} . The locus of the vector $(Z_{h+1})'$ is then no longer a circle, but one of the curves of fig. 77, corresponding to the value of $(p_{h+1})^2$. Since it is desirable that not only the response curve of circuit h but also that of circuit $h+1$ has a regular form, the value of $(p_{h+1})^2$ must be chosen fairly low. According to fig. 77, this will result in the locus of the $(Z_{h+1})'$ vector differing but little from that of a circuit without feedback and having a maximum impedance of

$$\frac{\hat{Z}_{h+1}}{1 - \frac{1}{2}(p_{h+1})^2}.$$

This expression will become clear when the minimum value of $(Y_{h+1})'$ is calculated from eq. (120*e*) (see also fig. 76). In the construction the $(Z_{h+1})'$ diagram is approached by the circular diagram of the vector of the above-mentioned expression.

If it is desired to give circuit h a feedback parameter p_h^2 , the stage in which this circuit h is connected to the grid of the valve must be designed for a smaller value of p^2 , viz.:

$$p^2 = \omega C_{ag} S' \hat{Z}_h \hat{Z}_{h+1}.$$

Since the actual amount of feedback is determined by:

$$p_h^2 = \omega C_{ag} S' \hat{Z}_h (\hat{Z}_{h+1})' = \omega C_{ag} S' \hat{Z}_h \cdot \frac{\hat{Z}_{h+1}}{1 - \frac{1}{2}(p_{h+1})^2},$$

the condition

$$p^2 = p_h^2 \left\{ 1 - \frac{1}{2}(p_{h+1})^2 \right\}$$

must be satisfied. Since $\frac{1}{2}(p_{h+1})^2$ is usually kept well below unity, p^2 need not differ appreciably from the chosen value of p_h^2 . An exact calculation of the required value of p_h^2 according to the rather complicated method indicated at the end of Section 6.3.2 is therefore not necessary, and in practice it will suffice to determine p_h^2 as if there were no feedback in the other stages and to use the value thus found in all further calculations. It should, however, be taken into account that the product $\omega C_{ag} S' \hat{Z}_h \hat{Z}_{h+1}$ is lower than the value of p_h^2 that determines the amount of feedback in stage h , by a factor $1 - \frac{1}{2}(p_{h+1})^2$.

It should be realized that this method becomes less accurate when heavy feedback is present. As a result of this feedback the difference between $(Z_{h+1})'$ and Z_{h+1} will then be considerable, so that the response curve of this circuit will deviate greatly from the desired shape. As a rule measures will then be taken to compensate these deviations, at least partially, by detuning and additionally damping circuit $h+1$, thus rendering $(Z_{h+1})'$ near its resonance again almost equal to the value prescribed by the staggering scheme. In this case also ϕ_h^2 can therefore be calculated as if feedback were present in stage h only. It will then, necessary be however, to fill in the corrected value for (Z_{h+1}) , which is almost equal to the value required by the staggering scheme.

6.3.5 Maximum permissible gain

It will now be assumed that the maximum permissible value of ϕ^2 has been determined in accordance with the preceding formulae. The maximum permissible gain G_{max} of each stage will then obviously be determined by the characteristics of the valve. For a staggered amplifier it follows from eq. (123) that:

$$(S'Z_r)^2 = \phi_r^2 \cdot \frac{S'}{\omega C_{ag}} = \phi_r^2 \cdot \frac{S_{max}}{2\pi f_r C_{ag}}. \quad (125)$$

This expression can be further simplified by introducing the concept of **stability reference frequency** f_s :

$$f_s = \frac{S_{max}}{2\pi C_{ag}}, \quad (126)$$

which finally gives:

$$G_{rmax} = \phi_{rmax} \sqrt{\frac{f_s}{f}}. \quad (127)$$

This expression shows that f_s is the frequency at which G_{max} would be equal to ϕ_{max} , assuming the above formulae to be valid even at the high frequencies concerned. This assumption, however, is by no means permissible, since at these frequencies the "dynamic value" of C_{ag} , which determines the feedback, is no longer equal to the "static value", valid at low frequencies. f_s is, therefore, only an extrapolated value by means of which the permissible gain, in the range for which eq. (125) is valid, can be determined.

In Section 2.2.2 it was shown that, at the mid frequency, G_h , i.e. the gain of stage h , is equal to G_r , the gain of a stage with the reference circuit

connected to the anode of the valve. Substitution of the value of p_r from eq. (124) therefore gives:

$$G_h \leq p_h \sqrt{\sin \alpha_h \sin \alpha_{h+1}} \cdot \sqrt{\frac{f_s}{f}}. \quad (128a)$$

As already shown, a reasonable value for p_h^2 is, say, 0.5. In practice $p_h \sqrt{\sin \alpha_h \sin \alpha_{h+1}}$ can be about 0.5. This roughly amounts to:

$$G_{h\max} \approx 0.5 \sqrt{\frac{f_s}{f}}, \quad (128b)$$

or (at the mid frequency!), for an amplifier with n stages:

$$G_{\text{tot max}} \approx \left(0.5 \sqrt{\frac{f_s}{f}}\right)^n. \quad (128c)$$

Example

What will be the maximum permissible gain per stage of an I.F. amplifier for 35 Mc/s with a flat staggered quintuple if valves EF 80 are used and the circuit is also to remain stable (with a safety factor 4) during trimming?

According to Table 3 (p. XX) the smallest value of $\sin \alpha_h$ is 0.31. Combining this value with $\sin \alpha_{h+1} = 1$ gives:

$$\sqrt{\sin \alpha_h \sin \alpha_{h+1}} = 0.56.$$

Table 1 (p. 168) shows that, for the EF 80, $f_s = 17 \cdot 10^4$ Mc/s, so that:

$$G_{h\max} = 0.7 \cdot 0.56 \sqrt{\frac{17 \cdot 10^4}{35}} = 27.$$

If the sequence of the circuits were chosen less favourable so that the two values $\sin \alpha_h = 0.31$ and $\sin \alpha_{h+1} = 0.31$ are combined, the maximum permissible gain would be considerably less, viz.:

$$G_{h\max} = 0.7 \cdot 0.31 \sqrt{\frac{17 \cdot 10^4}{35}} = 15.$$

A slightly higher value of $G_{h\max}$ could be afforded in this case, since the limit of instability cannot be approached unless both circuits are considerably mistuned.

6.3.6 Coupling by means of band-pass filters (I.F. transformers)

It would as a rule result in a reduction of the maximum permissible gain if the same stringent requirements were imposed on circuits coupled by band-pass filters as on those coupled by single-tuned circuits.

This may be illustrated by the following example. The transimpedance of a band-pass filter with $q = 0$ is also zero, and so is the gain of an amplifier containing such stages. The input and output impedances of the band-pass filters, however, differ from zero, so that the circuit may become unstable even at zero gain.

If the circuit is required to remain stable during trimming (without special precautions being taken) the maximum permissible gain per stage is smaller by a factor of at least 2 than in single tuned circuits.

In the most unfavourable case the mutual detuning of the grid and anode circuits of one particular valve is such that the risk of spurious oscillations is greatest, whilst the other circuits are detuned to such an extent that their influence can be disregarded. The condition for stability is then:

$$p^2 = \omega C_{ag} S R_p R_s < 2.$$

If all band-pass filters are identical and symmetrical ($R_p = R_s = R$), as is often the case with I.F. transformers in the sound channel of T.V. receivers, the maximum gain per stage is:

$$G_{max} = SR \cdot \frac{q}{1 + q^2} = p \cdot \frac{q}{1 + q^2} \cdot \sqrt{\frac{f_s}{f}}. \tag{127a}$$

The fraction $q/(1 + q^2)$ is at the utmost 0.5, so that the maximum permissible gain is indeed smaller by a factor 2.

To avoid instability during trimming special measures are often taken, such as heavily damping all circuits except that which is being trimmed, or avoiding the unstable region. In that case higher values of p^2 are permissible and either the risk of instability at correct tuning or the irregularities in the response of the amplifying stage caused by the feedback are then taken as the criterion for the maximum permissible value of p^2 .

In order to be able to judge the latter irregularities, it is necessary to calculate the output admittance curve at the input band-pass filter, the influence of the feedback being taken into account. It will as a rule suffice to determine the output admittance of this band-pass filter, which can be done

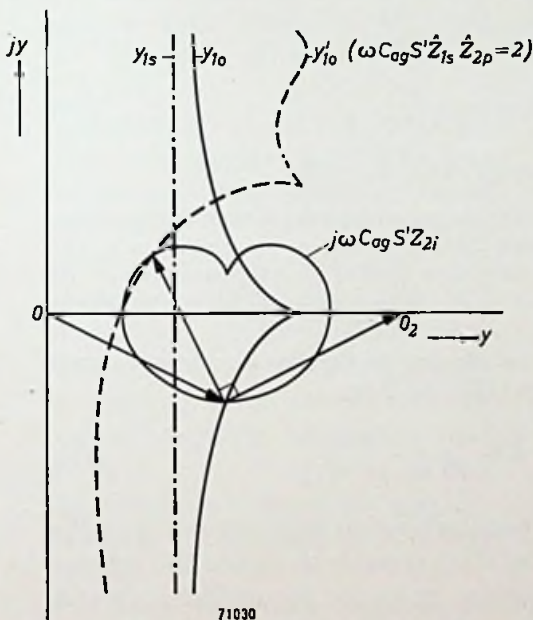


Fig. 80. Polar diagram of the output admittance of a band-pass filter at the input of an I.F. stage, with and without feedback, in which $q_1 = q_2 = 1$; $r_1 = r_2 = r = 1$ and $\omega_{1p} = \omega_{1s} = \omega_{2p} = \omega_{2s}$.

similarly to the construction of fig. 76 according to fig. 79.

An example of such a polar diagram, with and without feedback, is given in fig. 80.

This procedure has the drawback of being rather cumbersome. A less accurate method that saves much time consists in roughly determining the magnitude of the maximum relative change to which the Y_h vector is subject when the feedback admittance is taken into account. In the case of a single circuit, the relation

$$|Y_h' - Y_h| : |Y_h| = 0.5$$

(at $p^2 = 0.5$) was taken to be permissible.

It may now be assumed that the permissible ratio is of the same order when the coupling consists of a band-pass filter, Y_h then representing the output admittance of this filter at the grid side.

In order to apply this procedure to stagger-damped band-pass filters of which $Q_p = \infty$, the admittances Y_i and Y_o of such a band-pass filter must first be expressed in terms of the quantities x_s and q_s , which are related to the secondary only, namely:

$$Y_i = \hat{Y}_s \frac{C_1}{C_2} \left(jx_s + \frac{q_s^2}{1 + jx_s} \right), \quad (129)$$

and

$$Y_o = \hat{Y}_s \left(1 + jx_s + \frac{q_s^2}{jx_s} \right), \quad (130)$$

in which

$$\hat{Y}_s = R_s, \quad x_s = \beta_s Q_s \quad \text{and} \quad q_s = k Q_s.$$

From these formulae it follows that the output admittance is the minimum when $x_s = \pm q_s$. For the frequencies at which this is the case, at a variation of x_s , the phase of Y_o changes much more quickly than that of Y_i . Y_o' passes through its minimum value in close proximity to $|x_s| = q_s$, which — as far as stability is concerned — is the most critical area.

From the staggering scheme it can easily be derived that, for the reference circuit in this region, $x_r \approx 1$. Hence, from eqs (129) and (130):

$$|Z_h| \cdot |Z_{h+1}| \approx \hat{Z}_r^2 \cdot \frac{\sqrt{1 + \sin^2 \alpha_{h+1}}}{\sin \alpha_h \cdot \sin \alpha_{h+1}}. \quad (131)$$

It is clear that the maximum permissible gain largely depends on the staggering scheme in this case also. It is possible to choose this scheme so that eq. (131) assumes its minimum value for the critical stages. A rough calculation in which the mean value of $\sin \alpha$ is taken to be approximately 0.7 gives:

$$G_{\max} \approx 0.8 \sqrt{\frac{I_s}{I}}, \quad (128d)$$

which appears to be slightly higher than the value of G_{\max} found for the case where single circuits are used. It should, be realized however, that in the deduction of the formula for single circuits the exact point of the

response curve was considered at which the effect of the feedback was most detrimental, whereas in this case some point of the response curve "in the proximity of" this point is considered. An additional safety factor must therefore be observed, so that the maximum permissible gain is actually slightly lower than that of single circuits.

The disadvantage attached to the above procedure for quickly estimating the maximum permissible gain is that the results are rather vague and no insight is obtained into the difficulties which may be experienced at a slightly larger gain. It is therefore desirable to have a simple method for ascertaining at what gain the circuit becomes unstable when all circuits are correctly tuned. This can be done by means of the following data:

- (a) The polar diagram of Z_o of the band-pass filter at the grid side;
- (b) the polar diagram of Z_i of the band-pass filter at the anode side.

Both diagrams must be provided with a frequency scale. The two diagrams are then placed on top of each other so that the poles O coincide, whilst the real axis of the anode impedance leads over 90° . When doing this, the reflected image of the grid impedance diagram must be taken, i.e. the direction of the real axis remains unchanged, but $+j$ and $-j$ are interchanged, so that the frequency scale of this diagram now runs in the opposite direction (see fig. 81).

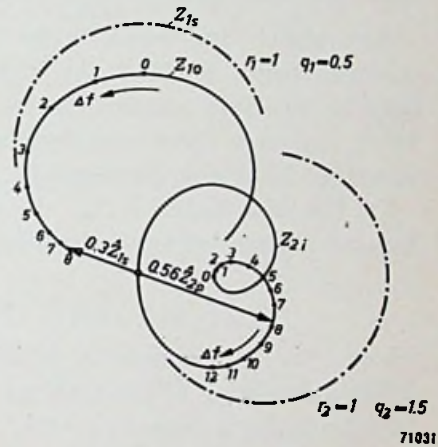


Fig. 81. Polar diagrams of Z_o and Z_i from which the maximum permissible gain can be ascertained. $r = Q_s |Q_p| = 0.5$. The circuit becomes unstable when:

$$\omega C_{ag} S' 0.3 \hat{Z}_{1s} 0.56 \hat{Z}_{2p} = 1,$$

or

$$\omega C_{ag} S' \hat{Z}_{1s} \hat{Z}_{2p} = \frac{1}{0.3 \cdot 0.56}.$$

A line is then drawn through the origin, so as to intersect the two diagrams at the same frequency. This is the frequency at which the circuit starts to oscillate provided the gain is sufficiently high. Denoting the absolute magnitude of the two impedances for this frequency by $|Z_a'|$ and $|Z_g'|$ respectively, then the condition for stability becomes:

$$\omega C_{ag} S |Z_a'| |Z_g'| < 1. \tag{132}$$

This method can be applied also when the coupling network between

the stages is of a more complex nature and consists, for example, of a circuit with wave traps for suppressing undesired signals.

The above method can easily be derived from the Nyquist criterion, in which case the polar diagrams of the complex gain $\gamma = E_a/E_g$ and of the complex feedback factor β are determined. For the circuit to become unstable it is necessary that the sum of the phase angles of these two diagrams be zero, whilst the product $|\gamma \cdot \beta|$ must moreover be equal to or exceed unity at the frequency at which this condition is satisfied.

These conditions can be expressed by:

$$\gamma\beta = \omega C_{ag} S |Z_a'| |Z_g'| \geq 1.$$

6.3.7 Deviations at higher frequencies

The above comments apply to I.F. amplifiers operating at frequencies below 30 Mc/s. At higher frequencies however, it is necessary to take into account the fact that the dynamic feedback capacitance C_{ag}' may differ considerably from the static value C_{ag} (see Other Forms of Feedback, Section 6.6).

In the first instance C_{ag}' decreases with the frequency and finally assumes a negative value. In this range:

$$C_{ag}' = C_{ag} \left\{ 1 - \left(\frac{f}{f_s'} \right)^2 \right\}, \quad (133)$$

where f_s' is the frequency at which C_{ag}' is zero.

The calculation of the maximum permissible gain could be corrected by introducing a quantity f_s which depends on the signal frequency. It is, however, simpler to determine f_s from the static value of C_{ag} and to correct the equation for the maximum permissible gain as follows:

$$G_{\max} = \phi_{\max} \sqrt{\frac{f_s}{f \left\{ 1 - \left(\frac{f}{f_s'} \right)^2 \right\}}}. \quad (128d)$$

The values of f_s' are not valve constants, but also depend to a certain extent on the wiring, the valve holders, etc. For an EF 80 tube $f_s' \approx 70$ Mc/s in normal circuits.

At frequencies exceeding f_s' the maximum permissible gain G_{\max} rapidly decreases. Since the sign of the feedback admittance is now reversed, damping occurs at those detunings at which originally regeneration occurred, and vice versa.

When the signal frequency is further increased the transit time τ usually also starts to play a part in the stability condition. Although the magnitude of S' remains practically unchanged, the phase shift may become quite considerable at frequencies from 100 Mc/s to 200 Mc/s. It is

due to this phase shift that the distortion of the response curve caused by the feedback is of a more symmetrical nature. When $f\tau = \frac{1}{2}$ this distortion is purely symmetrical.

6.4 FEEDBACK BY THE CATHODE-TO-GRID ADMITTANCE

The investigation of the effect of feedback by the cathode-to-grid admittance is again based on equations (115) and (117). The admittances Y_3 and Y_5 (see fig. 72) are assumed to be zero, so that ρ and Y_7 also become zero. This gives:

$$Y_0' = Y_1 = Y_0,$$

and
$$F_s = \frac{Y_0}{Y_0 + Y_4 + S_k} \approx \frac{1}{1 + S_k Z_k \left(1 + \frac{j\omega C_{gk}}{S_k}\right)}. \quad (134)$$

The input admittance is thus:

$$Y_i' = Y_2 + \frac{Y_0 Y_4}{Y_0 + Y_4 + S_k}. \quad (135)$$

Eq. (135) is now applied to a few practical circuits, where the input admittance of the valve is governed by:

- the capacitance C_{g1} of the control grid to earth (Y_2),
- the capacitance C_{g1k} of the control grid to the cathode (Y_4),
- the capacitance C_{g1g2} of the control grid to the screen grid (Y_2),
- the conductance g_{g1} of the control grid to earth (Y_2),
- the conductance of the control grid to the cathode (Y_4), i.e. mainly the transit time damping g_τ , and
- the impedance in the cathode lead, consisting of a real component and an imaginary component connected in parallel, i.e.:

$$\frac{1}{Z_0} = Y_0 = g_0 + jb_0.$$

Eq. (135) can be developed to:

$$Y_i' = g_{g1} + j\omega(C_{g1} + C_{g1g2}) + \frac{g_\tau g_0 - \omega C_{g1k} b_0}{g_0 + g_\tau + S_k + j\omega C_{g1k} + jb_0} + j \frac{\omega C_{g1k} g_0 + b_0 g_\tau}{g_0 + g_\tau + S_k + j\omega C_{g1k} + jb_0}.$$

By eliminating the imaginary components from the denominator the third term becomes:

$$\frac{(g_\tau g_0 - \omega C_{g1k} b_0) \{ (g_0 + g_\tau + S_k) - j(\omega C_{g1k} + b_0) \}}{(g_0 + g_\tau + S_k)^2 + (\omega C_{g1k} + b_0)^2},$$

and the fourth term becomes:

$$j \frac{(\omega C_{g1k} g_0 + b_0 g_\tau) \{ (g_0 + g_\tau + S_k) - j(\omega C_{g1k} + b_0) \}}{(g_0 + g_\tau + S_k)^2 + (\omega C_{g1k} + b_0)^2}.$$

The input damping is thus ¹⁾

$$g_i' = g_{g1} + \frac{(g_{\tau}g_0 - \omega C_{g1k}b_0)(g_0 + g_{\tau} + S_k) + (\omega C_{g1k} + b_0)(\omega C_{g1k}g_0 + b_0g_{\tau})}{(g_0 + g_{\tau} + S_k)^2 + (\omega C_{g1k} + b_0)^2},$$

which may also be written as:

$$g_i' = g_{g1} + \omega C_{g1k} \cdot \frac{\omega C_{g1k}g_0 - b_0S_k}{(g_0 + g_{\tau} + S_k)^2 + (\omega C_{g1k} + b_0)^2} + \\ + g_{\tau} \cdot \frac{g_0^2 + b_0^2 + g_0(S_k + g_{\tau})}{(g_0 + g_{\tau} + S_k)^2 + (\omega C_{g1k} + b_0)^2}. \quad (136)$$

The magnitude of the imaginary component of Y_i' is now:

$$(Y_i')_{\text{imaginary}} = \omega C_{g1} + \omega C_{g1g2} + \\ + \frac{(\omega C_{g1k} + b_0)(\omega C_{g1k}b_0 - g_0g_{\tau}) + (\omega C_{g1k}g_0 + b_0g_{\tau})(g_0 + g_{\tau} + S_k)}{(g_0 + g_{\tau} + S_k)^2 + (\omega C_{g1k} + b_0)^2},$$

which corresponds to an input capacitance of:

$$C_i' = C_{g1} + C_{g1g2} + C_{g1k} \cdot \frac{g_0(g_0 + S_k) + b_0 \left\{ b_0 + \omega C_{g1k} + (g_{\tau} + S_k) \cdot \frac{g_{\tau}}{\omega C_{g1k}} \right\}}{(g_0 + g_{\tau} + S_k)^2 + (\omega C_{g1k} + b_0)^2}. \quad (137)$$

By means of eqs (136) and (137) it will now be shown how the various cathode impedances influence the input circuit. Once the input conductance g_i has been calculated from eq. (136) for a particular case, the simplified expression thus obtained will be used to calculate the input conductance when other effects are considered. The following effects are of importance:

- (1) the damping caused by the self-inductance of the cathode lead,
- (2) the compensation of this damping when using an additional cathode capacitor,
- (3) the variation of the input capacitance by incorporating a small resistance in the cathode lead,
- (4) the variation of g_i' and C_i' if a resistor shunted by a fairly small capacitor is included in the cathode lead.

6.4.1 Self-inductance in the cathode lead

It is assumed that a very small self-inductance L_k is present in the cathode lead, so that:

$$\omega L_k S_k \ll 1 \quad \text{or} \quad \left| \frac{S_k}{b_0} \right| \ll 1,$$

while

$$\left| \frac{g_{\tau}}{b_0} \right| < \left| \frac{S_k}{b_0} \right| \ll 1.$$

¹⁾ It is only in this section that, in analogy with the convention of p. 85, the input damping is denoted by g_i' .

If the frequencies for which

$$\omega^2 L_k S_k C_{g1k} \ll 1 \quad \text{or} \quad \left| \frac{\omega C_{g1k}}{b_6} \right| \ll 1$$

are considered, i.e. only the frequency range below the resonance frequency of L_k - C_{g1k} , then, since g_6 is zero, according to eq. (136) the **input conductance** is:

$$g_i' = g_{g1} + \frac{g_\tau b_6^2 - \omega C_{g1k} b_6 S_k}{b_6^2 \left(\frac{g_\tau^2}{b_6^2} + \frac{2g_\tau S_k}{b_6^2} + \frac{S_k^2}{b_6^2} + \frac{\omega^2 C_{g1k}^2}{b_6^2} + \frac{2\omega C_{g1k}}{b_6} + 1 \right)}$$

The fractions with the square of b_6 in the denominator are very small compared with unity and may therefore be ignored, which gives:

$$g_i' \approx g_{g1} + \left(g_\tau - \frac{\omega C_{g1k} S_k}{b_6} \right) \left(1 - \frac{2\omega C_{g1k}}{b_6} \right),$$

or by putting $b_6 = -1/\omega L_k$:

$$g_i' = g_{g1} + (g_\tau + \omega^2 L_k C_{g1k} S_k) \left(1 + 2 \frac{f^2}{f_{g1k}^2} \right), \quad (136a)$$

where

$$f_{g1k} = \frac{1}{2\pi \sqrt{L_k C_{g1k}}}$$

In eq. (136a) $\omega^2 L_k C_{g1k} S_k$ represents the "feedback damping" caused by

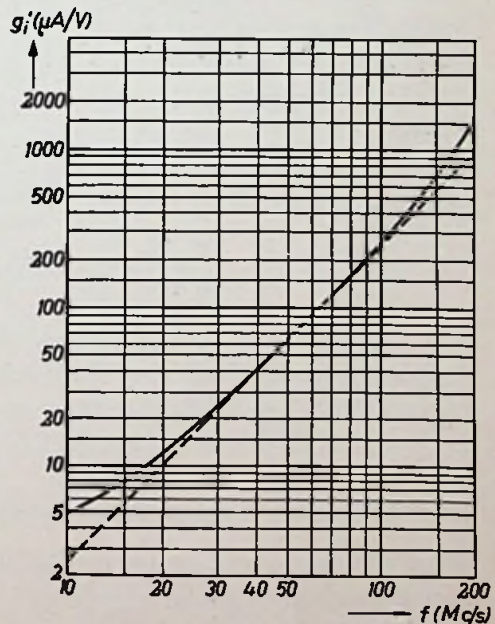


Fig. 82. Example of the frequency-dependence of g_i' . If the relation were truly quadratic this dependence would be represented by the broken line.

the self-inductance in the cathode lead. To a first approximation the input conductance g_i' is a second-power function of the frequency, but the term g_{g1} and the second factor between brackets give rise to deviations at both low and high frequencies. Both these deviations result in an increase of g_i ; cf. fig. 82.

Provided the frequency differs sufficiently from f_{g1k} (i.e. the resonant frequency of L_k-C_{g1k}) without, however, being too low, then:

$$g_i' \approx \omega^2 S_k (\tau^2 F_\tau + C_{g1k} L_k),$$

where τ represents the transit time of the electrons from the cathode to the control grid and the factor F_τ depends on the ratio of the distances between g_2-g_1 and g_1-k and on the ratio of the effective potential in the plane of g_2 to that in the plane of g_1 .

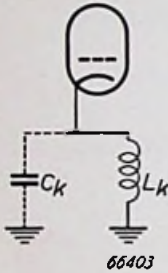


Fig. 83. Cathode lead having a self-inductance L_k and a stray capacitance C_k .

Another cause of the increase of g_i' at high frequencies is the capacitance C_k' from cathode to earth (e.g. the cathode-to-filament capacitance). A calculation of b_g for the circuit of fig. 83 gives:

$$b_g = \omega C_k - \frac{1}{\omega L_k} = - \frac{1}{\frac{\omega L_k}{1 - \omega^2 L_k C_k}}$$

The deduction of eq. (136a) is obviously still valid, provided ωL_k is replaced by:

$$\frac{\omega L_k}{1 - \frac{f^2}{f_k^2}},$$

where

$$f_k = \frac{1}{2\pi\sqrt{L_k C_k}},$$

which gives:

$$g_i' = g_{g1} + \left\{ g_\tau + \frac{\omega^2 C_{g1k} L_k S_k}{1 - \frac{f^2}{f_k^2}} \right\} \left\{ 1 + \frac{2 \frac{f^2}{f_{g1k}^2}}{1 - \frac{f^2}{f_k^2}} \right\}. \tag{136b}$$

This shows that both the "feedback damping" and the deviation due to the factor $(1 + 2f^2/f_{g1k}^2)$ increase as the frequency f_k (i.e. the resonant frequency of L_k-C_k) is approached.

6.4.2 Reducing the conductance by means of a cathode capacitor

An undamped grid circuit can be obtained by incorporating an additional capacitor C_k' in the cathode lead (see fig. 84) and can be investigated similar to the procedure in Section 6.4.1.

It is clear that in this case:

$$\frac{1}{b_g} = -\omega L_k \left(1 - \frac{1}{\omega^2 L_k C_k'} \right).$$

Disregarding the small deviations and putting

$$fk' = \frac{1}{2\pi\sqrt{L_k C_k'}},$$

from eq. (136a) the input conductance is found to be:

$$g_i' = g_{g1} + g_\tau + \omega^2 C_{g1k} L_k S_k \left(1 - \frac{(fk')^2}{f^2} \right). \quad (136c)$$

Complete compensation of the damping due to the input conductance at a frequency f is obtained by tuning the cathode lead to a frequency slightly above f , namely to:

$$f \sqrt{\frac{g_l + g_\tau}{g_l}}.$$

When this limit is approached the amplifier will obviously show a tendency to oscillate; cf. fig. 85.

In this circuit also the capacitance C_k of the cathode to earth has an adverse effect. This may

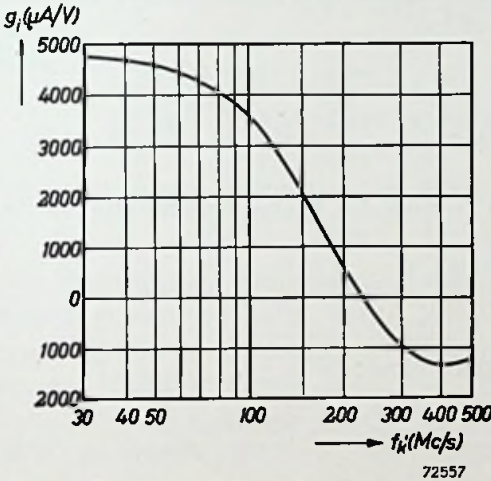


Fig. 85. Example of the influence of f_k' on g_i at $f = 200$ Mc/s.

be explained, by means of fig. 86, from which follows:

$$b_g = \omega C_k - \frac{1}{\omega L_k \left(1 - \frac{1}{\omega^2 L_k C_k'} \right)},$$

so that, in analogy with eq. (136c):

$$g_i' = g_{g1} + g_\tau + \omega^2 C_{g1k} L_k S_k \cdot \frac{1 - \frac{(fk')^2}{f^2}}{1 - \frac{f^2}{fk'^2} \cdot \left(1 - \frac{(fk')^2}{f^2} \right)}. \quad (138)$$

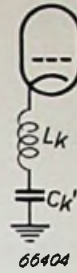


Fig. 84.

Cathode lead the self-inductance L_k of which is compensated by an additional capacitor C_k' .

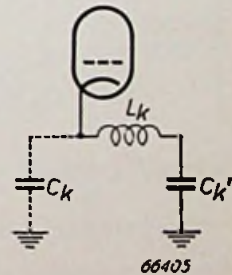


Fig. 86. Circuit similar to that of fig. 84, in which the stray capacitance C_k is also indicated.

Hence

$$g_i' = g_{g1} + g_\tau - g_t \cdot \frac{\Psi}{1 + \Psi \cdot \frac{f^2}{f_k^2}}, \quad (136d)$$

in which

$$\Psi = \frac{(fk)^2 - f^2}{f^2}.$$

For frequencies higher than f_k it becomes difficult to render Ψ sufficiently large to ensure satisfactory compensation. The required high value of the cathode impedance then increases the difficulties caused by the anode-to-cathode capacitance C_{ak} (see Section 6.5).

6.4.3 Small resistance in the cathode lead

From eq. (137) the **input capacitance** of a valve with very small self-inductance in the cathode lead is:

$$C_i' = C_{g1} + C_{g1g2} + C_{g1k} \cdot \frac{b_0^2 \left\{ 1 + \frac{\omega C_{g1k}}{b_0} + \frac{(g_\tau + S_k)g_\tau}{b_0 \omega C_{g1k}} \right\}}{b_0^2 \left\{ \frac{g_\tau^2}{b_0^2} + 2 \frac{g_\tau S_k}{b_0^2} + \frac{S_k^2}{b_0^2} + \frac{\omega^2 C_{g1k}^2}{b_0^2} + \frac{2 \omega C_{g1k}}{b_0} + 1 \right\}}.$$

As in the calculation of g_i' in Section 6.4.1, the denominator of the third term may be taken to equal

$$1 + \frac{2\omega C_{g1k}}{b_0},$$

so that replacement of b_0 by $-1/\omega L_k$ gives:

$$C_i' = C_{g1} + C_{g1g2} + \frac{C_{g1k} (1 - \omega^2 L_k C_{g1k})}{1 - 2\omega^2 L_k C_{g1k}} - \frac{L_k g_\tau (g_\tau + S_k)}{1 - 2\omega^2 L_k C_{g1k}},$$

whence:

$$C_i' = C_{g1} + C_{g1g2} + C_{g1k} \left(1 + \frac{f^2}{f_{g1k}^2} \right) - L_k \cdot \frac{g_\tau S_k \left(1 + K_2 \cdot \frac{f^2}{f_1^2} \right)}{1 - 2 \frac{f^2}{f_{g1k}^2}},$$

where $K_2 = g_\tau / (g_\tau + g_t)$.

For frequencies which are not too high, this expression can be simplified to:

$$C_i' = C_{g1} + C_{g1g2} + C_{g1k} - L_k g_\tau S_k. \quad (137a)$$

It should be noted that C_{g1k} depends on the space charge between cathode and grid and therefore varies when the gain is controlled by

changing the grid bias. This effect can be compensated by the following means.

If only a small resistance R_k is incorporated in the cathode lead, then, according to eq. (137), the input capacitance is:

$$C_i' = C_{g1} + C_{g1g2} + C_{g1k} \cdot \frac{\frac{1}{R_k} \cdot \left(\frac{1}{R_k} + S_k \right)}{\left(\frac{1}{R_k} + g_\tau + S_k \right)^2 + \omega^2 C_{g1k}^2},$$

or

$$C_i' = C_{g1} + C_{g1g2} + C_{g1k} \cdot \frac{1 + S_k R_k}{1 + 2(g_\tau + S_k)R_k + (g_\tau + S_k)^2 R_k^2 + \omega^2 C_{g1k}^2 R_k^2}.$$

Since $(S + g_\tau)/2\pi C_{g1k}$ is approximately equal to (GB) :

$$C_i' = C_{g1} + C_{g1g2} + \frac{C_{g1k}}{\{1 + 2\varphi(g_\tau + S_k)R_k\} \{1 - S_k R_k + S_k^2 R_k^2\}}, \quad (137b)$$

in which

$$\varphi = 1 + R_k(g_\tau + S_k) \left(1 + \frac{f^2}{(GB)^2} \right). \quad (139)$$

When the frequency is not too high it is clear that:

$$\varphi \approx 1 + S_k R_k. \quad (140)$$

Disregarding the second and higher powers of $S_k R_k$, the denominator of the third term of eq. (137b) becomes $1 + S_k R_k$, so that the expression for C_i' can be simplified to:

$$C_i' = C_{g1} + C_{g1g2} + \frac{C_{g1k}}{1 + S_k R_k}, \quad (137c)$$

provided $S_k R_k$ is small compared with unity. By giving $S_k R_k$ a suitable value, the third term of eq. (137c) may be made far less sensitive to grid bias variations than C_{g1k} ; cf. fig. 87.

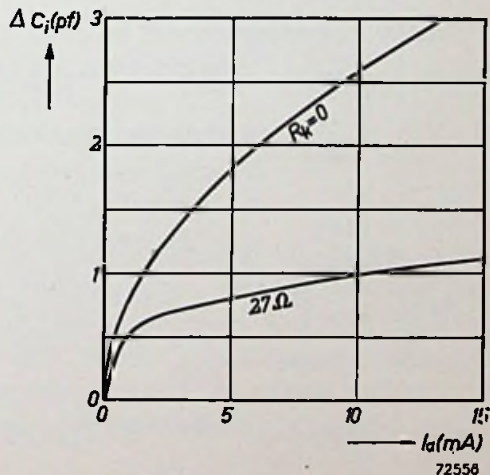


Fig. 87. Example of the reduction of ΔC_i due to the use of a small cathode resistance (at $f = 50$ Mc/s).

The input conductance of a valve when the cathode lead con-

tains only a small resistor can again be determined from eq. (136):

$$g_i' = g_{01} + \frac{\frac{\omega^2 C_{g1k}^2}{R_k} + \frac{g_\tau}{R_k^2} + \frac{g_\tau}{R_k} \cdot (S_k + g_\tau)}{\left(\frac{1}{R_k} + g_\tau + S_k\right)^2 + \omega^2 C_{g1k}^2}$$

By multiplying the numerator and denominator by R_k^2 , the latter becomes:

$$1 + 2\varphi(g_\tau + S_k)R_k \approx 1 + 2\varphi S_k R_k z/1 + 2S_k R_k,$$

so that, putting $g_\tau + S_k \approx S_k$:

$$g_i' = g_{01} + \frac{\omega^2 C_{g1k}^2 R_k}{1 + 2S_k R_k} + g_\tau \cdot \frac{1 + S_k R_k}{1 + 2S_k R_k}$$

It is clear, therefore, that if f is sufficiently small compared with (GB) and f_1 , and if also $S_k R_k$ is sufficiently small compared with unity, this expression for g_i' can be simplified to:

$$g_i' = g_{01} + \frac{\omega^2 C_{g1k}^2 R_k}{1 + 2S_k R_k} + \frac{g_\tau}{1 + S_k R_k}. \quad (136e)$$

6.4.4 Stabilization of the input admittance

Finally, consideration will be given to a valve in the cathode lead of which there is a self-inductance L_k , and a capacitor C_k' shunted by a resistor R_k (see fig. 88). It is assumed that both $\omega L_k/R_k$ and $\omega C_k' R_k$ are very small compared with unity, as is often the case in practice.

In these circumstances:

$$Z_0 = j\omega L_k + \frac{1}{\frac{1}{R_k} + j\omega C_k'} \approx j\omega L_k + R_k(1 - j\omega C_k' R_k),$$

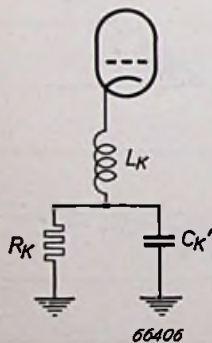
and

$$Y_0 \approx \frac{1}{R_k - j\omega C_k' R_k^2 + j\omega L_k} = \frac{1}{R_k} - j\omega \left(\frac{L_k}{R_k^2} - C_k' \right),$$

whence

$$g_0 = \frac{1}{R_k} \quad \text{and} \quad b_0 = -\frac{\omega L_k}{R_k^2} + \omega C_k'. \quad (141)$$

Fig. 88. Cathode lead having a self-inductance L_k , and a compensating capacitor C_k' shunted by a small resistor R_k .



When g_i' and C_i' are again determined by means of eqs (136) and (137),

and the numerators and denominators are divided by $g_0^2 = 1/R_k^2$, the denominators become:

$$1 + 2(g_\tau + S_k)R_k + (g_\tau + S_k)^2 R_k^2 + \left(\omega C_{g1k} - \frac{\omega L_k}{R_k^2} + \omega C_k'\right)^2 R_k^2,$$

which may be written as:

$$1 + S_k R_k \left\{ 2 \left(1 + K_2 \frac{f^2}{f_1^2} \right) + \left(1 + K_2 \frac{f^2}{f_1^2} \right)^2 S_k R_k + \left(\frac{\omega C_{g1k}}{S_k} - \frac{\omega L_k}{S_k R_k} + \frac{\omega C_k'}{S_k} \right)^2 S_k R_k \right\} \approx \\ \approx 1 + S_k R_k \left[2 \left(1 + K_2 \frac{f^2}{f_1^2} \right) + S_k R_k \left\{ \left(1 + K_2 \frac{f^2}{f_1^2} \right)^2 + \left(\frac{f}{GB} + \frac{\omega C_k' R_k}{S_k R_k} - \frac{\omega L_k}{S_k R_k} \right)^2 \right\} \right].$$

Provided f is sufficiently small compared with f_1 and (GB) , this expression becomes:

$$1 + S_k R_k (2 + S_k R_k) + \left(\omega C_k' R_k - \frac{\omega L_k}{R_k} \right)^2 \approx 1 + 2S_k R_k.$$

Hence the **input conductance** is:

$$g_i' = g_{g1} + \frac{\omega^2 C_{g1k}^2 R_k}{1 + 2S_k R_k} + \frac{\omega^2 C_{g1k} L_k S_k - \omega^2 C_{g1k} C_k' S_k R_k^2}{1 + 2S_k R_k} + \\ + \frac{g_\tau}{1 + 2S_k R_k} \cdot \left\{ 1 + R_k^2 \left(\omega C_k' - \frac{\omega L_k}{R_k^2} \right)^2 + R_k S_k \left(1 + \frac{f^2}{f_1^2} \right) \right\}.$$

The expression between braces is to a good approximation equal to $(1 + S_k R_k)$, which gives:

$$g_i' = g_{g1} + \frac{\omega^2 C_{g1k}^2 R_k}{1 + 2S_k R_k} + \frac{\omega^2 C_{g1k} L_k S_k - \omega^2 C_{g1k} C_k' S_k R_k^2}{1 + 2S_k R_k} + \frac{g_\tau}{1 + S_k R_k}. \quad (136f)$$

By ignoring a few terms the **input capacitance** is again:

$$C_i' = C_{g1} + C_{g1g2} + \frac{C_{g1k}}{1 + S_k R_k}. \quad (137c)$$

This expression shows that the input capacitance can be influenced by means of a cathode resistor, and advantage may be taken of this effect to compensate, for example, the capacitance variation occurring when applying automatic gain control. When the cathode resistor is given such a value that optimum compensation of the capacitance variations is obtained, the relation between g_i' and S can be determined by substituting this value for R_k in eq. (136f).

The value of the input conductance g_i' is then not yet entirely fixed, since C_k' can still be chosen arbitrarily. C_k' can be given a value such that the effect of variations of S on g_i' is the minimum. A rough approximation of the value required for this purpose can be found by assuming the

denominators in eq. (136f) to be constant and disregarding g_r . In that case g_i' appears to be independent of S when:

$$\omega^2 C_{g1k} L_k S_k - \omega^2 C_{g1k} C_k' S_k R_k^2 = 0,$$

or:
$$C_k' = \frac{L_k}{R_k^2}. \quad (142)$$

In eq. (142) ω no longer appears, i.e. the compensation is to a first approximation independent of the frequency.

Alternatively, g_i' could be rendered independent of S by tuning the cathode lead by means of a series capacitor, but the compensation is then highly dependent on the frequency, so that the circuit is apt to become unstable. There is no such risk in the case discussed above, where the cathode capacitance is usually smaller than in the case of series tuning of the cathode lead.

In some cases the capacitance of the cathode pin (and the connected screens) to earth is large enough for the purpose in view. The capacitance C_k of the cathode itself to earth should not be taken into account here, since this is not shunted across C_k' . This is demonstrated by the expression:

$$b_6 = \frac{-\omega L_k (1 - \omega^2 L_k C_k)}{R_k^2} - \omega C_k', \quad (141a)$$

which shows that C_k has not the same effect on b_6 as C_k' .

6.4.5 Valves with double cathode connection

The input conductance g_i of some valves is given a low value by providing two cathode connections which should be connected in parallel; by this artifice L_k is approximately halved.

When it is desired to undamp the grid circuit by tuning the cathode circuit it is not advisable to tune only one of the cathode leads and to use the other as a supply lead for the direct current, nor should the two leads be tuned to different frequencies. This might lead to instability due to the combination of the two cathode leads being in parallel resonance for one or several particular frequencies.

Furthermore, if ΔC_i compensation is not applied in the cathode circuit, advantage can be taken of the double cathode connection to reduce appreciably the active cathode lead impedance L_k by connecting the lower end of the grid circuit to the one cathode pin and the return lead of the anode circuit to the other pin ¹). To avoid instability the lower end

¹) Cf. M. J. O. Strutt and A. van der Ziel, A Variable Amplifier with Double Cathode Connection suitable for Metre Waves, Philips Techn. Review 5, p. 357, 1940 (No. 12).

of the grid circuit must also in this case be screened from the anode. Since the screening can of the anode circuit has to be connected to the lower end of this circuit, the anode return lead must be connected to earth, and the grid circuit thus remains floating. The capacitance to earth of this floating circuit and the inductance of both cathode leads give rise to another form of feedback, which may lead to instability at frequencies well above 100 Mc/s.

6.5 FEEDBACK BY THE ANODE-TO-CATHODE CAPACITANCE

The inclusion of an impedance Z_6 in the cathode lead will result in feedback to the cathode by the anode-to-cathode capacitance C_{ak} , after which feedback to the control grid occurs via the grid-to-cathode capacitance C_{g1k} . The anode-to-cathode capacitance C_{ak} , therefore, has a similar effect in these circumstances to that of the anode-to-grid capacitance C_{ag1} . As can be deduced from eqs (115) and (116):

$$Y_i' = Y_2 + Y_4 \cdot \frac{Y_6 + Y_7}{Y_6 + Y_4 + Y_7 + S_k - \rho S_a},$$

which, to a fair approximation, may be written:

$$Y_i' = Y_2 + Y_4 \cdot \frac{Y_6}{Y_6 + Y_4 + Y_7 + S_k} + Y_4 \cdot \frac{Y_7}{Y_6 + Y_4 + Y_7 + S_k} + Y_4 \cdot \frac{\rho S_a}{Y_6 + Y_4 + Y_7 + S_k},$$

provided $Y_6 > S_k$. By substituting

$$\rho = \frac{Y_5}{Y_1 + Y_5} \approx \frac{Y_5}{Y_1}$$

and

$$Y_7 = (1 - \rho)Y_5 \approx Y_5,$$

and disregarding Y_7 in the denominator,

$$Y_i' = Y_2 + Y_4 \cdot \frac{Y_6}{Y_6 + Y_4 + S_k} + \frac{Y_4 Y_5}{Y_6 + Y_4 + S_k} \cdot \left(1 + \frac{S_a}{Y_1}\right).$$

Provided the gain is not too small, this expression may be approximated as:

$$Y_i' = Y_2 + Y_4 \cdot \frac{Y_6}{Y_6 + Y_4 + S_k} + \frac{Y_4 Y_5}{Y_1} \cdot \frac{S_a}{Y_6 + Y_4 + S_k}.$$

The "feedback term" (containing Y_5) is now compared with the effect of the direct feedback from the anode to the control grid. This effect is expressed by (see eq. (120)):

$$\frac{Y_3}{Y_1} \cdot S',$$

or, from eq. (115), by setting $\rho = 0$ and $Y_7 = 0$:

$$\frac{Y_3}{Y_1} \cdot \frac{S_a Y_6}{Y_6 + Y_4 + S_k}.$$

The feedback via the cathode circuit is therefore equivalent to a direct feedback produced by an admittance Y_3' equal to:

$$Y_3' = \frac{Y_5 Y_4}{Y_6}. \quad (143)$$

Substituting $j\omega C_{ak}$ for Y_5 , $j\omega C_{g1k}$ for Y_4 and $j\omega C_{ag1}'$ for Y_3' , eq. (143) becomes:

$$C_{ag1}' = C_{ak} \cdot j\omega C_{g1k} Z_6. \quad (144)$$

This means that if a capacitor C_k' is included in the cathode lead, the capacitance C_{ag1}' should not exceed the maximum permissible value.

The value of C_{ag1}' can be calculated from eqs (126), (127) and (144), which give:

$$\frac{S_{\max}}{2\pi C_{ak}} = \omega C_{g1k} Z_6 f \cdot \frac{G_{\max}^2}{p_{r \max}^2}, \quad (145)$$

provided $S_k Z_6 < 1$.

6.6 OTHER FORMS OF FEEDBACK

At frequencies exceeding 50 Mc/s the self-inductances and mutual inductances of various connecting leads of the valves will give rise to other forms of feedback.

Space does not permit full investigation of these effects, but it may be stated that their influence can be considered as a variation of C_{ag1}' .

Due to the effects summarized below, C_{ag1} contains other terms in addition to C_{ag1} and $j\omega C_{ak} C_{g1k} Z_6$.

Mutual inductance M_{ag1} between the anode and the control-grid leads gives rise to an additional term:

$$+\omega^2 C_a C_{g1} M_{ag1}.$$

Self-inductance L_{g2} of the screen-grid lead gives rise to an additional term:

$$-\omega^2 C_{ag2} C_{g1g2} L_{g2}.$$

Mutual inductance M_{g1g2} between the control-grid and screen-grid leads gives rise to an additional term:

$$-\omega^2 C_{g1} C_{ag2} M_{g1g2}.$$

Self-inductance L_s of the earth lead of the screening cage (s) gives rise to an additional term:

$$-\omega^2 C_{as} C_{g1s} L_s .$$

Mutual inductance M_{ks} between the cathode lead and the earth lead of the screening cage gives rise to an additional term:

$$\omega^2 (C_{as} C_{g1k} + C_{ak} C_{g1s}) M_{ks} .$$

It is difficult to determine accurately the effects of all these terms, but it will be clear that the deviation of C_{ag1}' from the static value of C_{ag1} increases with the frequency.

In practice the negative terms appear to predominate, so that C_{ag1}' first decreases with increasing frequency. At the self-neutralizing frequency, f_s' , $C_{ag1}' = 0$. From this frequency onwards C_{ag1}' becomes negative. In the vicinity of f_s' , C_{ag1}' assumes a parabolical form as a function of the frequency (see fig. 89), viz.:

$$C_{ag}' = C_{ag} \left\{ 1 - \left(\frac{f}{f_s'} \right)^2 \right\} .$$

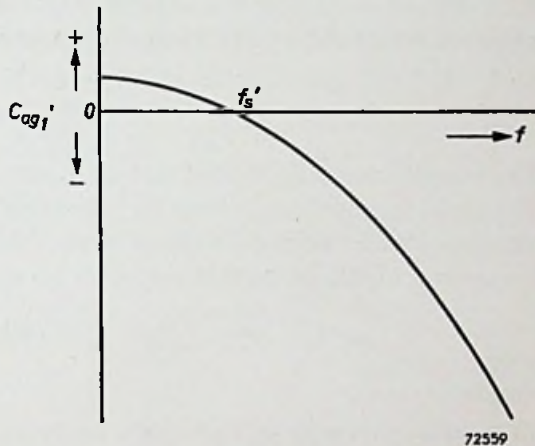


Fig. 89. Variation of the effective anode-to-grid capacitance C_{ag1}' as a function of the frequency f . At f_s' the effective anode-to-grid capacitance is zero.

At much higher frequencies, in the vicinity of f_s'' , deviations occur and C_{ag1}' again becomes positive beyond f_s'' due to the influence of terms containing higher powers of f . It is clear that the performance at these high frequencies and the magnitude of f_s' depend not only on the construction of the valve, but also on the wiring of the circuit.

7. PRACTICAL CONSIDERATIONS FOLLOWING ON THE THEORY

It will now be shown how the preceding calculations can be used when designing circuits for I.F. amplification in television receivers.

7.1 SENSITIVITY

The sensitivity required for a given amplifier will first be investigated. The minimum field strength for various frequencies at which a signal-to-noise ratio of 5 (= 14 db) can be attained is shown in fig. 70. From this curve it is possible to ascertain the smallest field strength H_{\min} that can be amplified to give full output. Once this choice has been made, the voltage across the input circuit of the amplifier is given by eq. (17):

$$V_i = \frac{H_{\lambda}}{2\pi} \cdot w.$$

The transformer ratio w need not be known if the required sensitivity at the aerial terminals only is to be calculated, since the voltage at these terminals is smaller than the voltage across the input circuit by a factor w . For a normal dipole aerial this voltage is given by:

$$V_{\min} = \frac{H_{\min}\lambda}{2\pi} = \frac{50 H_{\min}}{f}.$$

Example

A television receiver for 50 Mc/s with a bandwidth of 5 Mc/s must be capable of giving maximum output signal even when the signal-to-noise ratio at the output drops to 2 or even less. What should the sensitivity be at the aerial terminals?

From fig. 70 (broken lines, corresponding to conditions of minimum cosmic noise) the maximum output signal may be obtained at field strengths of approximately:

$$\frac{2}{5} \cdot 60 = 24 \mu\text{V/m}.$$

Hence, according to the above formula:

$$V_{\min} = \frac{50 H_{\min}}{50} = 24 \mu\text{V}.$$

7.2 GAIN

In the case of a T.R.F. receiver the total gain G_{tot} , calculated from the aerial terminals to the anode circuit of the last I.F. tube, is given by the expression:

$$G_{\text{tot}} = w \cdot G^n.$$

In a superheterodyne receiver with a tuner, the gain G_{tuner} of which is given, the total gain can be calculated from:

$$G_{\text{tot}} = G_{\text{tuner}} \cdot G^n.$$

7.2.1 Gain of the input circuit

The gain of the input circuit of a receiver can be determined by means of eq. (13b) in the frequency range below f_0' , or by means of eq. (10b) for frequencies exceeding f_0' . The voltage gain G' thus found is the ratio of the voltage across the input circuit to the voltage at the aerial at zero load. (If the gain is understood to be the ratio w of the voltage across the input circuit to the voltage at the aerial terminals, twice this value must be taken, since $w/2 = G'$.)

In practice the admittance of the aerial circuit is not always negligibly small compared with the input admittance of the valve and the additional damping resistance. Since it is not possible to reduce g_c below the extreme value $g_{c\text{min}}$, it is clear that:

- (a) G_0' cannot exceed $1/\sqrt{4R_{\text{ant}}g_{c\text{min}}}$, and
 (b) f_0' cannot be lower than $f\sqrt{4R_{\text{ant}}g_{c\text{min}}}$.

Maximum gain is obtained when the circuit is not additionally damped, see fig. 90.

Apart from the transitional point at f_0' being somewhat more rounded off, this diagram has the same form as fig. 3. As G_0' (and thus also f_0') approaches the above-mentioned boundary value, the effect of this curvature on the $\log G' = f(\log f)$ curve steadily increases; by keeping a factor of about 2 below the boundary value the rounding-off will be less than 10 %.

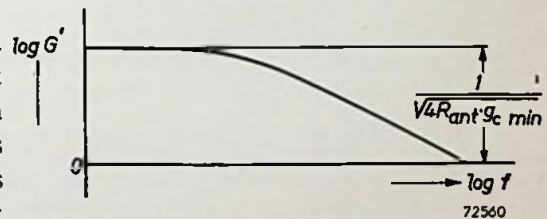


Fig. 90. Diagram showing the variation of $\log G'$ as a function of $\log f$. In contrast to fig. 3 the circuit conductance is constant, viz. $g_{c\text{min}}$.

7.2.2 Gain of the I.F. amplifier

In the calculation of G_{tot} the term G^n is always the main factor. To evaluate G^n it must first be investigated whether the valves operate above or below f_0 (cf. eq. (12a)). As a rule the latter will be the case, so that G can be calculated from eq. (13a):

$$B \cdot G = F_s F_z (GB).$$

If the valves operate above f_0 , then $G = G_{\max}$, which can be calculated from eq. (10a):

$$G_{\max} = F_s \left(\frac{f_1}{f} \right)^2 .$$

The bandwidth B is calculated in the following way. For television receivers with a normal response curve the total bandwidth B_{tot} between the 3 db points is approximately 10 % smaller than the distance between

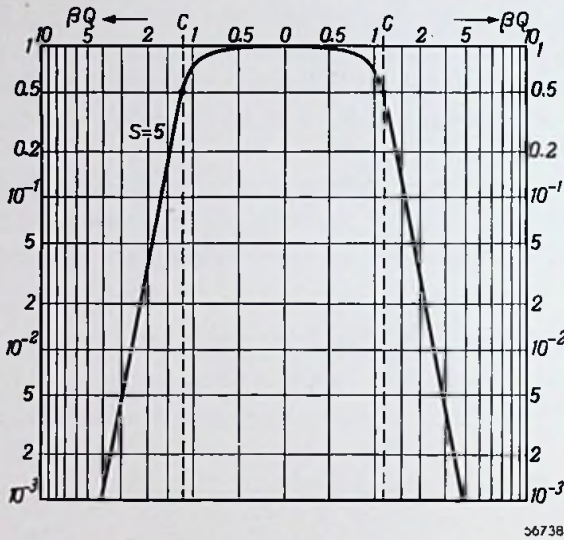


Fig. 91. Simplified response curve of a T.V. receiver. It should be noted that the scale of the abscissa consists of a linear and two logarithmic parts. The position of the carrier is indicated by C .

the 6 db points (see fig. 91), which, to a first approximation, may be taken to be equal to the distance between the image and sound carriers. When B_{tot} has thus been determined, B can be calculated from eq. (20):

$$B = \frac{B_{\text{tot}}}{F_B} .$$

If a band-pass filter is used for the coupling, F_B may be taken to be from 1.5 to 2, but when single-tuned circuits are used F_B is at the most equal to unity. The chosen value of F_B must be verified after the staggering scheme has been selected.

Once the bandwidth B has thus been determined, the values of F_s , F_x and (GB) must be chosen. It is most convenient first to ascertain how

many amplifying stages should be used. For this purpose F_s , F_x and w (or G_{tuner}) are roughly estimated, assuming, for example, that:

$$G_{\text{tot}} = G_{\text{tuner}} \left\{ \frac{F_B F_s F_x (GB)}{B_{\text{tot}}} \right\}^n.$$

7.3 SELECTION OF THE VALVES

From the foregoing considerations a relation has been established between the values of (GB) and n and the required value of G_{tot} . From eq. (32) the required value of f_1 can be evaluated for a given staggering scheme, whilst a condition can also be imposed on the value of F_s . The valves can now be chosen according to their (GB) product and gain reference frequency f_1 .

It may be useful to draw a diagram showing these two quantities, from which the performance obtainable with these valves can be ascertained. For this purpose the required values of (GB) and f_1 are calculated from eqs (13a) and (20) and from eq. (32) after the values valid for the design have been filled in for the other data.

Example

In fig. 92 a number of areas are shown which correspond to the various applications.

Each application covers a certain area in the graph due to the fact that some freedom of choice is permissible in designing a receiver. From this it will be seen that the (GB) product and the gain reference frequency f_1 may assume different values.

A given application with the desired number of valves of a given type is now possible if their (GB) product and gain reference frequency f_1 are equal to or larger than the values of (GB) and f_1 in any part of the (GB) - f_1 area of the application concerned.

The receivers taken as an example in fig. 92 have almost the same sensitivity, and have other comparable properties. The factor F_r (see eq. (147), p. 124), for example, is assumed to be unity in all cases, which means that the valves are not controlled. No band-pass filter coupling is employed in any of the circuits, although it would be possible to reduce the required (GB) product in this way.

When a large gain per stage is required, valves with a high (GB) product will obviously be chosen. The performance of valves with an identical (GB) product may, however, differ appreciably: one type of valve may have a much higher mutual conductance and a much larger input capacitance than another type of valve having the same (GB) product. In that case the valve having the highest product $F_x \cdot (GB)$, i.e. the largest valve with the highest mutual conductance, is often preferred.

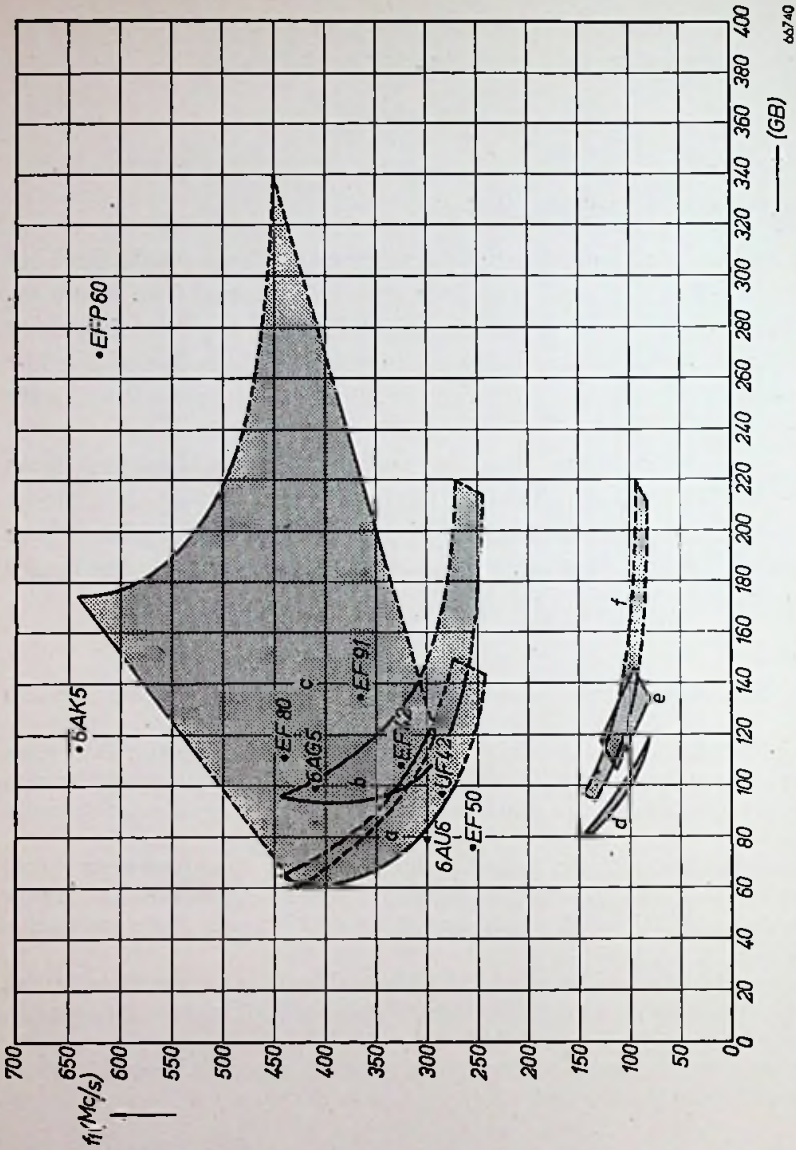


Fig. 92. Diagram in which f_1 and (GB) have been plotted for a number of valves. The shaded areas apply to various circuits, as indicated in the table below. It is inadvisable to choose a point in the vicinity of the broken lines.

area	a	b	c	d	e	f
type	T.R.F. receiver			superheterodyne		
T.V. band (Mc/s)	40-70			180-210	40-70	
bandwidth (Mc/s)	3	4.5	3	4.5	11	3
number of H.F./I.F. valves (including the mixer valve)	4	4	3	5	8	4

Very large valves, however, are less suitable for these applications, due to the following facts.

- (a) The gain reference frequency f_1 of a large valve is as a rule comparatively low. Particularly at high frequencies there is then a risk that the maximum gain per stage will no longer be limited by the (GB) product but by the gain reference frequency f_1 . The influence of the input capacitance of the valve on f_1 may be explained by as follows.

Assume for the sake of simplicity that

$$g_i \approx \omega^2 L_k C_{g1k} S_k,$$

and

$$\left(\frac{f_1}{f}\right)^2 = \frac{S}{g_i}.$$

Since the cathode connection is substantially independent of the choice of C_{g1k} and S_k , L_k may be taken to be constant. Hence:

$$f_1 \approx \text{constant} \cdot C_{g1k}^{-1/2}.$$

- (b) Beyond a given limit the value of F_x increases but little with the mutual conductance of the valve, whereas the increase in physical dimensions, price and current drain becomes quite considerable.
- (c) F_x has an optimum value above which the total gain begins to decrease with increasing value of F_x . This optimum value of F_x of a particular amplifier depends on various factors: in the first place on the question whether the amplifier operates on a frequency above or below f_0 and f_0' , in other words whether the maximum gain of each stage is limited by f_1 or by (GB) .

As shown on p. 12, one of the two following conditions usually applies:

- (1) the signal frequency is lower than f_0 and f_0' , or
 (2) the signal frequency is lower than f_0 but higher than f_0' (in this case the receiver is usually provided with a tuner with additional H.F. amplifying valves).

In the first case F_x can be evaluated in the following way: Assume that

$$a = \frac{C_i}{C_i + C_o}, \quad b = \frac{C_y}{C_x} \quad \text{and} \quad x = \frac{C_x}{C_i + C_o},$$

where C_x denotes the stray capacitance of each I.F. stage and C_y is the stray capacitance of the input circuit. The gain is then proportional to

$$(C_i + C_y)^{-1/2} \cdot \left(1 + \frac{C_x}{C_i + C_o}\right)^{-n} = C_x^{-1/2} \left(\frac{a}{x} + b\right)^{-1/2} (1 + x)^{-n} = X.$$

When x is varied at constant values of a , b and C_x , X will be the maximum at

$$\frac{dX}{dx} = 0, \text{ or } \frac{\frac{1}{2}aX}{ax + bx^2} - \frac{nX}{1+x} = 0,$$

whence

$$x_{\text{opt}} = \frac{a}{2b} \cdot \left(1 - \frac{1}{2n}\right) \pm \sqrt{\frac{a^2}{4b^2} \cdot \left(1 - \frac{1}{2n}\right)^2 + \frac{a}{2bn}}.$$

If a is given a value between 0.5 and 0.7 and b is from 0.5 to 1, whilst the number of stages n may vary between 3 and 8, the value of x_{opt} will be from 0.095 to 0.04, which gives for $F_x = 1/(1+x)$, a value of 0.92 to 0.96.

When the circuits are coupled by band-pass filters the results are very similar.

It can be shown in an analogous way that, when a tuner is used, the larger I.F. gain due to a further increase of the dimensions of the I.F. amplifying valves is outweighed by the smaller gain of the tuner. The optimum value depends on the design of the tuner and the valves with which it is equipped. As a rule little is gained by choosing larger valves than correspond to $F_x = 0.8$.

7.4 STAGGERED TUNING SYSTEM

The (GB) product and the value of n having been determined, a detailed staggered tuning system can now be worked out, from which the values of F_B , F_s and F_x and the performance of the amplifier can be determined with greater accuracy.

In designing this tuning system it should be taken into account that it will usually be necessary to incorporate a number of traps to eliminate certain undesired signals originating from adjacent channels and the sound channel of the wanted transmission.

As can be seen from the response curve shown in fig. 91, the attenuation of these signals by the H.F. and I.F. circuits is inadequate: the required additional attenuation is given by the difference between this curve and the desired response curve.

The incorporation of a trap also affects the response curve on either side of the frequency which has to be suppressed; the greater the attenuation, the more serious is the influence on the response curve. To evaluate the influence of the traps¹⁾, the following two quantities must be calculated:

- (1) The relative quality factor r , i.e. the ratio Q_t/Q of the quality factor of the trap to that of the circuit to which it is connected.
- (2) The separation s , i.e. the relative detuning of the trap with respect

¹⁾ J. A vins, Electronics, Jan. 1950.

to the circuit, multiplied by the quality factor Q_t of the trap, viz.:

$$s = \left(\frac{\omega_t}{\omega_0} - \frac{\omega_0}{\omega_t} \right) Q_t = \beta_t Q_t, \quad (146)$$

where ω_t and ω_0 are the resonant frequencies of the trap and of the circuit respectively.

The values of r and s having been determined, the changes to which the response curve is subject at a given attenuation can be derived from one of the graphs given in figs 113a to l of Appendix I.

These graphs are based on the theory of detuned band-pass filters with two resonant circuits and can be derived from the response curves of four single circuits whose quality factors and resonant frequencies are related to the properties of the circuit and the trap and their mutual coupling.

The changes to which the response curve is subject as a result of the presence of traps must be corrected when these lie within the pass band range of the video signal. This is achieved by slightly changing the tuning and damping of the I.F. circuits. The effects of these modifications can be determined by means of figs 113m and n of Appendix I.

The influence of the traps cannot be neutralized completely over the entire pass band. This is not objectionable, since the purpose in view is only to obtain an acceptable response curve which gives a satisfactory step function.

It is further of interest to investigate to what extent the corrected response curve is situated above or below the original curve. As a rule the differences will be small, so that the total gain is hardly affected by the incorporation of traps.

It is now possible to design a corrected staggered tuning system. In the corresponding diagram the top extremities of the perpendiculars no longer coincide with the points dividing the semi-circle into equal parts, as is the case in fig. 8. The tunings and dampings of the various circuits are now exactly known and so are the tunings of the traps and the tightness with which they are coupled to the circuits. It is therefore possible to determine the total capacitance C_x of the circuit and consequently the value of F_x with greater accuracy.

It is now necessary to ascertain whether the staggered tuning system chosen can indeed be achieved without any of the stages operating at a frequency exceeding f_0 . If this is not possible, additional capacitance will have to be added to the stage concerned in order to reduce the bandwidth of that stage sufficiently. In this case, however, the gain of this stage will also be reduced owing to the lower value of F_x .

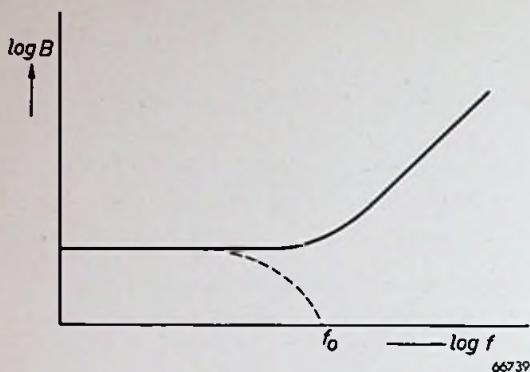


Fig. 93. Graph showing the variation of $\log B$ as a function of $\log f$ in the vicinity of f_0 . The full line applies to non-controlled valves and the broken line to a cut-off valve.

If the gain of the receiver is controlled by varying the mutual conductances of the valves the inherent variation of the input conductance Δg_i may result in a variation of the bandwidth. This effect is most marked when a valve, operating around the value f_0 , is controlled without compensating Δg_i (see fig. 99); the damping of the grid circuit is then almost entirely controlled by g_i . If now the valve is cut off, g_i decreases approximately in proportion to S_{eff} (see Section 6.4), thereby also reducing the bandwidth.

If the bandwidth with the valve cut off is denoted by B_{co} , it can be deduced from eqs (6) and (9) that

$$\frac{B_{\text{co}}}{B_0} = \frac{g_c}{g_i + g_o + g_c} = 1 - \frac{f^2}{f_0^2},$$

or

$$\Delta B_0 = B_0 - B_{\text{co}} = B_0 \cdot \frac{f^2}{f_0^2}.$$

In order to reduce $\Delta B_0/B_0$ it will therefore be necessary to remain below the frequency f_0 by a factor F_r . It is obvious that where the variations Δg_i are not compensated:

$$F_r = \left(\frac{\Delta B_0}{B_0} \right)^{-1/2}. \tag{147}$$

In practice F_r may be from 1 (when there is no gain control) to 5; higher values will not be required.

Eq. (32) now becomes:

$$B_{\text{tot}} \sin \alpha \geq F_B F_x F_r (GB) \left(\frac{f}{f_1} \right)^2. \tag{148}$$

In order to satisfy this condition a valve with a given minimum value of f_1 is required. This value of f_1 can be found by solving f_1 from eq. (148) after the staggered system has been chosen.

In the case of superheterodynes with intermediate frequencies of about 20 Mc/s the values thus required are usually not excessively high, but in

7.4 Staggered tuning system

the case of T.R.F. receivers it may be found that no valves are available which have the required value of f_1 . In that case the design may be adapted to the requirements thus imposed by one of the following means:

- (1) Reduction of F_r . This may be achieved by improving the compensation of Δg_i or by not controlling those valves the grid circuits (and possibly the anode circuits) of which have a narrow bandwidth.

As a rule not only Δg_i but also ΔC_i will be compensated. For this purpose a resistor R_k shunted by a capacitor C_k' must be incorporated in the cathode lead (see Section 6.4.4.).

It follows from eq. (137c) that for compensating ΔC_{g1k} the following condition must be satisfied:

$$S_{k\max} R_k \approx \frac{\Delta C_{g1k}}{C_{g1k}},$$

where $S_{k\max}$ denotes the maximum cathode transconductance. The required value of R_k is therefore determined within certain limits. The most favourable value can best be ascertained experimentally.

The required value of C_k' can be calculated from eq. (136f). First the relatively small correction due to $S_k R_k$ in the denominators is disregarded, which gives:

$$g_i \approx g_{g1} + \omega^2 C_{g1k}^2 R_k + \omega^2 C_{g1k} L_k S_k - \omega^2 C_{g1k} C_k' S_k R_k^2 + g_\tau.$$

g_i no longer varies with S_k when

$$g_\tau + \omega^2 C_{g1k} L_k S_{k\max} \approx \omega^2 C_{g1k} C_k' S_{k\max} R_k^2,$$

which may be written as:

$$g_\tau + g_l \approx \frac{\omega^2 \Delta C_{g1k}^2 C_k'}{C_{g1k} S_{k\max}},$$

or

$$C_k' \approx \frac{C_{g1k} S_{k\max} (g_l + g_\tau)}{\omega^2 \Delta C_{g1k}^2}.$$

The most suitable value of C_k' is again determined experimentally. The resulting input conductance will now be approximately:

$$g_i \approx g_{g1} + \omega^2 C_{g1k}^2 R_k,$$

or, after substitution of the optimum value of R_k :

$$g_i \approx g_{g1} + \frac{\omega^2 C_{g1k} \Delta C_{g1k}}{S_{k\max}} = g_{g1} + g_l'.$$

The second term of this expression may be estimated from:

$$g_t' \approx g_t \cdot \frac{\Delta C_{g1k}}{C_{g1k}} \cdot \left(\frac{f_1}{(GB)} \right)^2 \cdot \left(\frac{C_{g1k}}{C_i + C_o} \right)^2.$$

The loss of gain due to the compensation is approximately:

$$F_s \approx \frac{1}{1 + S_{k\max} R_k} \approx \frac{C_{g1k}}{C_{g1k} + \Delta C_{g1k}} > 0.75,$$

except in those cases where R_k has such a high value that the mutual conductance is reduced by the resulting grid bias. On the other hand, F_x is slightly improved because the input capacitance of the valve will now be about equal to the cut-off value of C_i throughout the control range.

- (2) Choice of a more suitable staggered tuning system, with larger values of $\sin \alpha$. In such a system F_B will usually be smaller, so that the bandwidth B_r of the reference circuit may have to be increased considerably. The extreme values between which the gain reference frequency f_1 thus required may be varied are given on the one hand by $(n + 1)$ synchronous circuits and, on the other hand, by a flat staggered $(n + 1)$ tuple.

When these changes have been made it will be obvious that, due to the increase of B_r , a higher (GB) product is required in order to obtain the same total gain G_{tot} .

- (3) Rendering the most critical circuit less sensitive to Δg_t variations. This may be achieved by increasing the damping across the circuit and adding extra capacitance. The advantage of this method is that the circuit also becomes less sensitive to variations of the input capacitance of the controlled valve, but on the other hand the gain decreases so, that valves with a higher (GB) product are required to obtain the same gain. As a rule, however, there is no need to apply this method to all stages, so that the required increase of the (GB) product is less than the required decrease of the gain reference frequency f_1 .

When the staggered tuning system has been chosen and the gain per stage has been calculated according to Section 7.2, it still remains to be investigated whether the gain is permissible with a view to stability. For each stage eq. (128a) applies, namely:

$$G_{h\max} \leq p_h \sqrt{\sin \alpha_h \sin \alpha_{h+1}} \sqrt{\frac{f_s}{f}}.$$

It has been shown in Section 6.3.2 that, in order to avoid irregular-

ities of the response curve, the value of p_h^2 must in any case remain below 0.5.

Example

It is required to design an I.F. amplifier for 23.75 Mc/s (picture carrier) preceded by a given tuner having a gain of 15. The overall sensitivity at 23.75 Mc/s should be approximately $20 \mu V$ for a direct voltage of 1 V at the detector. Contrast control should be provided.

The F.M. audio signal should also be amplified in two of the I.F. video stages, after which it is separated. At the video detector the audio signal should be weaker by a factor of at least 20 than the image carrier; the ratio of the image to the sound carrier at the aerial terminals is assumed to be 2 : 1. The interval between the sound and image carriers is 5.5 Mc/s.

Signals originating from adjacent channels should be suppressed to such an extent that they are weaker by a factor of at least 50 than the image carrier, but suppression should not deteriorate appreciably when the allocation of the adjacent channels differs slightly from the standards.

The supply is 220 V AC/DC (without mains transformer).

Fig. 94 gives the required overall response curve of the receiver, whilst fig. 95 gives the response curve of the tuner.

The response curve of the I.F. part of the receiver should therefore be approximately as shown in fig. 96 with a width of about 5 Mc/s between the 3 db points.

The design will be based on the use of a flat-staggered tuning system with $F_B = 1$, so that B_T of each circuit is 5 Mc/s.

It is obvious that traps will have to be added to most of the circuits. In this connection, and in view of the available coils and other components, C_x of each of the stages may be taken to be approx. 10 pF. F_x is therefore likely to assume a fairly low value, for example $F_s F_x \approx 0.5$. The product $F_s F_x \cdot (GB)$ may, therefore, amount to approx. 50 Mc/s and the gain per stage to about 10.

The total gain in the centre of the response curve should be approximately $2 \times 1 V / 20 \mu V = 10^5$. Taking the gain of the tuner to be 15 and the detector efficiency to be 50 %, the required gain of the I.F. amplifier is therefore $10^5 / 15 \times 0.5 \sqrt{2} \approx 10^4$.

Four stages of I.F. amplification may therefore suffice, provided the valves have a relatively high (GB) product and are not too small, i.e. their high (GB) product

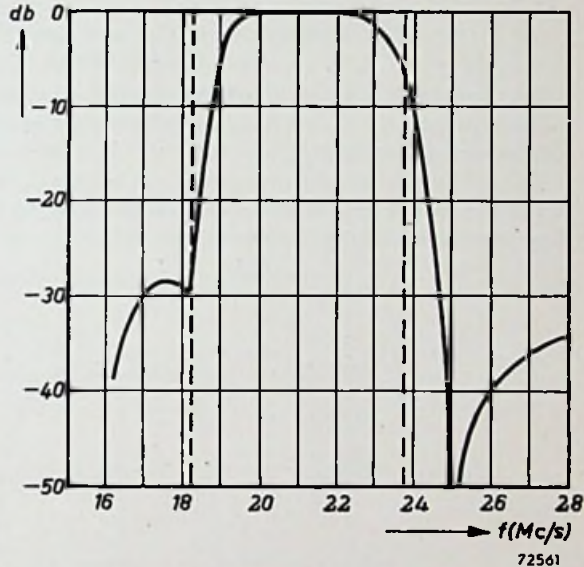


Fig. 94. Required overall response curve of the receiver.

may not be due to their low input capacitance, their mutual conductance being relatively small.

A high-slope valve such as the EF 42 or EF 91 pentode is unsuitable for a receiver

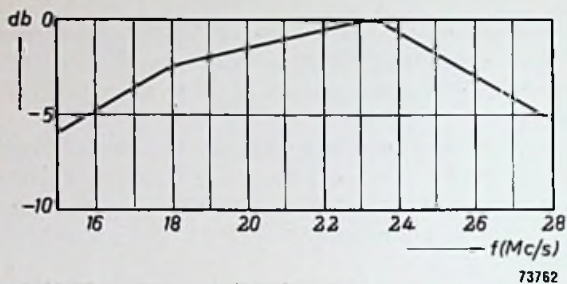


Fig. 95. Response curve of the tuner preceding the I.F. amplifier to be designed.

without mains transformer, whilst the UF 42 pentode for AC/DC mains is less suitable because of its somewhat smaller (GB) product and smaller value of the gain reference frequency f_1 .

The EF 80 pentode is more convenient, although the value of F_x is slightly smaller. In the case of the EF 80 valve, $G = 100 \times 0.5/5 = 10$. The required sensitivity may thus be reached with four EF 80 valves.

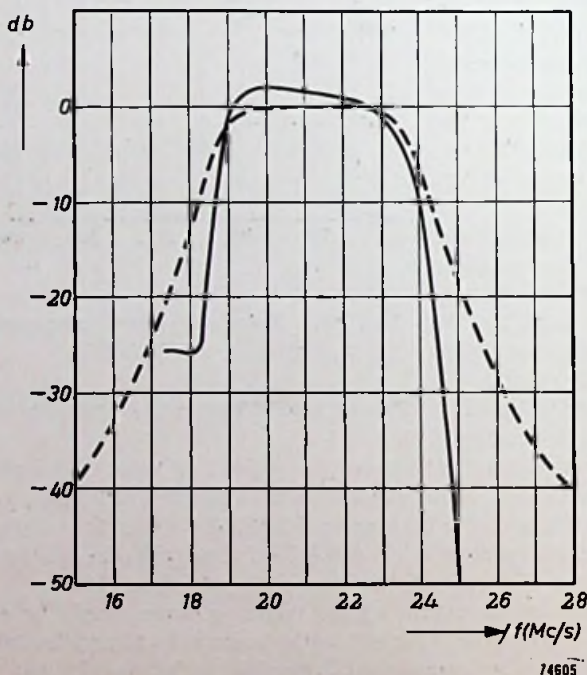


Fig. 96. Required response curve of the I.F. part of the receiver (fully drawn line) and the response curve according to the staggering system of fig. 97 (broken line):

7.4 Staggered tuning system

A staggered tuning system will now be designed for five I.F. circuits, the detunings of which are respectively -2.5 Mc/s, -1.5 Mc/s, 0 Mc/s, $+1.5$ Mc/s and $+2.5$ Mc/s.

The last I.F. circuit should be tuned to a frequency near the image carrier, and its damping should not be too small in view of the damping caused by the following diode detector. The latter imposes a fairly heavy damping, which, moreover, depends to some extent on the signal amplitude. For crystal diodes the calculation given on p. 14 is applicable, but if a vacuum diode is used the calculation given on pp. 13 and 14 holds for large signals only. At small signals R_d assumes a lower value, depending on the shape of the diode current characteristic in the vicinity of $V_d = 0$. To avoid any marked dependency of the response curve upon the signal amplitude, it is undesirable to damp the circuit exclusively by R_d .

The first three circuits should be tuned to frequencies close to the sound carrier, since the I.F. audio signal is also amplified in these stages (the audio and video signals are separated after the third stage). Gain control is applied only to the first two stages, so that it has no effect on the ratio of the video signal to the audio signal. It would, in fact, be inadvisable to control the other two stages in view of the sensitivity of the two weakly damped grid circuits to variations of the input conductance and capacitance. Another objection against controlling the last I.F. stages is the serious distortion resulting when controlling valves which are fully driven by a large signal.

The sequence of the circuits is therefore chosen as indicated in fig. 97.

The impedance of the reference circuit can be evaluated from $C_r \approx 18$ pF, $B_r = 5$ Mc/s, $g_r = 2\pi \cdot 5 \times 18 = 550$ μ A/V, which gives $R_r = 1.8$ k Ω according to eq. (6). The damping resistances for the various circuits then become respectively 5.5 k Ω , 2.2 k Ω , 1.8 k Ω , 2.2 k Ω and 5.5 k Ω .

In order to determine the tuning and required suppression of the traps, the desired I.F. response curve is compared with that obtained with the above-mentioned

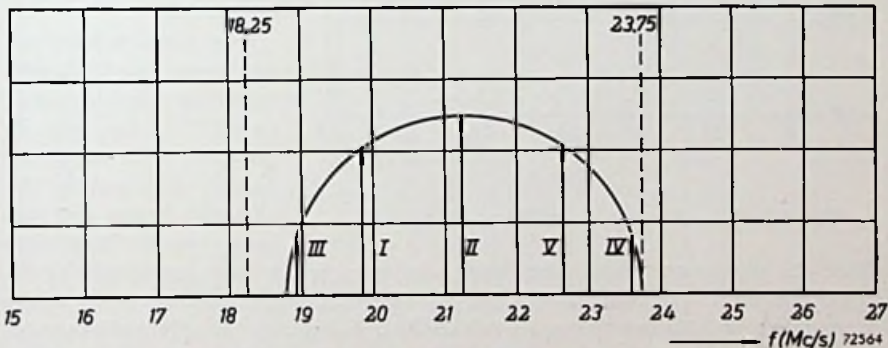


Fig. 97. Provisional design of the staggered tuning system.

staggered tuning system; cf. fig. 96. It is seen that at 25.25 Mc/s and at 18.25 Mc/s some 20 db of additional attenuation is required. It is therefore necessary to adjust two traps near these frequencies. In order to render these traps as effective as possible, the separation s should preferably be small, whilst the relative quality factor r should be high. For this purpose the traps should be coupled to circuits V and III respectively (see fig. 97).

It is true that if the 25.25 Mc/s trap were connected to circuit IV an even smaller

separation could be obtained, but the relative quality factor of the trap would then be smaller. When connected to circuit *V*, this trap, which should suppress the adjacent sound, gives rise to a sharp dip in the response curve, i.e. a strong absorption of the interfering signal in the close proximity of the pass band.

The purpose of the 18.25 Mc/s trap connected to circuit *III* is to suppress the sound carrier to such an extent that the audio signal does not noticeably interfere with the video signal. This trap is so adjusted that the overall response curve is substantially flat in the vicinity of the sound carrier. In this way the frequency modulation of the sound carrier is not converted into amplitude modulation, which would result in the audio signal becoming visible in the picture.

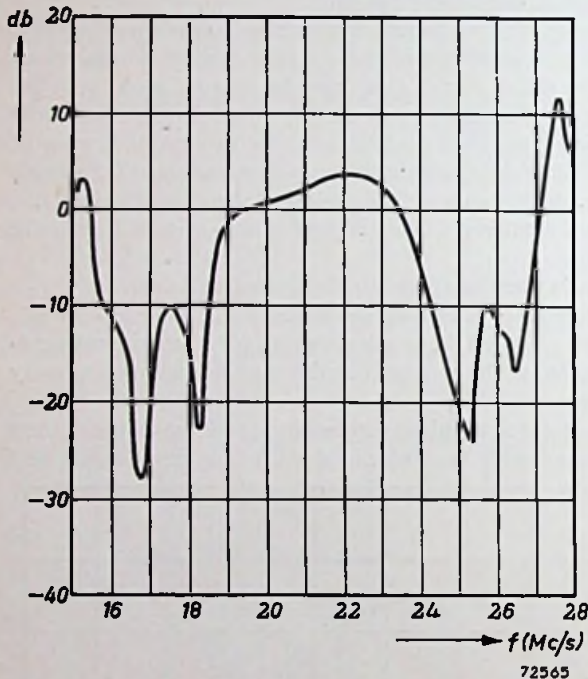


Fig. 98. Overall response curve of all traps.

will be the maximum when these traps are tuned to the same frequencies as the traps connected to circuits *V* and *I*. For the case of an experimental system where it is uncertain how the interfering signals are distributed over the adjacent channels, it is preferable, however, to tune these traps so that they eliminate the peaks of the response curve caused by the traps connected to circuits *V* and *I* and keep the entire response curve beyond the pass band as low as possible. These peaks are situated close to the attenuated frequencies, viz. at about 26.5 and 15.75 Mc/s respectively. By tuning the traps of circuits *IV* and *II* to these frequencies the overall response curve of all traps will be as shown in fig. 98. This diagram is constructed by adding the responses of all traps. These responses can be determined from figs 113 *a* to *l*. For the calculation of s and r the values of Q_s were taken to be about 75.

In addition to the audio signal of the transmission being received and the audio signal on the adjacent channel, the video carrier of an adjacent transmitter must be sufficiently attenuated. As a rule this is easier to achieve than the suppression of the two signals mentioned above. The I.F. frequency originating from this signal is usually 16.75 Mc/s, and since circuit *III* is already trapped, this trap can best be connected to circuit *I*.

Two circuits have not yet been provided with traps, namely circuits *II* and *IV*. These may be provided with traps for further attenuating the adjacent image and adjacent sound. Attenuation

7.4 Staggered tuning system

It is seen that the traps give rise to a distortion of the response curve within the pass band, which must be corrected by slightly altering the original staggered tuning system.

Fig. 99 shows the final staggered tuning system thus obtained, whilst fig. 100 gives the corresponding overall response curve.

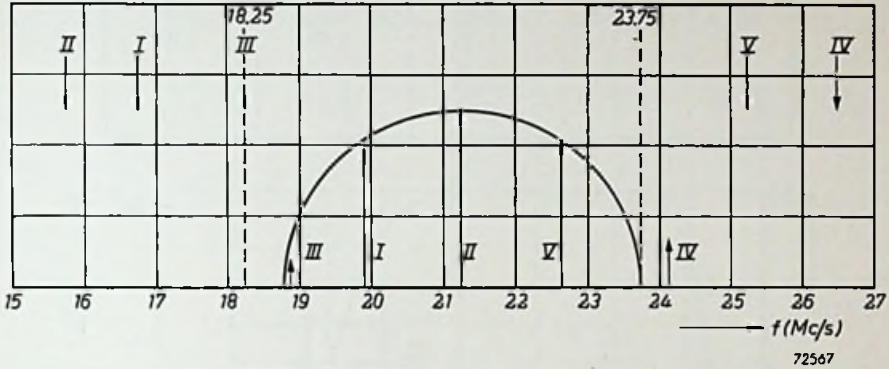


Fig. 99. Final staggered tuning system.

By means of this response curve the amplitude and phase characteristics can be constructed (fig. 101), from which the real and imaginary modulation response

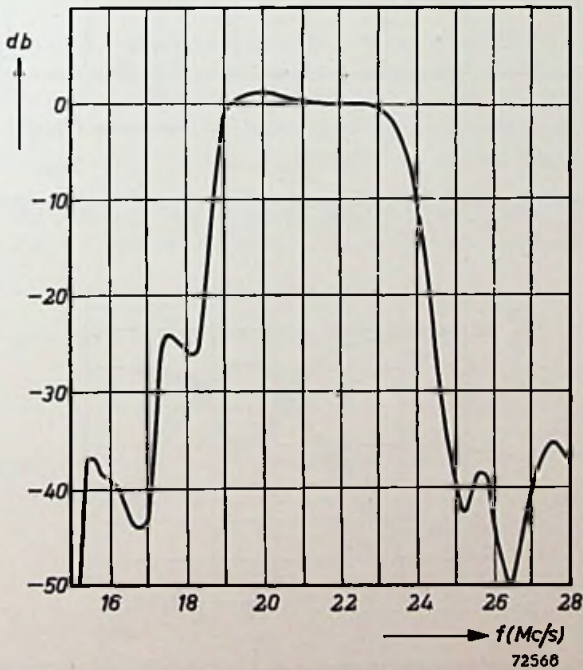
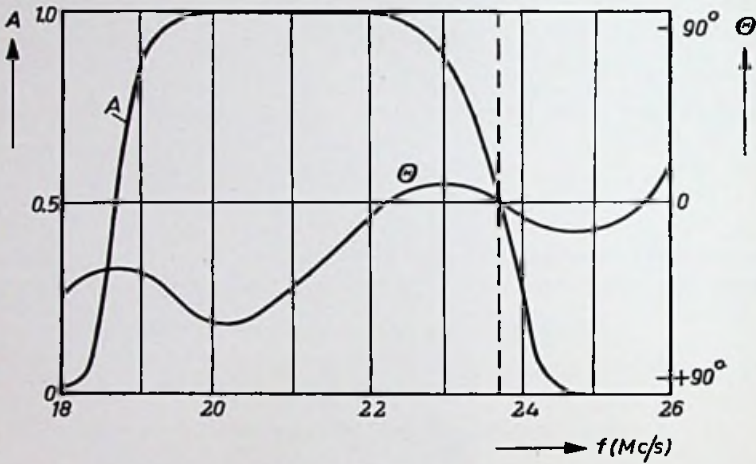


Fig. 100. Overall response curve of the staggered tuning system of fig. 99.

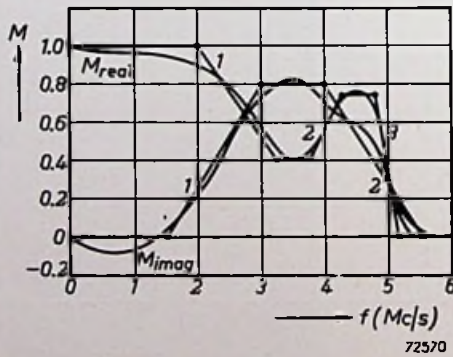
curves are derived (fig. 102). These are approximated by the series of straight lines, the inclined line segments of which are given by the following data:

Segment	No.	h	f'	f''/f'
M_{real}	1	0.6	3.3	0.6
	2	-0.35	4.3	0.9
	3	0.75	5.25	0.9
M_{imag}	1	-0.85	3.0	0.5
	2	+0.85	5.5	0.75



72569

Fig. 101. Amplitude and phase characteristics A and Θ corresponding to the response curve of fig. 101.



72570

Fig. 102. Real and imaginary components of the modulation response curves M_{real} and M_{imag} derived from the phase characteristic of fig. 101.

7.4 Staggered tuning system

Fig. 103 gives the step function $S_{tot} + C_{tot}$ which has been graphically derived from fig. 102.

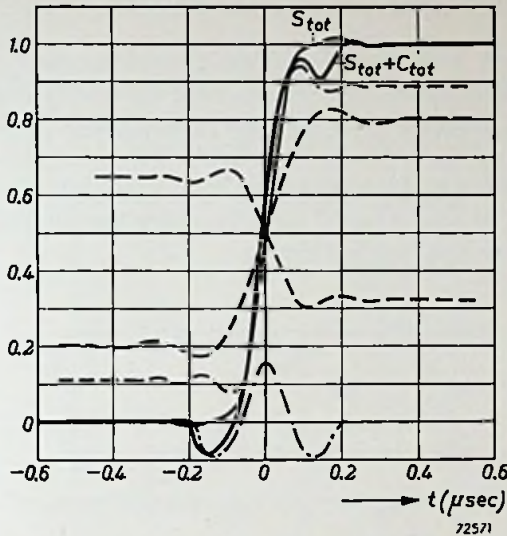


Fig. 103. Step function $S_{tot} + C_{tot}$ constructed from the modulation response curves plotted in fig. 102.

The main data of the design have thus been determined. If required, the changes which must be made in the staggered tuning system when the valves are controlled, and what the consequences of controlling the valves will be on the response curve and step function, can be investigated. The change of the step function with increasing modulation depth can be investigated by adding the quadrature component.

To ensure that the frequency response and the step function are not affected by feedback via C_{ag} , a check of this effect should be made by means of eq. (128a). Setting

$$G_h = 10, \quad p_h^2 = 0.5 \quad \text{and} \quad f = 21 \text{ Mc/s},$$

this equation gives for $f_s = 17 \times 10^4 \text{ Mc/s}$:

$$\sin \alpha_h \sin \alpha_{h+1} \geq \frac{100}{0.5} \cdot \frac{21}{17} \cdot 10^{-4} \approx 0.02.$$

The actual value of this product is tabulated below:

Stage h	$\sin \alpha_h$	$\sin \alpha_{h+1}$	product
1	0.8	1.0	0.8
2	1.0	0.15	0.15
3	0.16	0.3	0.05
4	0.3	0.8	0.24

APPENDIX I

TUNED CIRCUITS AND BAND-PASS FILTERS

In this Section several well-known formulae, used without further explanation in the preceding sections, will be briefly commented upon. This may also be useful in clarifying the meaning of several symbols.

- (a) By generalizing and introducing a few approximations the stationary oscillations of single-tuned circuits under various conditions can be expressed by one single formula.

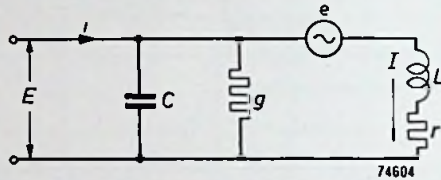


Fig. 104. Diagram of a tuned circuit for expressing E and I .

Assume that a tuned circuit consisting of a capacitance C and an inductance L with a series resistance r and parallel damping g is excited by a current i fed to the top of the circuit, and that a voltage e is induced in the inductance (see fig. 104). Both signals have an angular frequency ω (radians per second). The current I flowing through L and the voltage E across C can now be expressed in simple formulae by setting:

$$\omega_0^2 LC = 1, \quad \frac{g}{\omega_0 C} = \delta_C, \quad \frac{r}{\omega_0 L} = \delta_L \quad \text{and} \quad \frac{\omega}{\omega_0} - \frac{\omega_0}{\omega} = \beta.$$

Assuming now that ω differs relatively little from ω_0 , then the factor ω_0/ω can be disregarded in all formulae. A further simplification is obtained by assuming, moreover, that $\delta_C \ll 1$ and $\delta_L \ll 1$, so that δ_C and δ_L no longer occur separately in the formulae ($\delta_C + \delta_L$ does, however, occur and will henceforth be denoted by δ).

For the further calculation it is therefore immaterial whether the circuit losses are caused by a series resistance or a parallel damping. It will be shown that for the losses thus generalized $1/\delta = Q$, where Q is a measure for the selectivity of the circuit.

Setting furthermore:

$$\beta/\delta = x \quad \text{and} \quad 1 + jx = a,$$

it may be written:

$$E = (\omega_0 L i - j e) Q/a,$$

and

$$I = (\omega_0 C e - j i) Q/a.$$

In these expressions only a depends on the angular frequency ω of the signal. The frequency response curve of the tuned circuit is therefore determined by $a = 1 + jx$.

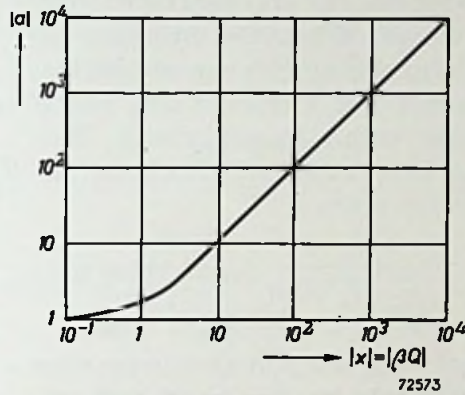


Fig. 105. Absolute value of a as a function of the absolute value of x .

The absolute value of a , given by

$$|a| = \sqrt{1 + x^2},$$

has been plotted in fig. 105, whilst the phase angle φ_a , given by

$$\tan \varphi_a = x \quad \text{or} \quad \varphi_a = \arctan x,$$

has been plotted in fig. 106.

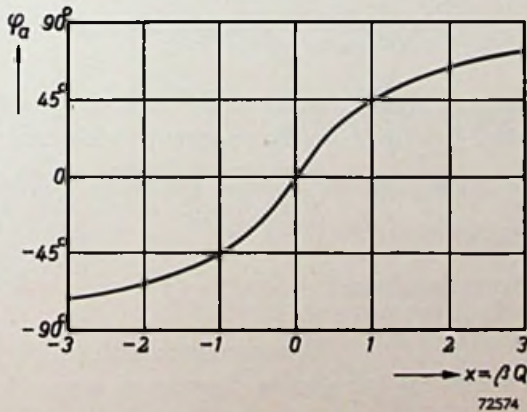


Fig. 106. Phase angle φ_a as a function of x .

The relation between amplitude and phase is shown by the polar diagram. Fig. 107 gives, by way of example, the admittance diagram of a parallel tuned circuit:

$$Y = \frac{i}{E} = \hat{Y}a,$$

where \hat{Y} denotes the admittance at resonance.

The curves for $a = Y/\hat{Y}$ are called the relative admittance curves. When the frequency is changed the locus of the vector representing the complex quantity a is a straight line, which may be provided with a frequency scale. This scale is to all intents and purposes linear, as shown by the expression:

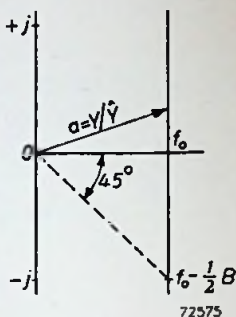


Fig. 107. Relative admittance diagram
 $Y = \hat{Y}a.$

$$x = \beta Q = \left(\frac{\omega}{\omega_0} - \frac{\omega_0}{\omega} \right) Q = \frac{(\omega - \omega_0)(\omega + \omega_0)}{\omega_0 \omega} Q \approx 2Q \frac{\omega - \omega_0}{\omega_0}.$$

The absolute value of a is at a minimum when $\omega = \omega_0 = 1/\sqrt{LC}$. A second point of the frequency scale is found by determining one of the frequencies at which the real part of a is equal to its imaginary part. This is the case at:

$$x = \pm 1, \quad |a| = \sqrt{2} (= 3 \text{ db}), \quad \varphi_a = \pm 45^\circ.$$

Denoting the difference in frequency (in $c/s!$) by B , then it is clear that for these points:

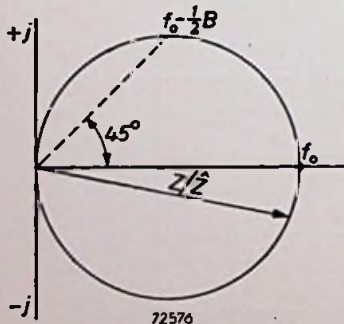


Fig. 108. Relative impedance diagram of a single-tuned circuit of which $Z = \hat{Z}/a.$

$$|x| = |\beta Q| = 1 \quad \text{or} \quad 2Q \frac{\frac{1}{2}(2\pi B)}{\omega_0} = 1,$$

so that $BQ = f_0$ or $Q = f_0/B$.

For a circuit with exclusively parallel damping g (hence $r=0$), it then follows from $\delta = \delta_C = g/\omega_0 C = 1/Q$ that:

$$g = \frac{\omega_0 C B}{f_0} = 2\pi B C,$$

in accordance with eq. (6) in Section I.1.

Fig. 108 shows the impedance diagram of a parallel tuned circuit of which $\hat{Z} = 1/\hat{Y} = \omega_0 L Q = Q/\omega_0 C$.

- (b) Now the properties of band-pass filters (I. F. transformers) consisting of two inductively coupled circuits tuned to the angular frequencies ω_p and ω_s will be investigated. It will again be assumed that the factors ω_p/ω and ω_s/ω are about unity, and moreover that $\delta_p \ll 1$ and $\delta_s \ll 1$.

From the formula for single-tuned circuits it follows that:

$$I_p = (\omega_p C_p e_p - j i) Q_p a_p,$$

and

$$I_s = \omega_s C_s e_s Q_s / a_s,$$

where

$$a_p = 1 + j \beta_p Q_p,$$

and

$$a_s = 1 + j \beta_s Q_s.$$

(see fig. 109)

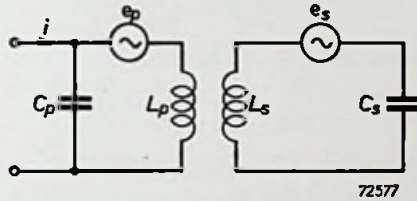


Fig. 109. Band-pass filter (I.F. transformer) consisting of two inductively coupled circuits.

The mutually induced voltages in the circuits are given by:

$$e_p = j\omega M I_s \quad \text{and} \quad e_s = j\omega M I_p,$$

from which it can be derived that:

$$\frac{I_p}{i} = \frac{-j Q_p / a_p}{1 + \omega^2 \omega_p \omega_s C_p C_s M^2 Q_p Q_s / a_p a_s},$$

and

$$\frac{I_s}{i} = \frac{\omega_p \omega_s C_s M Q_p Q_s}{a_p a_s + \omega^2 \omega_p \omega_s C_p C_s M^2 Q_p Q_s / a_p a_s}.$$

To simplify these expressions, M will be replaced by $k \sqrt{L_p L_s}$, whilst $k \sqrt{Q_p Q_s} = q$, which gives for $\omega_p/\omega \approx \omega_s/\omega \approx 1$:

$$\frac{I_p}{i} = \frac{-j Q_p a_s}{a_p a_s + q^2},$$

and

$$\frac{I_s}{i} = \frac{q \sqrt{Q_p Q_s} \sqrt{\frac{\omega_s C_s}{\omega_p C_p}}}{a_p a_s + q^2}.$$

From

$$E_p = \frac{I_p}{j\omega C_p} = I_p j\omega L_p$$

and

$$E_s = \frac{I_s}{j\omega C_s} = I_s j\omega L_s$$

it is now possible to derive the well-known formulae:

$$Z_i = \frac{E_p}{i} = \frac{\omega L_p Q_p a_s}{a_p a_s + q^2} = \hat{Z}_p \frac{a_s}{a_p a_s + q^2},$$

and

$$Z_t = \frac{E_s}{i} = \frac{jq\sqrt{\omega_p L_p Q_p \omega_s L_s Q_s}}{a_p a_s + q^2} = \frac{jq\sqrt{\hat{Z}_p \hat{Z}_s}}{a_p a_s + q^2}.$$

In analogy with the formula for Z_i ,

$$Z_o = \hat{Z}_s \frac{a_p}{a_p a_s + q^2},$$

whilst, moreover

$$\frac{E_s}{E_p} = \frac{Z_t}{Z_i} = j \frac{q}{a_s} \sqrt{\hat{Z}_s / \hat{Z}_p}.$$

- (c) The response curves of a band-pass filter consisting of two coupled tuned circuits are given by the denominator of the formula for Z_t , viz.:

$$N = a_p a_s + q^2.$$

This expression may be written as a product of two factors, both containing an imaginary term $jx = j\beta/\delta$, whilst the real term is independent of the frequency. These factors may, therefore, be regarded as the admittances of two single-tuned circuits which are not coupled¹⁾. Hence:

$$N = \alpha a' a'' = \frac{(\delta' + j\beta')(\delta'' + j\beta'')}{\delta_p \delta_s}.$$

Provided the four characteristic quantities δ' , β' , δ'' and β'' can be determined, the response curve of the band-pass filter can therefore be derived from the so-called α -diagram of a single-tuned circuit. For this purpose it is assumed that:

$$\beta = \frac{1}{2}(\beta_p + \beta_s), \quad \delta = \frac{1}{2}(\delta_p + \delta_s), \quad m = \frac{1}{2}(\beta_p - \beta_s), \quad l = \frac{1}{2}(\delta_p - \delta_s), \quad \text{and}$$

$$w = \sqrt{\frac{k^2 - l^2 + m^2}{2}}.$$

¹⁾ B. D. H. Tellegen, Coupled Circuits, Philips Research Reports 2, p. 1, 1947 (No. 1).

It is possible to carry out the following calculations:

$$\gamma = w \sqrt{1 + \sqrt{1 + \frac{l^2 m^2}{w^4}}}$$

and

$$\epsilon = w \sqrt{-1 + \sqrt{1 + \frac{l^2 m^2}{w^4}}}$$

Now:

$$\beta' = \beta + \gamma, \quad \beta'' = \beta - \gamma, \quad \delta' = \delta \mp \epsilon \quad \text{and} \quad \delta'' = \delta \pm \epsilon,$$

in which the upper sign applies when lm is positive.

For the further calculation of N the product of the standardized admittance curves of both fictitious circuits is determined. This product then has to be multiplied by the factor

$$\alpha = \frac{\delta' \delta''}{\delta_p \delta_s}$$

When the primary and secondary circuits are tuned to the same frequency, ϵ becomes zero, so that $\delta' = \delta'' = \frac{1}{2}(\delta_p + \delta_s)$. Both fictitious circuits then have the same value of Q , which results in the response curve becoming symmetrical. This curve is then identical to that of two circuits connected in cascade having the same value of Q and an equally large but opposed detuning $\Delta f = \pm \frac{1}{2} f \sqrt{k^2 - l^2}$ with respect to the resonant frequency. From the above formulae it follows that this detuning is determined by δ_p , δ_s and k . It is clear that at $\delta_p = 0$, δ_s and k can be so chosen that the detunings and dampings of the fictitious circuits correspond to the values required for flat staggering. It is on this principle that the stagger damping system is based by making $\delta' = \frac{1}{2}\delta_s = (\sin \alpha_h)/Q_r$ and $k = 1/Q$, which gives:

$$\Delta f = \pm \frac{f}{2Q_r} \cdot \sqrt{1 - \sin^2 \alpha_h} = \pm \frac{1}{2} B_r \cos \alpha_h$$

- (d) The case where the primary and secondary circuits are tuned to the same frequency will now be investigated. Assuming that

$$Q_s/Q_p = r \quad \text{and} \quad x = \beta \sqrt{Q_p Q_s},$$

then:

$$a_p = 1 + \frac{jx}{\sqrt{r}} \quad \text{and} \quad a_s = 1 + jx \sqrt{r}.$$

This gives:

$$Z_t = \frac{jq \sqrt{\hat{Z}_p \hat{Z}_s}}{1 + q^2 + jx \left(\sqrt{r} + \frac{1}{\sqrt{r}} \right) - x^2}$$

(The expression $\sqrt{r} + \frac{1}{\sqrt{r}}$ may also be written: $\sqrt{2 + \frac{1}{r} + r}$.)

Eq. (61) can now be deduced directly by setting:

$$\hat{Z}_p = R_p \quad \text{and} \quad \hat{Z}_s = R_s.$$

It is moreover seen that

$$Z_i = \frac{\hat{Z}_p}{1 + \frac{jx}{\sqrt{r}} + \frac{q^2}{1 + jx\sqrt{r}}}$$

and

$$Z_o = \frac{\hat{Z}_s}{1 + jx\sqrt{r} + \frac{q^2}{1 + \frac{jx}{\sqrt{r}}}}.$$

At resonance

$$Z_i = \frac{\hat{Z}_p}{1 + q^2}, \quad \hat{Z}_o = \frac{\hat{Z}_s}{1 + q^2} \quad \text{and} \quad \hat{Z}_t = \frac{q}{1 + q^2} \sqrt{\hat{Z}_p \hat{Z}_s} = q \sqrt{\hat{Z}_i \hat{Z}_o}.$$

The above considerations yield no practical results when, for example, Q_p is infinitely large. In that case:

$$Z_t = \frac{j k Q_p Q_s \sqrt{\omega^2 L_p L_s}}{a_p a_s + k^2 Q_p Q_s} = \frac{j k / \omega \sqrt{C_p C_s}}{k^2 + j \beta / Q_s + (j \beta)^2},$$

so that

$$\hat{Y}_t = \frac{1}{Z_t} = -j \omega k \sqrt{C_p C_s},$$

whilst

$$Z_i = \frac{\hat{Z}_s \frac{C_s}{C_p}}{j x_s + \frac{q_s^2}{a_s}}, \quad \text{so that} \quad \hat{Z}_i = \frac{\hat{Z}_s}{q_s} \cdot \frac{C_s}{C_p},$$

where $q_s = k Q_s$. Moreover:

$$Z_o = \frac{\hat{Z}_s}{a_s + \frac{q_s^2}{j x_s}}, \quad \text{so that} \quad \hat{Z}_o = 0.$$

- (e) The following comments will again be confined to band-pass filters the primary and secondary of which are tuned to the same frequency (tuned I. F. transformers).

The polar diagram of

$$y = \frac{q \sqrt{\hat{Z}_p \hat{Z}_s}}{Z_t} = j (1 + q^2) \frac{Y_t}{\hat{Y}_t}$$

then passes through the point $j(1 + q^2)$, i.e. the top of a parabola which can be constructed by plotting on the abscissa the real component of N and on the ordinate its imaginary component (fig. 110). From eq. (61) it may then be written:

$$\left. \begin{aligned} Y &= 1 + q^2 - x^2 \\ X &= x \sqrt{2 + r + \frac{1}{r}} \end{aligned} \right\} \text{(a)}$$

The response curve is flattest when the length of the vector having the parabola as locus is as constant as possible at small values of x . The calculation of the values of the parameters q

and r at which this will be the case will be based on the equation of a circle given by $X^2 + Y^2 = R^2$ with centre O and coinciding with the parabola for small values of X .

Since the circle must run through the top of the parabola, $R = 1 + q^2$, so that

$$X^2 + Y^2 = (1 + q^2)^2. \quad \text{(b)}$$

To determine the point of intersection of this circle with the parabola, the values of X and Y which satisfy eq. (a) are substituted in eq. (b), thus giving:

$$(1 + q^2 - x^2)^2 + \left(x \sqrt{2 + \frac{1}{r} + r}\right)^2 = (1 + q^2)^2,$$

or

$$x^4 - 2(1 + q^2)x^2 + \left(2 + r + \frac{1}{r}\right)x^2 = 0.$$

This equation is satisfied by two points $x = 0$. After having divided the equation by x^2 , so that these points are eliminated, two points of intersection remain, which are determined by

$$x^2 - 2(1 + q^2) + 2 + r + \frac{1}{r} = 0.$$

In order to ensure that the parabola approximates as near as possible to the circle at $x = 0$, these two points of intersection will

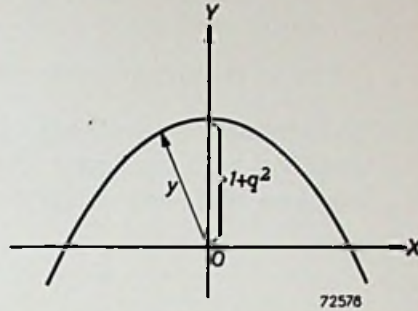


Fig. 110. Polar diagram of y for a band-pass filter.

also be made to lie at $x = 0$. The condition to be satisfied for this purpose is

$$q = \sqrt{\frac{r + \frac{1}{r}}{2}}$$

This is the condition for transitional coupling given by eq. (64).

- (f) To determine the feedback via the anode-to-grid capacitance C_{ag} in amplifiers with band-pass filters, it is important to know the polar diagrams of Z_i and Z_o (or Y_i and Y_o) of a band-pass filter. Now

$$Y_i = \frac{1}{R_p} \left(a_p + \frac{q^2}{a_s} \right),$$

or

$$Y_i = Y_p + \frac{q^2}{R_p} \cdot \frac{Z_s}{R_s}$$

From these formulae it is seen that the construction of the polar diagram of Y_i is analogous to that of the admittance of a grid circuit in the case of feedback from anode to grid. In fact, it is necessary to add to the Y_p vector a Z/R vector the extremity of which is situated on a circle moving along the Y_p line and having a diameter q^2/R_p . This construction is given in fig. 111.

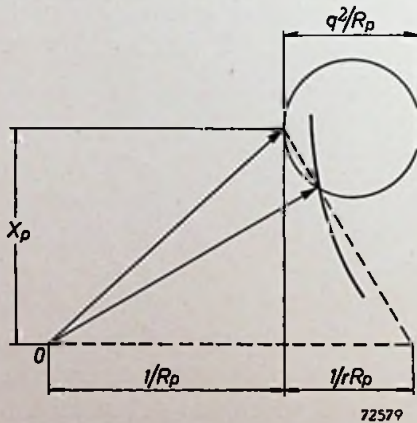


Fig. 111. Construction of the polar diagram of Y_i . When the scale of this diagram is multiplied by rR_p , the shape of the curves depends only on kQ_s and the location of the origin only on r .

The Y_i diagrams obtained at various values of q and r are given in figs 112a and b.

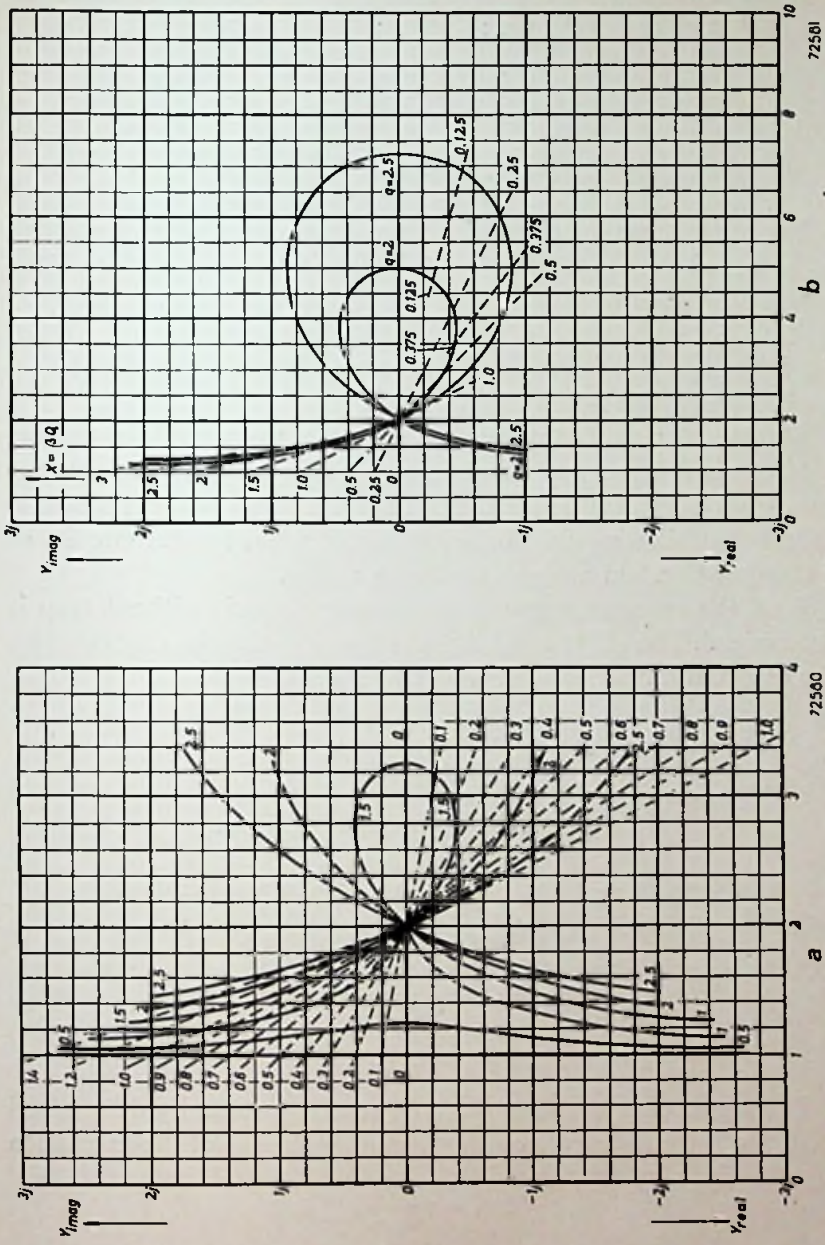


Fig. 112a and b. Polar diagrams of τY_i at various values of q and $\tau = 1$. These diagrams can also be used for $\tau \neq 1$, by substituting βQ_s for x , kQ_s for q and placing the origin in $1 - \tau$.

When the Z_i diagram is derived from the Y_i diagram a curve is obtained which resembles a cardioid at normal values of q .

If Q_p is made infinitely large, Y_i and Y_o can be expressed in $x_s = \beta Q_s$ and $q_s = kQ_s$, viz.:

$$Y_i = \hat{Y}_s \frac{C_1}{C_2} \left(jx_s + \frac{q_s^2}{1 + jx_s} \right),$$

and

$$Y_o = \hat{Y}_s \left(1 + jx_s + \frac{q_s^2}{jx_s} \right).$$

The latter locus coincides with the polar diagram of Y_s , but when x_s is varied from $-\infty$ to $+\infty$ this line is traversed twice. The minimum values of Y_o are then situated at $x_s = \pm q_s$.

- (g) An interstage circuit provided with a trap may be considered as a double tuned band-pass filter.

When both circuits are tuned to the same frequency (Z_i coupling) the response curve can be determined from the Z_i diagrams for band-pass filters, but when the tunings are different it is preferable to use the following method, particularly when several circuits of a staggered system are provided with a trap.

First the response curve of the primary circuit without trap is determined. The effect of adding the trap can then be expressed by the attenuation factor a_t of the trap, that is:

$$a_t = \frac{a_p a_s + q^2}{a_p a_s}.$$

Setting

$$\beta_s Q_p = x_t, \quad \frac{Q_s}{Q_p} = r \quad \text{and} \quad \beta' Q_p = s,$$

where $\beta' = \omega_p/\omega_s - \omega_s/\omega_p$, then, to a good approximation:

$$\beta_p Q_p = x_t - s \quad \text{and} \quad \beta_s Q_s = x_t r,$$

so that

$$|a_t| = \sqrt{\frac{\left(1 + \frac{q^2}{1 + r^2 x_t^2}\right)^2 + \left(x_t - s - \frac{q^2 r x_t}{1 + r^2 x_t^2}\right)^2}{1 + (x_t - s)^2}}$$

The absorption curve of the trap can be graphically determined from the response curves of four circuits by means of the expression

$$a_t = \alpha \frac{a' a''}{a_p a_s},$$

in agreement with the method outlined in Appendix Ic.

The diagrams for $|a_t|$, at various values of r and s , have been plotted in figs 113a—l. In each of these diagrams the variation of the coupling is such that given, fixed values of the maximum suppression $|a_t|$ are obtained. The x_t scale is related to the x_p scale by the following rule: $x_t = s$ at the resonant frequency of the primary circuit; the 3 db points of this circuit are located at $x_t = s \pm 1$.

Figs 113 m and n have been graphically derived from the response curves of two circuits according to the expression $a'' = a'/a$, where a' applies to the corrected circuit and a to the original circuit. These curves are used for determining the small corrections of the staggering system.

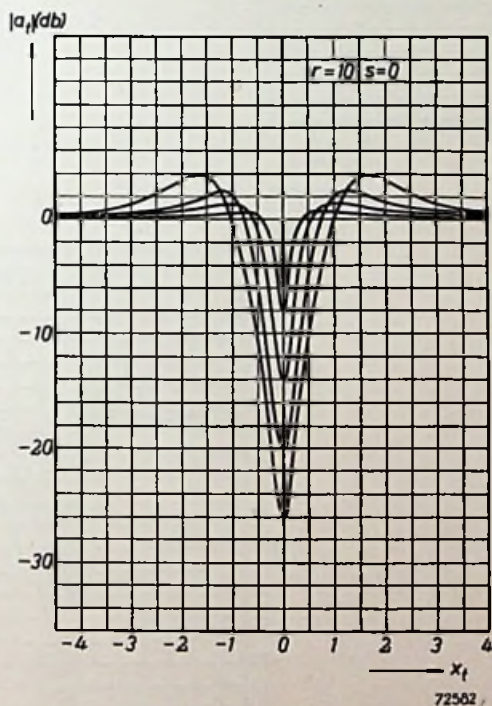


Fig. 113a. $|a_t|$ as a function of x_t at $r = 10$ and $s = 0$.

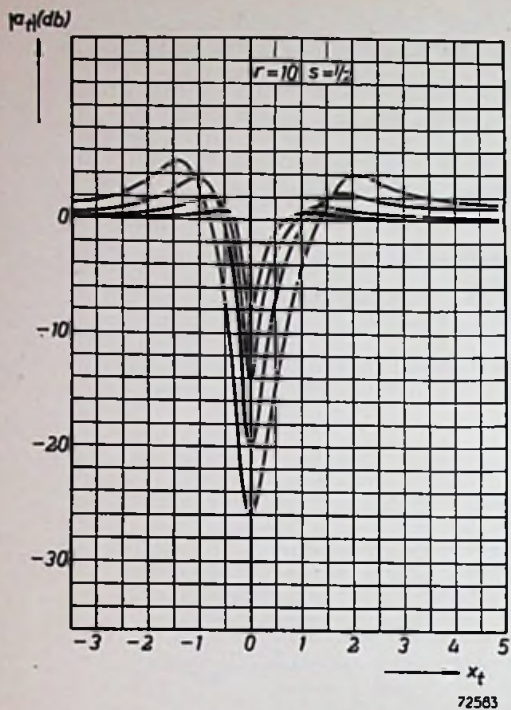


Fig. 113b. $|a_t|$ as a function of x_t at $r=10$ and $s=1/2$.

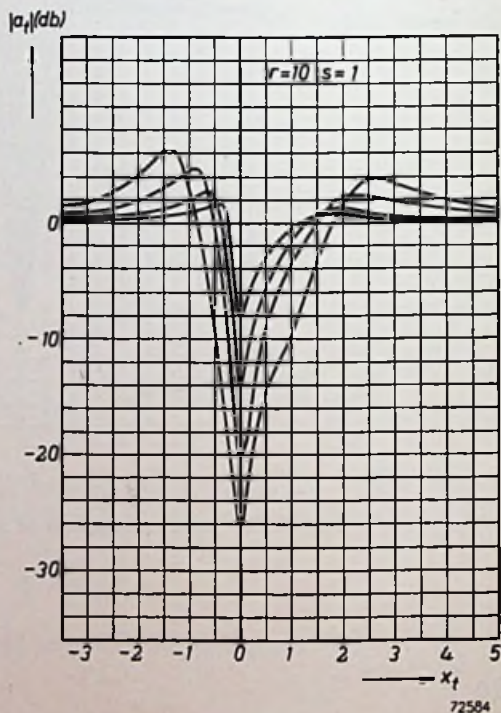


Fig. 113c. $|a_t|$ as a function of x_t at $r=10$ and $s=1$.

Fig. 113d. $|a_t|$ as a function of x_t at $r = 10$ and $s = 2$.

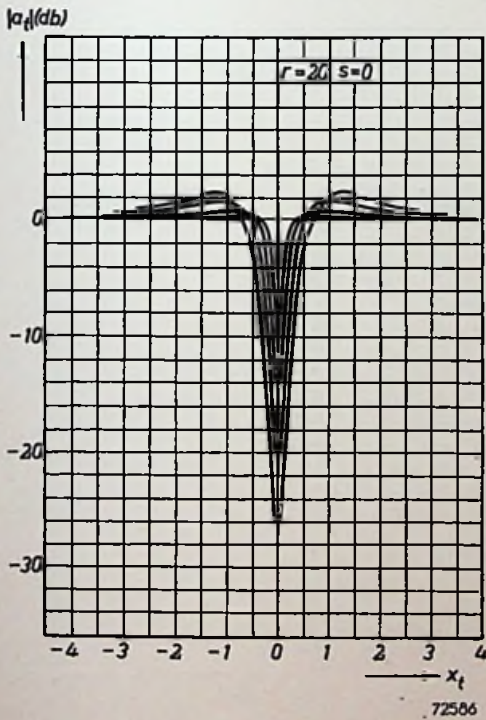
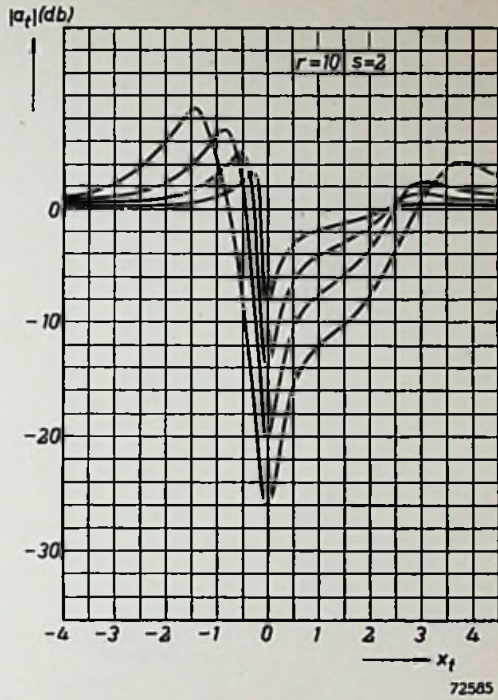


Fig. 113e. $|a_t|$ as a function of x_t at $r = 20$ and $s = 0$.

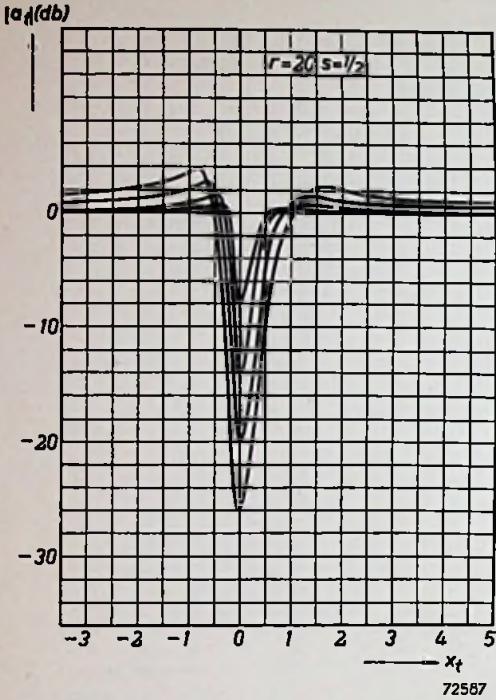


Fig. 113f. $|a_t|$ as a function of x_t at $r=20$ and $s=1/2$

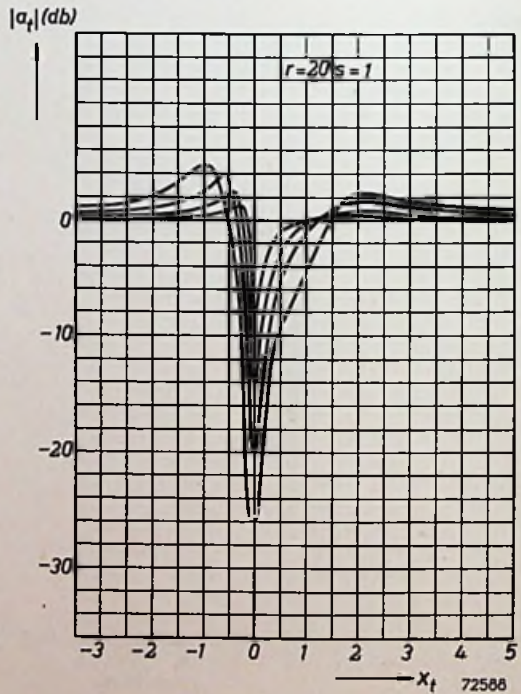
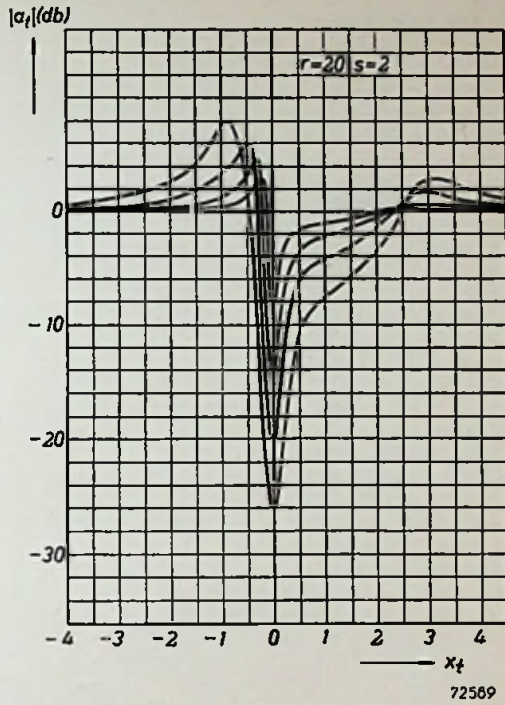
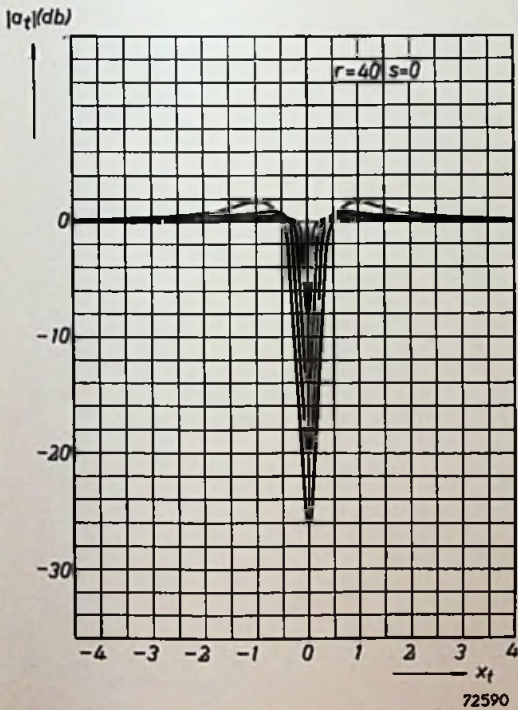


Fig. 113g. $|a_t|$ as a function of x_t at $r=20$ and $s=1$.

Fig. 113*h*. $|a_t|$ as a function of x_t
at $r = 20$ and $s = 2$.



72569



72590

Fig. 113*i*. $|a_t|$ as a function of x_t at
 $r = 40$ and $s = 0$.

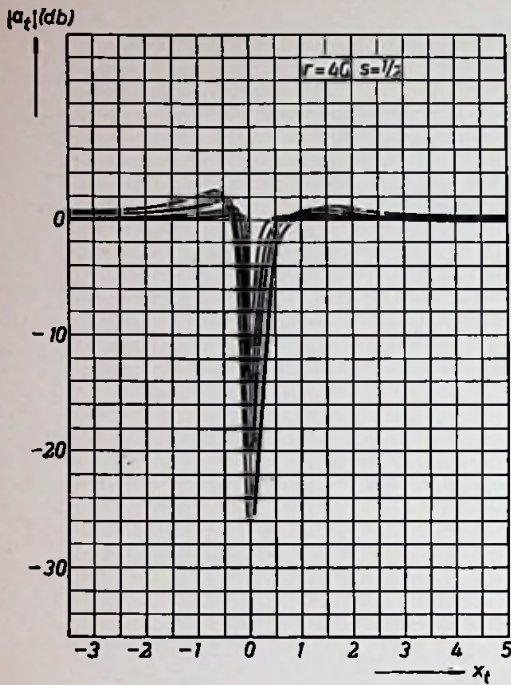


Fig. 113j. $|a_t|$ as a function of x_t at $r = 40$ and $s = 1/2$.

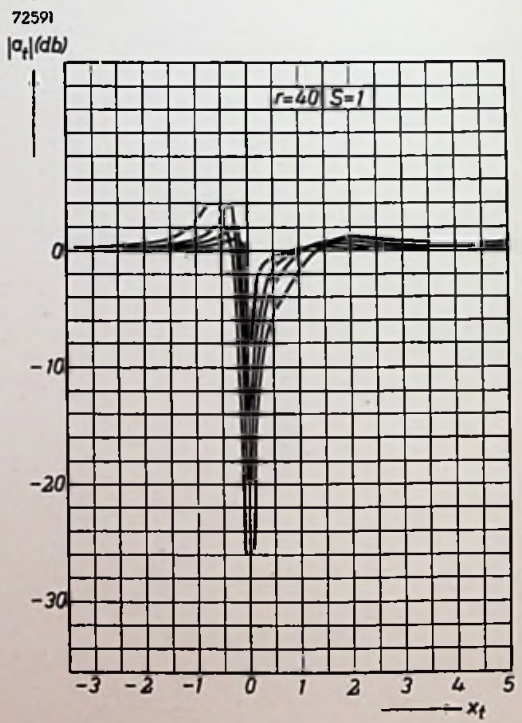


Fig. 113k. $|a_t|$ as a function of x_t at $r = 40$ and $s = 1$,

Fig. 113l. $|a_t|$ as a function of x_t at $r = 40$ and $s = 2$.

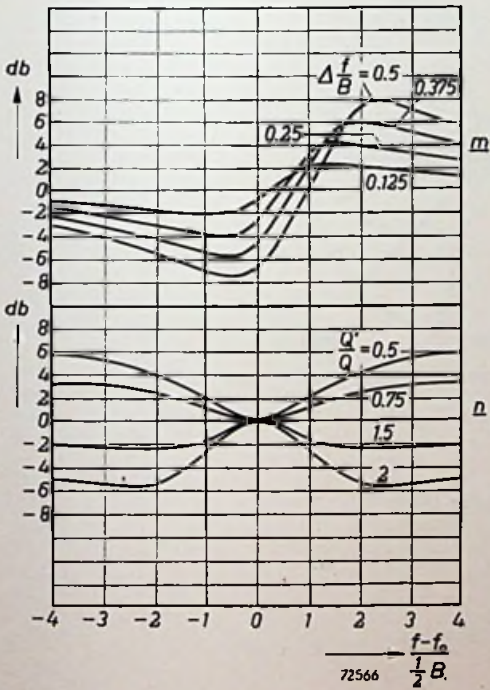
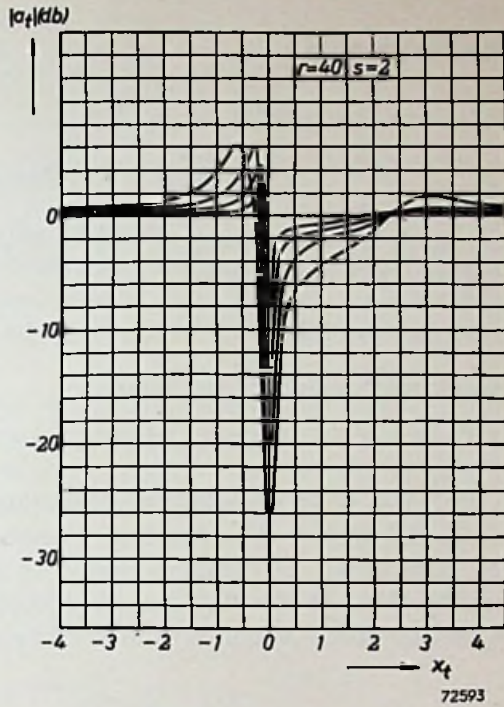


Fig. 113m. Modification a^* of the response curve due to the detuning of one of the circuits.

n. Modification a^* of the response curve due to a change of the quality factor of one of the circuits.

APPENDIX II

To prove the validity of eq. (29):

$$\prod_{h=1}^{h=s} (1 + x^2 + 2x \cos \alpha_h) = 1 + x^{2s},$$

the term between brackets will be transformed by writing $\cos^2 \alpha_h + \sin^2 \alpha_h$ for 1, which gives:

$$x^2 + 2x \cos \alpha_h + 1 = x^2 + 2x \cos \alpha_h + \cos^2 \alpha_h + \sin^2 \alpha_h = (x + \cos \alpha_h)^2 + \sin^2 \alpha_h,$$

which may factorised as follows:

$$(x + \cos \alpha_h + j \sin \alpha_h) (x + \cos \alpha_h - j \sin \alpha_h).$$

For the sake of simplicity the quantities $\cos \alpha_h + j \sin \alpha_h$ and $\cos \alpha_h - j \sin \alpha_h$ will be denoted x_h and x_h^* respectively. x_h and x_h^* can be represented as complex quantities on a circle with radius $r = 1$, see fig. 114. If the flat staggered tuning system is adhered to (see p. 18), all points x_h and x_h^* are evenly distributed over the whole circle.

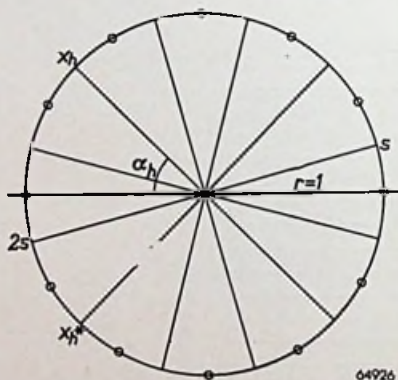


Fig. 114. Diagram representing the quantities x_h and x_h^* .

As shown by fig. 114,

$$\prod_{h=1}^{h=s} (x + x_h) (x + x_h^*)$$

may also be written as:

$$\prod_{h=1}^{h=2s} (x + x_h).$$

This product can be worked out, giving:

$$\prod_{h=1}^{h=2s} (x + x_h) = \sum_{h=0}^{2s} E_h x^{2s-h},$$

where $E_0 = 1$,

$$E_1 = x_1 + x_2 + \dots + x_{2s}, \text{ and}$$

$$E_2 = x_1 x_2 + x_1 x_3 + \dots + x_{2s-1} x_{2s}, \text{ etc.}$$

Summarizing, E_n always contains all possible products of n terms x_h .

All coefficients of the power series from E_1 to E_{2s-1} are now obviously zero, since each product, say $x_p \cdot x_q \cdot \dots \cdot x_r$, has a "twin" with opposite sign.

The last term $x_1 \cdot x_2 \cdot \dots \cdot x_{2s}$, on the other hand, is equal to unity, since for each factor of this product there is again a "twin", which is now conjugate complex, and as the product of each pair of conjugate complexes is unity, this is also the case with the entire term.

Concluding, only the first and last terms of the whole power series

$$\sum_{h=0}^{2s} E_h x^{2s-h}$$

remain, which gives:

$$\prod_{h=1}^{h=2s} (x + x_h) = x^{2s} + 1.$$

APPENDIX III

- (a) A general method for determining the step function from the amplitude response curve is based on the Fourier analysis of the signal. According to the integral theorem of Fourier, a function $y(t)$ may, under certain conditions, be described by:

$$y(t) = \int_{-\infty}^{+\infty} c| \omega t Y(\omega) d\omega, \quad (c)$$

where $e^{j\omega t}$ stand for $\cos \omega t + j \sin \omega t$. $Y(\omega)$ is termed the spectral amplitude of the function $y(t)$, and is given by:

$$Y(\omega) = \frac{1}{2\pi} \int_{-\infty}^{+\infty} e^{-j\omega t} y(t) dt. \quad (d)$$

Applied to the function $H(t)$ of eq. (33), this gives:

$$H(t) = \frac{1}{2} + \frac{1}{\pi} \int_0^{\infty} \frac{\sin \omega t}{\omega} d\omega. \quad (e)$$

The spectral amplitude of this function is, therefore, $1/2\pi j\omega$.

For the function $H(t-\tau)$, representing a unit step at $t = \tau$, the spectral amplitude is given by $e^{-j\omega\tau}/2\pi j\omega$.

The Fourier components of the input signal applied thus having been determined, it is possible to derive from the amplitude response curve the corresponding Fourier components of the output signal, after which the step function can be determined from the latter components.

This principle will now be applied to the envelope of the H. F. signal. The step-like variation of the signal amplitude is analysed into sinusoidal modulation components:

$$E_i = E_b + E_s \left(\frac{1}{2} + \frac{1}{\pi} \int_0^{\infty} \frac{\sin \omega t}{\omega} d\omega \right). \quad (f)$$

After the amplitude and phase of these components have been changed in the amplifier, the following equation applies:

$$\frac{E_o}{G} = E_b + E_s \left[\frac{1}{2} + \frac{1}{\pi} \int_0^{\infty} \frac{A(\omega)}{\omega} \sin \omega \left\{ t - D(\omega) \right\} d\omega \right]. \quad (g)$$

$A(\omega)$ and $D(\omega)$ are determined by the complex modulation response curve $M(\omega)$. Once $M(\omega)$ is known, E_o/G , i.e. the step

function, can be determined, and, conversely, $M(\omega)$ can be derived from the step function.

The value of $M(\omega)$ corresponding to the frequency ω can be found by considering that the gain and the modulation response curve $M(\omega)$ convert the Fourier component with angular frequency ω of the input signal into a component of E_o of the same frequency. Hence:

$$E_i(\omega) \cdot M(\omega) \cdot G = E_o(\omega). \quad (h)$$

- (b) The step function without overshoot depicted in fig. 115 will be taken as a starting point.

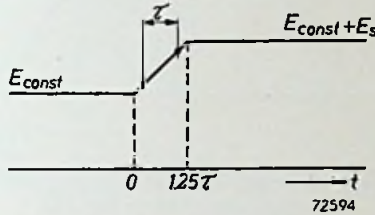


Fig. 115. Idealized step function without overshoot.

The step function can be analysed in the following way:

$$E_o(t) = E_{const} + 0.8 E_s \frac{t}{\tau} \{1 - H(t - 1.25\tau)\} + 0.8 E_s H(t - \tau).$$

The corresponding amplitude response curve will now be derived without considering whether this can indeed be realized physically. The gain is assumed to be unity and the delay $D(\omega)$ is taken to be zero and $A(\omega)$ is then calculated. Disregarding the frequency zero, the spectral amplitude of E_i is given by:

$$E_i(\omega) = \frac{E_s}{2\pi j\omega}.$$

Moreover, from eq. (d):

$$E_o(\omega) = \frac{1}{2\pi} \int_{-\infty}^{+\infty} E_o(t) e^{-j\omega t} dt = \frac{0.8 E_s}{2\pi} \int_0^{1.25\tau} \frac{t}{\tau} e^{-j\omega t} dt + 0.8 E_s \frac{e^{-j\omega\tau/0.8}}{2\pi j\omega}$$

Hence:

$$E_o(\omega) = \frac{0.8 E_s}{2\pi(j\omega)^2} \cdot \frac{1 - e^{-j\omega\tau/0.8}}{\tau}.$$

From eq. (h):

$$M(\omega) = \frac{1 - e^{-j\omega\tau/0.8}}{1.25 j\omega\tau} \quad \text{and} \quad A(\omega) = |M(\omega)| = \frac{\sin 1.25 \pi / \tau}{1.25 \pi / \tau}.$$

For $\omega = 0$, $A(\omega) = 1$ (see fig. 116). The 3 db point is situated at $1.25 \pi f \tau = 1.39$. Assuming that the H. F. amplitude response curve is symmetrical, the distance between the 3 db points is $1.25 \pi B \tau = 2.78$, from which it follows that:

$$B \tau = \frac{2.78}{1.25 \pi} = 0.7.$$

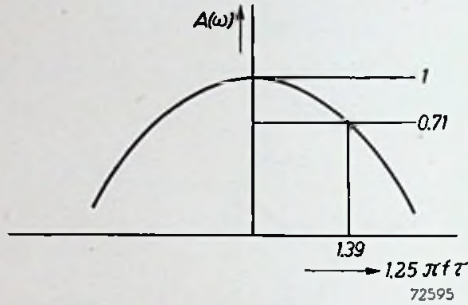


Fig. 116. Amplitude response curve corresponding to the step function depicted in fig. 115.

- (c) It will now be shown what form the step function will assume when the (symmetrical) amplitude response curve is as shown in fig. 117, all modulation components up to the frequency $B/2$ being passed unattenuated and the phase angle being proportional to the frequency.

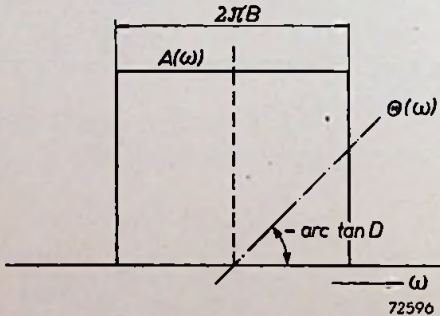


Fig. 117. Symmetrical amplitude response curve with a constant delay D .

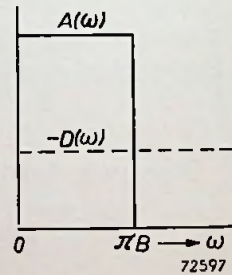


Fig. 118. Modulation response curve corresponding to the amplitude response curve depicted in fig. 117.

Fig. 118 shows the corresponding modulation response curve.

E_o can now be calculated from E_i by means of eq. (g). It then follows from fig. 118 that:

$$E_o = E_b + E_s \left\{ \frac{1}{2} + \frac{1}{\pi} \int_0^{\pi B} \frac{\sin \omega(t-D) d\omega}{\omega} \right\} = E_b + E_s \left(\frac{1}{2} + \frac{1}{\pi} \text{Si } \pi B' \right).$$

By means of a table for $\text{Si}(x)$ ¹⁾ it is now possible to plot the envelope of the output signal (fig. 119).

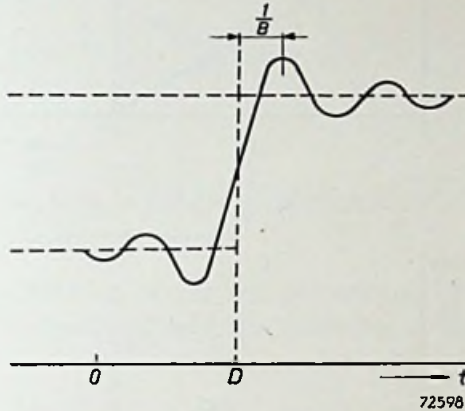


Fig. 119. Envelope of the output signal corresponding to the modulation response curve of fig. 118.

One point situated on the practically straight part of the flank is:

$$\text{Si } \pi B' = \pm \frac{\pi}{2} \quad \text{at} \quad |\pi B'| = 1.925.$$

Linear interpolation then gives:

$$B\tau = \frac{0.8 \times 2 \times 1.925}{\pi} = 0.97.$$

The maximum of $\text{Si}(x)$ is 1.85. Hence:

$$\delta = \frac{1.85}{\pi} - 0.5 = 9\%.$$

- (d) The modulation response curve of fig. 120a will now be considered. This curve descends linearly between $f = 0$ and f_1 , whilst its phase shift is zero.

This response curve may be considered as a superposition of the flat response curve discussed in the previous section (fig. 120b) upon a response curve which ascends linearly (fig. 120c), i.e.:

$$A = A_1 - A_2.$$

¹⁾ See Jahnke-Emde, Tables of Higher Functions, 4th edition 1948, B. G. Teubner, Leipzig.

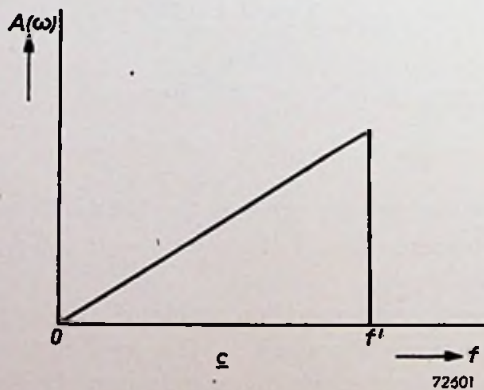
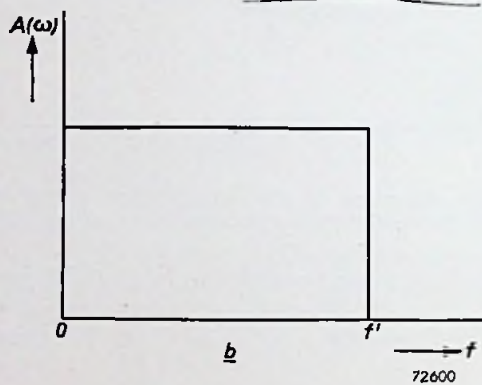
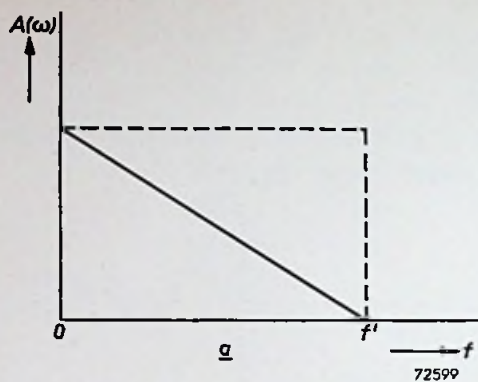


Fig. 120. (a) Linearly descending response curve which may be considered as the superposition of a flat response curve (b) upon a linearly ascending response curve (c).

As shown in Appendix IIIc, the contribution of A_1 towards E_o is:

$$E_{o1} = E_b + E_s \left\{ \frac{1}{2} + \frac{1}{\pi} \text{Si} (2\pi f_1 t') \right\},$$

whilst the contribution of A_2 towards E_o is:

$$E_{o2} = \frac{E_s}{\pi} \int_0^{2\pi f_1} \frac{\sin \omega t'}{2\pi f_1} d\omega = \frac{E_s}{\pi} \cdot \frac{1 - \cos 2\pi f_1 t'}{2\pi f_1 t'},$$

yielding:

$$E_o = E_{o1} + E_{o2} = E_b + E_s \left[\frac{1}{2} + \frac{1}{\pi} \left\{ \text{Si} (2\pi f_1 t') - \frac{1 - \cos 2\pi f_1 t'}{2\pi f_1 t'} \right\} \right].$$

The term between braces will be denoted by $S(f't')_0$. The term $S(x)_0$ can be developed into the following series:

$$\text{Si} (2\pi x) = 2\pi x - \frac{(2\pi x)^3}{3!3} + \frac{(2\pi x)^5}{5!5} \dots$$

$$\frac{1 - \cos 2\pi x}{2\pi x} = \frac{2\pi x}{2!1} - \frac{(2\pi x)^3}{4!1} + \frac{(2\pi x)^5}{6!1} \dots$$

$$f(x) = \frac{2\pi x}{2!1} - \frac{(2\pi x)^3}{4!3} + \frac{(2\pi x)^5}{6!5} \dots$$

Hence:

$$S(x)_0 = \frac{1}{2} + \frac{f(x)}{\pi} = \frac{1}{2} + \frac{1}{\pi} \left\{ \frac{2\pi x}{2!1} - \frac{(2\pi x)^3}{4!3} + \frac{(2\pi x)^5}{6!5} \dots \right\}.$$

From the known property that for large values of x , the sine integral $\text{Si}(x) \approx \pi/2 - \frac{1}{x} \cos x$, it follows that in this range:

$$S(x)_0 \approx 1 - \frac{1}{2\pi^2 x}.$$

- (e) The modulation response curves dealt with in the preceding examples are very rough approximations of practical response curves. A further approximation is obtained by a modulation response curve which is partly flat and descends linearly beyond a given frequency (fig. 121).

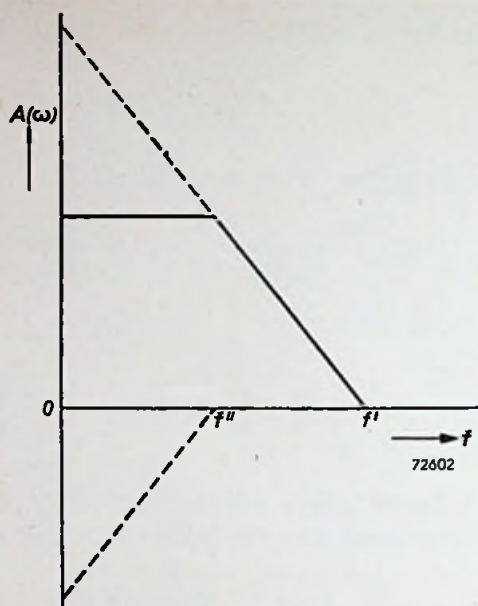


Fig. 121. Modulation response curve consisting of a flat and a linearly descending part (fully-drawn lines).

This response may be considered as being composed of one response with a linearly descending part and one with a linearly ascending part, as dealt with in the preceding section (broken lines in fig. 121).

It is clear that now:

$$S(f'v) = \frac{f'}{f-f''} S(f'v)_0 - \frac{f''}{f-f''} S(f''v)_0,$$

by which $S(f'v)$ is determined for any value of f_1''/f_1' .

In this way it is possible for any modulation response curve approximated by straight line segments (cf. fig. 122) to be analysed

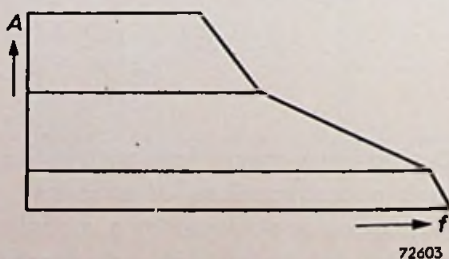


Fig. 122. Modulation response curve approximated by straight line segments and subdivided into trapezoidal parts.

into trapezoidal parts similar to the full-line modulation response curve in fig. 121.

It is on this principle that the method of analysis outlined in Section 3.4 is based.

- (f) The modulation response curve will again be taken to be flat as far as f_1 and then suddenly dropping to zero, as was the case in Appendix IIIc, but it will now be assumed that all sinusoidal modulation compents are shifted 90° in phase (imaginary response).

The output step function is then:

$$\frac{E_s}{\pi} \int_0^{2\pi f_1} \frac{\cos \omega t'}{\omega} d\omega = \frac{E_s}{\pi} \text{Ci}(2\pi f_1 t').$$

By giving the response curve a linearly descending and a linearly ascending part according to fig. 120a, an output step function is obtained which can be calculated to be:

$$E_s C(f't')_0 = \frac{E_s}{\pi} \left\{ \text{Ci}(2\pi f't') - \frac{\sin(2\pi f't')}{2\pi f't'} \right\}.$$

The form $C(x)_0$ can again be transformed into a series:

$$\begin{array}{r} \text{Ci}(2\pi x) = \text{const.} + \log_e 2\pi x - \frac{(2\pi x)^2}{2!2} + \frac{(2\pi x)^4}{4!4} - \frac{(2\pi x)^6}{6!6} \dots \\ \frac{\sin 2\pi x}{x} = 1 - \frac{(2\pi x)^2}{3!} + \frac{(2\pi x)^4}{5!} - \frac{(2\pi x)^6}{7!} \dots \\ \hline f(x) = \text{const.} + \log_e x - \frac{(2\pi x)^2}{3!2} + \frac{(2\pi x)^4}{5!4} - \frac{(2\pi x)^6}{7!6} \dots \end{array}$$

Hence:

$$C(x)_0 = \frac{1}{\pi} \left\{ \text{const.} + \log_e x - \frac{(2\pi x)^2}{3!2} + \frac{(2\pi x)^4}{5!4} - \frac{(2\pi x)^6}{7!6} \dots \right\}.$$

Since, according to the cosine integral tables, $\text{Ci}(x) \approx \sin x/x$ at large values of x , in this range $C(x)_0 \approx 0$. At very small values of x , $C(x)_0$ and $\log_e x$ approach $-\infty$.

When $C(ft')$ diagrams are plotted with a logarithmic time scale they approximate to parallel straight lines at small values of x . In fact, for a trapezoidal component (see fig. 122) of the imaginary response curve:

$$\begin{aligned}
 C(f't) &= \frac{f'}{f' - f''} C(f't)_0 - \frac{f''}{f' - f''} C(f''t)_0 = \\
 &= C(f't)_0 + \frac{f''}{f' - f''} \{ C(f't)_0 - C(f''t)_0 \}.
 \end{aligned}$$

For small values of t' the second term must assume a finite value, because for small values of $f't'$ the lines $C(f't)_0$ and $C(f''t)_0$ run parallel. The proof that the output step function has a finite value when the (imaginary) response is zero for $f=0$ and $f=\infty$, is based on this property.

For this purpose a step function of the form:

$$h_1 C(f_1't) + h_2 C(f_2't) + h_3 C(f_3't) \dots$$

will be investigated. This step function may be written as:

$$\begin{aligned}
 &h_1 C(f_1't) + \\
 &+ h_2 C(f_1't) + h_2 \{ C(f_2't) - C(f_1't) \} + \\
 &+ h_3 C(f_1't) + h_3 \{ C(f_2't) - C(f_1't) \}.
 \end{aligned}$$

The sum of the left-hand terms of each line is zero because $h_1 + h_2 + h_3 = 0$. Since the lines $C(f_1't)$, $C(f_2't)$, $C(f_3't)$, etc. run parallel for small values of $f't'$, the forms between the large brackets must assume a finite value for small values of t' . The resultant thus also has a finite value.

APPENDIX IV

In order to calculate the noise figure of the circuit of fig. 31, R_c and R_r are replaced by R_1 , having a temperature $\alpha_1 T$. The circuit is then split up into four elementary four-terminal networks (fig. 123), the available power gains and noise figures of which can easily be determined. The overall noise figure can be calculated from these data by using eq. (90):

	R_{input}	R_{output}	$(G_p)^h$	$\prod_{k=0}^{h-1} (G_p)^k$	$N-1$	$(N-1) \cdot \prod_{k=0}^{h-1} (G_p)^k$
1	R_s	$\frac{R_s}{1+R_{sg1}}$	$\frac{1}{1+R_{sg1}}$	1	$\alpha_1 R_{sg1}$	$\alpha_1 R_{sg1}$
2	$\frac{R_s}{1+R_{sg1}}$	$\frac{R_s}{1+R_{sg1}}$	1	$\frac{1}{1+R_{sg1}}$	$\frac{R_{eq}-R_p}{R_s} (1+R_{sg1})$	$\frac{R_{eq}-R_p}{R_s} (1+R_{sg1})^2$
3	$\frac{R_s}{1+R_{sg1}}$	$\frac{R_s}{1+R_{sg1}+R_{sgt}}$	$\frac{1+R_{sg1}}{1+R_{sg1}+R_{sgt}}$	$\frac{1}{1+R_{sg1}}$	0	0
4	$\frac{R_s}{1+R_{sg1}+R_{sgt}}$	$\frac{R_s}{1+R_{sg1}+R_{sgt}}$	1	$\frac{1}{1+R_{sg1}+R_{sgt}}$	$\frac{R_p}{R_s} (1+R_{sg1}+R_{sgt})$	$\frac{R_p}{R_s} (1+R_{sg1}+R_{sgt})^2$

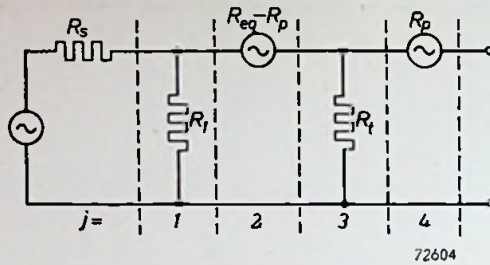


Fig. 123. Diagram in which the circuit of fig. 31 is split up into four elementary four-terminal networks. $R_1 = 1/g_1$ and $R_t = 1/g_t$.

From the last column of the above table it can be seen that

$$N = 1 + \alpha_1 R_s g_1 + \frac{R_{eq}}{R_s} (1 + R_s g_1)^2 - \frac{R_p}{R_s} (1 + R_s g_1)^2 + \frac{R_p}{R_s} (1 + R_s g_1 + R_s g_t)^2.$$

By putting $g_1 = g - g_t$, this gives:

$$N = 1 + 2 R_{eq} (g - g_t) + 2 R_p g_t + \frac{R_{eq}}{R_s} + R_s (g - g_t) F,$$

where

$$\begin{aligned} F &= \alpha_1 + R_{eq} (g - g_t) - R_p (g - g_t) + \frac{R_p g^2}{g - g_t} = \\ &= \alpha_1 + R_{eq} (g - g_t) + 2 R_p g_t + \frac{R_p g_t^2}{g - g_t}, \end{aligned}$$

in which

$$\alpha_1 = \frac{g_c + \alpha_\tau g_\tau}{g_c + g_\tau} \quad \text{and} \quad g = g_t + g_\tau + g_c.$$

In order to express these formulae as far as possible in the product $R_{eq} g_i$ the following substitutions are made:

$$\begin{aligned} g_c &= K_1 g_i, & g_t &= (1 - K_2) g_i, \\ g_\tau &= K_2 g_i, & R_p &= K_3 R_{eq}, \end{aligned}$$

which gives:

$$N = 1 + 2 R_{eq} g_i (K_1 + K_2) + 2 R_{eq} g_i K_3 (1 - K_2) + \frac{R_{eq}}{R_s} + R_{eq} g_i (K_1 + K_2) F \cdot \frac{R_s}{R_{eq}},$$

and

$$F = \frac{K_1 + a_\tau K_2}{K_1 + K_2} + R_{\text{eq}i} (K_1 + K_2) + 2R_{\text{eq}i} K_3 (1 - K_2) + R_{\text{eq}i} \cdot \frac{K_3 (1 - K_2)^2}{K_1 + K_2}.$$

Minimum noise is experienced when:

$$R_{s_i} = \sqrt{\frac{R_{\text{eq}i}}{K_1 + a_\tau K_2 + (K_1 + K_2)^2 R_{\text{eq}i} + (1 - K_2) (2K_1 + K_2 + 1) K_3 R_{\text{eq}i}}}$$

giving a minimum noise figure:

$$N_{\text{opt}} = 1 + 2R_{\text{eq}i}(K_1 + K_2) + 2R_{\text{eq}i}K_3(1 - K_2) + 2 \sqrt{R_{\text{eq}i}(K_1 + K_2) \left\{ \frac{K_1 + a_\tau K_2}{K_1 + K_2} + R_{\text{eq}i}(K_1 + K_2) + \frac{2R_{\text{eq}i}K_3(1 - K_2)(2K_1 + K_2 + 1)}{K_1 + K_2} \right\}}.$$

At correct matching $R_{s_i}(K_1 + 1) = 1$, giving a practical noise factor:

$$N_{\text{pract}} = 1 + R_{\text{eq}i}(K_1 + K_2) \left(2 + \frac{K_1 + 1}{K_1 + K_2} + \frac{K_1 + K_2}{K_1 + 1} \right) + R_{\text{eq}i}K_3(1 - K_2) \left(2 + \frac{2K_1 + K_2 + 1}{K_1 + 1} \right) + \frac{K_1 + a_\tau K_2}{K_1 + 1}.$$

It should be noted that in these equations K_1 is much smaller than unity for frequencies above f_0 , while, according to eq. (99), $0 < K_2 < 1$ and $1/K_3 \approx 1 + S/8I_{g2}$.

The various special cases dealt with in Section 5.4 and many others can be calculated from the above expressions by substituting the required values of K_1 , K_2 and K_3 and putting $R_{\text{eq}i} = (f/f_n)^2$.

APPENDIX V

Eqs (II5), (II6) and (II7) may be derived as follows. The output voltage V_o is first expressed in V_i and V_k to eliminate V_o from V_{ag} and V_k :

$$V_o = -Z_1(S_a V_g + Y_3 V_{ag} + Y_5 V_a) = Z_1 S_a V_k + Z_1 Y_5 V_k + Z_1 Y_3 V_i - Z_1 S_a V_i - Z_1 Y_3 V_o - Z_1 Y_5 V_o,$$

or

$$V_o = V_k \cdot \frac{S_a + Y_5}{Y_1 + Y_3 + Y_5} - V_i \cdot \frac{S_a - Y_3}{Y_1 + Y_3 + Y_5}. \quad (j)$$

V_g can then be expressed in V_i :

$$I_6 = Y_4 V_g + Y_5 V_a + S_k V_g = V_i \left\{ Y_4 + S_k - \frac{Y_5(S_a - Y_3)}{Y_5 + Y_3 + Y_5} \right\} - V_k \left\{ Y_4 + Y_5 + S_k - \frac{Y_5(S_a + Y_5)}{Y_1 + Y_3 + Y_5} \right\},$$

and since

$$V_k = I_6 Z_6 = V_i Z_6 \left\{ Y_4 + S_k - \rho(S_a - Y_3) \right\} - V_k Z_6 \left\{ Y_4 + Y_5 + S_k - \frac{Y_5(S_a + Y_5)}{Y_1 + Y_3 + Y_5} \right\}, \quad (k)$$

this gives:

$$V_g = V_i \cdot \frac{Y_6 + Y_7 - \rho Y_3}{Y_6 + Y_4 + Y_7 + S_k - \rho S_a}, \quad (l)$$

Putting $I_a = S_a V_g = S' V_i$, the factor $F_S = S'/S_a$ becomes:

$$F_S = \frac{V_g}{V_i} = \frac{Y_6 + Y_7 - \rho Y_3}{Y_6 + Y_4 + Y_7 + S_k - \rho S_a}. \quad (115)$$

by which the solution of S' is given.

Eq. (k) can be simplified to:

$$V_k = V_i \cdot \frac{Y_4 + S_k - \rho(S_a - Y_3)}{Y_6 + Y_4 + Y_5 - \rho(S_a + Y_5) + S_k} \quad (m)$$

By substituting eq. (m) in eq. (j), V_o can be expressed in V_i , viz.:

$$V_o = V_i \left\{ \frac{S_a + Y_5}{Y_1 + Y_3 + Y_5} \cdot \frac{Y_4 + S_k - \rho(S_a - Y_3)}{Y_6 + Y_4 + Y_5 - \rho(S_a + Y_5) + S_k} - \frac{S_a - Y_3}{Y_1 + Y_3 + Y_5} \right\}.$$

Hence

$$V_{ag} = V_o - V_i = -\frac{V_i}{Y_1 + Y_3 + Y_5} \cdot \left[Y_1 + Y_5 + S_a - \frac{(S_a + Y_5) \{ Y_4 + S_k - \rho(S_a - Y_3) \}}{Y_6 + Y_4 + Y_5 - \rho(S_a + Y_5) + S_k} \right].$$

The form between square brackets may be written:

$$\begin{aligned} Y_1 + (S_a + Y_s) \cdot \frac{\{Y_6 + Y_4 + Y_s - \rho(S_a + Y_s) + S_k\} - \{Y_4 + S_k - \rho(S_a - Y_3)\}}{Y_6 + Y_4 + Y_s - \rho(S_a + Y_s) + S_k} = \\ = Y_1 + (S_a + Y_s) \cdot \frac{Y_6 + Y_s(1-\rho) - \rho Y_3}{Y_6 + Y_4 + Y_s(1-\rho) - \rho S_a + S_k} = \\ = Y_1 + (S_a + Y_s) \cdot \frac{Y_6 + Y_7 - \rho Y_3}{Y_6 + Y_4 + Y_7 + S_k - \rho S_a}. \end{aligned}$$

From eq. (115) it can then be written:

$$V_{ag} = -V_i \cdot \frac{Y_1 + F_S(S_a + Y_s)}{Y_1 + Y_3 + Y_6} = -V_i \cdot \frac{S' + Y_1 + F_S Y_6}{Y_1 + Y_3 + Y_6}. \quad (n)$$

Substitution of eq. (n) in the expression:

$$Y_i' = \frac{V_i}{I_i},$$

where $I_i = I_2 + I_4 - I_3$ and $I_3 = Y_3 V_{ag}$, gives:

$$Y_i' = Y_2 + Y_4 F_S + Y_3 \cdot \frac{S' + Y_1 + F_S Y_6}{Y_1 + Y_3 + Y_6}, \quad (116)$$

while substitution of eq. (n) in the expression:

$$V_{ag} = V_o - V_i$$

gives:

$$-\frac{V_o}{V_i} = \frac{S' - Y_3 - (1 - F_S)Y_6}{Y_1 + Y_3 + Y_6}. \quad (o)$$

Substitution of eq. (o) in the expression:

$$Y_o' = -S' \cdot \frac{V_i}{V_o}$$

finally gives:

$$Y_o' = \frac{Y_1 + Y_3 + Y_6}{1 - \frac{Y_3}{S'} - \frac{Y_6}{S'} \cdot (1 - F_S)}. \quad (117)$$

TABLE 1

Summary of the characteristic figures

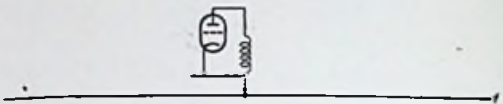
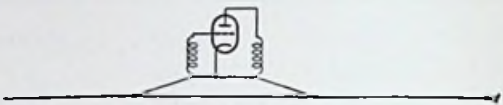
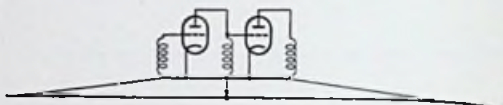
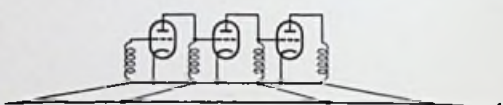
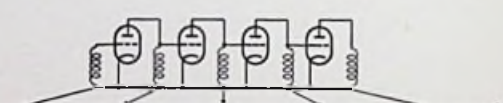
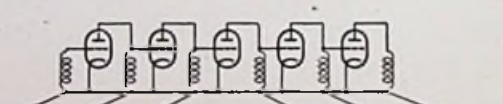
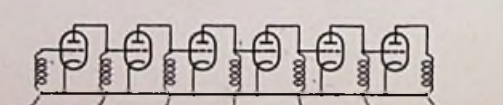
	EF 42	UF 42	EF 91	EF 80
W_f	2.1	2.1	1.9	1.9
V_a	250	170	250	170
V_{g2}	250	170	250	170
I_a	10	10	10	10
I_{g2}	2.4	2.8	2.5	2.5
V_{g1}	-2	-2	-2	-2
S	9	8	7.6	7.4
C_{ag1}	< 0.006	< 0.006	< 0.008*)	< 0.007
C_i (cold capacitance)	9.4	8.6	7.0	7.5
C_o	4.3	4.3	2.0	3.3
g_i (at 100 Mc/s)	850	1000	550	400
R_i ($= 10^3/g_i$)	1.2	1.0	1.8	2.5
R_{eq}	0.84	1.1	1.2	1.0
$(GB) = \frac{S}{2\pi(C_i + C_o)}$	100	100	130	110
$F_x(GB) = \frac{S}{2\pi(C_i + C_o + 6)}$ (for $C_{xi} = C_{xo} = 3$ pF)	75	65	80	70
$(GB)'' = \frac{S}{4\pi\sqrt{C_i C_o}}$	110	100	160	120
$F_x''(GB)'' = \frac{S}{4\pi\sqrt{(C_i + 3)(C + 3)}}$ (for $C_{xi} = C_{xo} = 3$ pF)	75	70	90	70
$(GB)' = \frac{32.5}{\sqrt{C_i}}$	10	11	12	12
$F_x'(GB)' = \frac{32.5}{\sqrt{C_i + 3}}$ (for $C_{xi} = C_{xo} = 3$ pF)	9	10	10	10
f_1 ($SR_i = 1$)	320	280	370	430
f_1' ($300 g_i = 10^6 \mu A/V$)	190	180	240	290
$f_s = \frac{S}{2\pi C_{ag}} >$	24	21	15	17
f_n ($R_{eq} g_i = 10^3$)	120	100	120	160

various valves

6FP 60	EF 50	6AK5	6CB6	6AU6	
2.3	1.9	1.1	1.9	1.9	W
250	250	180	200	250	V
150/250	250	120	150	150	V
20	10	7.7	9.5	10.8	mA
1.51	3	2.4	2.8	4.3	mA
-2.0	-2.0	-2.0	-2.2	-1.0	V
25	6.5	5.1	6.2	5.2	mA/V
0.004	< 0.007	0.02 *)	< 0.020	0.0035	pF
9.2	8.3	4.0	6.3	5.5	pF
6	5.2	2.8	1.9	5	pF
650	1000	125	460	580	μ A/V
1.5	1.0	8.0	2.2	1.7	k Ω
5.7	1.4	1.9	1.6	2.7	k Ω
260	75	120	120	80	Mc/s
190	55	65	70	50	Mc/s
270	80	120	140	80	Mc/s
190	55	65	70	50	Mc/s
10	11	16	13	14	(Mc/s) ^{1/2}
9	10	12	11	11	(Mc/s) ^{1/2}
620	250	640	350	300	Mc/s
220	180	510	270	240	Mc/s
100	15	4	7	24	10 ⁴ Mc/s
50	85	200	120	80	Mc/s

TABLE 2

Bandwidth factor F_B for several identical

Type of staggered group	Diagram of staggered group
one single circuit	
flat staggered pair	
flat staggered triplet	
flat staggered quadruple	
flat staggered quintuple	
flat staggered sextuple	
flat staggered septuple	

Groups in cascade at staggered tuning

sin α	Number of identical groups								
	1	2	3	4	5	6	7	8	9
1.00	1.00	0.64	0.51	0.44	0.39	0.35	0.32	0.30	0.28
0.71	1.00	0.80	0.71	0.65	0.62	0.59			
0.50	1.00	0.86	0.80	0.76	0.73				
0.38	1.00	0.90	0.84	0.81					
0.31	1.00	0.92	0.87						
0.26	1.00	0.93	0.90						
0.195	1.00	0.95							

TABLE 3

Unit function for several identical groups connected in cascade (double side-band systems).

Type of coupling network	t/s	δ in %	$B_r \cdot \tau$	$B_{tot} \cdot \tau$
Synchronous circuits	n	0	$0.7/F_B$	0.7
Flat staggered pairs	1	4.3	0.69	0.69
	2	6.25	0.90	0.72
Synchronous band-pass filters	3	7.7	1.05	0.75
Fed-back pairs	4	8.4	1.15	0.76
	6	10.0	1.34	0.79
Flat staggered triplets	1	8.15	0.73	0.73
	2	11.2	0.93	0.80
	4	14.2	1.14	0.78
Staggered quadruple Staggered band-pass filter pair	1	10.9	0.78	0.78
Staggered quintuple	1	12.8	0.82	0.82
Staggered sextuple Staggered band-pass filter triplet	1	14.3	0.85	0.85
Staggered septuple	1	15.4	0.89	0.89

t = number of identical stages

B_r = bandwidth of the reference circuit

s = number of mutually detuned circuits B_{tot} = total bandwidth

δ = overshoot

τ = rise time

TABLE 4

Bandwidth factor F_B'' for several identical groups in cascade at staggered damping, the bandpass filters being damped at one side only.

Number of identical groups	1	2	3	4	5	6	7
Identical band-pass filters	1	0.80	0.71	0.65	0.62	0.59	0.56
Staggered band-filter pairs	1	0.90	0.84	0.81	0.78	0.77	0.75
Staggered band-pass filter triplets	1	0.93	0.90	0.87	0.85		

In order to find F_B'' , the above numbers must be multiplied by a factor F_{B_1}'' according to fig. 48.

LIST OF SYMBOLS

<i>A</i>	amplitude response of an I.F. amplifier (fig. 19); amplitude of a signal	$C(f'')$	step function corresponding to a given modulation response curve (p. 161)
A_0	carrier amplitude	<i>D</i>	delay of a signal in an amplifier
A_m	amplitude of envelope modulation	<i>d</i>	diameter of dipole (fig. 6)
<i>a</i>	relative admittance of a parallel tuned circuit	E_b	initial magnitude of a carrier modulated by a unit step
<i>B</i>	bandwidth (between 3 db points)	E_n	noise voltage
B'	bandwidth of the aerial circuit (p. 10)	E_n^2	square of the r.m.s. value of E_n
B_h	bandwidth of circuit number <i>h</i>	E_s	change in magnitude of a carrier modulated by a unit step
B_n	noise bandwidth (p. 61)	E_s	signal voltage
B_r	bandwidth of the reference circuit (p. 18)	<i>e</i>	base of natural logarithm (2.71828...)
B_0	maximum bandwidth obtainable with a given valve at a gain G_0 (fig. 4)	<i>e</i>	induced voltage; charge of the electron
b_0	imaginary part of Y_0	F_a	factor expressing the anode current fluctuations due to emission and partition noise (p. 68)
C_c	capacitance of a tuned circuit (p. 2)	F_B	factor expressing the loss of bandwidth due to selective stages being connected in cascade (p. 15)
C_{01}	capacitance of control grid to earth	F_B''	factor expressing the loss of bandwidth in the case of band-pass filter coupling (p. 55).
C_{01k}	capacitance of control grid to cathode	F_{B1}''	factor of F_B'' depending on ν (p. 55)
C_{012}	capacitance of control grid to screen grid	F_k	space charge attenuation factor of emission noise (p. 67)
C_h	total capacitance of tuned circuit number <i>h</i>	F_p	partition noise factor in analogy with F_k (p. 68)
C_i	input capacitance of a valve	F_r	factor expressing the loss of bandwidth due to a valve being controlled (p. 124)
C_i'	input capacitance of a valve with feedback	F_s	factor expressing the loss of gain due to S_{eff} being smaller than S (p. 8)
C_o	output capacitance of a valve (p. 2)	F_x	factor expressing the loss of bandwidth due to stray capacitance (p. 8)
C_D	capacitance of a band-pass filter primary (fig. 47)	F_x'	factor expressing the loss of bandwidth of the aerial circuit due to stray capacitance (p. 11)
C_r	capacitance of the reference circuit		
C_s	capacitance of a band-pass filter secondary (fig. 47)		
C_x	stray capacitance (p. 7)		
$Ci(x)$	integral cosine of x : $\int_0^x \frac{\cos t}{t} \cdot dt$		

List of Symbols

F_z''	factor expressing the loss of bandwidth due to stray capacitance in the case of band-pass filter coupling (p. 54)	$(GB)'$	($= G'\sqrt{B'}$) gain bandwidth figure of an aerial circuit followed by a given valve (p. 11)
f	frequency	$(GB)''$	gain bandwidth figure of a valve (p. 54)
f', f''	characteristic frequencies in the linear approximations of a response curve (fig. 20)	g	($= 1/R$) conductance or damping
f_1	gain reference frequency (fig. 3)	g_a	anode conductance of a valve, excluding $1/r_a$ (p. 2)
f_1'	gain reference frequency for the aerial circuit (p. 11)	g_c	total conductance of a tuned circuit, excluding the valve damping
f_{01k}	frequency at which L_k is in resonance with C_{01k}	g_{01}	conductance of control grid to earth, excluding feedback damping and transit time damping
f_k	frequency at which L_k is in resonance with the cathode-to-earth capacitance	g_h	total damping of tuned circuit number h
f_k'	frequency at which L_k is in resonance with the cathode capacitor	g_i	input conductance of a valve
f_m	frequency of the modulation	g_i'	input conductance of a valve with feedback
f_n	noise reference frequency of a valve (p. 73)	g_o	($= g_a + 1/r_a$) output conductance of a valve (p. 2)
f_s	stability reference frequency of a valve (p. 97)	g_r	conductance of the reference circuit (p. 18)
f_s'	self-neutralising frequency of a valve (fig. 89)	g_t	feedback damping in a valve
f_o	maximum frequency at which a given gain G_o can be obtained with a given valve (fig. 3); frequency of carrier	g_0	real part of Y_0
f_o'	maximum frequency for the aerial circuit at which a given gain G_o' can be obtained with a given valve (fig. 5)	$g\tau$	transit time input damping of a valve
G	($= V_o/V_i$) voltage gain (p. 1)	H	electric field strength
G'	gain of the aerial circuit (p. 10)	$H(t)$	unit step at the instant t
G_h	voltage gain of stage number h	$H_s(t')$	step function
G_{max}	maximum obtainable or permissible voltage gain	h	magnitude of a component in linear approximations of a response curve (p. 32)
G_o	maximum gain obtainable with a given valve at a bandwidth B_o (fig. 3)	I	current or current variation
G_p	available power gain (p. 60)	I_a	anode current of a valve
$(G_p)_f$	power gain at the frequency f	I_a'	anode current fluctuation due to emission noise (p. 67)
$(G_p)_s$	power gain at the signal frequency	I_g	control grid current
G_{tot}	total voltage gain of an amplifier	I_{g2}	screen grid current
(GB)	gain bandwidth figure of a valve (p. 3)	I_k	cathode current
		I_p	current fluctuation due to partition noise (p. 68)
		j	square root of minus one
		K_1	ratio of circuit damping to valve input damping
		K_2	fraction of total input damping due to transit time effects

List of Symbols

K_3	fraction of total noise due to partition noise (p. 69)	P_{si}	signal power at the input of an amplifier
k	($= M/\sqrt{L_p L_s}$) coupling coefficient of two coils; Boltzmann's constant ($= 1.37 \times 10^{-23}$ J/°K)	P_{so}	signal power at the output of an amplifier
L	inductance	p^2	feedback parameter (pp. 87, 90)
L_c	inductance of an interstage circuit (p. 2)	p_h^2	value of p^2 for stage number h
L_k	inductance of the cathode lead	p_r^2	value of p^2 for a stage the anode and grid circuits of which are identical to the reference circuit (p. 91)
L_p	inductance of a band-pass filter primary, including M	Q	quality factor of a tuned circuit (p. 134); in a bandpass filter $Q = \sqrt{Q_p Q_s}$
L_s	inductance of a band-pass filter secondary, including M	Q_h	quality factor of tuned circuit number h
l	length of dipole (fig. 6)	Q_p	Q of a band-pass filter primary
M	mutual inductance of a band-pass filter (fig. 47); modulation response of an I.F. amplifier (fig. 19)	Q_s	Q of a band-pass filter secondary
M_{real}	real component of the modulation response (p. 34)	q	($= kQ$) relative coupling coefficient of a band-pass filter
M_{imag}	imaginary component of the modulation response (p. 35)	R	resistance
$M_{q \text{ real}}$	real component of the modulation response for the quadrature component of the carrier (p. 40)	R_a	anode load resistance of a valve, excluding R_c (p. 2)
$M_{q \text{ imag}}$	imaginary component of the modulation response for the quadrature component of the carrier (p. 40)	R_{ao}	feedback resistance between anode and grid
N	noise factor (p. 59)	R_{ant}	radiation resistance of an aerial (p. 9)
N_a	actual noise factor with a signal source of which $T_s \neq 288$ °K	R_c	parallel resistance of a tuned circuit (p. 2)
N_{pract}	noise factor at correct matching	R_d	resistance equivalent to loading by a detector
N_{st}	noise factor with a signal source of which $T_s = 288$ °K	R_g	grid leak resistance
n	number of stages of an amplifier	R_k	cathode resistance
P	available power of a signal source	R_l	load resistance of a diode detector (p. 13)
P_n	noise power	R_n	noise resistance (p. 63)
P_{ni}	noise power at the input of an amplifier	R_p	total parallel resistance of a band-pass filter primary, including valve damping (fig. 47)
P_{no}	noise power at the output of an amplifier	R_s	total secondary resistance of a band-pass filter secondary, including valve damping (fig. 47)
P_{nr}	noise power originating from a "noise resistance" (p. 62)	R_s	internal resistance of a signal source
P_s	signal power	R_t	input resistance of a valve due to feedback damping
		R_τ	($= 1/g\tau$) input resistance of a valve due to transit time damping

List of Symbols

r	(= Q_s/Q_p) ratio of the secondary to the primary quality factor of a band-pass filter (p. 53)	V_o	output voltage
r_a	(= μ/S) internal resistance of a valve (p. 2)	V_{rad}	e.m.f. in the aerial (p. 9)
S	mutual conductance of a valve (static value)	w	ratio of transformation of aerial circuit (fig. 6)
S_a	($\partial I_a/\partial V_g$) anode transconductance	x	(= $\beta Q = \Delta\omega/\pi B$) relative detuning expressed in half the bandwidth
S'	effective transconductance of a stage having feedback (p. 85); transconductance for the effective control voltage (p. 67)	x_h	value of x for circuit number h
S_{eff}	mutual conductance of a valve (dynamic value)	Y	admittance
S_k	($\partial I_k/\partial V_g$) cathode transconductance	\hat{Y}	value of Y at the resonant frequency
$Si(x)$	integral sine of x : $\int_0^x \frac{\sin t}{t} \cdot dt$	Y_h	admittance of circuit number h
$S(f')$	step function corresponding to a given modulation response curve (p. 33)	Y_h'	apparent value of Y_h due to feedback effects
S_{max}	maximum mutual conductance of a valve	Y_i	input admittance
s	number of staggered circuits in a flat staggered group (p. 17); (= $\beta'Q_p$) relative detuning of a trap with respect to the primary circuit expressed in half the bandwidth of the primary (p. 144)	Y_i'	input admittance of a stage with feedback (p. 85)
T	absolute temperature; standard value 288 °K (p. 60)	Y_o	output admittance
T_s	noise temperature of signal source (p. 60)	Y_o'	output admittance of a stage with feedback (p. 85)
t	time; number of tuned circuits in an amplifier	Y_t	transfer admittance
t'	(= $t + D$) time corrected for delay in an amplifier	$Y_{h, h+1}$	transfer admittance of the inter-stage circuit between stages h and $h + 1$
V_a	anode voltage	Y_1	admittance between anode and earth (fig. 72)
V_{ag}	voltage between anode and control grid	Y_2	admittance between grid and earth (fig. 72)
V_{ant}	output voltage of an aerial (p. 9)	Y_3	admittance between anode and grid (fig. 72)
V_g	control grid voltage	Y_4	admittance between grid and cathode (fig. 72)
V_k	cathode voltage	Y_5	admittance between anode and cathode (fig. 72)
V_i	input voltage	Y_6	admittance between cathode and earth (fig. 72)
		Y_7	auxiliary quantity (p. 85)
		Z	impedance
		\hat{Z}	value of Z at the resonant frequency
		Z_{ant}	characteristic impedance of an aerial (p. 9)
		Z_h	grid circuit impedance of stage number h
		Z_k	cathode impedance
		Z_i	input impedance
		Z_o	output impedance

List of Symbols

Z_r	impedance of the reference circuit of a staggering system		with respect to the reference circuit (fig. 8)
Z_t	transfer impedance	$\Delta\omega$	detuning of a signal with respect to the resonant frequency of a circuit (radn./sec)
Z_1, Z_2, \dots	inverse values of Y_1, Y_2, \dots (fig. 72)	δ	overshoot of a step function (fig. 13); loss angle (p. 134)
α	characteristic angle in staggering system (p. 18); ratio of noise temperature to standard temperature of 288 °K (p. 61)	η_D	detector efficiency
α_h	value of α for circuit number h	Θ	delay angle (p. 31)
α_τ	noise temperature attributed to $R\tau$ (p. 70)	λ	wavelength
β	(= $\omega/\omega_0 - \omega_0/\omega \approx 2\Delta\omega/\omega$) relative detuning	π	ratio of circumference to diameter of circle (3.14159...)
β_h	value of β for circuit number h	ρ	auxiliary quantity (p. 85)
ΔC_i	increase of input capacitance due to space charge	τ	rise time of a step function
Δ/h	detuning of circuit number h	τ_{k_v}	electron transit time from cathode to grid
		ω	angular frequency (radn./sec)
		ω_0	resonant frequency of a tuned circuit (radn./sec)

PHILIPS' TECHNICAL LIBRARY comprises 4 series of books:

- a. Electronic Valves
- b. Light and Lighting
- c. Miscellaneous
- d. Popular series

The series a, b and c published in 6" × 9" are cloth bound, gilt. The dimensions of the popular series are 3½" × 8½" bound in coloured "integral" binding. These books are mostly published in 4 languages: English, French, German and Dutch.

a. Series on ELECTRONIC VALVES:

- Book I "Fundamentals of Radio-Valve Technique" by J. Deketh
Book II "Data and Circuits of Receiver and Amplifier Valves"
Book III "Data and Circuits of Receiver and Amplifier Valves", 1st Suppl.
Book IIIA "Data and Circuits of Receiver and Amplifier Valves", 2nd Suppl.
by N. Markus and J. Otte
Book IIIB "Data and Circuits of Receiver and Amplifier Valves", 3rd Suppl.
by N. Markus
Book IIIC "Data and Circuits of Television Valves" by J. Jager
Book IV "Application of the Electronic Valve in Radio Receivers and Amplifiers", Volume I, by B. G. Dammers, J. Haantjes, J. Otte and H. van Suchtelen
Book V Idem, Volume 2
Book VI Idem, Volume 3
Book VII "Transmitting Valves" by P. J. Heyboer and P. Zijlstra
Book VIIIA "Television Receiver Design" 1, by A. G. W. Uitjens
Book VIIIB "Television Receiver Design" 2, by P. A. Neeteson
Books IIIB, IIIC and VI are in preparation.

b. Series "LIGHT AND LIGHTING"

1. "Physical Aspects of Colour" bij P. J. Bouma
2. "Gas Discharge Lamps" by J. Funke and P. J. Oranje
3. "Fluorescent Lighting" by Prof. C. Zwikker c.s.
4. "Artificial Light and Architecture" by L. C. Kalf
5. "Artificial Light and Photography" by G. D. Rieck and L. H. Verbeek
6. "Manual for the Illuminating Engineer on Large-Size Perfect Diffusors"
by H. Zijl
7. "Calculation and Measuring of Light" by H. A. E. Keitz

Books 4 and 7 exist in German only. An English edition of book 7 is in preparation

c. Series "MISCELLANEOUS"

- a. "Television" by Fr. Kerkhof and W. Werner
- b. "Low Frequency Amplification" by N. A. J. Voorhoeve
- c. "Metallurgy and Construction" by E. M. H. Lips

- d. "Strain Gauges" by Prof. J. J. Koch
- e. "Introduction to the study of Mechanical Vibrations" by G. W. v. Santen
- f. "Data for X-Ray Analysis" I by W. Parrish and B. W. Irwin
- g. "Data for X-Ray Analysis" II by W. Parrish, M. G. Ekstein and B. W. Irwin
- h. "X-Rays in Dental Practice" by G. H. Hepple
- i. "Industrial Electronics" by R. Kretzmann

Books b, c, e, f, g and i are in preparation.

"POPULAR SERIES"

The books of Philips' Technical Library are on a rather high level. Again and again we received requests for technical books on a somewhat lower level. It was decided to comply with these requests and to bring such books in a "popular" series. Popular does not mean here superficial, but intelligible to a larger group of readers.

- 1. "Remote Control by Radio" by A. H. Bruinsma
- 2. "Electronic Valves for L.F. Amplification" by E. Rodenhuis
- 3. "The Odes and Trons Family" by J. Haantjes
- 4. "Application of small Transmitting Valves for High Frequency and Transmission" by H. H. Mulder, D. Zaayer and P. J. Zijlstra
- 5. "Photo Valves" by E. Rodenhuis.

Books 2, 3, 4 and 5 are in preparation.